

AFFDL-TR-78-169

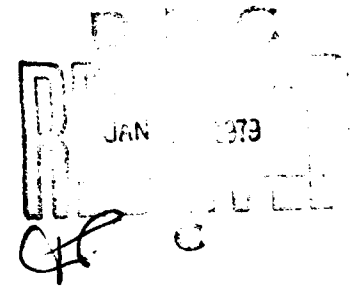
**LEVEL**

2

AD A063497

**SIMULATION OF THE DYNAMIC TENSILE  
CHARACTERISTICS OF NYLON PARACHUTE MATERIALS**

Robert E. McCarty  
Recovery and Crew Station Branch  
Vehicle Equipment Division



November 1978

DDC FILE COPY.

TECHNICAL REPORT AFFDL-TR-78-169  
Final Report for Period 1 November 1973 - 1 November 1976

Approved for public release; distribution unlimited.

AIR FORCE FLIGHT DYNAMICS LABORATORY  
AIR FORCE WRIGHT AERONAUTICAL LABORATORIES  
AIR FORCE SYSTEMS COMMAND  
WRIGHT-PATTERSON AIR FORCE BASE, OHIO 45433

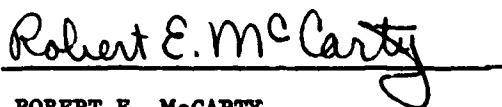
08

NOTICE

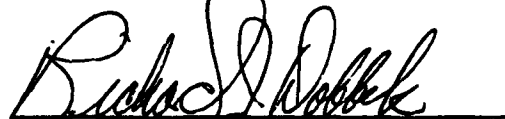
When Government drawings, specifications, or other data are used for any purpose other than in connection with a definitely related Government procurement operation, the United States Government thereby incurs no responsibility nor any obligation whatsoever; and the fact that the government may have formulated, furnished, or in any way supplied the said drawings, specifications, or other data, is not to be regarded by implication or otherwise as in any manner licensing the holder or any other person or corporation, or conveying any rights or permission to manufacture, use, or sell any patented invention that may in any way be related thereto.

This report has been reviewed by the Information Office (OI) and is releasable to the National Technical Information Service (NTIS). At NTIS, it will be available to the general public, including foreign nations.

This technical report has been reviewed and is approved for publication.

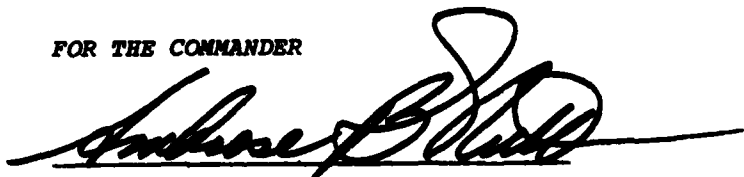


ROBERT E. McCARTY  
Project Engineer



RICHARD J. DOBBEK  
Group Leader  
Recovery Systems Dynamic Analysis Group

FOR THE COMMANDER



AMBROSE B. NUTT  
Director  
Vehicle Equipment Division

"If your address has changed, if you wish to be removed from our mailing list, or if the addressee is no longer employed by your organization please notify AFFDL/FER, W-PAFB, OH 45433 to help us maintain a current mailing list".

Copies of this report should not be returned unless return is required by security considerations, contractual obligations, or notice on a specific document.

UNCLASSIFIED

SECURITY CLASSIFICATION OF THIS PAGE (When Data Entered)

REPORT DOCUMENTATION PAGE		READ INSTRUCTIONS BEFORE COMPLETING FORM
1. REPORT NUMBER AFFDL-TR-78-169	2. GOVT ACCESSION NO.	3. RECIPIENT'S CATALOG NUMBER (9)
4. TITLE (and Subtitle) SIMULATION OF THE DYNAMIC TENSILE CHARACTERISTICS OF NYLON PARACHUTE MATERIALS	5. TYPE OF REPORT & PERIOD COVERED Final Report, 1 Nov 1973 - 1 Nov 1976	6. PERFORMING ORG. REPORT NUMBER
7. AUTHOR(s) Robert E. McCarty	8. CONTRACT OR GRANT NUMBER(s)	
9. PERFORMING ORGANIZATION NAME AND ADDRESS Air Force Flight Dynamics Laboratory Wright-Patterson Air Force Base, Ohio 45433	10. PROGRAM ELEMENT, PROJECT, TASK AREA & WORK UNIT NUMBERS Project 2402 Task 240203 Work Unit 24020312	
11. CONTROLLING OFFICE NAME AND ADDRESS Air Force Flight Dynamics Laboratory Wright-Patterson Air Force Base, Ohio 45433	12. REPORT DATE November 1978	
14. MONITORING AGENCY NAME & ADDRESS (if different from Controlling Office) (12) 183 p.	13. NUMBER OF PAGES 182	
	15. SECURITY CLASS. (of this report) Unclassified	
	15a. DECLASSIFICATION/DOWNGRADING SCHEDULE	
16. DISTRIBUTION STATEMENT (of this Report) Approved for public release; distribution unlimited.		
17. DISTRIBUTION STATEMENT (of the abstract entered in Block 20, if different from Report)		
18. SUPPLEMENTARY NOTES		
19. KEY WORDS (Continue on reverse side if necessary and identify by block number) Computer Models Impact Nylon Material Properties Subroutines		
20. ABSTRACT (Continue on reverse side if necessary and identify by block number) The empirical development of nylon material subroutines for use in computer analysis of parachute system dynamics is discussed. The subroutines account for material plasticity, creep and hysteresis. They predict peak forces and strains accurately (+5%) and are valid over broad ranges of strain rate (three decades) and tensile load (zero to minimum breaking strength). The strain rate sensitivity of nylon is shown to be a manifestation of material creep. Previous models are simplistic by comparison and have been, in general, unsatisfactory. A package		

DD FORM 1 JAN 73 1473

EDITION OF 1 NOV 65 IS OBSOLETE

UNCLASSIFIED

SECURITY CLASSIFICATION OF THIS PAGE (When Data Entered)

012070

Jover

r/B

**SECURITY CLASSIFICATION OF THIS PAGE(When Data Entered)**

A
DATE
REC
FILE NO.
SERIAL
EY
DATE
FILE

**SECURITY CLASSIFICATION OF THIS PAGE(When Data Entered)**

## FOREWORD

This report describes an in-house work effort conducted in the Recovery and Crew Station Branch (FER), Vehicle Equipment Division (FE), Air Force Flight Dynamics Laboratory, Air Force Wright Aeronautical Laboratories, Wright-Patterson Air Force Base, Ohio, under Project 2402, "Vehicle Equipment Technology", Task 240203, "Aerospace Vehicle Recovery and Escape Subsystems", Work Unit 24020312, "Crew Escape and Recovery System Performance Assessment".

The work reported herein was performed during the period of 1 November 1973 to 1 November 1976 by the author, Mr. Robert E. McCarty (AFFDL/FER), project engineer. The report was released by the author in March 1978.

# TABLE OF CONTENTS

SECTION		PAGE
I	INTRODUCTION	
	1. Background	1
	2. Approach	7
	3. Scope	8
II	DATA ACQUISITION	
	1. Methods	10
	2. Apparatus	10
	3. Material Samples	12
	4. Static Data	20
	5. Creep Data	20
	6. Dynamic Data	21
	7. Data Reduction	23
III	DATA ANALYSIS	
	1. Method	28
	2. Creep	28
	3. Loading Characteristic	32
	4. Plasticity	36
	5. Hysteresis	44
	6. Damping	50
IV	COMPUTER SUBROUTINES	
	1. Data Processing	53
	2. Subroutine Models	56
V	RESULTS	59
VI	CONCLUSIONS	62
VII	RECOMMENDATIONS	63
	APPENDIX A MODEL/DATA CORRELATION	65
	APPENDIX B SUBROUTINE LISTINGS	138
	REFERENCES	161

## LIST OF ILLUSTRATIONS

FIGURE		PAGE
1	Loading Characteristics of Nylon	2
2	Hysteresis of Nylon	2
3	Plastic Strain of Nylon	3
4	Creep Behavior	4
5	Schematic for Tensile Impact Test Fixture	11
6	Drop Sled and Weight Plates	13
7	Weighted Drop Sled with LVDT Probe, Zero Strain Weight and Load Link	14
8	Tensile Impact Test Fixture	15
9	Load Link Attachment and Sled Release Mechanism	16
10	Drop Sled Probe in LVDT	17
11	Nylon Cord and Fabric Test Samples	19
12	Test Sample Dimensions	20
13	Typical Creep Strain Data	21
14	Tensile Impact Test Oscillograph Record	24
15	Calibration Error Determination	25
16	Load Calibration Error Correction	25
17	Displacement Calibration Error Correction	26
18	Creep Strain Histories for Fabric	28
19	Creep Strain Model	30
20	Creep Strain Rate Model	31
21	Creep Strain Rate History	32
22	Ideal Creep Test	33
23	Actual Creep Test	33
24	Fabric Fill Loading Characteristics	34
25	Creep Contribution to Total Strain	35
26	Loading Characteristics with Creep Effects Subtracted Out	36
27	Model with Creep Effect	38
28	Residual Strain as a Function of Maximum Strain	38

## LIST OF ILLUSTRATIONS (Concluded)

FIGURE		PAGE
29	Repeated Loading Characteristics	39
30	Initial and Subsequent Loading	41
31	Model with Creep and Plasticity Effects	41
32	Continuous Loading Characteristic	42
33	Residual Strain for Material under Load and under Zero load	43
34	Representation of Unloading Characteristics	45
35	FD versus ELS Data	45
36	Ratioed FD versus ELS Data	46
37	FD Ratios as a Function of ELM1	47
38	Model with Creep, Plasticity, and Hysteresis Effects	48
39	Model Unloading Discontinuity	49
40	Model with Continuous Loading Term	50
41	VSFD versus Strain Rate	51
42	Typical Model-Data Phase Correlation	52
43	Data Processing Flow Diagram	54



## LIST OF TABLES

TABLE		PAGE
1	Impact Test Fixture Components	18
2	Tensile Test Parameters	23
3	Load and Displacement Data Calibration Errors Assumed	27

# LIST OF SYMBOLS

<u>Symbol</u>	<u>Units</u>	<u>Definition</u>
AX	ft/sec <sup>2</sup>	Component of relative acceleration of two end points of tensile member in the direction parallel the member. Same as P(1).
CSR(I,J) I = 1,6 J = 1,3	sec <sup>-1</sup>	Array of values for creep strain rate. Used as the dependent variable in creep model. It is a function of both time, TC(I) and tensile load, FC(J).
DEC	sec <sup>-1</sup>	Current creep strain rate calculated from TBL2. Differs from current creep strain rate, P(3), only by a scalar multiple.
DELO	sec <sup>-1</sup>	Strain rate of tensile member based on original unstressed length of tensile member, LO.
DELOMAX	sec <sup>-1</sup>	Maximum positive strain rate experienced by tensile member during its loading history.
DPA(I) I = 1,6	-	Array of abscissae for the six fixed knots in the cubic spline fit used to represent material unloading characteristic.

# LIST OF SYMBOLS (Continued)

<u>Symbol</u>	<u>Units</u>	<u>Definition</u>
DPC(I,J) I = 1,5 J = 1,3	-	Array of cubic spline coefficients used with DPA(I) and DPO (I) to represent material unloading characteristic. DPA(I), DPO(I) and DPC (I,J) define load FD4 as a function of normalized strain ELS.
DPO(I) I = 1,6	lb for cord lb/in for fabric	Array of ordinates for the six fixed knots in cubic spline fit used to represent material unloading characteristic.
EC	in/in	Creep strain in tensile member.
EDOT	sec <sup>-1</sup>	Initial, maximum strain rate experienced by tensile member during drop weight testing.
EL	in/in	Strain in tensile member based on original unstressed length, L0. Includes residual strain, ELR, and creep strain, EC.
ELM	in/in	Maximum strain experienced by tensile member during its loading history.
ELM1	in/in	Maximum strain experienced by tensile member during the current loading cycle only.

# LIST OF SYMBOLS (Continued)

<u>Symbol</u>	<u>Units</u>	<u>Definition</u>
ELO	in/in	Strain of tensile member based on original unstressed length, $L_0$ . Includes residual strain, ELR, but excludes creep strain, EC.
ELOT	in/in	Linear transform of strain, ELO, in tensile member. Has the form $(ELO - ELR) ELM / (ELM - ELR)$ .
ELR	in/in	Residual strain in tensile member. This plus creep strain, EC, equals the total plastic strain in tensile member. Total plastic strain is that strain exhibited by tensile member when load is reduced to zero.
ELRL	in/in	Upper bound for residual strain, ELR, as a function of maximum strain, ELM.
ELRR	in/in	Lower bound for residual strain, ELR, as a function of maximum strain, ELM.
ELS	-	Normalized strain used to calculate load, $FD_4$ , during unloading of tensile member. Has the form $(ELM_1 - ELO) / (ELM_1 - ELR)$ .
EXA(I) I = 1,6	in/in	Array of abscissae for the six fixed knots in the cubic spline fit used to represent the material loading characteristic.

# LIST OF SYMBOLS (Continued)

<u>Symbol</u>	<u>Units</u>	<u>Definition</u>
EXC(I,J) I = 1,5 J = 1,3	-	Array of cubic spline coefficients used with EXA(I) and EXO(I) to represent the material loading characteristic. EXA(I), EXO(I) and EXC(I,J) define the initial tensile load FSO as a function of strain ELO, and repeated tensile loads FSR as a function of the transformed strain ELOT.
EXO(I) I = 1,6	lb for cord lb/in for fabric	Array of ordinates for the six fixed knots in the cubic spline fit used to represent the material loading characteristic.
FC(I) I = 1,3	lb for cord lb/in for fabric	Array of values for tensile load. Used as one of the independent variables in the creep model.
FD	lb for cord lb/in for fabric	The current unloading decrement derived from load FD2. Value depends on the relative acceleration of tensile member end points, P(1). When relative acceleration is negative or zero, FD has the value of FD2. When relative acceleration is positive, FD reduces the magnitude of FD2 by the ratio of current negative strain rate to maximum negative

# LIST OF SYMBOLS (Continued)

<u>Symbol</u>	<u>Units</u>	<u>Definition</u>
		strain rate. This drives the unloading decrement to zero as negative strain rates approach zero.
FD1	lb for cord lb/in for fabric	The same load as FD3 but limited to the value zero whenever strain rate is zero or positive.
FD2	lb for cord lb/in for fabric	Same as FD1 except that is has the value zero whenever tensile member length is less than the current unstressed length, L.
FD3	lb for cord lb/in for fabric	Value of load FD4 scaled for current cycle maximum strain and modified by a linear viscous damping term. It is also limited to values between zero and the current tensile load, FS. This prevents compression in flexible members since unloading decrements are subtracted from tensile loads to model unloading.
FD4	lb for cord lb/in for fabric	Load calculated from the cubic spline fit for the material unloading characteristic. DPA(I), DPO(I), and DPC(I,J) are required for the calculation of FD4 as a function of normalized strain, ELS.

# LIST OF SYMBOLS (Continued)

<u>Symbol</u>	<u>Units</u>	<u>Definition</u>
FS	lb for cord lb/in for fabric	The current load in tensile member during loading. Equal to the value of FS1.
FSO	lb for cord lb/in for fabric	Tensile load calculated from the cubic spline fit for the material initial loading characteristic. EXA(I), EXO(I), and EXC(I,J) are required for the calculation of FSO as a function of strain, ELO.
FSOL	lb for cord lb/in for fabric	Same as FSO but limited to positive values only.
FSR	lb for cord lb/in for fabric	Tensile load calculated from the cubic spline fit for the material repeated loading characteristic. EXA(I), EXO(I), and EXC(I,J) are required for the calculation of FSR as a function of the transformed strain, EL0T.
FSRL	lb for cord lb/in for fabric	Same as FSR but limited to positive values only.

# LIST OF SYMBOLS (Continued)

<u>Symbol</u>	<u>Units</u>	<u>Definition</u>
FSW(A,B,C,D)	-	External FORTRAN function. Equals B if A is less than zero, C if A equals zero, D if A is greater than zero.
FS1	lb for cord lb/in for fabric	Same as FS2 but has the value zero whenever tensile member length is less than the current unstressed length, L.
FS2	lb for cord lb/in for fabric	Has the value of FSOL for initial loading of material and the value of FSRL for repeated loading of the material.
FT	lb for cord lb/in for fabric	Tensile load. The difference between the load FS and the load FD. Has the value FS whenever strain rate is zero or positive since FD is zero for these cases.
FTR	lb	Tensile load FT multiplied by material width WIDTH. For cords, webs, and tapes the value is the same as FT. For fabric, FTR represents a total load for a given width of fabric whereas FT represents linear stress in lb/in.
g	ft <sup>2</sup> /sec	Acceleration of gravity.



# LIST OF SYMBOLS (Continued)

<u>Symbol</u>	<u>Units</u>	<u>Definition</u>
IER	-	Error parameter related to routine TBL2.
IMODE	-	Alphanumeric parameter used in program MADLOT (Section IV.1). Not required by subroutine model.
KCR	-	A scalar quantity used to alter the magnitude of P(3) during model development. Should have the value 1.
KDP	-	A scalar quantity used to alter the magnitude of FD3 during model development. Should have the value 1.
KPU	-	A scalar quantity used in program BOUNCE (Section IV.1) Not required by subroutine model.
KRL	-	A scalar quantity used to alter the magnitude of ELR during model development. Should have the value of 1.
L	ft	Current unstressed length of tensile member. Includes residual strain, ELR. Excludes creep strain, EC.
LO	ft	Original unstressed length of tensile member.

# LIST OF SYMBOLS (Continued)

<u>Symbol</u>	<u>Units</u>	<u>Definition</u>
M	sl	Total mass of drop weight sled used in dynamic tensile testing.
NDX	-	Number of elements in array TC. Same as NY.
NX	-	Number of elements in array FC.
NY	-	Number of elements in array TC.
P(1)	ft/sec <sup>2</sup>	Component of relative acceleration of two end points of tensile member in the direction parallel the member.
P(2)	ft/sec	Component of relative velocity of two end points of tensile member in the direction parallel the member.
P(3)	sec <sup>-1</sup>	Creep strain rate in tensile member.
RATIO	-	A scalar quantity used to adjust the magnitude of load, FD3. It is a cubic polynomial function of the current cycle peak strain, ELM1.
RLIM(A,B,C)	-	An external FORTRAN function. When A is less than B, the value of B is assigned to A. When A is greater than C, the value of C is assigned to A.

# LIST OF SYMBOLS (Continued)

<u>Symbol</u>	<u>Units</u>	<u>Definition</u>
RMAXD1	sec <sup>-1</sup>	Has the value of strain rate DELO when strain rate is negative. Arbitrarily assigned the value of -1.E-6 when strain rate is positive.
RMAXD2	sec <sup>-1</sup>	Maximum negative strain rate experienced by tensile member during the current unloading cycle only.
T	sec	Current time.
TBL2	-	Double linear interpolation routine used to calculate current creep strain rate from tensile load FT and cumulative time under load TF.
TC(I) I - 1,6	sec	Array of values for time. Used as one of the independent variables in the creep model.
TF	sec	Cumulative time for which tensile member experienced nonzero load.
TN	sec	Current Time.
TS	sec	Cumulative time for which tensile member experienced zero load.
TSS	-	Ratio of TS to value of relaxation time for the material. Used to interpolate value of residual

# LIST OF SYMBOLS (Continued)

<u>Symbol</u>	<u>Units</u>	<u>Definition</u>
		strain, ELR, between its bounds, ELRL and ELRR.
TT	sec	Value of time T when TF was last calculated.
VSFD	-	Linear function of maximum strain rate, DELOMAX. Used as a linear viscous damping term in expression for load FD3.
VSFDM	sec	Linear viscous damping coefficient. Used as slope in term for linear viscous damping, VSFD.
VX	ft/sec	Component of relative velocity of two end points of tensile member in the direction parallel the member.
WIDTH	in	Width of fabric samples. Has the value of 1.0 for cords, webs, and tapes.
X	ft	Length of tensile member including residual strain, ELR, and creep strain, EC.
Y(1)	ft/sec	Component of relative velocity of two end points of tensile member in the direction parallel the member.
Y(2)	ft	Length of tensile member.

LIST OF SYMBOLS (Concluded)

<u>Symbol</u>	<u>Units</u>	<u>Definition</u>
Y(3)	in/in	Creep strain in tensile member.

## SECTION 1 INTRODUCTION

### 1. Background

Computer programs have contributed much to the design and analysis of deployable aerodynamic decelerator systems. Most of the major parachute analysis computer programs developed over the last decade include in some form a mathematical model for the properties of the materials comprising the system. The task of modelling the behavior of parachute materials in such a manner has come to be regarded as both an indispensable element in computer analyses and a major roadblock to full success of the same computer analyses. It is essential because the dynamics of parachute systems prove to be very sensitive to material properties, and at the same time becomes an obstacle primarily because the behavior of parachute materials is so complex.

A review of the typical tensile behavior of the most widely used parachute material, nylon, will serve to explain the difficulty encountered in modelling its properties. The load-strain characteristic, referred to in this report as the loading characteristic, of a nylon tensile member is quite nonlinear and demonstrates a strong sensitivity to strain rate, as can be seen from Figure 1. For a parachute structural member in tension the strain rate is defined to be the difference between the lengthwise velocity components of the member ends divided by the length of the member. It will be reported in units of  $\text{sec}^{-1}$ . Positive strain rates imply that the member is growing longer, negative ones that it is growing shorter. The word loading will be used to imply positive strain rates, the word unloading to imply negative strain rates.

During unloading, nylon exhibits strong hysteresis, that is, it unloads along a characteristic load-strain curve which is considerably different from the one along which it loads as illustrated in Figure 2. The area contained by the two

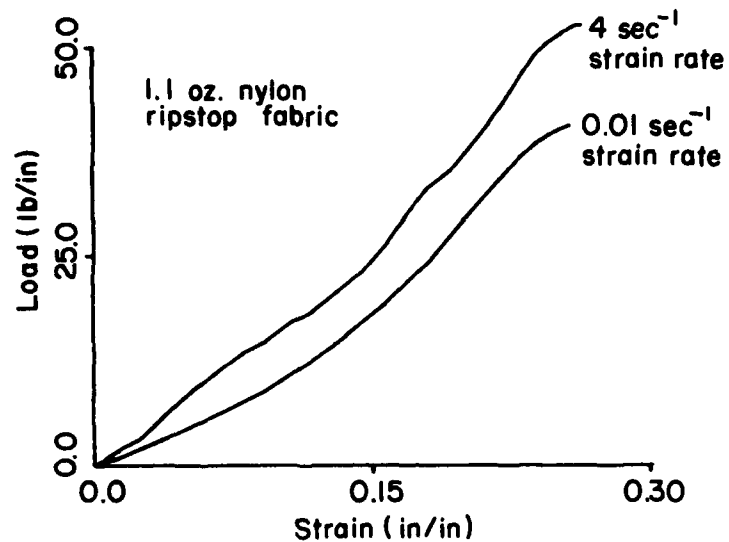


Figure 1. Loading Characteristics of Nylon.

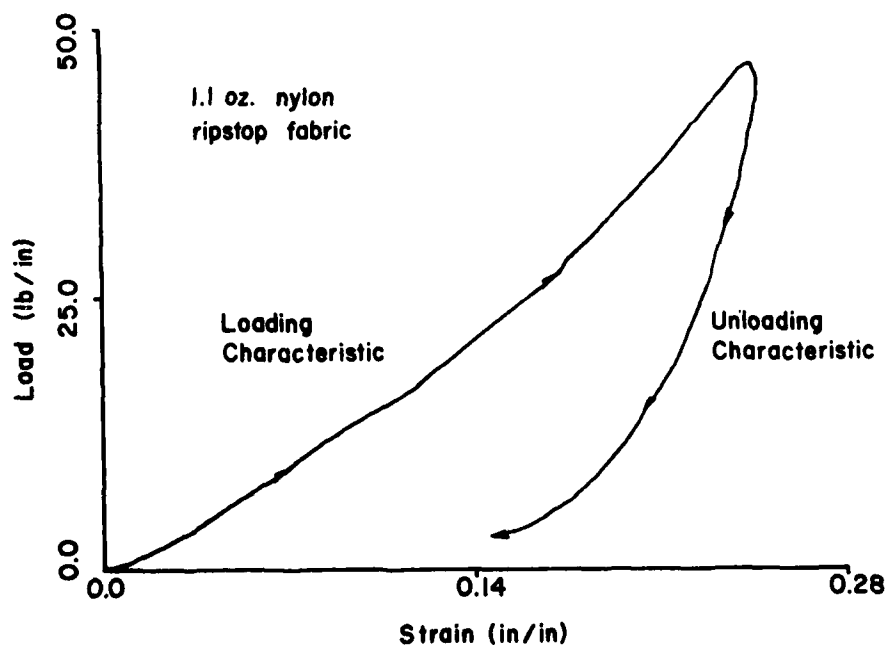


Figure 2. Hysteresis of Nylon.

characteristics represents the kinetic energy dissipated per unit length of material.

Another significant aspect of nylon tensile behavior is the large plastic strain exhibited by the material. Figure 3 illustrates this. Plastic strain is defined to be that strain

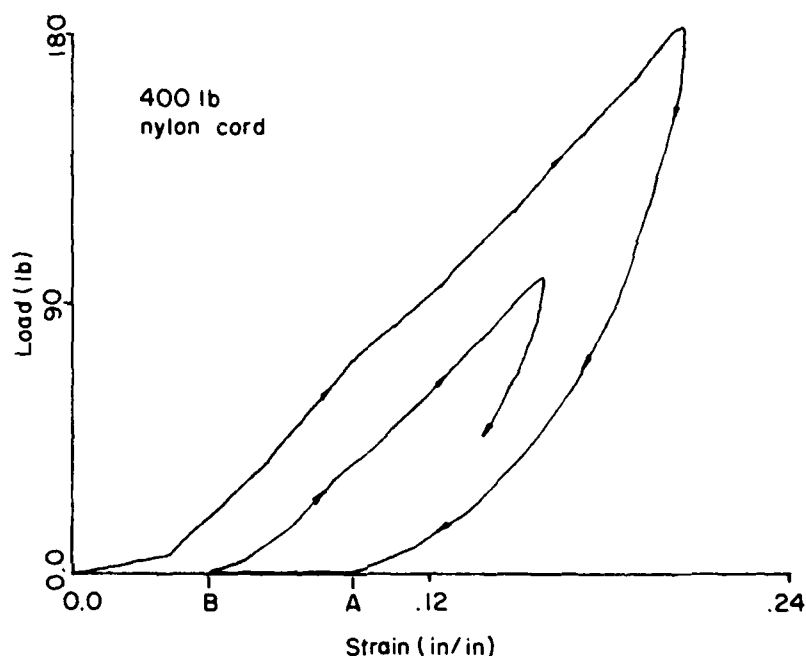


Figure 3. Plastic Strain of Nylon.

remaining in a tensile member when the load is zero after having been loaded. Figure 3 indicates that nylon plastic strain has two components, one time dependent and one not. Immediately upon unloading, the material exhibits the large plastic strain A. After the passage of some time at zero load it exhibits the smaller plastic strain B (at the beginning of the second loading cycle). Plastic strain B is independent of time, or permanent. The material process of shrinking from initial strain A to later strain B is referred to as relaxation.



Yet another significant aspect of the tensile properties of nylon is the presence of creep which is defined as that strain suffered by the material as a function of time under static tensile load. Figure 4 depicts typical creep behavior

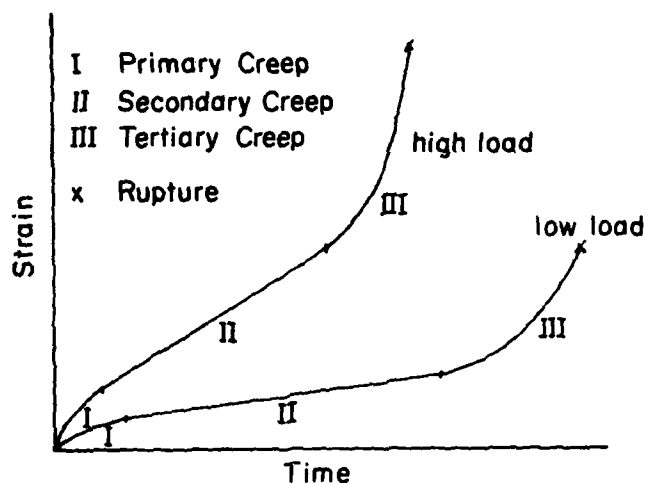


Figure 4. Creep Behavior

including its three stages: primary, secondary, and tertiary. Primary creep is characterized by decreasing strain rate with time, secondary by constant minimum strain rate, and tertiary by rapidly increasing strain rate to the point of material rupture. The creep strain history can change dramatically for different static load levels, so in general creep in nylon is a function of both time and tensile load.

Studies, such as those in References 1 and 2, have shown that the number of these mechanical properties included in

(1) Priesser, J.S. and Green, G.C., "Effect of Suspension Line Elasticity on Parachute Loads," *Journal of Spacecraft and Rockets*, Vol. 7, No. 10, Oct. 1970, pp. 1278-1280.

(2) Poole, L.R., "Effect of Suspension-Line Viscous Damping on Parachute Opening Load Amplification," *Journal of Spacecraft and Rockets*, Vol. 10, No. 1, Jan. 1973, pp. 92-93.

the mathematical model of a parachute material has a marked effect upon computer analyses utilizing that model. As has been mentioned earlier, successful computer analysis of parachute systems depends heavily on the availability of realistic material math models.

A considerable variety of parachute material computer models already exist. The simplest, such as that used in Reference 3, assume that the material is linearly elastic, i.e., that the loading characteristic is linear and that the material exhibits no strain rate sensitivity, hysteresis, plasticity or creep. Others, for example those in References 4, 5, and 6, vary this approach somewhat by assuming a non-linear elastic model. Some researchers have tried to account for the effects of hysteresis by assuming the presence of viscous damping in the material. Modelling this damping component of the tensile load as a single constant multiplied by material strain rate, as in References 7 and 8, implies linear viscous damping. Allowing a variable coefficient or a matrix of coefficients to multiply material strain rate implies non-linear viscous damping. The material model cited in

(3) Mullins, W.M., et al., Investigation of Prediction Methods for the Loads and Stresses of Apollo Type Spacecraft Parachutes, Volume 2: Stresses, NASA-CR-134231, 1970.

(4) Houmard, J.E., Stress Analysis of the Viking Parachute AIAA Paper 73-444, 1973.

(5) Reynolds, D.T., and Mullins, W.M., An Internal Loads Analysis for Ribbon Parachutes, NVR 75-12, Northrop Corp., Ventura Division, 1975.

(6) McVey, D.F., and Wolf, D.F., "Analysis of Deployment and Inflation of Large Ribbon Parachutes," Journal of Aircraft, Vol. 11, No. 2, February 1974, pp. 96-103.

(7) Ibrahim, S.K., and Engdahl, R.A., Parachute Dynamics and Stability Analysis, NASA-CR-120326, February 1974.

(8) Sundberg, W., Finite-Element Modelling of Parachute Deployment and Inflation, AIAA Paper 75-1380, 1975.

Reference 9 was used in analysis of the Viking Mars Lander parachute recovery system deployment and inflation. It assumed nonlinear viscous damping, nonlinear elasticity and an arbitrary history of plastic strain. Notwithstanding the fact that this model was the most sophisticated ever developed, its authors have written that "Significant voids in the knowledge of... suspension system physical properties appear to be a major obstacle to obtaining very accurate (parachute dynamics) simulations and to the use of the analytical model in a predictive mode." This theme is repeated in Reference 10: "A continuing effort is needed to obtain data ... to definitize the behavior of ...(parachute) components under dynamic conditions."

These statements and others like them reflect the consensus that material math models better than those which have been available will be required before parachute system computer analyses can become real predictive tools and as a consequence, make a broader impact on system design and analysis.

These circumstances led to the start in November 1973 of an in-house program in the Recovery and Crew Station Branch, Vehicle Equipment Division, of the Air Force Flight Dynamics Laboratory (AFFDL/FER) to develop improved math models for the dynamic tensile behavior of nylon parachute materials. The approach taken during this work effort is discussed in the following section.

(9) Talay, T.A., Parachute Deployment-Parameter Identification Based on an Analytical Simulation of Viking BLDT AV-4, NASA-TN-D7678, August 1974.

(10) Bobbit, P.J., "Recent Advances and Remaining Voids in Parachute Technology," AIAA Aerodynamic Deceleration Systems Tech Committee Position Paper, Astronautics and Aeronautics, October, 1975, pp. 56-63.

## 2. Approach

Since earlier attempts to model the properties of parachute materials all seemed to share a theoretical approach and to have achieved only limited success, the AFFDL/FER program was planned to be more empirical in nature. Instead of assuming some viscoelastic model for the material behavior at the outset and then struggling to acquire data (elastic and viscous damping coefficients) to fit, it was intended to develop the formulation of a realistic model from appropriate loading data alone. The mathematical expression of the observed data was to be the goal of the effort, not the first step.

An experimental phase of the program was planned to acquire a limited data base for some parachute material of interest. This was to be followed by an analytical phase to search for aspects of the data lending themselves to general mathematical expression over a wide range of load levels and strain rates; i.e., to develop math models of the data acquired. Finally, it was planned to code the math models as computer subroutines for general use in large parachute analysis computer programs. The material subroutines would serve to realistically model the dynamic tensile load-strain behavior of nylon components within the larger computer program, be it for parachute system stress analysis, opening dynamic analysis, stability analysis or design purposes. After one test case, that is after the successful development of one parachute material computer subroutine, it was further intended to automate the process as much as possible by writing data processing computer programs to generate additional material subroutines from new sets of data following the general form developed for the test case.

The goal of the program then was to demonstrate the capability to empirically develop computer subroutines which could realistically model the tensile behavior of nylon parachute components. These subroutines would be generated

semiautomatically through data processing of limited data bases acquired for the materials of interest.

### 3. Scope

The work outlined in the previous section resulted in two-and-one half man-years of work and involved a nylon cord and fabric used widely in personnel parachute fabrication. Only uniaxial tensile behavior of materials was addressed. The first material selected for modelling was a core-sleeve nylon cord used widely in suspension systems of personnel parachutes: 400 lb minimum breaking strength, MIL-C-5040E, Type II, nylon cord.

An apparatus was fabricated to provide dynamic load-strain data for material samples and was used to acquire data for load levels up to 300 lb and over a range of strain rates from 1.2 to 6.9  $\text{sec}^{-1}$ .

By early 1975, a computer subroutine modelling the cord behavior had been demonstrated and was documented in Reference 11. This cord subroutine was used with encouraging results in parachute opening dynamics studies conducted in-house during the same time period as reported in Reference 12.

A second test series was accomplished to acquire data for uniaxial samples in both the warp and fill directions of a light ripstop nylon fabric also used extensively in fabrication of personnel parachutes: 1.1-oz per square yard, MIL-C-7020F, Type I. The warp direction is that of the yarns which run parallel the length of a bolt of fabric as it is woven. The fill direction is normal to the warp direction and is that of the yarns which run back and forth across the bolt of fabric as it is woven. This time, data was acquired up to rupture

(11) McCarty, R., A Computer Subroutine for the Load-Elongation of Parachute Suspension Lines, AIAA Paper 75-1362, 1975.

(12) Keck, E.L., A Computer Simulation of Parachute Opening Dynamics, AIAA Paper 75-1379, 1975.

loads and over a range of strain rates from 1.3 to 4.9  $\text{sec}^{-1}$ .

Seven small data processing computer programs were written to automate the generation of material subroutines as much as possible. These programs were used to derive subroutines from both the fabric warp and fill data bases.

The purpose of this report is to document the overall work effort and publish the nylon material computer subroutines developed. It is also to encourage the application of these subroutines and the development of additional subroutines for other parachute materials by means of the efficient data processing capability now available for their generation.

## SECTION II

### DATA ACQUISITION

#### 1. Methods

This work effort involved a nylon cord and fabric used widely in personnel parachute fabrication, and the primary inhouse application of the computer subroutines developed was intended to be in simulation of personnel parachute opening dynamics, as reported in Reference 12. For these reasons, a test method was sought which would duplicate to a considerable extent the dynamic loading environment experienced by these materials in personnel parachute applications. All constant strain rate methods were rejected because strain rates experienced during parachute operation are not constant but rather suffer large excursions and sign changes. A drop-weight test method was adopted because it provided periodic variation of strain rate and would allow data acquisition over the full range of loading and strain rates (0 to  $4.5 \text{ sec}^{-1}$ ) occurring during conventional deployment and inflation of personnel parachutes.

#### 2. Apparatus

A test fixture was designed and fabricated which would allow tensile impact loads to be applied to samples of parachute materials over a wide range of initial strain rates and impact energies. Figure 5 illustrates the device. Material samples were oriented vertically in the fixture, the upper end being fixed and the lower being attached to a weighted sled. The main component was a 120-inch high tower fixed along its length to a concrete block wall. The tower supported two hard aluminum rails which served to guide the weight sled

(12) Keck, E.L., A Computer Simulation of Parachute Opening Dynamics, AIAA Paper 75-1379, 1975.

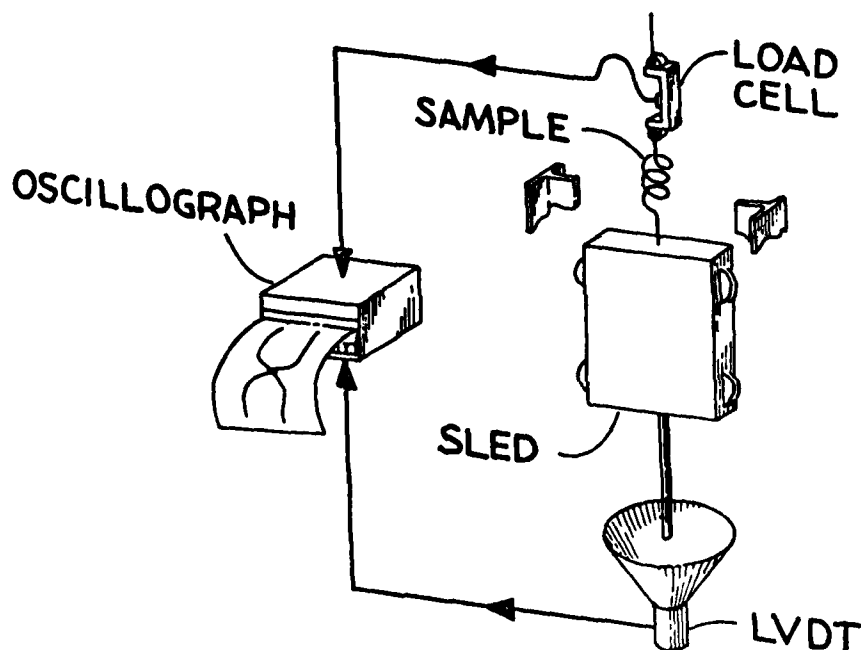


Figure 5. Schematic for Tensile Impact Test Fixture.

as it moved vertically. The rails engaged the flanges of four ball bearing wheels, two on either side of the weight sled. A solenoid-operated device on the tower provided for release of the drop weight sled from various heights. Combinations of drop height and drop weight were selected to obtain the initial strain rates and impact energies desired during testing. Rubber bungee cords were used in some tests to yield sled accelerations exceeding one gravity.

The upper attachment point for material samples was a strain gage load link used to acquire load history data during a test. The weighted drop sled had extending downward from its bottom center a 36-inch-long rod the tip of which entered a 30-inch Linear Variable Differential Transformer (LVDT) used to acquire sled displacement data during a test. Signals from the load link and LVDT were conditioned and used to drive galvanometers in a direct writing type oscillograph. An automatic test sequencer drove the release



mechanism and data acquisition equipment. Data was recorded for at least three full loading cycles (bounces) on every test. Figures 6 through 10 show details of the test fixture. Table 1 contains the list of equipment used in the tensile impact test fixture.

### 3. Material Samples

Length of the material samples tested in the tensile impact fixture were dictated by the range of strain rates desired in testing. Since the geometry of the test fixture prevented drop heights exceeding the length of the sample, the maximum initial strain rate available for (no rubber bungee) drop tests follows Equation (1). The sample lengths

$$EDOT_{\max} = [(2g)/LO]^{1/2} \quad (1)$$

$EDOT_{\max}$  - maximum possible initial strain rate

$g$  - acceleration of gravity

$LO$  - unstressed length of sample

that were selected allowed cord strain rates up to  $4.2 \text{ sec}^{-1}$  and fabric strain rates up to  $4.9 \text{ sec}^{-1}$ .

Cord samples had the ends doubled back and zig-zag stitched to allow steel pin attachments in the test fixture. The ends of warp and fill fabric samples were sandwiched between thin aluminum plates with an epoxy resin. Holes drilled in these end plates provided the same steel pin attachment used for the cord samples. Fabric samples were cut slightly wider than desired, then after epoxying on the end plates, extra yarn ends were cut from both sides of the sample to obtain the desired sample width. All fabric samples had the same number of longitudinal yarn ends. Figures 11 and 12 illustrate the material samples used. In each case, all samples were cut from the same lot of material. All samples were tested at temperatures between 66 and 88 degrees Fahrenheit.



Figure 6. Drop Sled and Weight Plates.

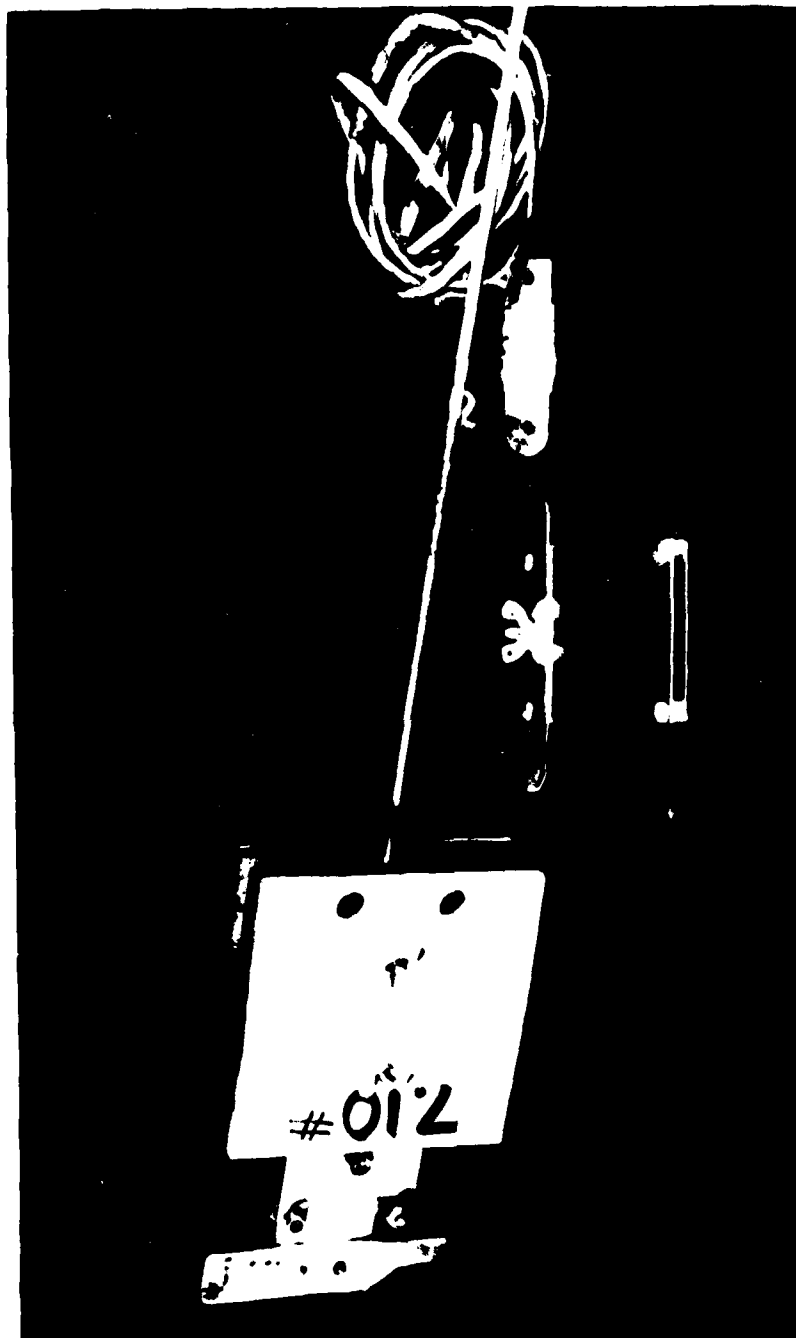


Figure 7. Weighted Drop Sled with LVDT Probe, Zero Strain Weight, and Load Link.

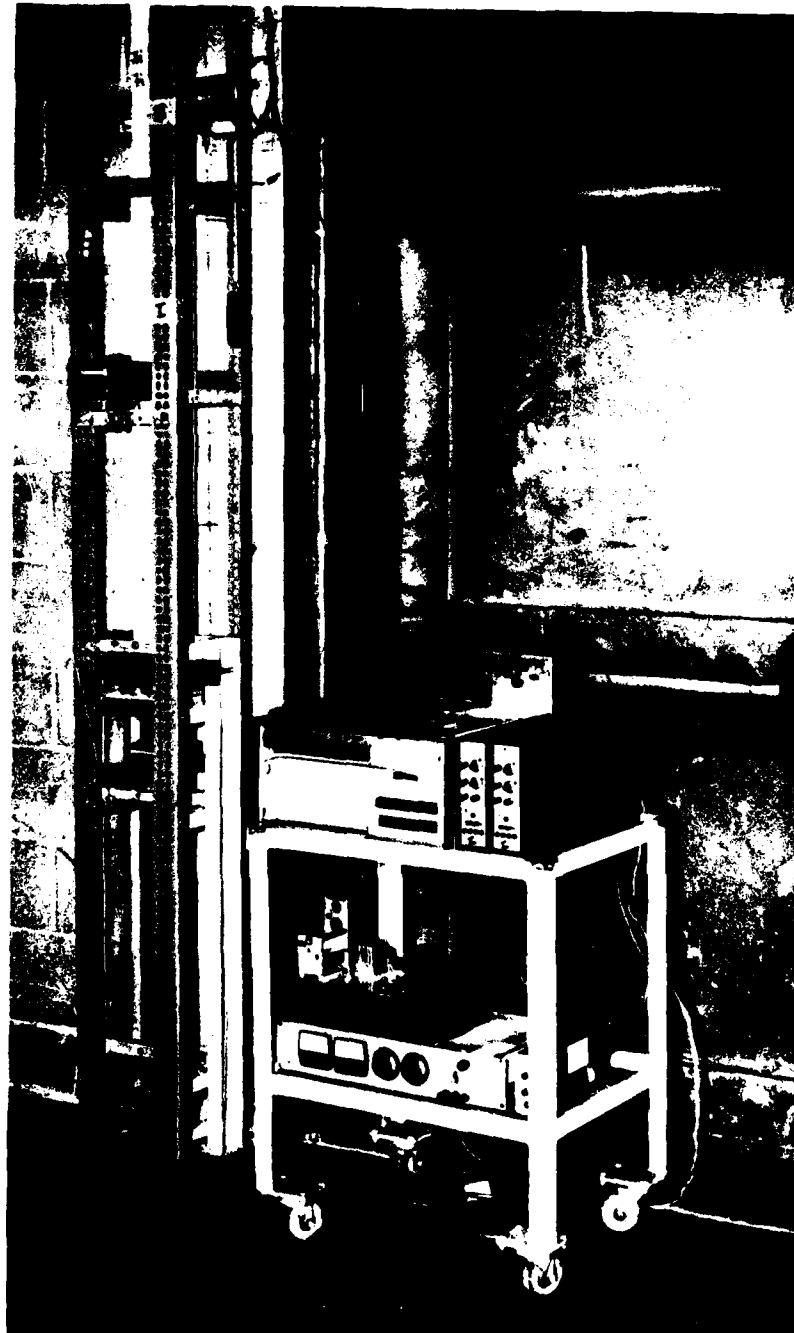


Figure 8. Tensile Impact Test Fixture.



Figure 9. Load Link Attachment and Sled Release Mechanism.

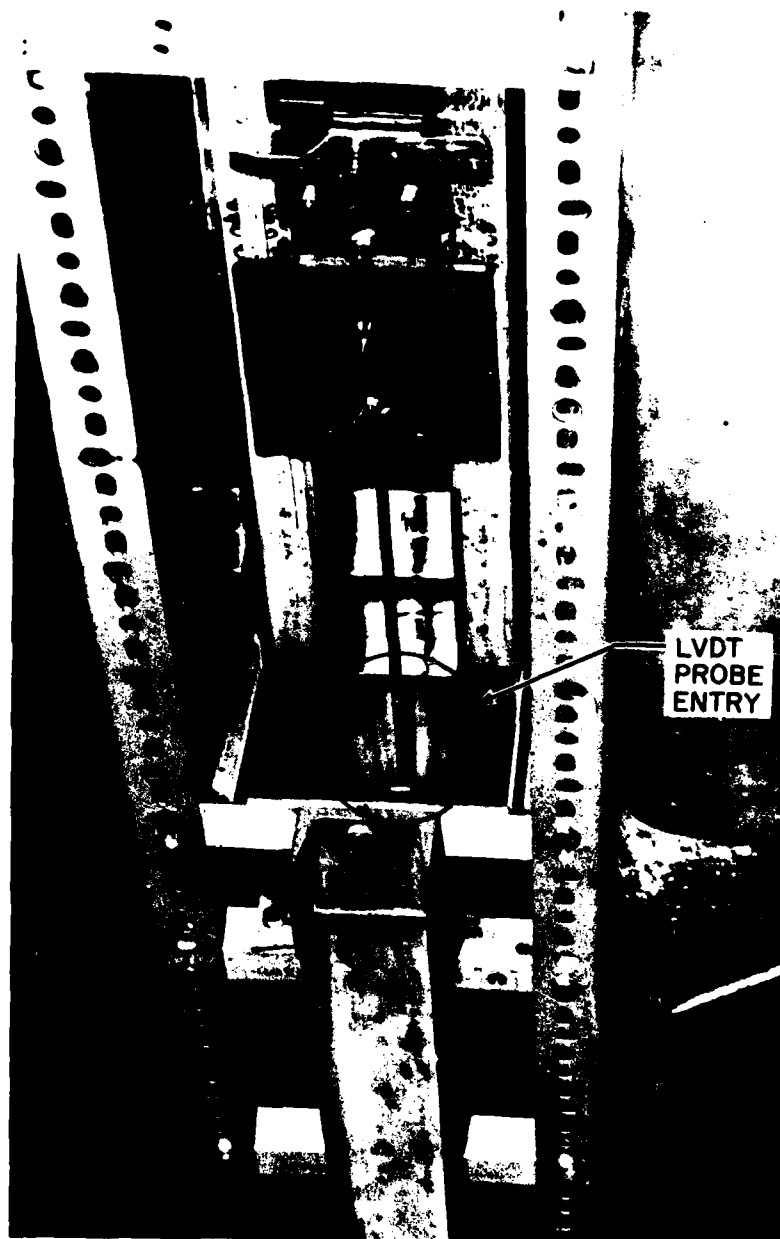


Figure 10. Drop Sled Probe in LVDT.

TABLE 1  
IMPACT TEST FIXTURE COMPONENTS

Component	Model	Performance
steel strain gage link, bending	S/N D-1 (FER)	0-60 lb or 0-140 lb
aluminum strain gage link, tension	S/N 300-1 (FER)	0-300 lb
Schaevitz LVDT	P/N 10000 HR	$\pm 10$ in displ.
Schaevitz signal conditioner	P/N SCM 025	(displ. channel)
SOLA regulated power supply	Cat. 80-36-1300	-
Bell & Howell signal conditioner	P/N 8-115-1	(loads channel)
Honeywell Visicorder	1508-T13679HK000 (oscillograph)	-
Honeywell galvanometer	M-1000 (fluid damped)	0-600 Hz (loads channel)
Honeywell galvanometer	M200-120	0-120 Hz (displ. channel)

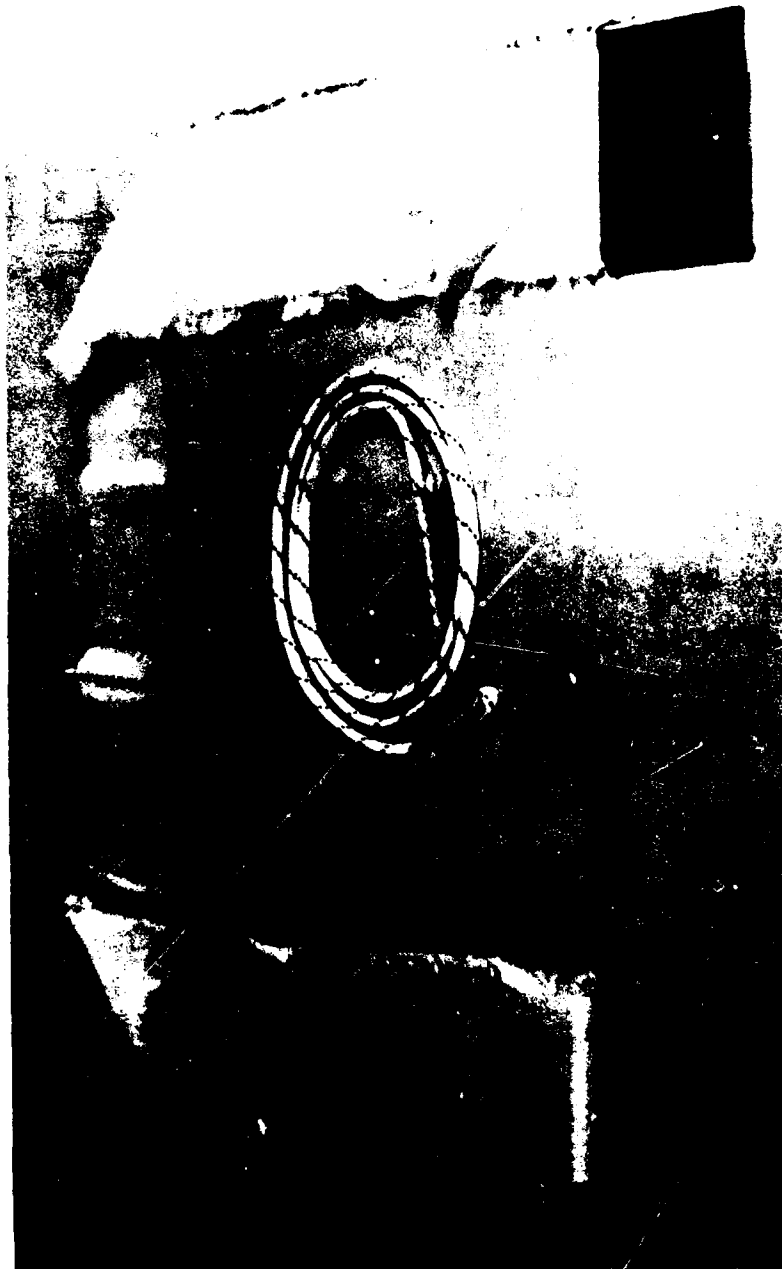


Figure 11. Nylon Cord and Fabric Test Samples.



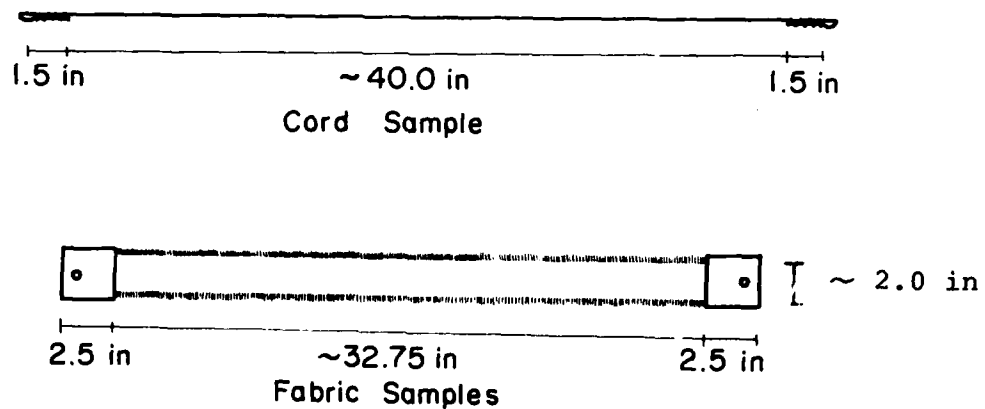


Figure 12. Test Sample Dimensions.

#### 4. Static Data

The Composites and Fibrous Materials Branch, Non-Metallic Materials Division of the Air Force Materials Laboratory (AFML) performed static testing of cord, fabric warp and fill samples. Tests were performed on an Instron machine at strain rates of  $0.01 \text{ sec}^{-1}$ . Rubber lined pressure grips were used to fix samples; all sample gauge lengths were 20 inches. This static data served as a baseline from which to measure strain rate effects in the high strain rate data acquired during subsequent dynamic (drop weight) testing. Load-strain plots made from the reduced AFML data are contained in Appendix A. Static test parameters may be found in Table 2.

#### 5. Creep Data

Creep strain data was acquired for fabric warp and fill samples by suspending the weight sled from a material sample on the Tensile Impact Test Fixture. The oscillograph was used to record the static tensile load and the resulting

strain history exhibited by the material sample. Creep data was recorded under three different loading conditions. A sample of reduced creep data is shown in Figure 13. No data

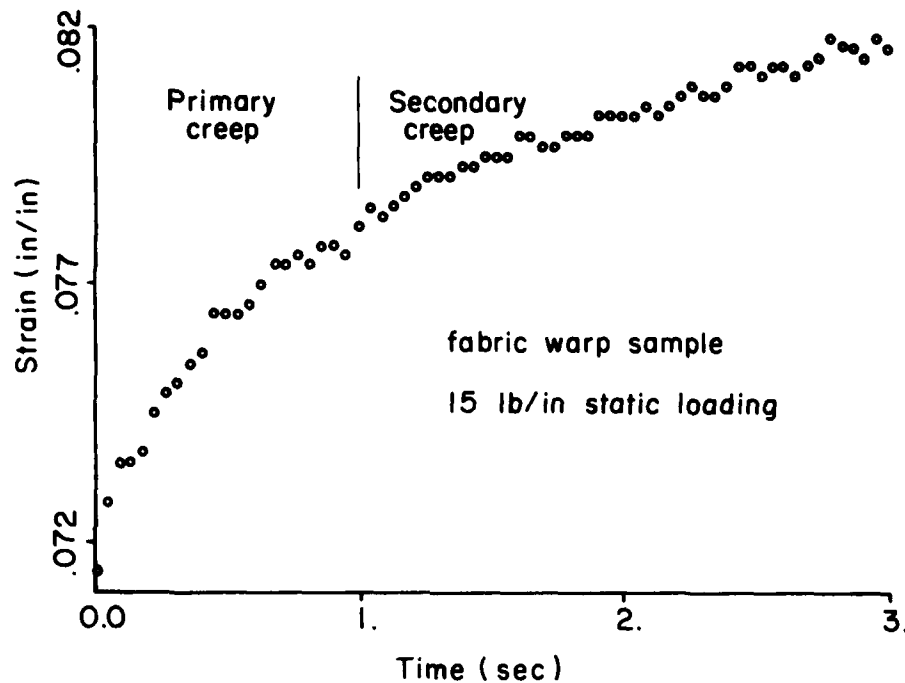


Figure 13. Typical Creep Strain Data.

was acquired for the tertiary stage of creep; i.e., no creep tests were conducted which resulted in material failure.

#### 6. Dynamic Data

Each dynamic, or drop weight, test was conducted with a previously unloaded material sample. Cord samples were tested at eleven different combinations of drop weight and drop height, fabric fill samples at nine combinations, and fabric warp samples at nine combinations. Three tests were performed at each test condition for a total of 87 tensile

impact tests. Table 2 lists parameters for one test at each condition. Parameters for those remaining tests not shown on Table 2 are very similar for any particular test condition, the differences being due primarily to small variations in the length of fabricated test samples. Sample length for cord samples was measured between centers of the steel pins used to mount the samples in the fixture. Sample length for fabric samples was measured between edges of the aluminum end plates as shown in Figure 12. Drop height was defined to be the distance between the sled release position and the sled position at the instant the recorded tensile load rose above zero. Figure 14 shows a typical oscillograph test and illustrates how the sled position at load rise was determined. This position was referred to as the sled zero displacement point and also served as the point from which to measure material sample strain.

#### 7. Data Reduction

The analog load-time and displacement-time traces on each oscillograph record were digitized at uniform intervals, 25 increments per loading cycle including values for peak load and peak displacement. Each data set was checked for reduction errors and corrected accordingly when any were found. Since load data and displacement data channels were calibrated only once at the start of each test series, the following procedure was devised to measure calibration errors. It was assumed that no calibration error was present in the oscillograph timing marks. The load-time data for each drop weight test was pointwise fit with a natural cubic spline as described in Reference 13 and numerically integrated twice to calculate a corresponding sled displacement history. Friction between

(13) DeBoor, C., and Rice, J., Cubic Spline Approximation II-Variable Knots, Computer Science Department TR-21, Purdue University, April 1968.

TABLE 2  
TENSILE TEST PARAMETERS

Test Number		Sample Length (ft)	Drop Height (ft)	Drop Mass (sl)	Initial Strain Rate (sec <sup>-1</sup> )	Peak Load (lb)	Peak Strain (in/in)
1M1	a	3.31	0.35	0.052	1.43	17.7	0.042
2-2	a	3.23	0.27	0.275	1.29	50.2	0.079
3-3	a	3.28	0.32	0.497	1.38	76.8	0.105
4-1	a	3.29	1.59	0.052	3.07	40.9	0.067
5-3	a	3.28	1.57	0.274	3.07	95.0	0.131
6-1	a	3.27	1.60	0.492	3.10	136.7	0.162
7-2	a	3.28	2.82	0.052	4.11	53.2	0.079
8-2	a	3.28	2.86	0.274	4.13	125.3	0.165
9-2	a	3.29	2.87	0.492	4.13	190.0	0.212
10-3	a	3.27	2.85	0.714	4.14	255.4	0.244
11-1	a	3.32	***	0.052	6.88	85.0	0.120
*2C	a	1.67	-	-	.01	409.9	0.355
*3C	a	1.67	-	-	.01	396.0	0.348
1W1	b	2.72	0.22	0.943	1.38	46.1**	0.176
2W1	b	2.72	0.22	0.501	1.38	25.0**	0.121
3W1	b	2.71	0.21	0.167	1.35	10.8**	0.050
*1W4	b	2.70	1.45	0.498	3.58	52.9**	0.201
1W5	b	2.71	1.46	0.278	3.58	38.7**	0.160
6W3	b	2.70	1.45	0.062	3.57	13.6**	0.070
3W7	b	2.69	2.70	0.279	4.89	53.1**	0.203
8W2	b	2.70	2.70	0.166	4.88	39.2**	0.156
9W2	b	2.70	2.71	0.062	4.88	18.8**	0.101
*16W	b	1.67	-	-	.01	40.9**	0.207
*30W	b	1.67	-	-	.01	40.7**	0.209
1F3	c	2.72	0.22	0.943	1.39	46.5**	0.247
2F3	c	2.72	0.22	0.501	1.40	25.5**	0.174
3F2	c	2.70	0.21	0.167	1.35	10.8**	0.083
3F4	c	2.71	1.46	0.498	3.58	51.7**	0.264
5F2	c	2.72	1.47	0.279	3.57	35.1**	0.207
6F2	c	2.71	1.46	0.062	3.58	12.5**	0.099
*3F7	c	2.71	2.71	0.279	4.87	42.6**	0.235
8F1	c	2.71	2.71	0.166	4.87	33.7**	0.211
9F3	c	2.72	2.72	0.062	4.87	17.0**	0.126
*3F1	c	1.67	-	-	.01	39.3**	0.257
*30F	c	1.67	-	-	.01	40.3**	0.271

\*Material rupture occurred.    \*\* (lb/in)    \*\*\*Bungee cord used.

a - cord samples

b - warp samples

c - fill samples

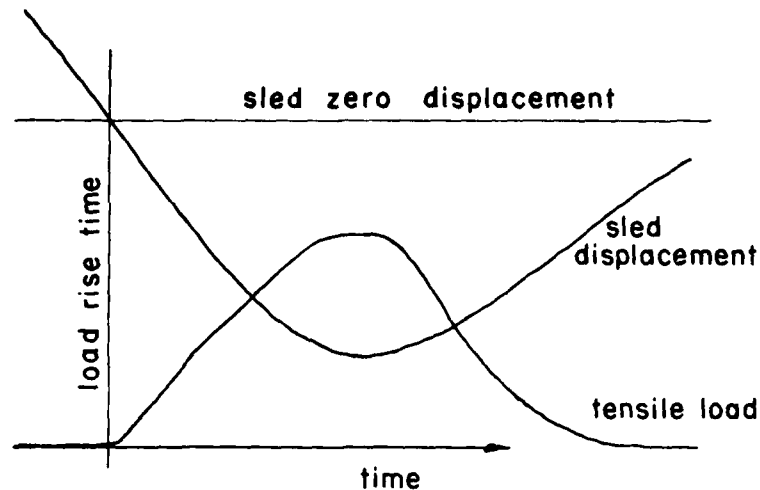


Figure 14. Tensile Impact Test Oscillograph Record.

sled and test fixture guide rails was assumed to be negligible in the calculation. The sled displacement data computed for a given test was compared with the sled displacement data recorded during that test. Figure 15 illustrates the method. Any difference between recorded and calculated periods of motion was taken as evidence of calibration error in the load data, since displacement data calibration error could not alter the recorded period of motion. Sled displacement history was then recalculated as a boundary value problem, assuming various load calibration errors until the one was found which resulted in agreement between recorded and calculated periods of motion. Figure 16 illustrates typical correlation after correction for load calibration error. Any remaining difference between the two maximum sled

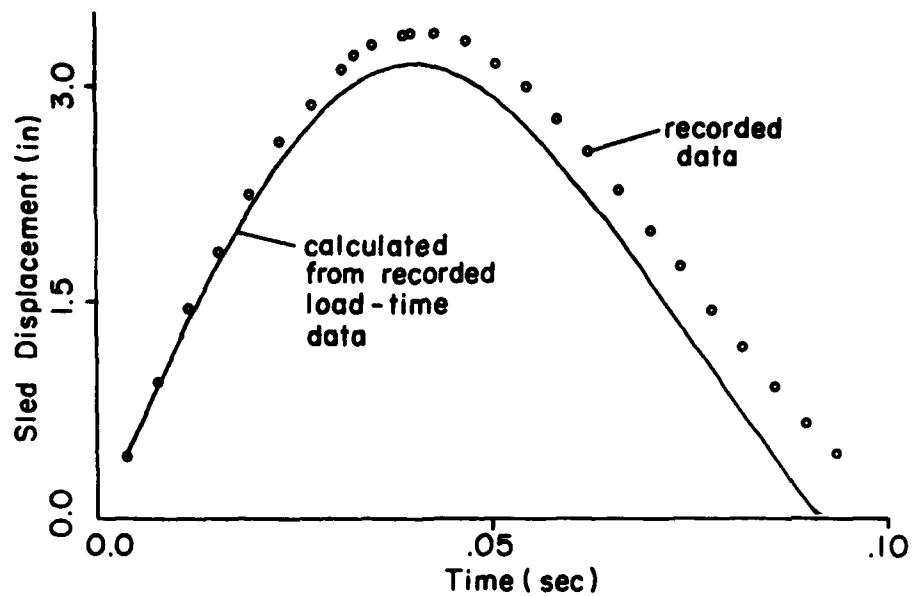


Figure 15. Calibration Error Determination.

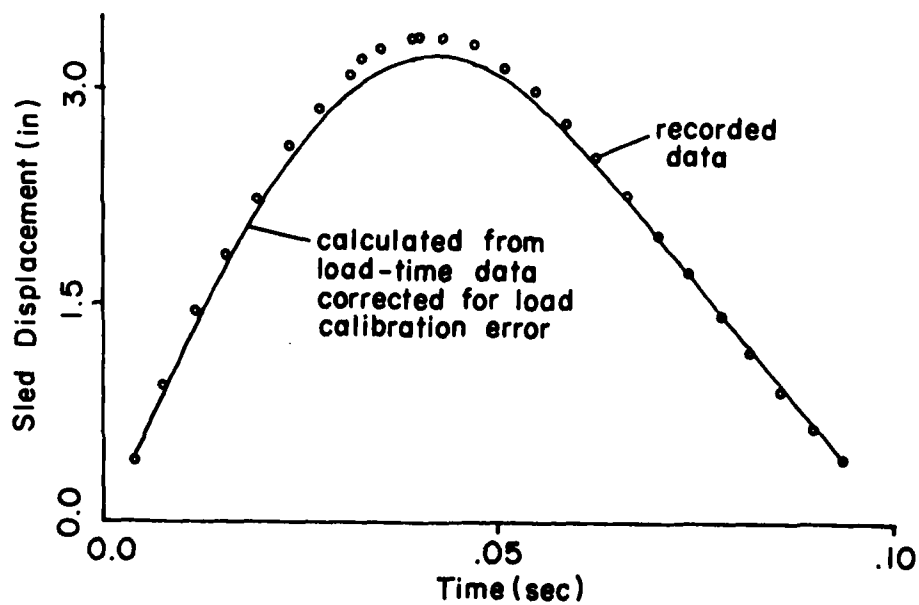


Figure 16. Load Calibration Error Correction.

displacements was attributed to calibration error in the displacement data. That displacement data calibration error which resulted in agreement between calculated and recorded maximum displacements was determined. Figure 17 shows typical correlation between the two sled displacement histories after correcting the data for those calibration errors implied by the method just described. The excellent agreement between shapes of the two displacement histories is

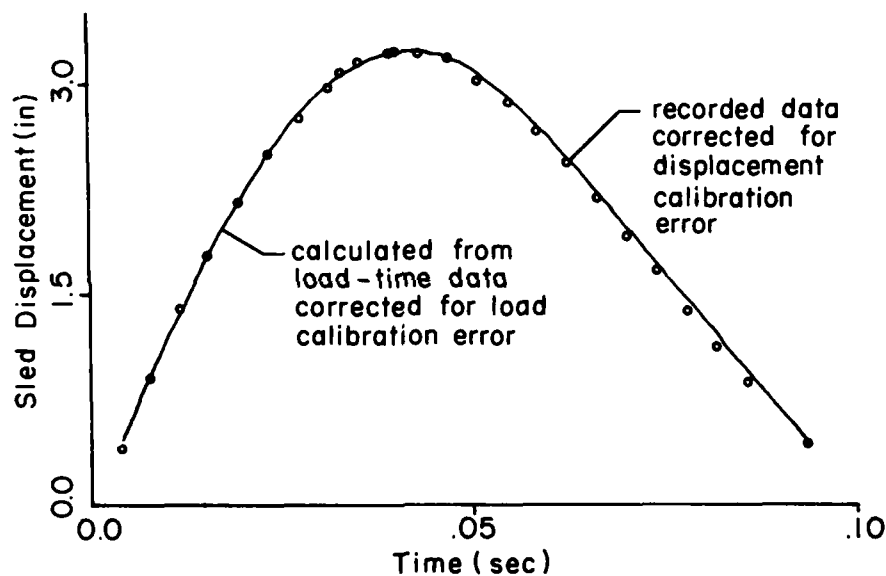


Figure 17. Displacement Calibration Error Correction.

taken as evidence that nonlinearities in transducers and recording equipment, friction in the tensile impact test fixture, and other random sources of recording and reduction errors were negligible for the purposes of this study. Table 3 lists calibration errors derived for those tests in Table 2. Load-strain and load-time plots of corrected data for these tests are contained in Appendix A.

**TABLE 3**  
**LOAD AND DISPLACEMENT DATA CALIBRATION ERRORS ASSUMED**

<u>Test Number</u>	<u>Percent Load Cal. Error</u>	<u>Percent Displacement Cal. Error</u>
1m1	3.0	7.0
2-2	1.0	4.0
3-3	6.0	5.0
4-1	0.0	6.0
5-3	5.0	5.0
6-1	-1.0	3.0
7-2	-2.0	7.0
8-2	-1.0	6.0
9-2	-1.0	4.0
10-3	-1.0	3.0
11-1	-2.0	0.0
1W1	4.0	-6.0
2W1	-2.0	-4.0
3W1	-2.0	-4.0
1W4	2.0	-7.0
1W5	3.0	-1.0
6W3	-3.0	1.0
3W7	4.0	0.0
8W2	5.0	-2.0
9W2	-1.0	-2.0
1F3	4.0	-7.0
2F3	-1.6	-5.3
3F2	-1.6	-5.3
3F4	4.0	-3.0
5F2	7.0	3.0
6F2	-5.0	-4.0
3F7	4.6	-1.3
8F1	6.0	5.0
9F3	-1.6	-1.3



### SECTION III DATA ANALYSIS

#### 1. Method

In developing math models from the data bases acquired, an attempt was made to isolate individual aspects of the material behavior. It was hoped that each of these features could be modelled independently and then that all could be combined to express the observed net behavior. Candidate features for doing this were drawn from the list discussed in Section I.1: nonlinear loading characteristic, strain-rate sensitivity, hysteresis, plasticity, and creep. The first feature selected for modelling was creep. This is discussed in the following section.

#### 2. Creep

The data which was acquired for creep is shown in Figure 18. It exhibits classic primary and secondary creep

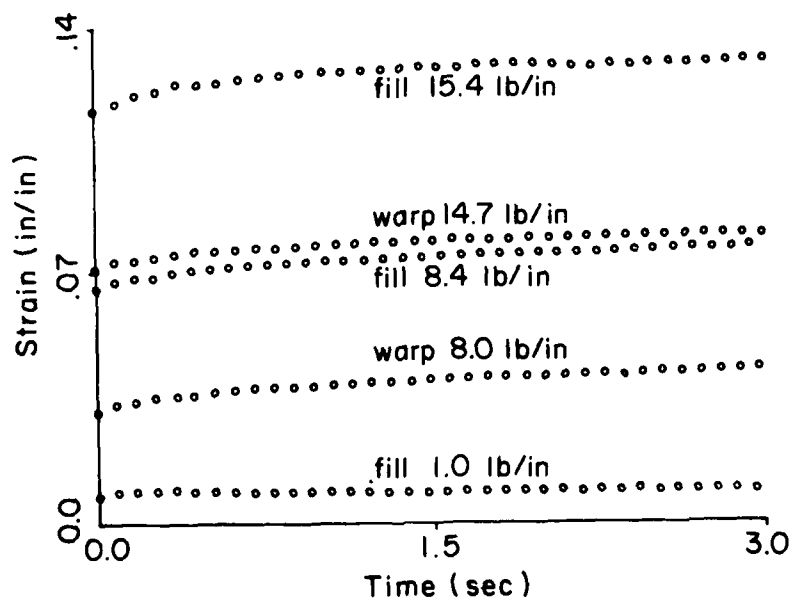


Figure 18. Creep Strain Histories for Fabric.

as defined in References 14 and 15. A great deal of similarity appears in all the creep data shown, aside from the fact that the initial strains under load differ widely. Little measurable creep resulted at very low loads (1 lb/in) on fill test samples. Nearly doubling the loading in the case of both warp and fill samples had little effect on the shape of the resulting strain-time curve. Similarly, no significant difference in curve shape can be seen between warp and fill data taken at about the same level of loading. Transition from primary to secondary creep occurs at about 1.8 seconds in all cases. Based on these observations and on the very limited data base acquired, a simple creep model was developed which proved sufficient for the purpose at hand and which threw a new light on the mechanism underlying the strain rate sensitivity of nylon. This latter result will be discussed more fully in Section III.3.

The creep model adopted assumes that creep behavior is independent of the construction of the particular component fabricated from nylon be it fabric, cord, webbing, etc. It further assumes no effects of material temperature. The model does assume that primary creep occurs from 0.0 to 1.8 seconds under any loading, and secondary creep from 1.8 seconds forward in time. Tertiary creep to material rupture is not modelled. The effect of this omission is discussed in the next section. Identical creep strain histories are assumed for all loadings above 20 percent of the minimum breaking strength for the material; i.e., at loadings above 20 percent of material breaking strength, creep ceases to be a function of static load and time and becomes a function of time alone.

(14) Crandall, S.H., and Dahl, N.C., An Introduction to the Mechanics of Solids, McGraw-Hill, 1959, pp 222-223.

(51) Bruhn, E.F., Analysis and Design of Flight Vehicle Structures, Tri-State Offset, 1965, pp. B1.12-B1.13.

For load levels between 0 and 20 percent breaking strength, the creep strain history is linearly scaled between zero and that creep strain history assumed for higher load levels. The model is extrapolated indefinitely in both independent variables: load and time. Figure 19 illustrates this model.

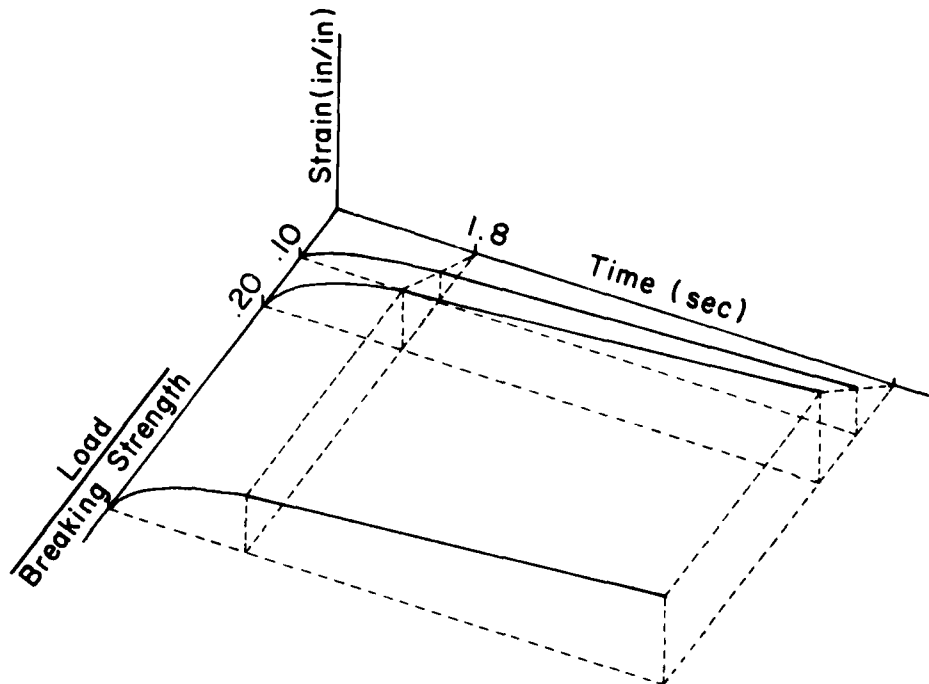


Figure 19. Creep Strain Model.

Values for initial strain (at  $t = 0$ ) have been subtracted out from the data in Figure 19. This surface representing strain as a function of load and time was differentiated with respect to time to yield a second surface representing creep strain rate as discussed further in Reference 16. Figure 20 shows this surface. Double linear interpolation on the second surface for a given load and time gives a corresponding creep strain rate. For the case of dynamic loading, a

(16) Polakowski, N.H., and Ripling, E.J., Strength and Structure of Engineering Materials, Prentice-Hall, 1966 p. 429.

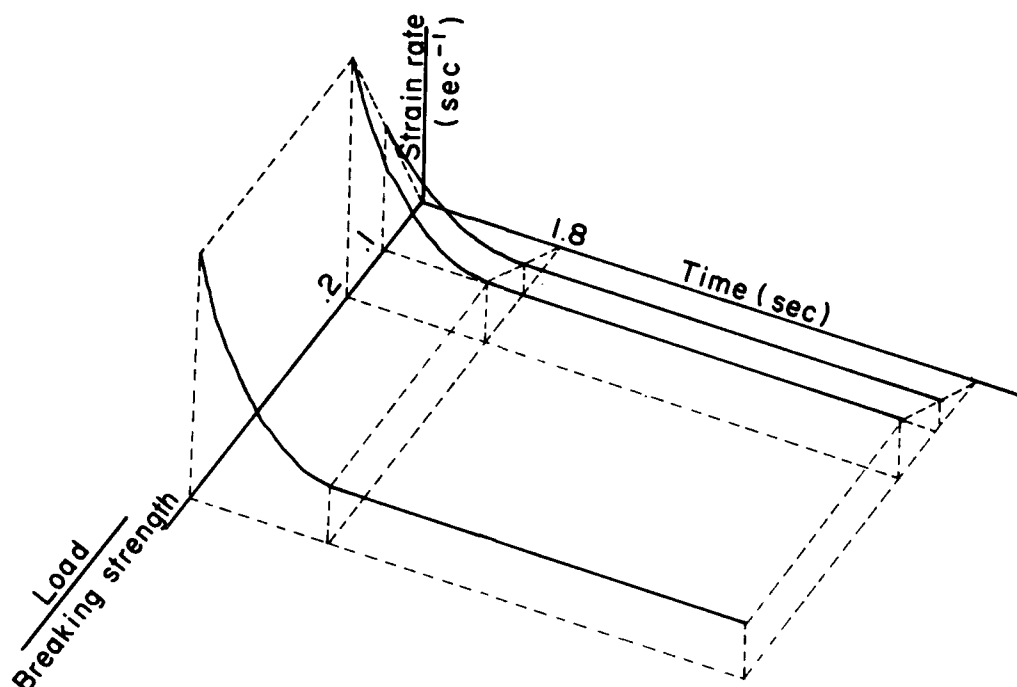


Figure 20. Creep Strain Rate Model.

series of creep strain rates can be determined which correspond to any given load-time path as shown in Figure 21. Integration along the creep strain rate path shown in Figure 21 yields instantaneous creep strain for the given loading history. This is the form in which the nylon creep model was adopted. Tabular data is used to represent the surface shown in Figures 20 and 21. Double linear interpolation and integration of the interpolated values is performed along the load-time path experienced by the material. The corresponding creep strain history is the result.

This creep model is probably more sound for secondary creep than for primary creep as a result of the test method used. The ideal creep strain test would provide for the instantaneous application of a static load and subsequent recording of strain-time data as shown in Figure 22. In practice, tensile loads were not applied instantaneously.

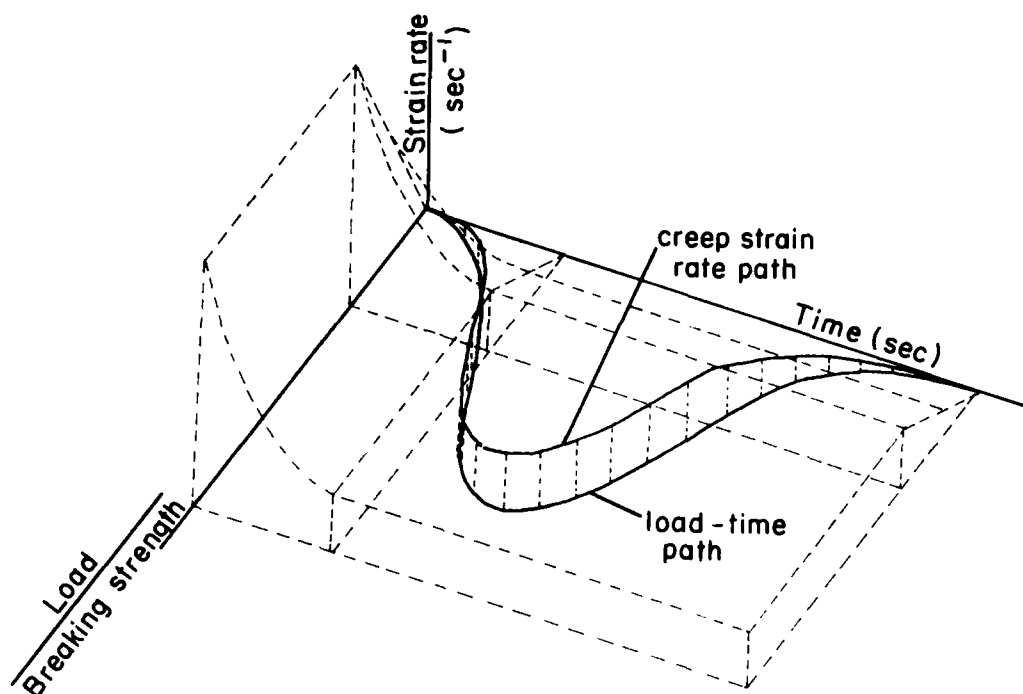


Figure 21. Creep Strain Rate History.

As a result, the early portion of the primary creep data was lost. Figure 23 illustrates that the effect of this would be to record values for primary creep strain rates which were too low. This concern was substantiated later in the analysis and will be discussed in greater detail in Section III.4. Data for secondary creep strain and strain rate remained unaffected by this technique-related problem.

### 3. Loading Characteristic

It was apparent from the data acquired that consideration of two behavioral aspects of nylon would be required in order to model the loading characteristic of the material. These were the nonlinearity of the loading characteristic and its sensitivity to strain rate. Figure 24 illustrates some dynamic and static loading characteristics from the fabric fill data. The nonlinearity is apparent and the dynamic behavior is considerably stiffer in every case. This latter fact plus the experience that had been gained in modelling

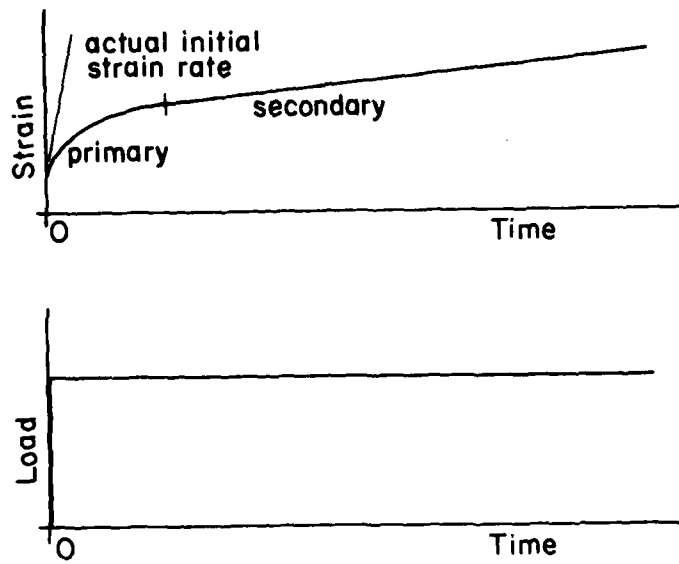


Figure 22. Ideal Creep Test.

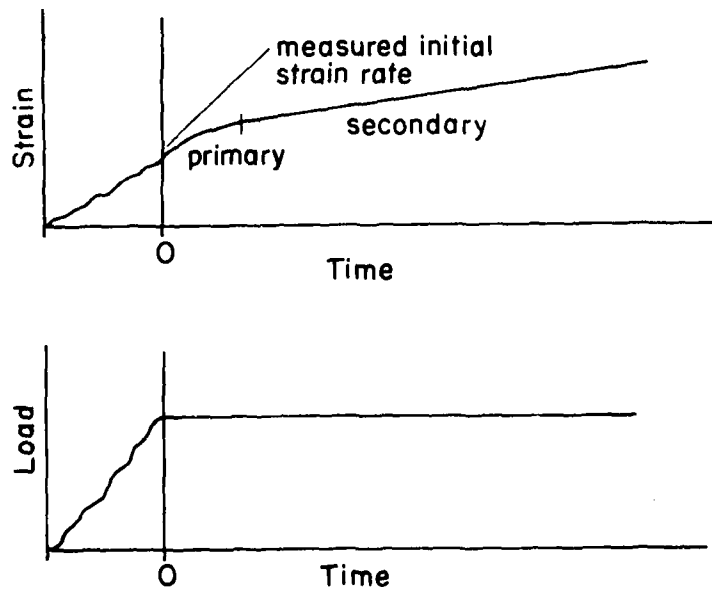


Figure 23. Actual Creep Test.

creep suggested that all or a part of the strain-rate sensitivity of nylon might simply be a manifestation of material creep. To test this hypothesis, the following steps were taken. The load-time histories for all tests (including static) of a material were input to the creep model shown in Figure 21 and described in the last section. The resulting creep strain rate history for each test was integrated to yield a corresponding creep strain history. This creep history was subtracted out from the loading characteristic for each test, making it stiffer in every case. Figure 25 illustrates this for a static test. The computed creep strain contribution for dynamic tests was much less significant than that illustrated for the static case. This result was to be expected since creep is time dependent and time under load was two orders of magnitude higher for

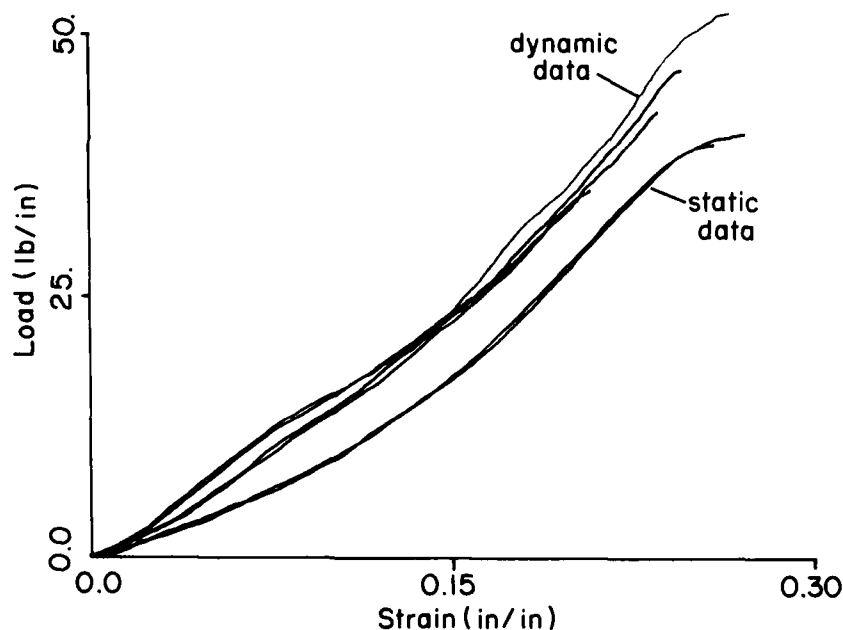


Figure 24. Fabric Fill Loading Characteristics.

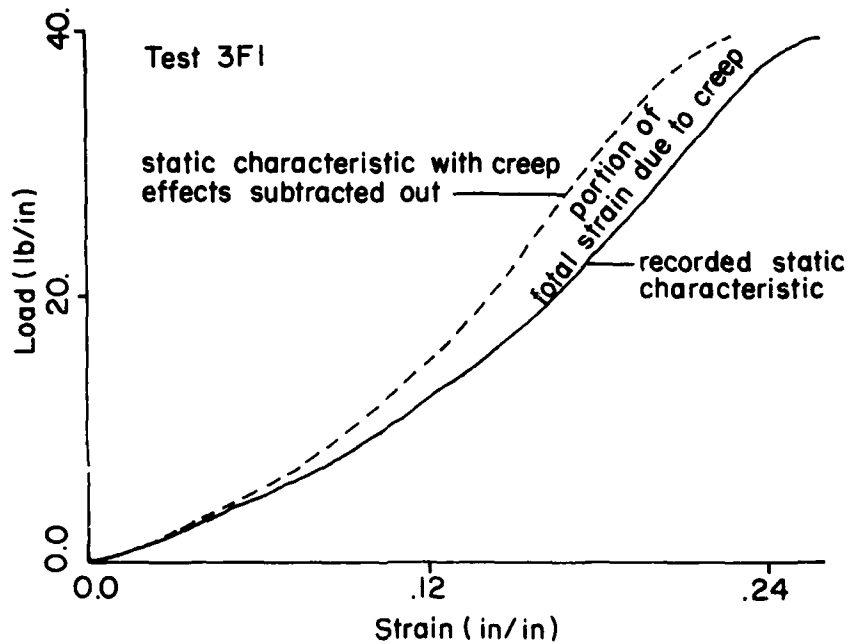


Figure 25. Creep Contribution to Total Strain.

static than for dynamic tests. The result of this exercise is shown in Figure 26. This is a plot of the same fabric fill loading characteristics shown in Figure 24 but for which the effects of creep have been subtracted out. The dispersion customarily associated with the strain rate sensitivity of nylon is no longer evident as in Figure 24. The only data lying outside the narrow band is that near material rupture from the static tests. Had the tertiary stage of creep been included in the creep model, much larger creep strains would have been computed in the vicinity of static rupture and these data points would have been moved closer to the narrow band of data.

Figure 26 implies that it is reasonable to think in terms of a strain rate independent loading characteristic for nylon. This thinking was followed in modelling loading characteristics. The data was least squares fit with a six-knot natural cubic spline which preserved the non-linearity of the data. The coupling of the previously



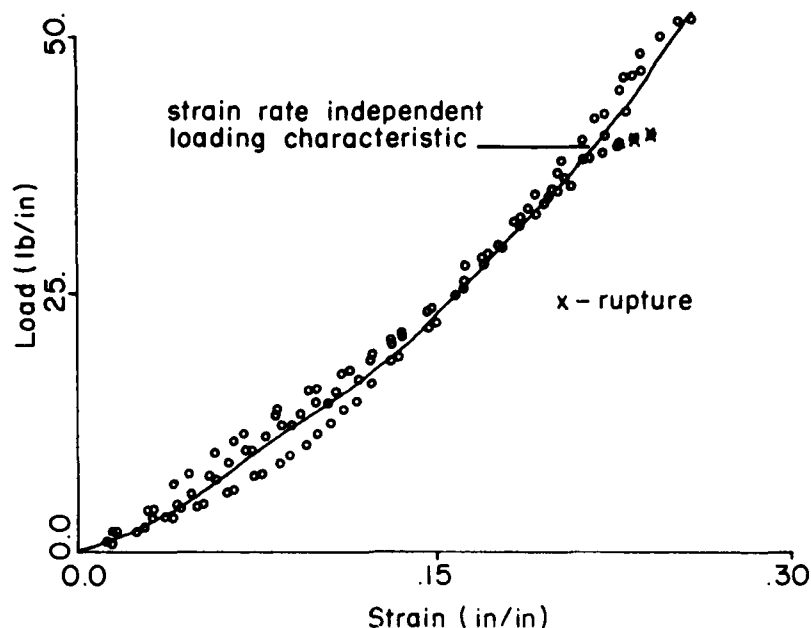


Figure 26. Loading Characteristics With Creep Effects Subtracted Out.

described creep model to this cubic spline fit then completed the definition of the loading characteristic. The spline fit provided the nonlinear strain rate independent behavior required while the creep model provided the necessary strain rate sensitivity. It should be emphasized that loading characteristics discussed thus far have been for initial loading of previously unloaded samples only. Subsequent or repeated loading behavior is treated in later sections.

#### 4. Plasticity

With the development of the creep and loading characteristic models just described it became possible to simulate accurately all of the data acquired (static and dynamic) for initial loading of material samples up to the point of maximum strain. Attention turned next to behavior beyond this point, in particular to the plastic strain resulting from this initial loading. At this point in its development, the

model predicted only a slight plastic strain at the beginning of the second loading cycle. This was a creep effect alone and is indicated as such in Figure 27. The difference between the smaller plastic strain predicted by the model with creep and the larger plastic strain observed in the data was defined as the residual strain, ELR, for modelling purposes. Dynamic tests were simulated using the current version of the model to generate plots similar to Figure 27, and values for residual strain were measured from these plots and tabulated. It was readily apparent from this that residual strain, ELR, increased with maximum strain, ELM. A plot of residual strain versus maximum strain shown in Figure 28 revealed a nearly cubic dependence so the data was fit with a cubic polynomial.

Having derived a simple expression for residual strain as a function of maximum strain, it remained to use this expression to correctly model subsequent or repeated loading characteristics for the material. It was observed that the slope of the recorded loading characteristic increased after each loading cycle and "pointed toward" a common vertex at the current maximum strain. This is illustrated in Figure 29. Other investigations, such as in Reference 17, have noted these same aspects of repeated loading behavior. This suggested that the expression derived for residual strain might be used to transform the expression for the loading characteristic. The transformation would be a linear one judging from the appearance of geometric similarity between first, second, and third loading characteristics. It would provide that the origin of the loading characteristic move from zero strain for the first loading cycle to the value of the current plastic strain for the second loading cycle and

(17) Groom, J.J., Investigation of a Simple Dynamic System with a Woven-Nylon Tape Member Displaying Nonlinear Damping, Thesis for Master of Science, Ohio State University, 1974, pp. 51-54.

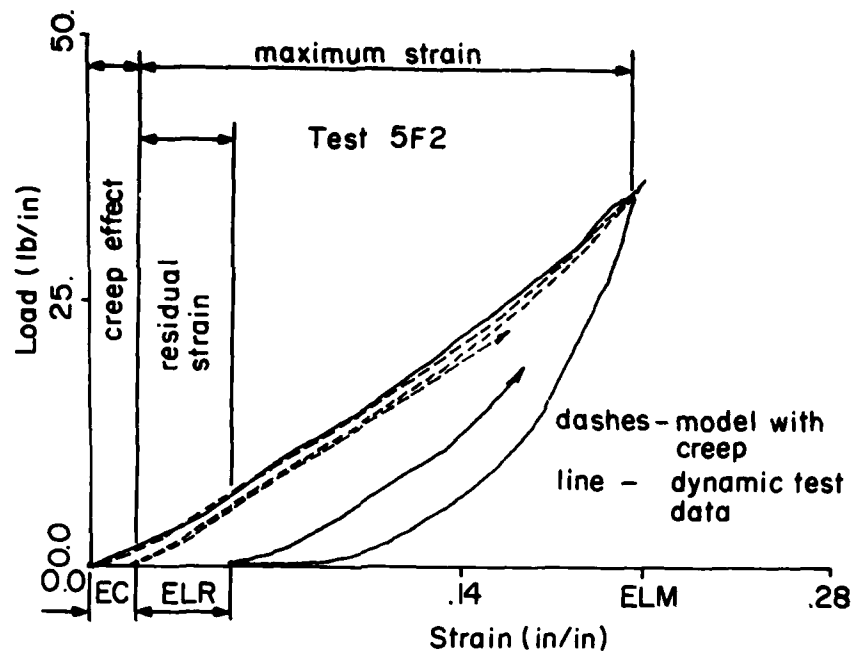


Figure 27. Model With Creep Effect.

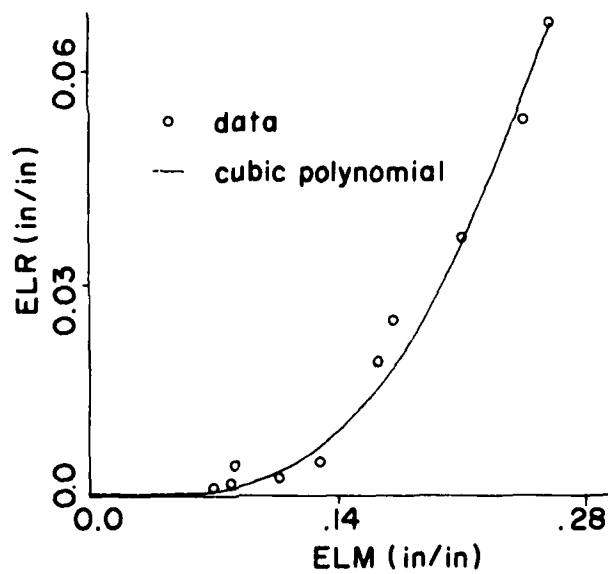


Figure 28. Residual Strain as a Function of Maximum Strain.

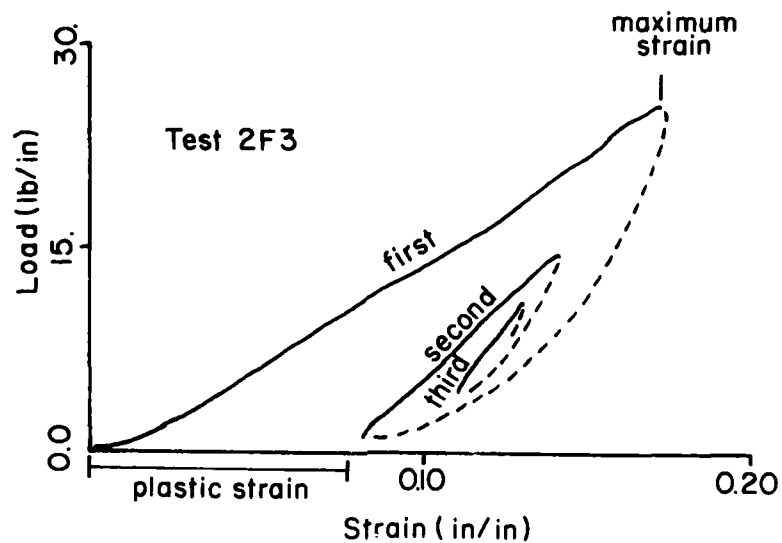


Figure 29. Repeated Loading Characteristics.

that all subsequent characteristics still pass through the point of maximum strain. The variable ELOT defined by Equation (2) was intended to meet all these requirements. Whenever material strain, ELO, is equal to the current residual strain, ELR, the value of ELOT becomes zero. When ELO is equal to the current maximum strain, ELM, the value of ELOT becomes ELM.

$$ELOT = (ELO - ELR)ELM / (ELM - ELR) \quad (2)$$

ELO - current material strain

ELR - current material residual strain

ELM - current material maximum strain

ELOT - transform of ELO, this provides for movement of the loading characteristic origin along the strain axis as a function of residual strain ELR.

After this definition of ELOT it became possible to use the cubic spline fit for the loading characteristic (Section III.3) to model both initial and repeated loading by substituting either ELO or ELOT as the independent variable as illustrated in Figure 30. The choice between the two was made by comparing instantaneous values of ELO and ELM during the loading history according to Equation (3). During initial loading, Equation (3-a) describes the loading because at any given time ELO equals ELM. During subsequent loading to

$$FT = f(ELO) \quad \text{if } ELO = ELM \quad (3-a)$$

$$FT = f(ELOT) \quad \text{if } ELO < ELM \quad (3-b)$$

FT - tensile load

ELM - current maximum strain

ELO - current strain

ELOT - transform of ELO

f - cubic spline function

strains less than the maximum strain attained during the initial loading, Equation (3-b) describes the behavior because ELO always remains less than ELM. During subsequent loading which exceeds all previous maximum strains, the behavior again reverts to Equation (3-a) since ELO equals ELM again. Figure 31 illustrates the behavior of the model at this point with creep and plasticity effects accounted for. The shift between first and second loading characteristics is due to both effects, the shift between second and third is due to the creep effect alone. All three loading characteristics are well simulated by the model. It should be noted that, as suspected (Section III.2), the level of primary creep originally modelled was too low by a factor of three or four and had to be increased to yield the level of correlation illustrated in Figure 31.

One case remained for which this version of the math model failed to model loading behavior satisfactorily. That was the case for which the tensile load never returned to

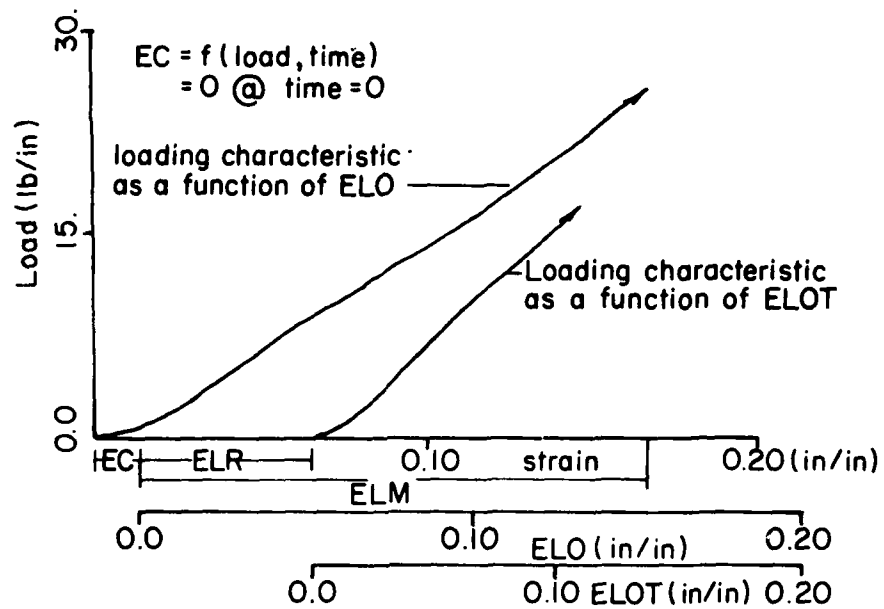


Figure 30. Initial and Subsequent Loading.

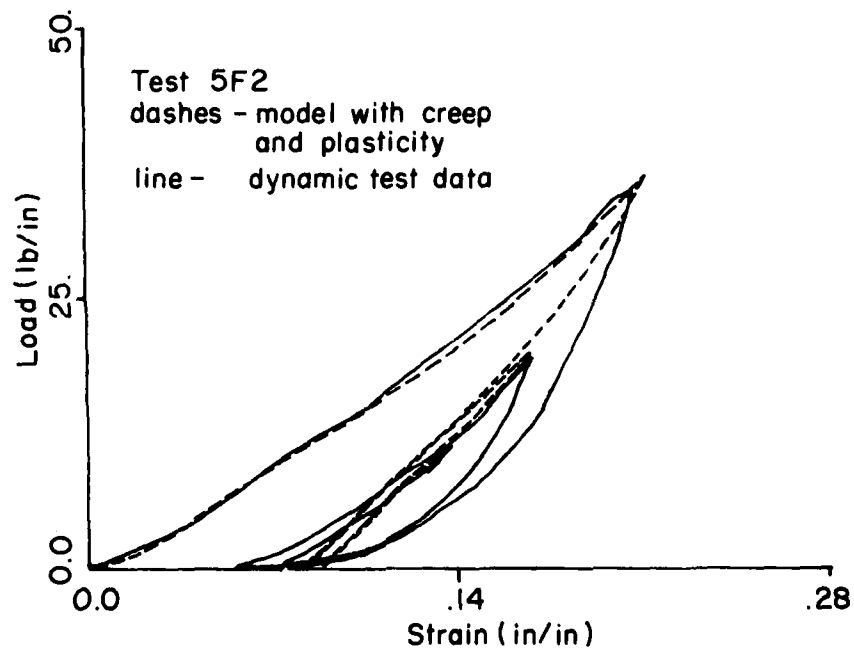


Figure 31. Model with Creep and Plasticity Effects.

zero after initial loading as shown in Figure 32. Estimation of residual strain as a function of maximum strain for such continuously loaded samples showed the same cubic dependence as that shown in Figure 28 for samples which periodically experienced zero load. But for the continuously loaded samples, the observed residual strain was always greater for the same level of maximum strain. This difference was attributed to the fact that for samples periodically seeing zero load the accumulated residual strain had time to relax while for continuously loaded sample no relaxation could occur (Section I.1). This behavior was modelled by using two curve fits like the one shown in Figure 28, one serving as an upper bound and one as a lower bound to residual strain.

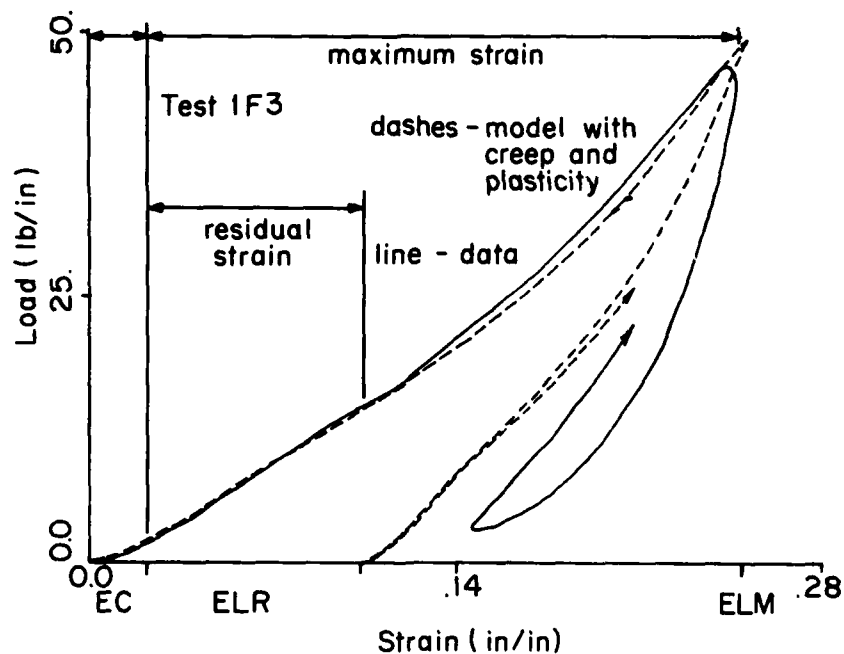


Figure 32. Continuous Loading Characteristics.

Accumulative time under zero load was tracked and used to interpolate linearly between the two. An example is illustrated in Figure 33. Immediately upon unloading from a maximum strain of 0.10 in/in the material exhibits the large

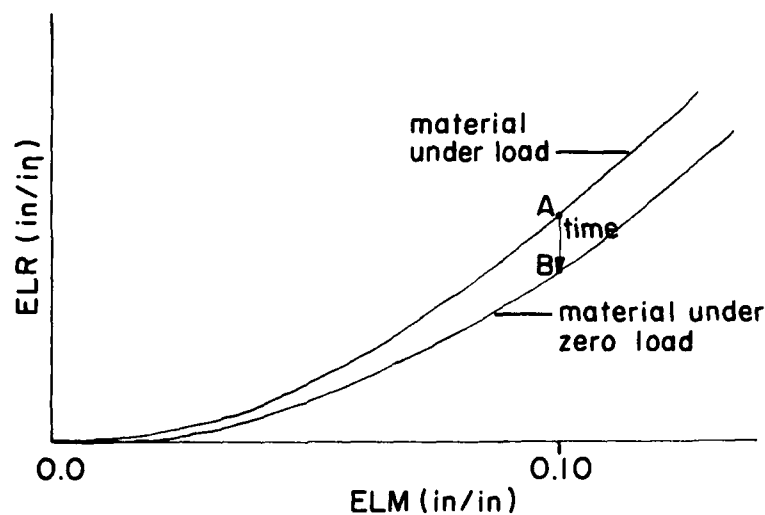


Figure 33. Residual Strain for Material under Load and under Zero Load.

plastic strain A. With the passage of time under zero load, the plastic strain relaxes or grows less following the path indicated from A to B. After sufficient time passes, the plastic strain ceases to relax further, permanently assuming the value represented by B. Data for both curves shown in Figure 33 and for related relaxation times were extracted from the test data, then this refinement was added to the plasticity portion of the model. At this point, all static and dynamic, initial and repeated loading characteristics could be simulated satisfactorily by the model. The only feature missing was realistic unloading behavior; the strong hysteresis observed in the data had not yet been accounted for. The development of this feature of the model is discussed in the following section.



## 5. Hysteresis

The first observation made regarding unloading behavior was the apparent geometric similarity among all unloading characteristics. This similarity has been noted by other authors, for example Reference 17, and led to the following approach to modelling unloading.

To provide a common denominator by which to describe unloading a normalized strain parameter, ELS, was defined having the form of Equation (4).

$$ELS = (ELM - ELO)/(ELM - ELR) \quad (4)$$

ELM - current maximum strain

ELO - current strain

ELR - current residual strain

ELS - normalized strain

When material strain is maximum, i.e., when ELO equals ELM, the value of ELS is zero. When the material has unloaded to its current plastic strain, i.e., when ELO equals ELR, ELS assumes the value of 1. Figure 34 shows that every unloading action then, no matter from what maximum strain or to what plastic strain, involves the variable ELS assuming values over the range of 0 to 1. To further specify unloading, the variable FD, as illustrated in Figure 34 was defined to be the difference between that load predicted by the current version of the model and that load observed in the data at a given strain during material unloading. Plots similar to Figure 34 were generated for all data on hand with the model results being linearly scaled such that computed and experimental peak load and strain would coincide exactly. From these plots tables of FD as a function of ELS were developed in an attempt to quantify unloading behavior. Plots of FD versus ELS for various tests are shown in Figure 35. The shape of the plots showed general similarity

(17) Groom, J.J., Investigation of a Simple Dynamic System with a Woven-Nylon Tape Member Displaying Nonlinear Damping, Thesis for Master of Science, Ohio State University, 1974.

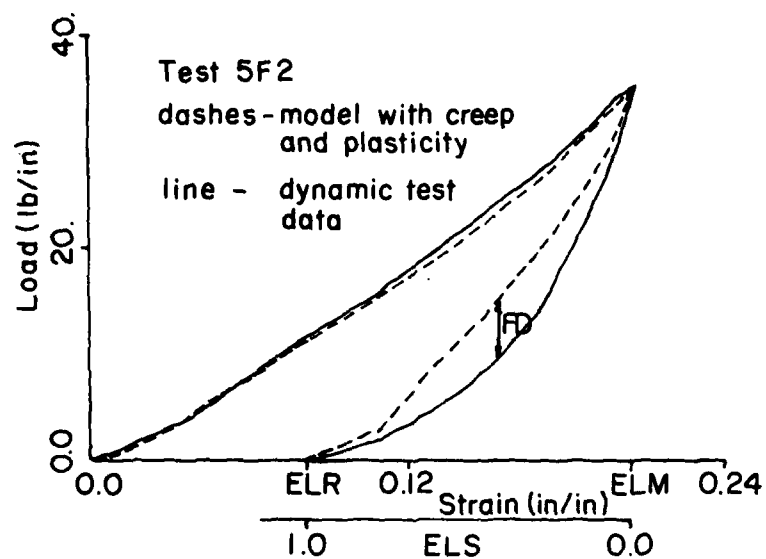


Figure 34. Representation of Unloading Characteristics.

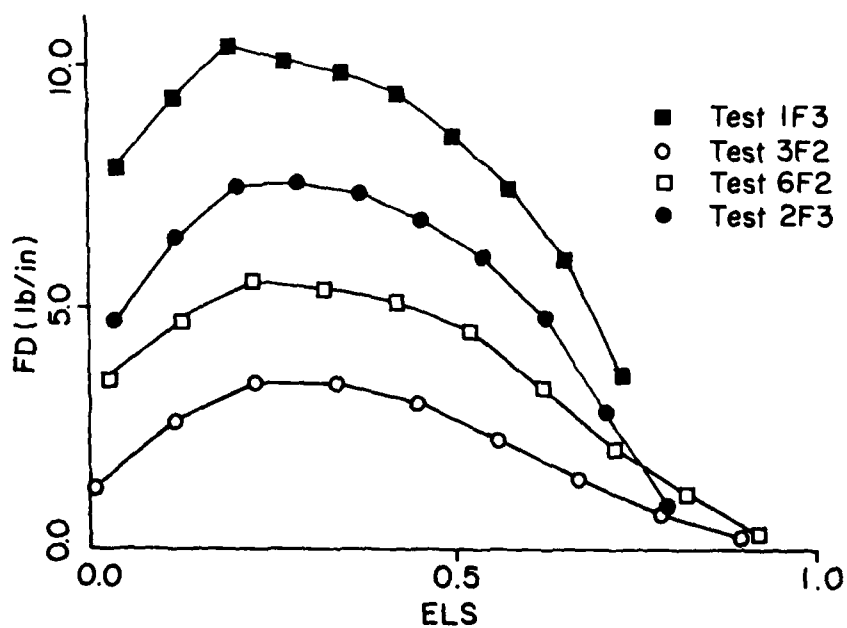


Figure 35. FD versus ELS Data.

for all tests but the magnitudes varied over a very wide range. It was observed, however, that the magnitudes varied directly with the maximum strain experienced by the material during the test. To determine the form of this dependence, the following steps were taken. One of the FD versus ELS curves for the material was selected arbitrarily and integrated in order to determine the area beneath the curve. All other FD versus ELS curves for the same material were multiplied by a ratio with a value such that the area under each became equal to the arbitrarily chosen reference area. The resulting group of data points was fit with a cubic spline as shown in Figure 36. This fit was forced to pass through zero at ELS = 0.0 and ELS = 1.0. The ratios required to equate areas in this manner were found to be a simple function of maximum strain as shown in Figure 37 and were least squares fit with a cubic polynomial.

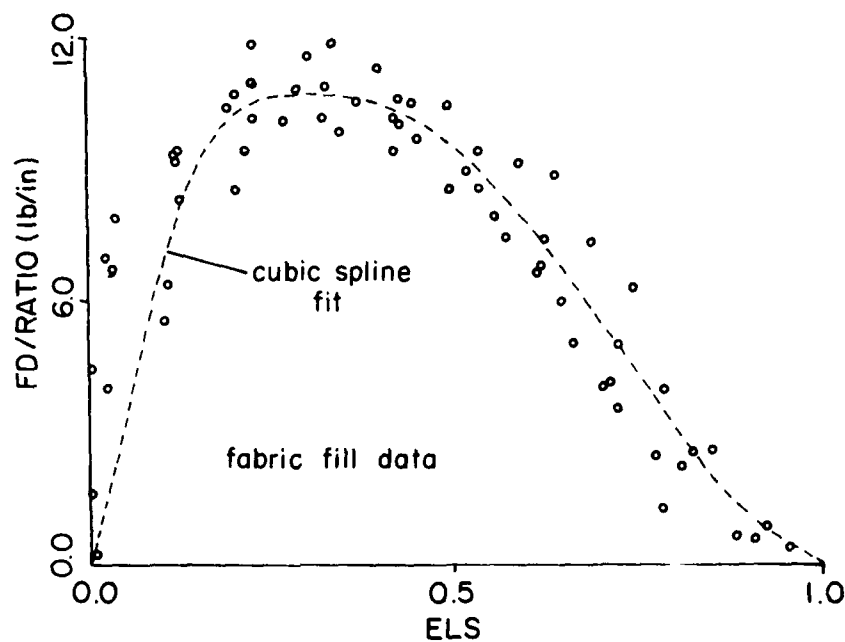


Figure 36. Ratioed FD versus ELS Data.

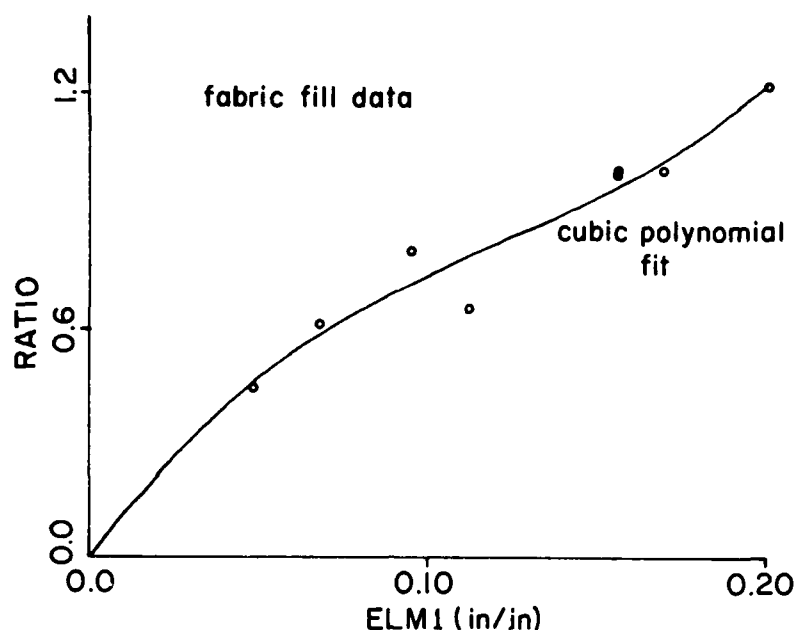


Figure 37. FD Ratios as a Function of ELMI.

The analysis just described provided a simple and general definition of unloading. The form of the expression is shown in Equation (5). It implies that three pieces of information are required in order to calculate FD: The value of  $\frac{FD}{RATIO}$  which is a function of normalized strain

$$FD = \frac{FD}{RATIO} RATIO \frac{(ELMI - ELR)}{(ELM - ELR)} \text{ when } EDOT \leq 0 \quad (5)$$

$$= 0 \text{ when } EDOT > 0$$

$\frac{FD}{RATIO}$  - six knot least squares fit cubic spline (Figure 36)

RATIO - least squares fit cubic polynomial (Figure 37)

(ELS), the value of RATIO which is a function of maximum strain (ELMI), and the value of ELM (and ELR which is a function of ELM per Figure 28). The value of  $\frac{FD}{RATIO}$  is determined

from the curve fit illustrated in Figure 36, and the value of  $RATIO$  is determined from the curve fit illustrated in Figure 37.  $ELS$ ,  $ELM1$ ,  $ELM$  and  $ELR$  are continuously calculated by the material model. Equation (5) also implies that the value of  $FD$  is zero whenever material strain rate is positive. When the material is loading, no  $FD$  contribution is felt by the model. But, whenever the material is unloading, a positive value of  $FD$  is calculated and subtracted from the current load.

The approach just outlined served very well to model all drop weight test data which periodically experienced zero load. This is illustrated in Figure 38. It should be noted that the third term in Equation (5) was added to properly scale  $FD$  for subsequent or repeated loading cycles. In this way, for example,  $FD$  loads for the third loading cycle shown in Figure 38 are scaled for the maximum strain experienced during that loading cycle instead of for the overall

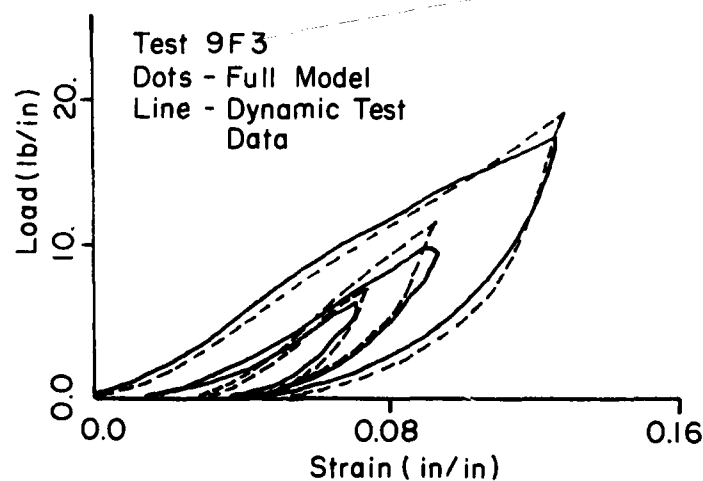


Figure 38. Model with Creep, Plasticity, and Hysteresis Effects.

maximum strain which had occurred earlier in the first loading cycle.

This description of material unloading failed for one class of drop weight tests, however, that being those tests during which the material sample was continuously loaded; i.e., those tests for which the drop weight sled did not bounce. Figure 39 shows that since unloading was modelled by subtracting an appropriate load component only when the material strain rate was negative, a force discontinuity was generated by the model whenever the strain rate changed from negative to positive at nonzero values of tensile load. This undesirable feature of the model was overcome by arbitrarily adding a strain rate term to the overall expression for FD. This term is only active when negative strain rates are decreasing, i.e., when material strain rates are negative and acceleration of sample end points is positive. The rate term is a ratio of current negative strain rate to maximum

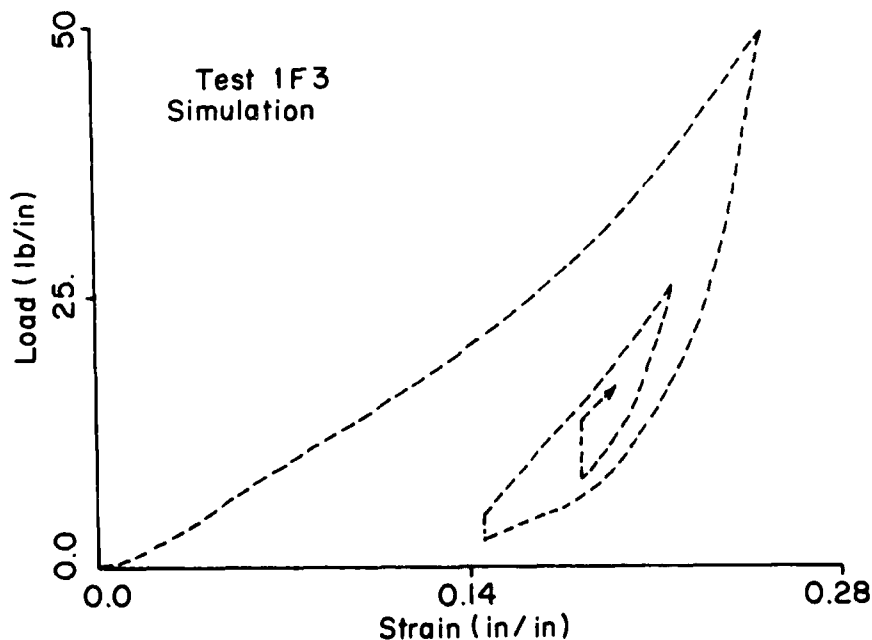


Figure 39. Model Unloading Discontinuity.

negative strain rate during the current unloading cycle. It is used to drive FD to zero as the current material negative strain rate approaches zero as shown in Figure 40. Load histories resulting from this approach still had discontinuous first and second derivatives with time.

At this point in its development, the model included all the major features of material behavior outlined in Section I.1. It provided the strong nonlinearity characteristic of nylon, the sensitivity to strain rate, significant hysteresis, large plastic strains, and creep effects. The model had not been used to simulate load-time or strain-time behavior of the material, however, When force-time correlation was first studied, room for improvement became apparent. The next section deals with this final stage of model development.

#### 6. Damping

As discussed in Section I.1, the area included within a load-strain diagram for one loading/unloading cycle of the

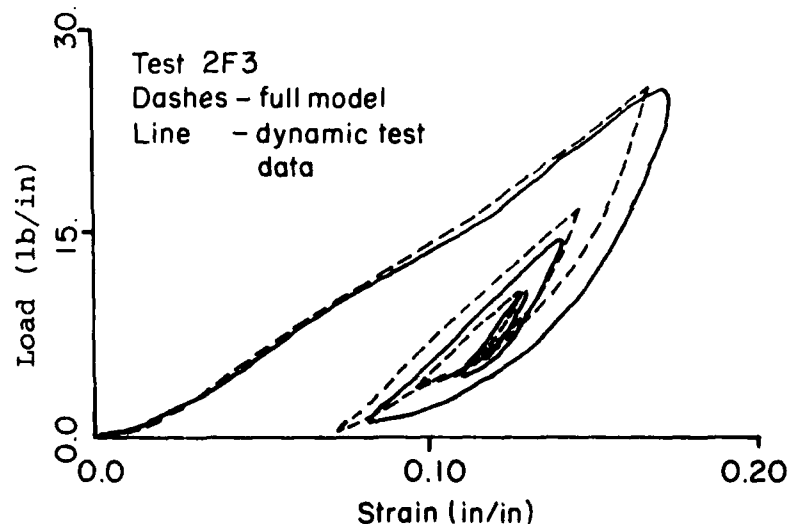


Figure 40. Model with Continuous Loading Term.

material represents the kinetic energy dissipated during that cycle. The magnitude of this energy dissipation determines among other things the resulting unforced period of motion or free damped natural frequency for simple mass-material systems. In view of this, the following approach was taken to optimize load-time correlation. A multiplicative constant VSFD was added to the expression for FD already described in Equation (5). For each data set a value of VSFD was determined which resulted in the best load-time correlation. It became apparent from doing this that greater values of VSFD were required for those tests performed at higher strain rates. A graph of VSFD versus strain rate as shown in Figure 41 revealed a linear dependence, the first and only evidence of linear viscous damping encountered during data analysis.

A linear fit was made to the VSFD data and was added as an additional term to the steadily growing expression for FD as shown by Equation (6).

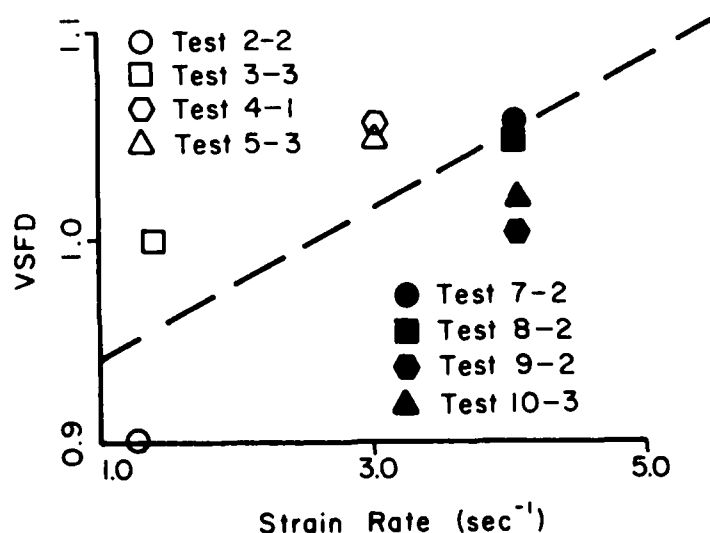


Figure 41. VSFD versus Strain Rate.



$$FD = \frac{FD}{RATIO} RATIO \frac{(ELM1 - ELR)}{(ELM - ELR)} VSFD \text{ when } EDOT \leq 0 \quad (6)$$

= 0 when  $EDOT > 0$

$\frac{FD}{RATIO}$  - see Equation (5)

RATIO - see Equation (5)

VSFD - linear viscous damping term

The first and second terms have already been discussed in Equation (5). The third term is that discussed in Section III.5 to scale FD for repeated loading cycles, and the fourth term is the linear viscous damping term just described.

This final expression for FD improved the load-time or phase correlation obtained to a satisfactory level as shown in Figure 42. Development of math models for the dynamic loading of nylon parachute materials was not carried beyond this point.

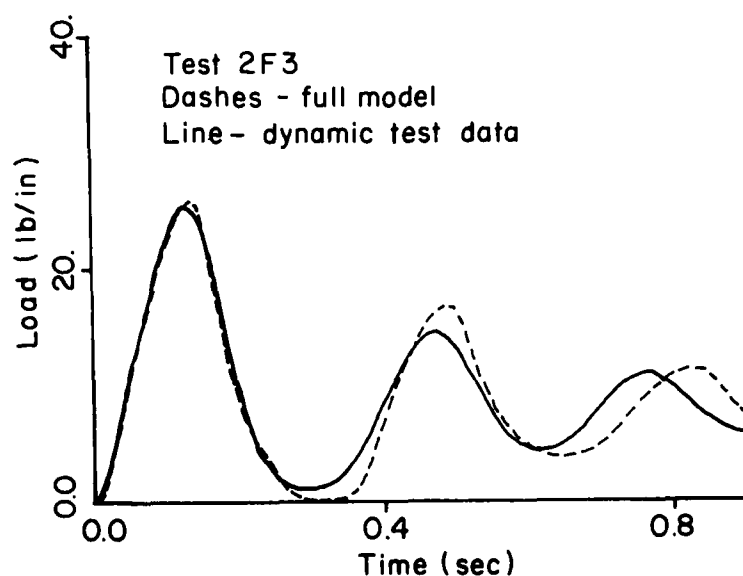


Figure 42. Typical Model-Data Phase Correlation.

## SECTION IV

### COMPUTER SUBROUTINES

#### 1. Data Processing

As already discussed in Section I.2, one of the goals of this work effort was to develop the capability through automatic data processing computer programs to generate additional models for a variety of parachute materials as the needs arose. To this end, and after obtaining satisfactory results with the manual development of one model as a test case, as documented in Reference 11, several plotting and data processing computer programs were written. Each of these was intended to automate as much as possible one of the data manipulation and fitting processes discussed in Section III. The flow chart in Figure 43 illustrates the following discussion. Each box in the figure represents a data processing computer program. The section in this report which discusses the analysis performed by each program is included in parenthesis in the same box. The following is a brief description of each program in the order in which they are executed during data processing:

1. Program OKDATA reads raw load, displacement, and time data acquired from drop weight testing. Reduction errors are also read and are used to correct the data accordingly. Corrected force-time data is pointwise fit with a cubic spline and integrated twice to calculate corresponding displacement-time data. Experimental and calculated displacement-time data are overplotted for visual correlation as shown in Figure 15. Subsequent runs of OKDATA are used to determine values for displacement and load data calibration errors following Figure 16 and 17 and to correct the data accordingly for these.

(11) McCarty, R.E., A Computer Subroutine for the Load-Elongation Characteristics of Parachute Suspension Lines, AIAA paper 75-1362, 1975.

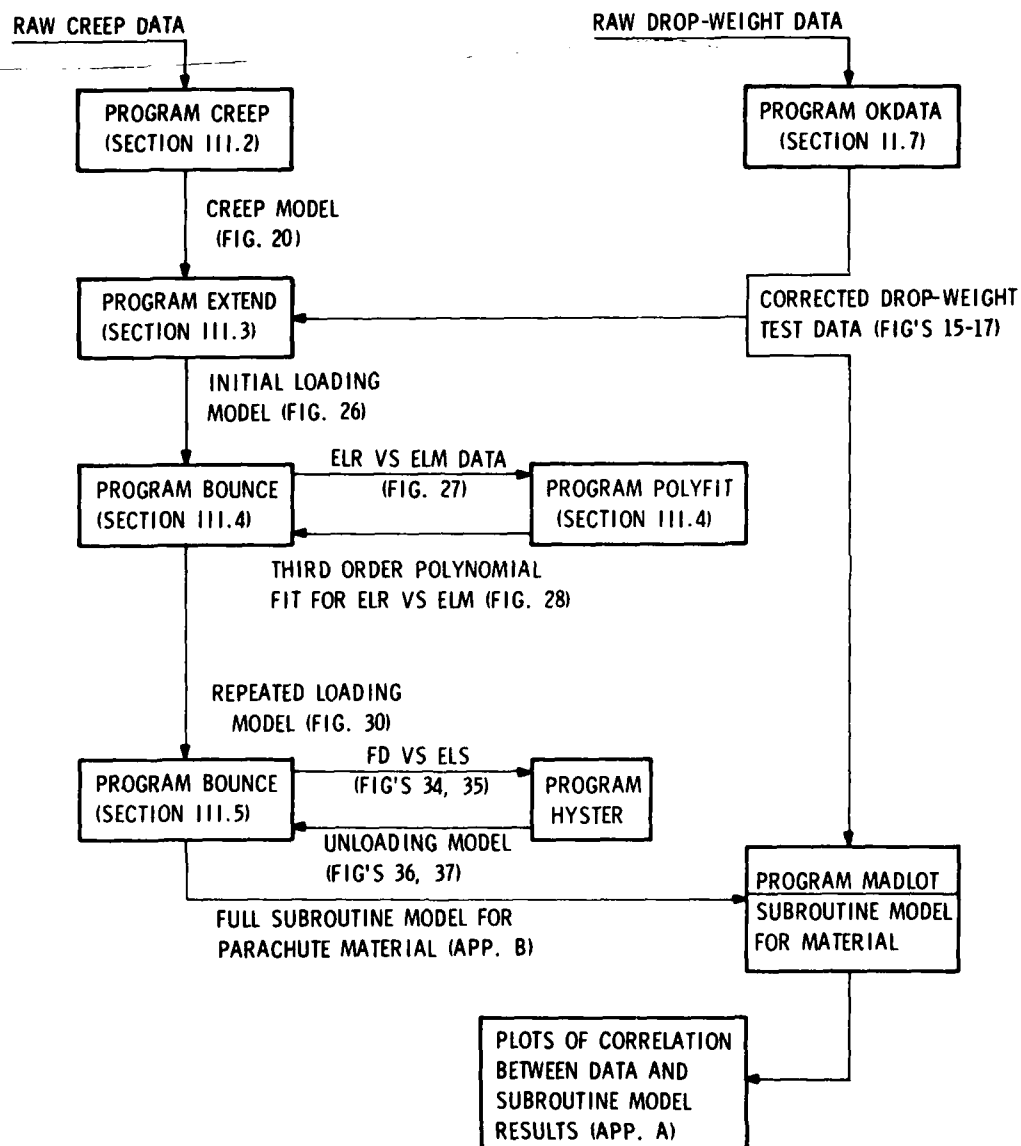


Figure 43. Data Processing Flow Diagram.

2. Program CREEP is designed to smooth and differentiate creep strain data (strain versus time). Tabular data is generated for a surface such as that illustrated in Figure 20 as a function of load and time.

3. Program EXTEND requires two types of input, the first being the creep strain rate table generated by program CREEP and the second being corrected load, strain, and time data generated by program OKDATA. Data for all initial loading characteristics are isolated. Creep effects are calculated for each loading history and subtracted out from the corresponding loading characteristic. Finally, all altered loading characteristics are overplotted and least squares fit with a cubic spline as illustrated in Figure 26. The two arrays and one matrix required to define the spline fit are printed out.

4. Program BOUNCE is a Control Data Corporation 777 Interactive Graphics System program, per Reference 18, which allows the interactive determination of residual strain from plots similar to Figure 27. Tabular data for residual strain as a function of maximum strain is output for all data sets processed.

5. Program POLYFIT reads residual strain tabular data generated by program BOUNCE and fits it with a third order polynomial constrained to pass through the origin as shown in Figure 28.

6. Program BOUNCE also serves to generate plots similar to Figure 34. Tabular data for FD as a function of the normalized strain parameter, ELS, are generated.

7. Program HYSTER reads the FD versus ELS tabular data generated by program BOUNCE. It performs the analysis discussed in Section III.5 required to generate plots like Figures 36 and 37. Coefficient arrays for the FD cubic spline fit and the RATIO polynomial fit are printed.

(18) 777 Interactive Graphics System, Version 2.1, Reference Manual, Control Data Corporation publication number 17321800, Revision B, 30 October 1975.

8. Program MADLOT (Mathematical Analog for the Dynamic Loading of Textiles) incorporates the finished material model as a subroutine. It simulates the dynamics of the drop weight test apparatus used for this work and overplots computed and experimental results. Either static or dynamic data may be simulated. All plots in Appendix A were generated using program MADLOT in conjunction with the appropriate material subroutine.

## 2. Subroutine Models

The three subroutine models developed with the aid of the seven data processing programs described in Section IV.1 are listed in Appendix B. The first is a model for 400 lb strength nylon parachute cord, the second for 1.1 oz nylon rip stop parachute fabric warp, and the third for 1.1 oz nylon rip stop parachute fabric fill. Data in them which was derived directly from execution of the seven data processing programs is labeled as such at the beginning of each subroutine model. Two external functions and one interpolation routine required by the subroutine models are listed at the end of Appendix B. The subroutine models are written in FORTRAN Extended Version 4, per Reference 19. All variable names used in the subroutine models are defined in the list of symbols at the beginning of this report.

The parameters involved in calling the subroutine models from other FORTRAN programs or subroutines are T, Y, and P as indicated in the listings. T is a scalar quantity which represents current time in seconds. Y is a vector quantity of dimension three. Y(1) is the component of relative velocity in ft/sec of the two end points of a tensile member taken in the direction parallel the member. A positive value implies that the ends are moving away from each other. Y(2) is the

(19) FORTRAN Extended, Version 4, Reference Manual, Control Data Corporation publication number 60305600, Revision J, 5 March 1976.

current tensile member length in ft.  $Y(3)$  is the current creep strain in the tensile member measured in in/in. The vector  $Y$  carries input data to the subroutine models.  $P$  is also a vector quantity of dimension three. It carries output data from the subroutine models to an integration routine (a fourth order Runge Kutta routine is used in MADLOT).  $P(1)$  is the component of relative acceleration in  $\text{ft/sec}^2$  of the two end points of a tensile member taken in the direction parallel to the member. It serves as the integrand in computing a new value of  $Y(1)$ .  $P(2)$  is the same as  $Y(1)$ . It serves as the integrand in computing a new value of  $Y(2)$ .  $P(3)$  is the current material creep strain rate measured in  $\text{sec}^{-1}$ . It serves as the integrand in computing a new value of  $Y(3)$ .

The two variables of primary interest in applications of the subroutine models are  $EL$  and  $FTR$ .  $EL$  represents current strain in in/in of the tensile member based on the original unstressed length.  $FTR$  represents the current tensile load in lb for cords (tapes, webs) and in lb/in for fabrics. Values for both variables are carried from the subroutine models through the labeled common block named INFO.

Since the subroutine models were used to simulate only single degree of freedom systems for the purposes of this report, the dimensions of all load and strain variables is one. To apply these subroutine models to systems involving many tensile structural elements will require modification. For example, for a system of  $N$  tensile elements the arrays  $Y$  and  $P$  might be dimensioned  $Y(N,3)$  and  $P(N,3)$  and do-loops added accordingly.

The following values should be preset prior to calling the subroutine models for the first time from a main program:

$KRL = 1.0$	$ELM1 = 0.0$
$KCR = 1.0$	$EC = 0.0$
$KDP = 1.0$	$TF = 0.0$
$RMAXD2 = 1.E-6$	$TS = 0.0$
$ELM = 0.0$	$DELOMAX = 0.0$

They are carried to the subroutine model through the labeled common block named INFO.

It is the intent of this report to publish the subroutine models in a rough format, leaving additional modifications of a more general nature to be accomplished through a variety of future applications.

All data included in the subroutine models follows the British Engineering system of units. Time is measured in seconds, load in pounds force, and mass in slugs.

It should be noted that material rupture is not modelled in any manner by the subroutine models. Instead, print flags are set for the two variables ELO and EL0T, the current strain and the transformed strain. Valid ranges for these variables are defined for each subroutine model. When the valid ranges are exceeded a printed message results. After printed messages occur, the models continue to function, but with potentially meaningless results. For some applications, it may be desirable to modify the subroutine models such that the tensile load is set to zero above a critical strain in an attempt to simulate rupture.

## SECTION V

### RESULTS

Appendix A contains plots to illustrate the correlation obtained between subroutine models and all static and dynamic experimental data acquired. Plots are grouped by material type in the order of cord, warp, and fill. The materials are more specifically identified in Section I.3. Within each grouping dynamic data is presented first, then static. For each test a load-strain plot is presented first, then a load-time plot. Material rupture occurred on all static tests and on the higher energy dynamic tests. Test number and material strain rate are printed on each plot. For dynamic tests, the material strain rate indicated is the initial strain rate occurring at time zero. More specific parameters for each test are listed in Table 2.

Review of Appendix A reveals that the shape of simulated initial loading characteristics is quite good for the dynamic case in general, but somewhat worse for the static case. This is believed to be primarily due to coarseness in the creep model, the effects of which become significant only for the static case. Peak loads and strains calculated for dynamic tests vary less than 5 percent from the data in most cases, never more than 10 percent.

The shapes of the initial unloading characteristics are also accurate although the level or magnitude of the hysteresis is occasionally low or high as for tests 2F3 and 8F1 respectively. The effect of this error is reflected in the load-time plots for the same tests. Too little damping occurs during first cycle simulation for test 2F3 while too much occurs for test 8F1.

Load-strain correlation for second and third loading cycles varies from quite accurate to only moderately so. Test 8F1 results offer a worst case example. The primary shortcoming of the models seem to be the inability to predict correct slopes for second and third loading cycles. Slopes are satisfactory for tests which involve continuous loading



such as 1F3 and 2F3, but not so for tests during which the loads periodically return to zero such as 8F1. The simple rules adopted to model repeated loading characteristics (Section III.4) apparently do not provide the capability to model all loading characteristics very accurately.

A second unsatisfactory feature related to repeated loading is apparent from the warp test plots in particular. This is the fact that in addition to the slopes of second and third loading characteristics being awry, the predicted shape also is unrealistic. This is due to the fact that warp samples exhibited a characteristic 'hump' in the initial loading characteristic. Previously loaded warp samples failed to redisplay this hump. In dynamic warp test cases, the first loading characteristic always showed the hump while second and third ones did not. The subroutine models, however, represent repeated loading and unloading characteristics by linearly transforming the initial loading characteristics as discussed in Section III. This approach preserves the humped shape of initial loading and reproduces it in all subsequent loading characteristics. Again, it would appear that the approach taken to model subsequent loading characteristics by applying linear transformations to the initial characteristic (Section III.4) may be overly simplistic.

The slight shift to higher strain between second and third loading characteristics is modelled very accurately in every case. This is an effect of material creep alone and reflects the accuracy with which primary creep has been modelled.

The level of damping predicted by the models is very realistic. The envelope of peak loads on load-time plots calculated by the models agrees closely with that seen in the data in every case.

In the case of dynamic loading, the material models do very well in predicting the shape of the loading characteristic at or near material rupture. Tests 3F4 and 3W7 provide examples of this respectively.

For static rupture, however, the model performance is poorer as can be seen for test STAT3OF. This is due to the fact that tertiary creep effects become significant near static rupture and that the tertiary stage of creep has not been included in any of the subroutine models (Section III.2 and III.3). In contrast, for dynamic rupture the times to material failures are so short that creep plays virtually no part at all in the simulation.

## SECTION VI

### CONCLUSIONS

An empirical approach to modelling the dynamic tensile behavior of nylon parachute materials is warranted. The capability of subroutine models of nylon material to simulate free oscillation data over very broad ranges of strain rate (nearly three decades) and tensile load has been demonstrated. This capability is unique and will contribute significantly to the improvement of parachute recovery system dynamic analyses.

The strain rate sensitivity so characteristic of nylon materials may be modelled accurately by coupling a strain rate independent loading characteristic for the material with a classical creep model as discussed in Section III.3.

Repeated loading characteristics may be modelled simply with moderate accuracy by means of a linear transformation of the initial loading characteristic. This transform is a function of residual strain and maximum strain as discussed in Section III.4.

Material unloading characteristics, or hysteresis, may be modelled by means of a generalized representation which is a function of a normalized strain parameter. The magnitude of the loads provided by this general rule is a function of both maximum strain and strain rate as discussed in Section III.5.

The capability exists to generate additional similar subroutine models for other parachute materials in short times (one week of data processing) and from limited data bases (digitized load and strain histories from ten drop weight tests).

## SECTION VII

### RECOMMENDATIONS

The subroutine models developed should be used in a variety of parachute applications involving forced vibration in an attempt to validate them for forced vibration problems in general. The areas of stress, opening dynamics, and stability analysis all promise such potential applications.

The subroutine models developed should be used to roughly model other similar materials. This could be done when maximum accuracy is not required simply by scaling minimum breaking strengths and strains. Experience in this area may show that all materials covered by one Military Specification can be represented by a single subroutine model which has been normalized for minimum breaking strength and strain. For example, one model might suffice to describe all the core-sleeve nylon cords defined by MIL-C-5040E because of their strong similarity in geometry of construction.

Since the mechanical properties of nylon materials can vary significantly from one lot to the next, specific subroutine models should be developed for particular applications. The time and data required to generate models are sufficiently small to allow this approach. As an example, during the development of a new spacecraft parachute recovery system, a small number of samples could be taken from the same material lots used to fabricate the parachute systems. Subroutine models could be developed quickly from tests of the material samples. This would allow accurate simulation of system dynamics prior to full-scale development.

Consideration should be given to the generation of libraries of subroutine models for many different parachute components and materials. The benefits would be considerable for the general purposes of parachute recovery system design and analysis.

Consideration should be given to development of sub-routine models from free vibration load-time data alone. Corresponding strain-time data could be generated by integration of the load-time data. This method would simplify the design of the drop-weight test apparatus to be used and reduce data acquisition requirements to the minimum.

Improvements to the math modelling approach outlined in this report should include the following.

1. A refined creep model developed along the same lines but from a larger data base to include the tertiary stage of creep and more load levels. This would serve primarily to improve low strain rate correlation.

2. The development and inclusion of material failure criteria in the subroutine models. This may evolve directly from development of an improved creep model.

3. The inclusion of temperature effects since these can become even more significant than strain rate effects according to Reference 20.

4. The development and inclusion of a relaxation model following the form of the creep model already developed. This would provide more realistic prediction of instantaneous plastic strain than the simplistic method described in Section III.4.

(20) Swallow, J.E., and Webb, Mrs. M.W., "Single and Repeated Snatch Loading of Textile Yarns, and the Influence of Temperature on the Dynamic Mechanical Properties", Journal of Applied Polymer Science, Vol. 8, pp. 257-282, 1964.

## APPENDIX A

### MODEL/DATA CORRELATION

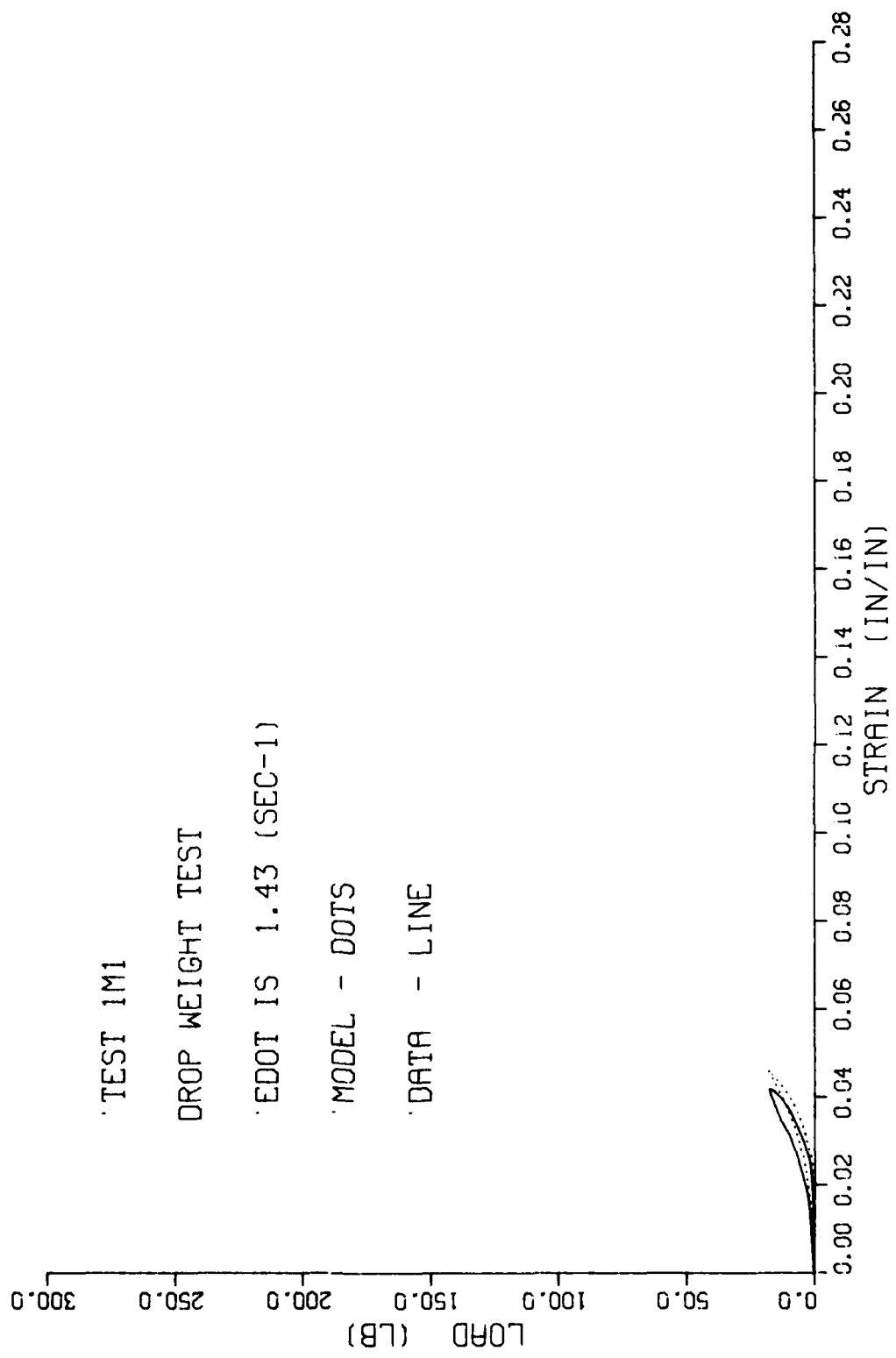
# APPENDIX A INDEX

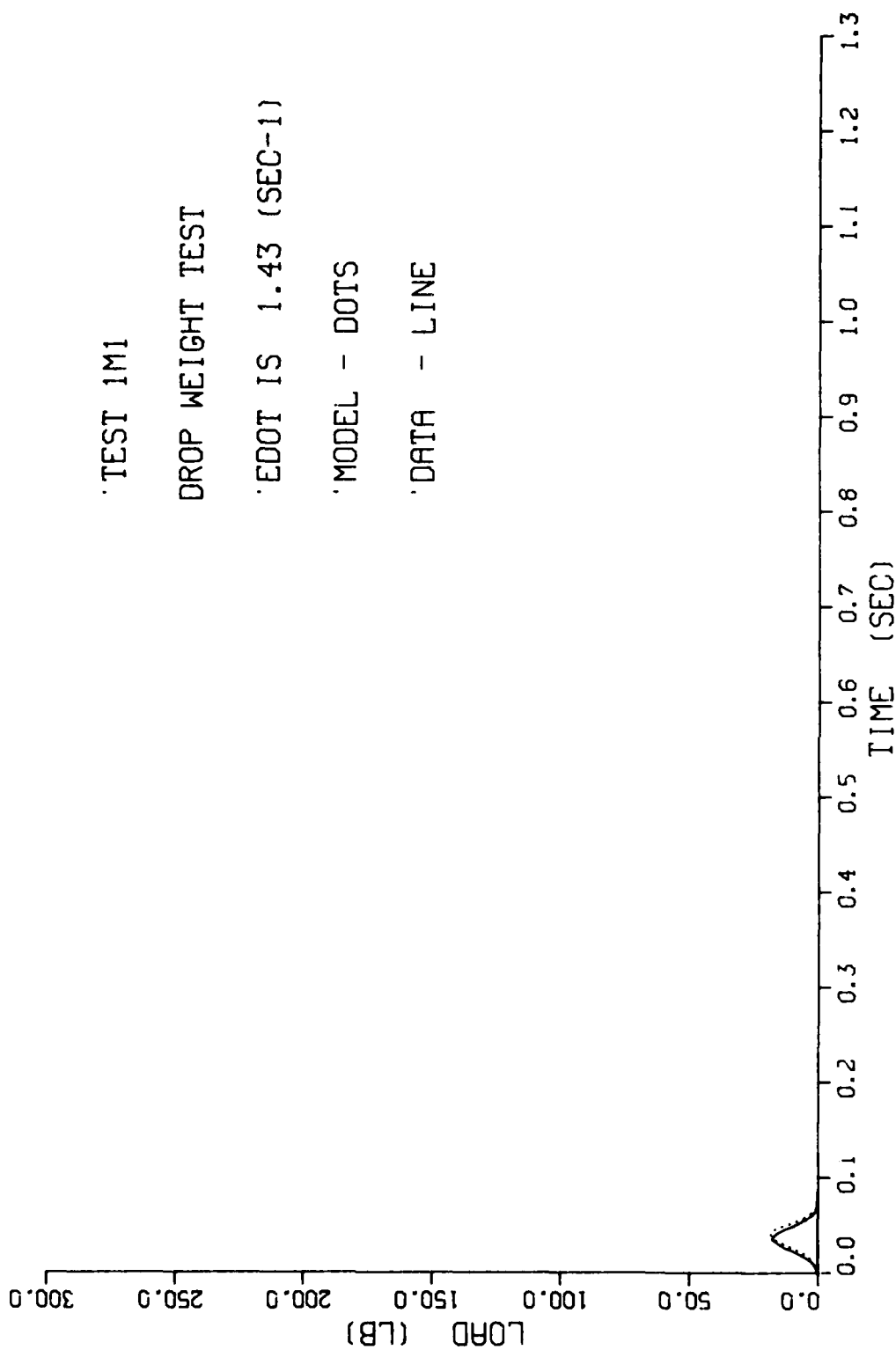
TEST	PAGE
1M1	68
2-2	70
3-3	72
4-1	74
5-3	76
6-1	78
7-2	80
8-2	82
9-2	84
10-3	86
11-1	88
2-C	90
3-C	92
1W1	94
2W1	96
3W1	98
1W4	100
1W5	102
6W3	104
3W7	106
8W2	108
9W2	110
16W	112
30W	114
1F3	116
2F3	118
3F2	120
3F4	122
5F2	124
6F2	126
3F7	128
8F1	130

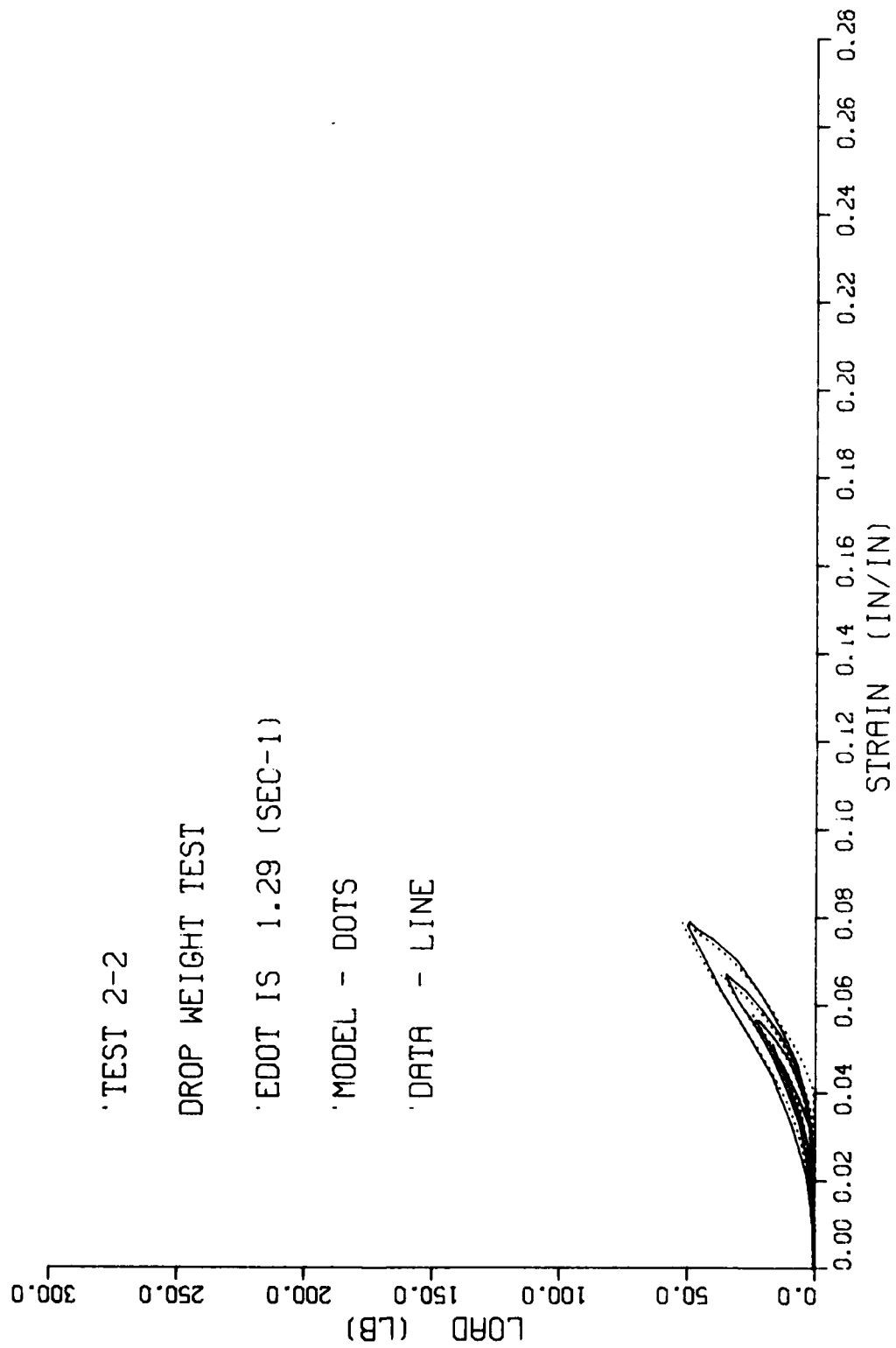
TEST  
9F3  
3F1  
30F

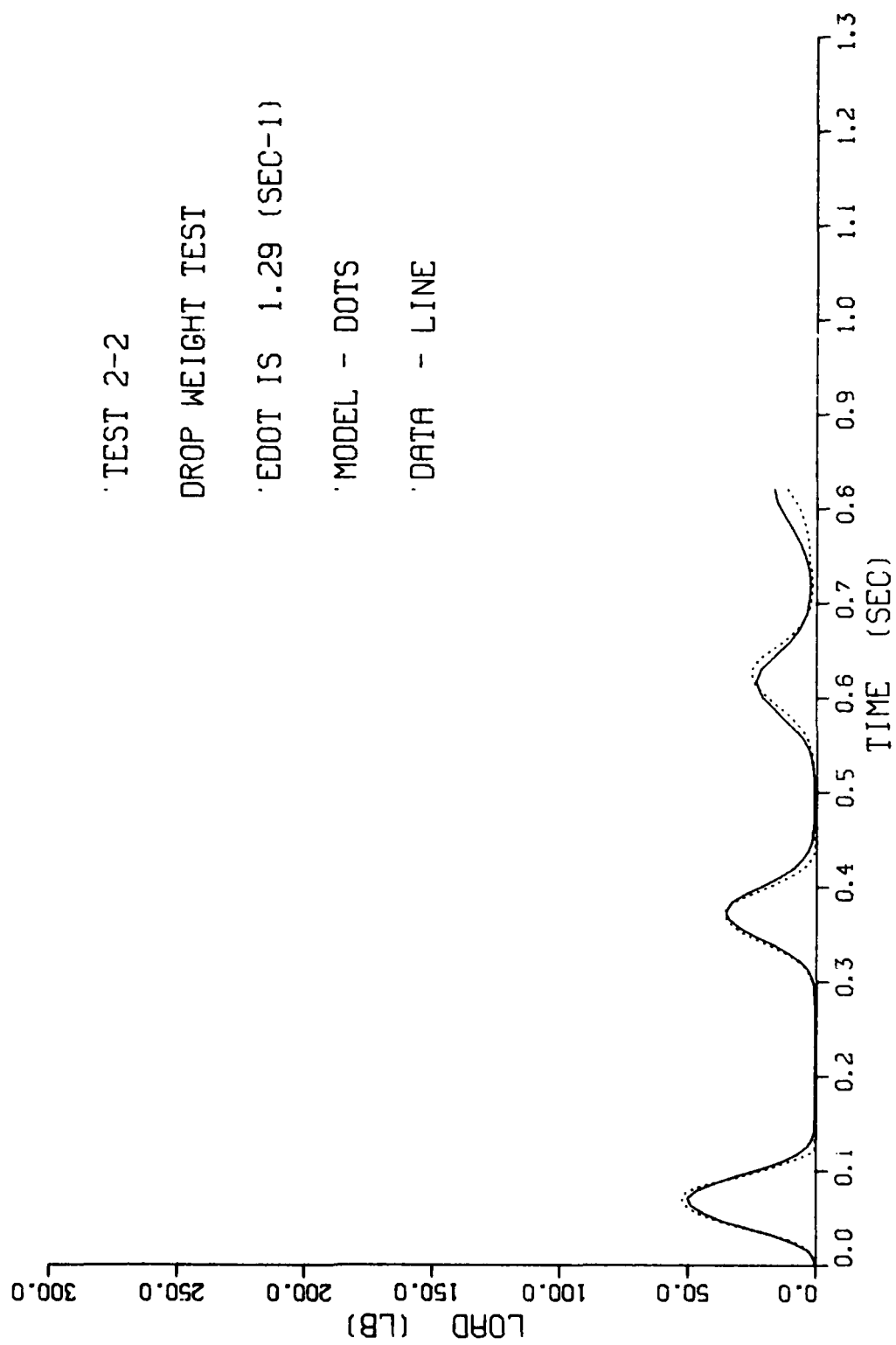
PAGE  
132  
134  
136

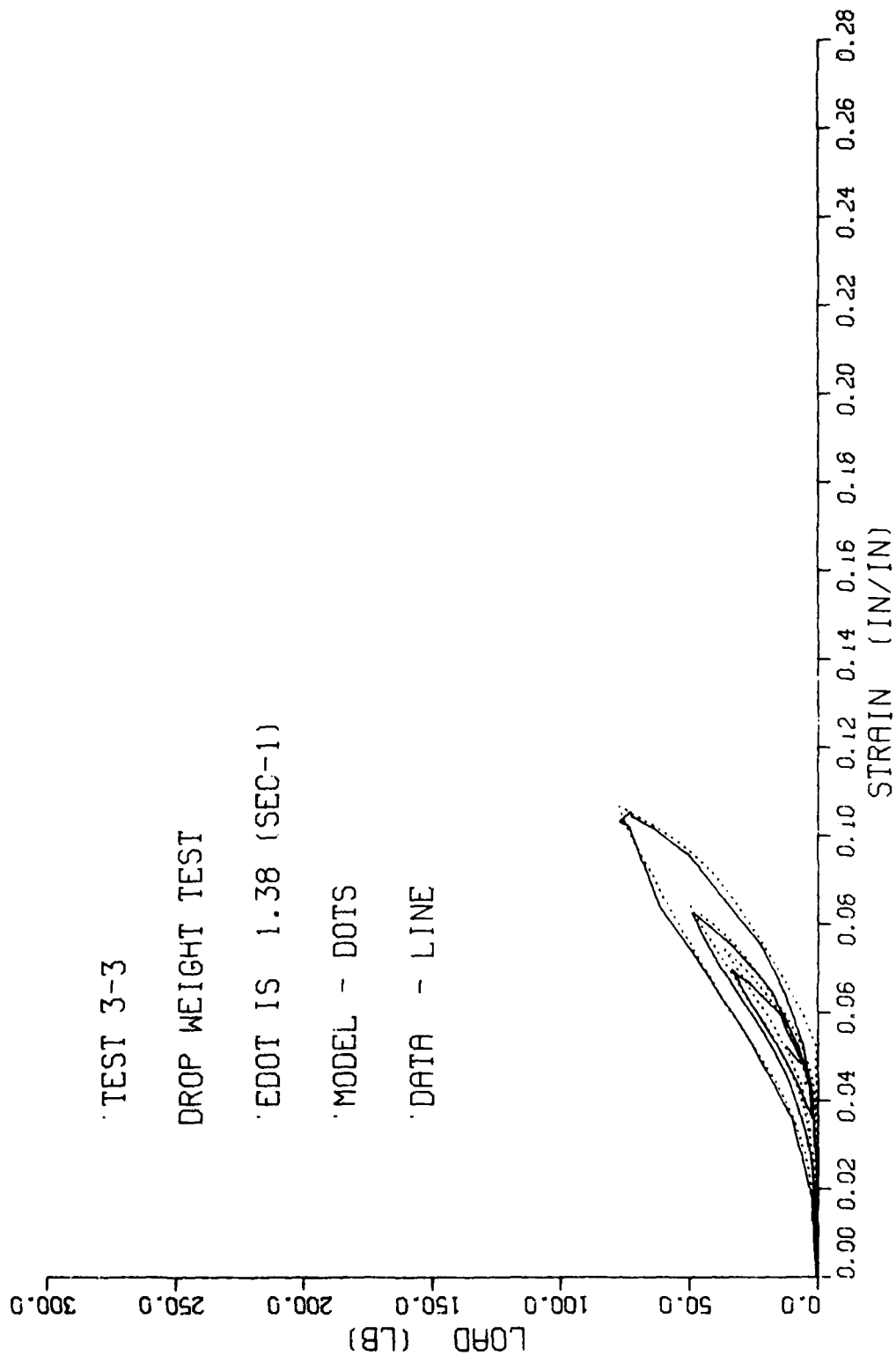












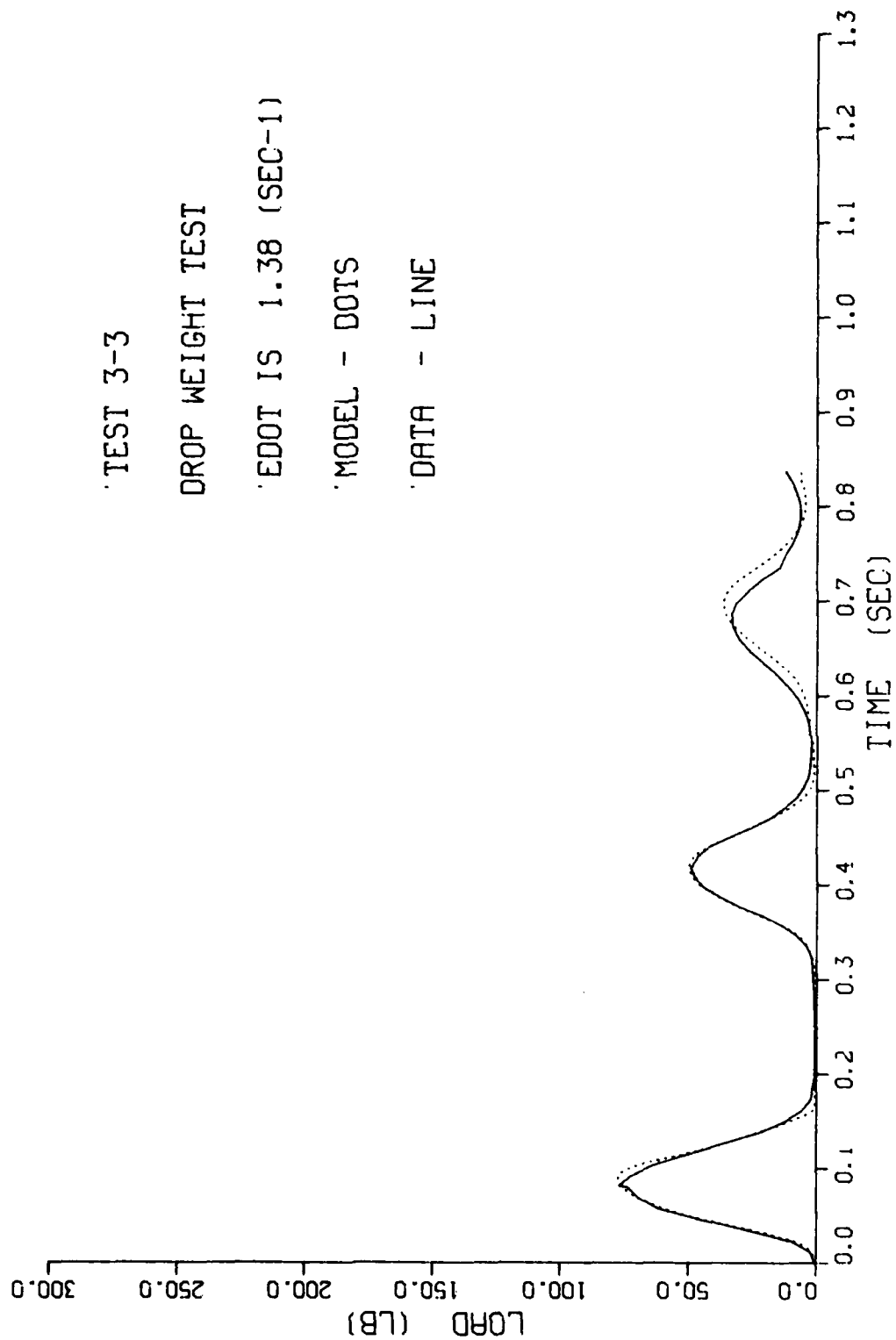
TEST 3-3

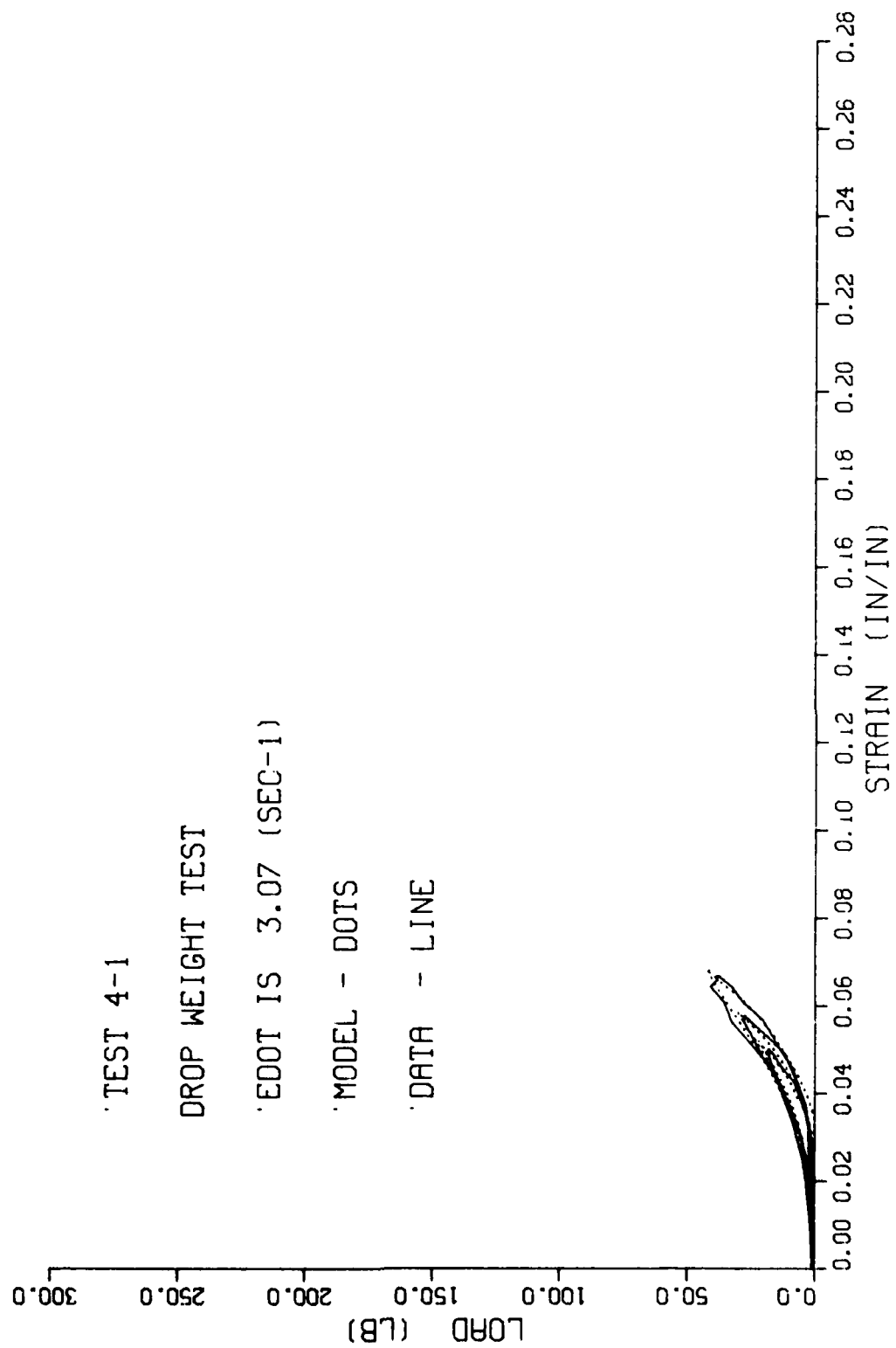
DROP WEIGHT TEST

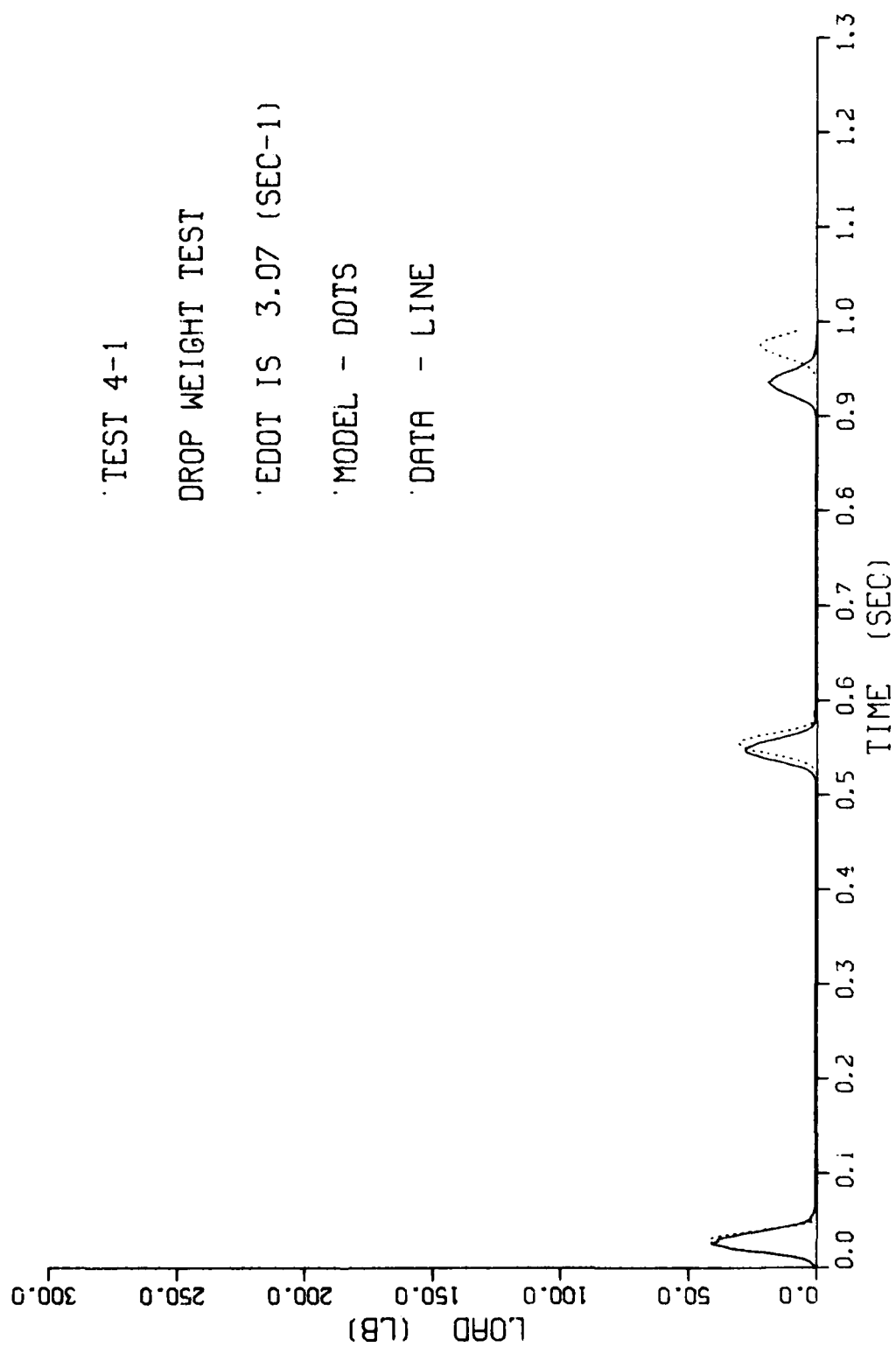
EDOT IS 1.38 (SEC-1)

MODEL - DOTS

DATA - LINE









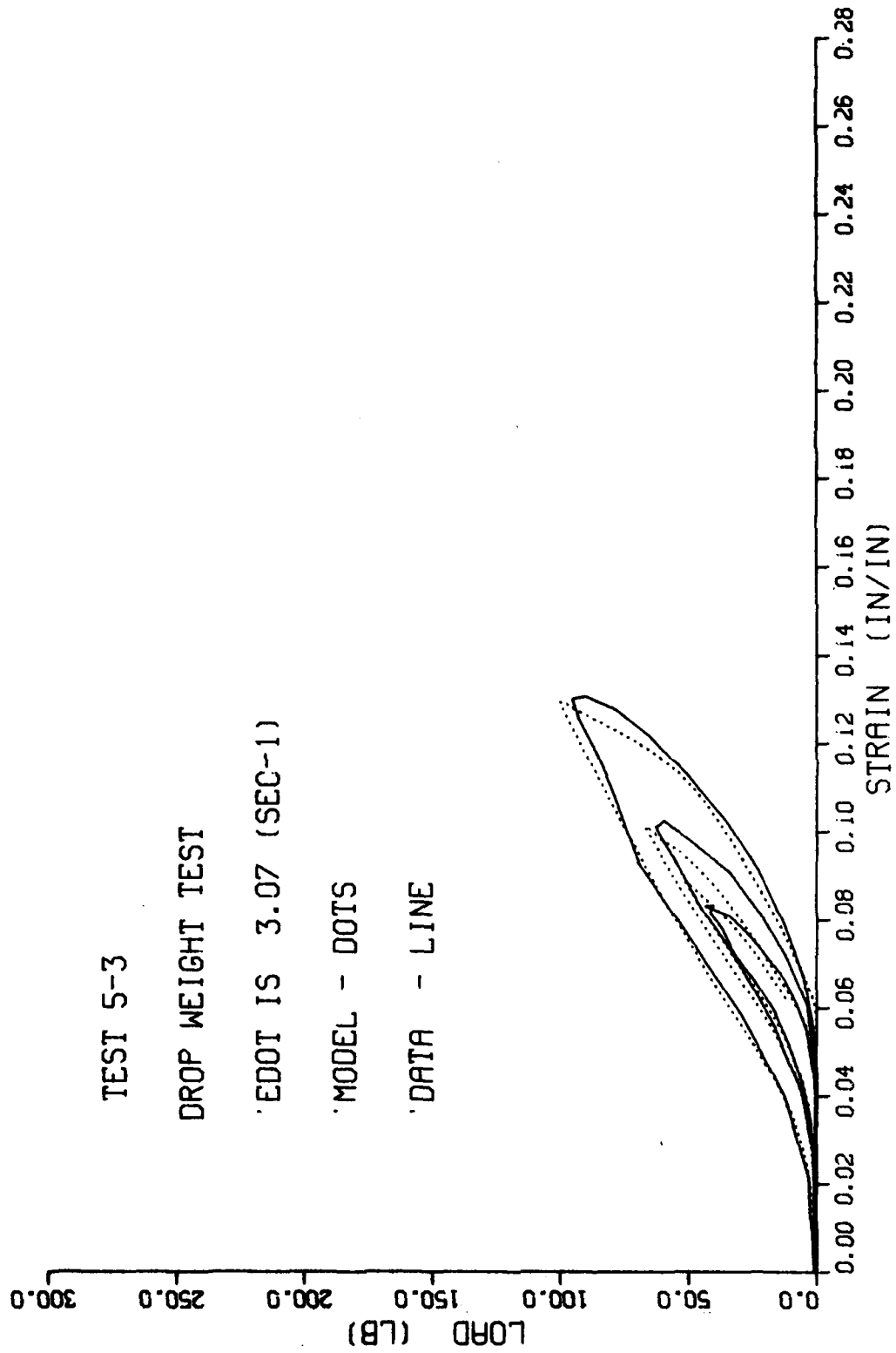
TEST 5-3

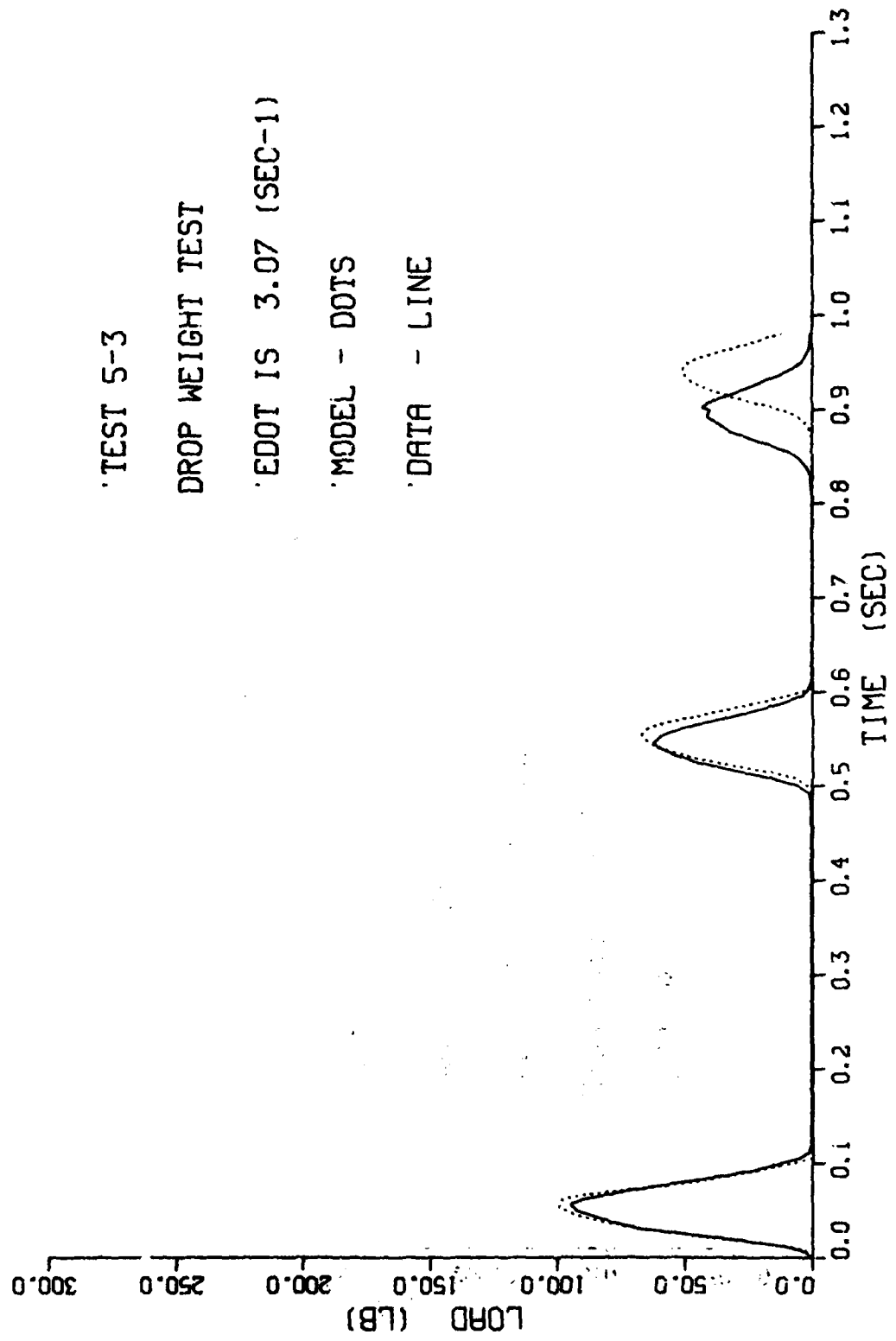
DROP WEIGHT TEST

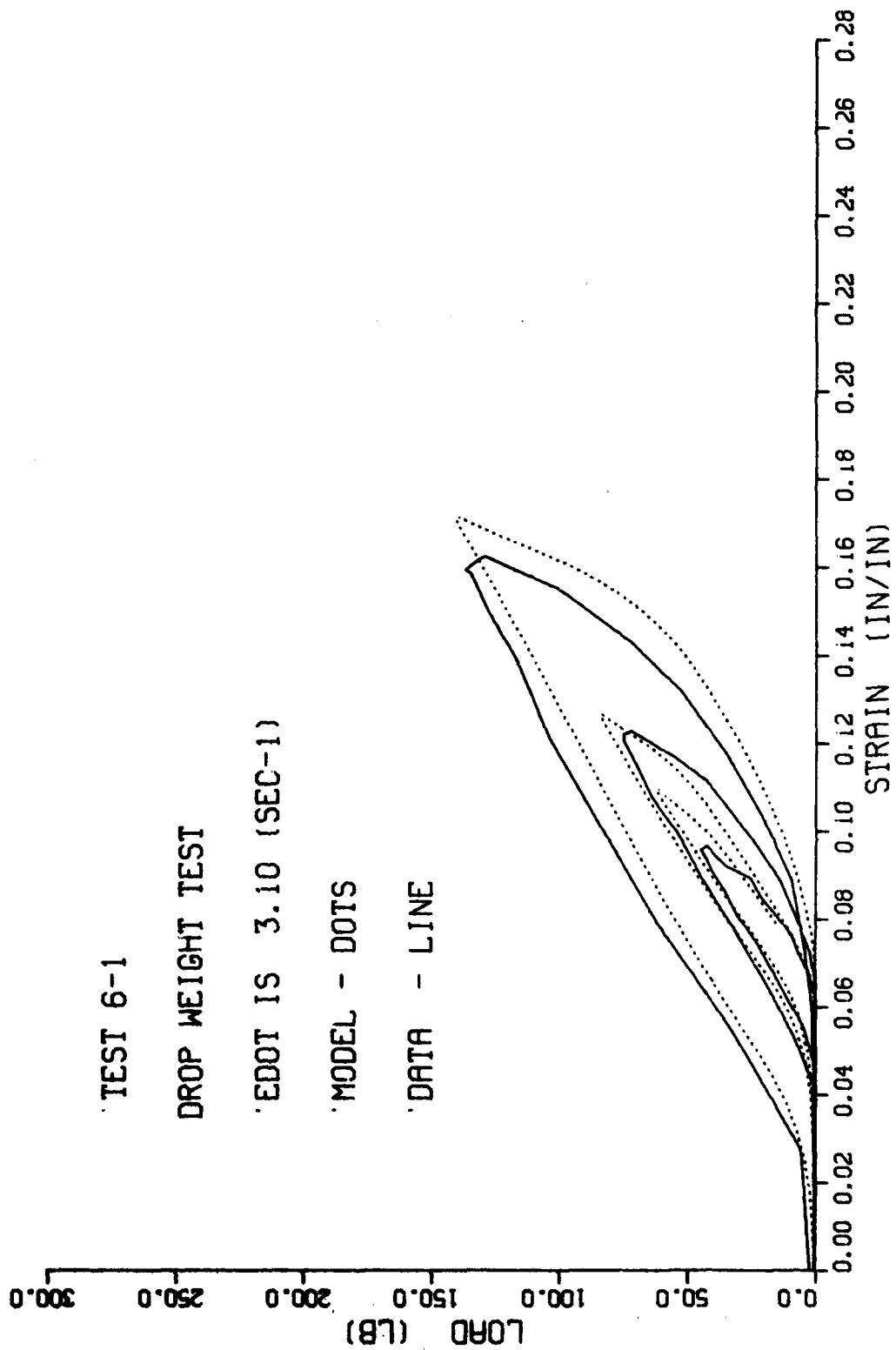
EDOT IS 3.07 (SEC-1)

MODEL - DOTS

DATA - LINE







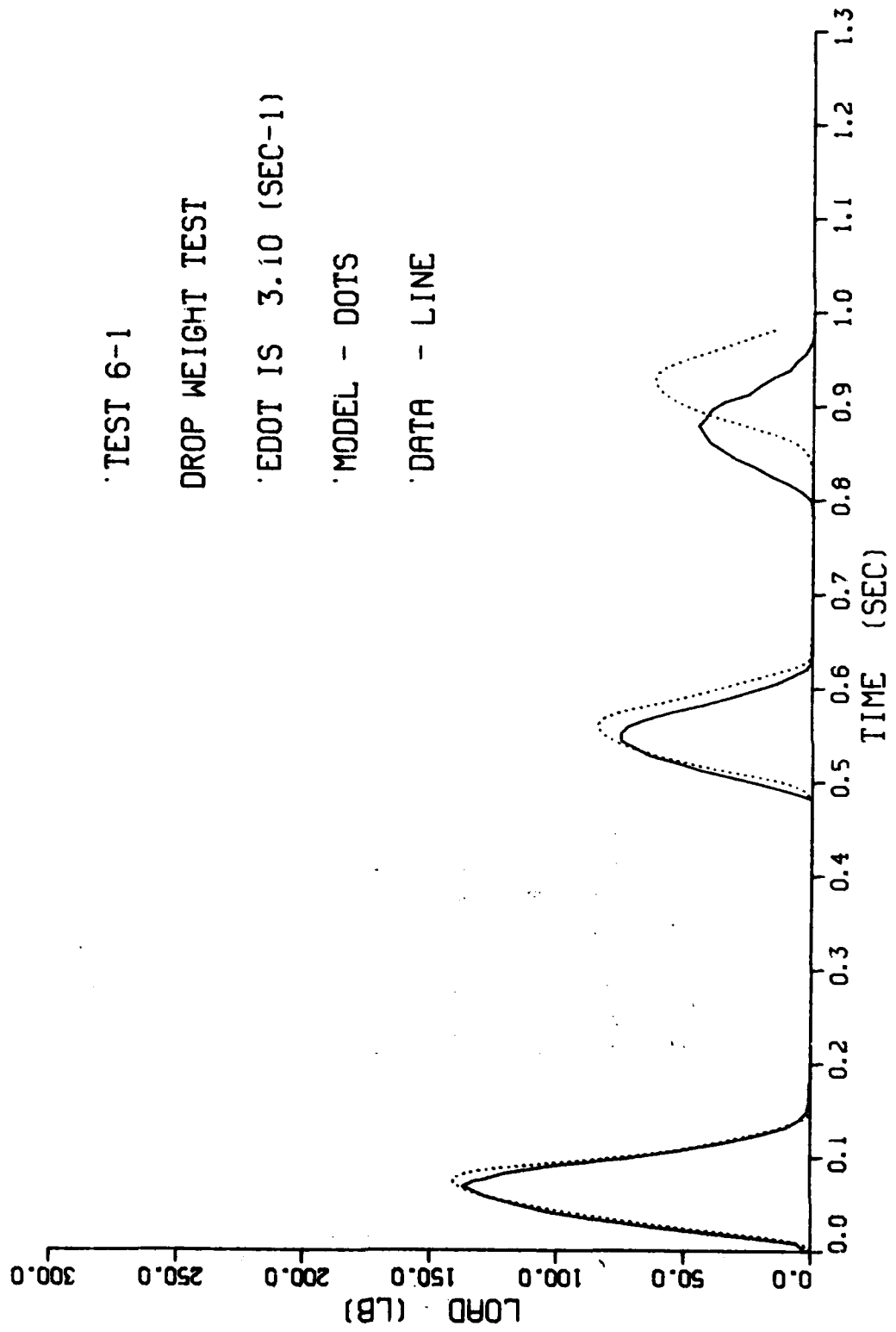
TEST 6-1

DROP WEIGHT TEST

EDOT IS 3.10 (SEC-1)

MODEL - DOTS

DATA - LINE



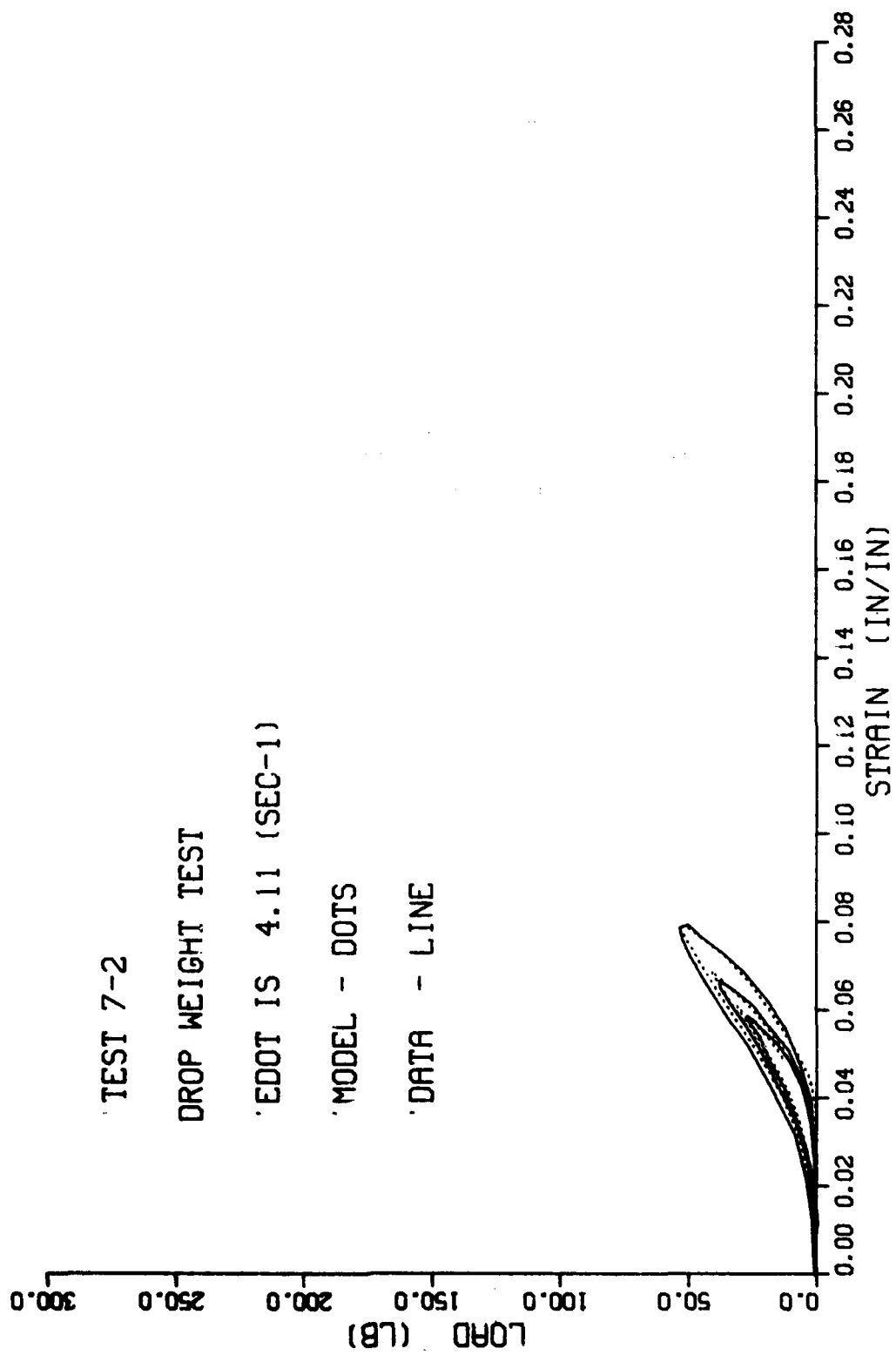
TEST 7-2

DROP WEIGHT TEST

EDOT IS 4.11 (SEC-1)

MODEL - DOTS

DATA - LINE



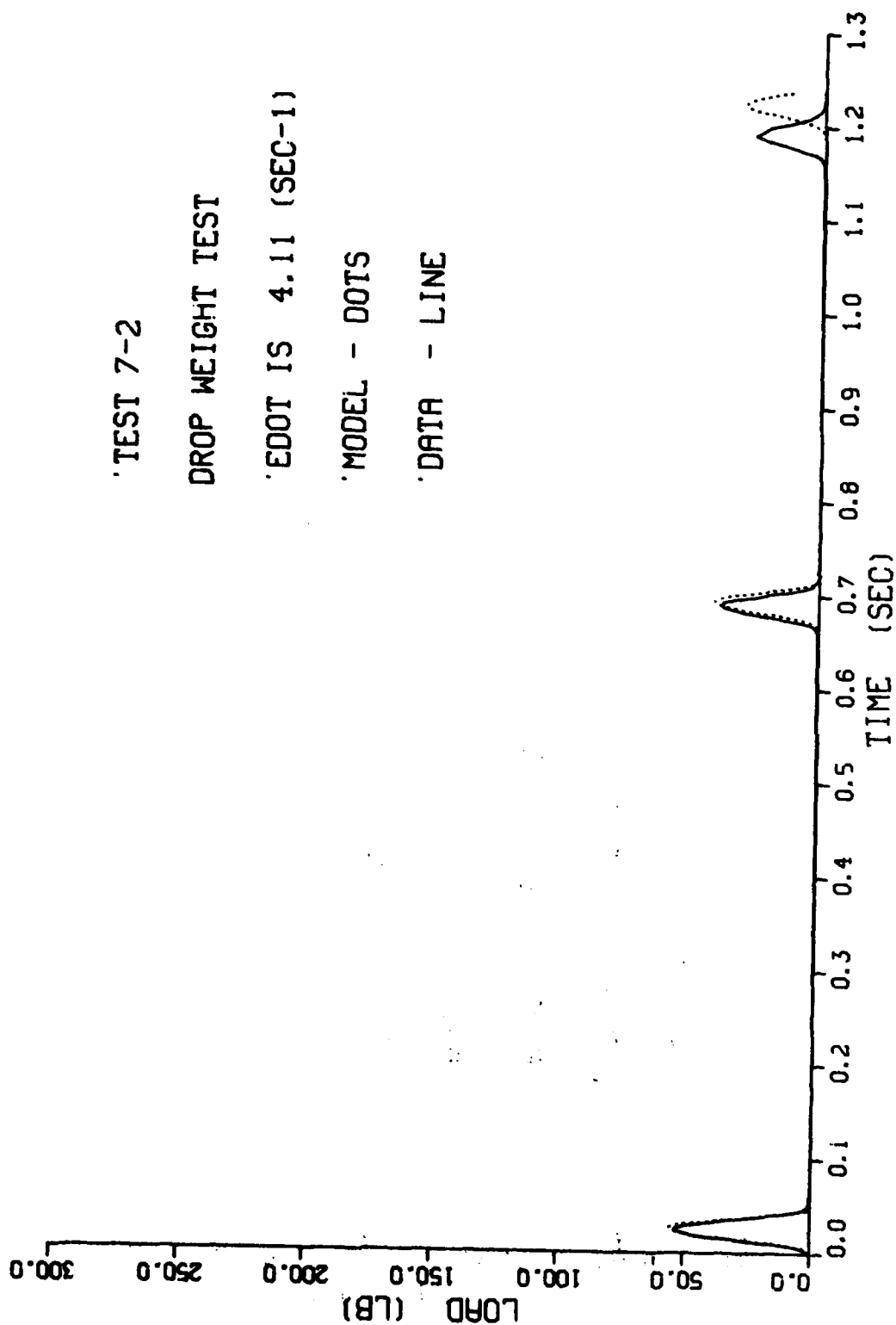
'TEST 7-2

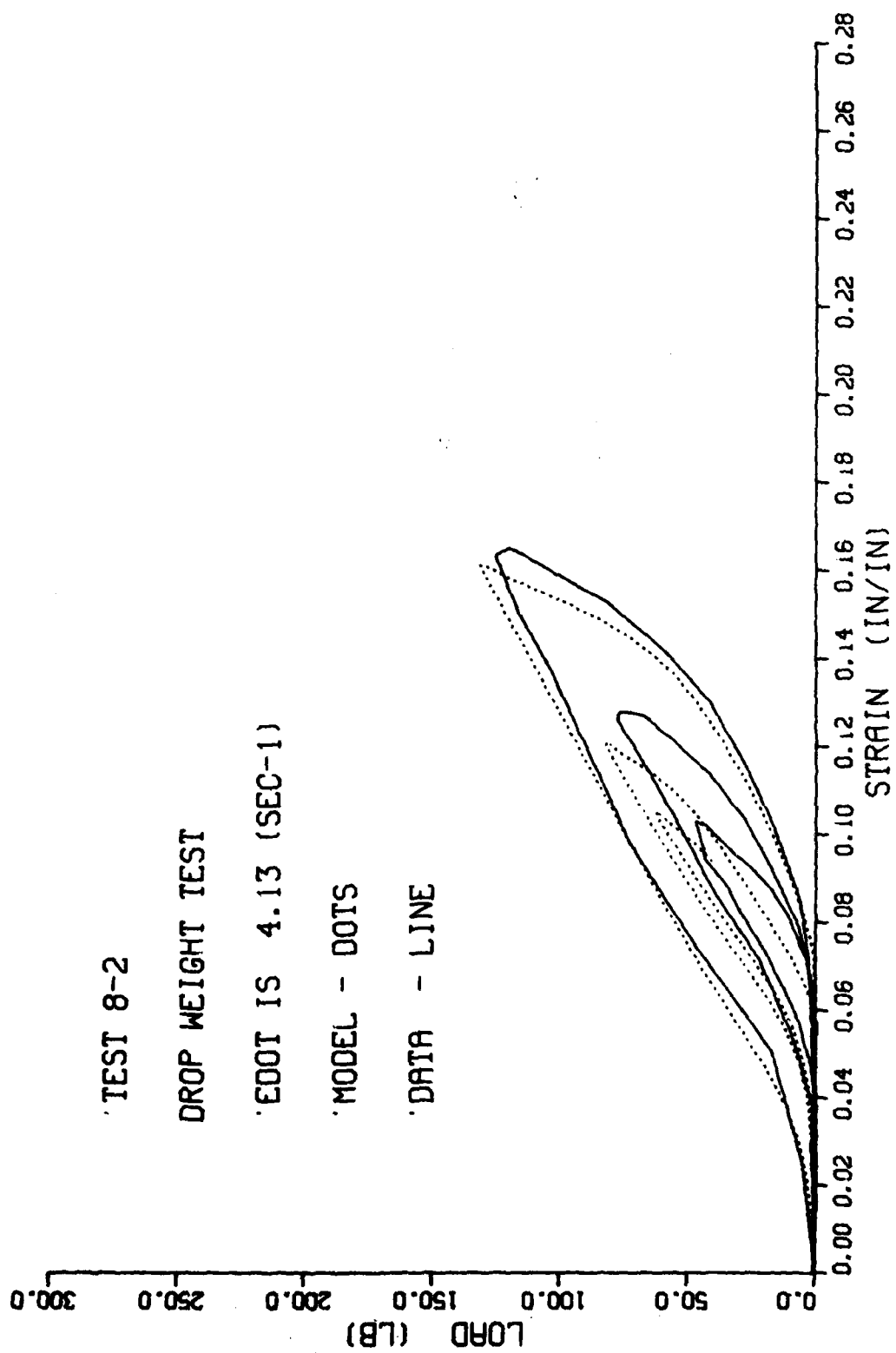
DROP WEIGHT TEST

'EDOT IS 4.11 (SEC-1)

'MODEL - DOTS

'DATA - LINE





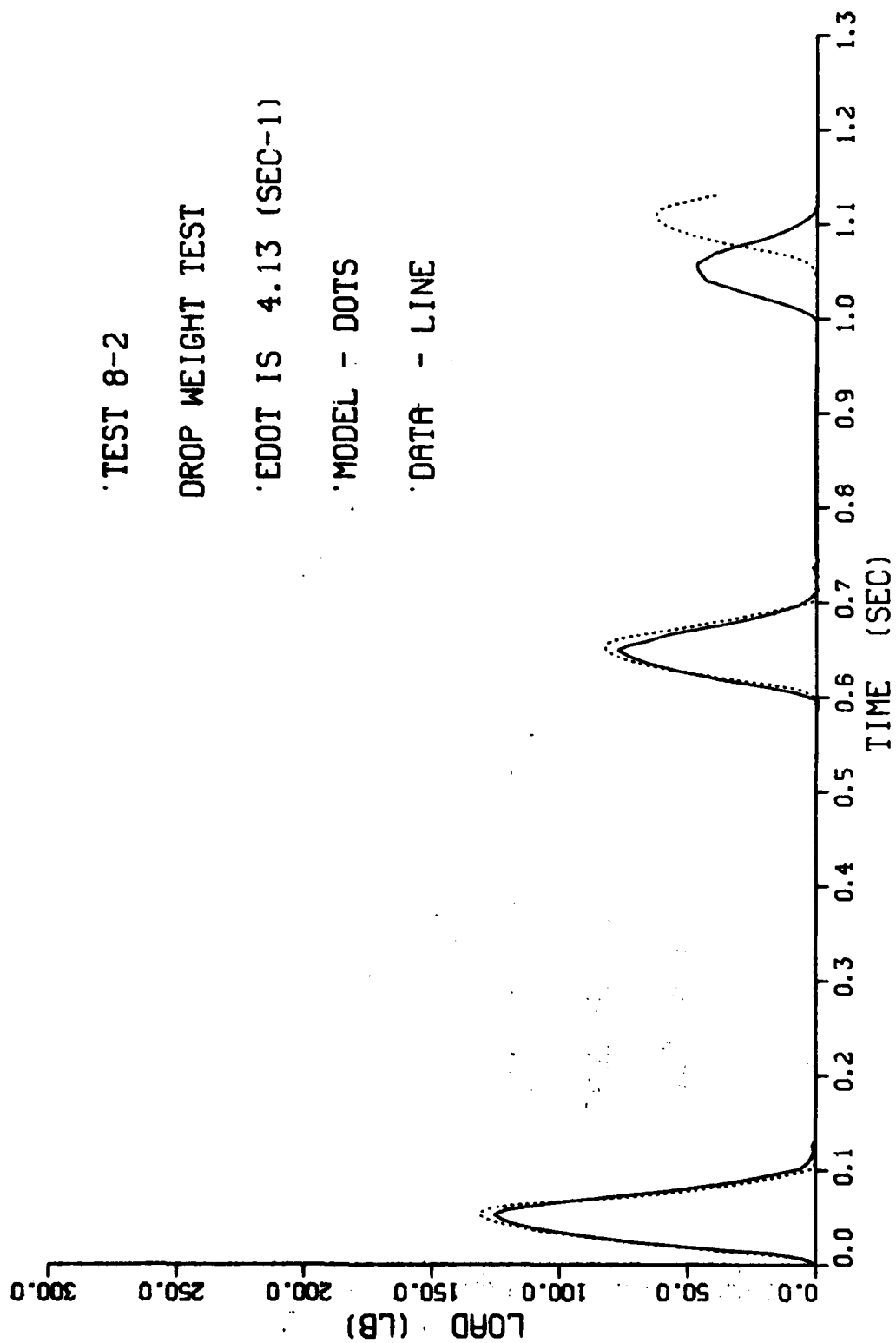
TEST 8-2

DROP WEIGHT TEST

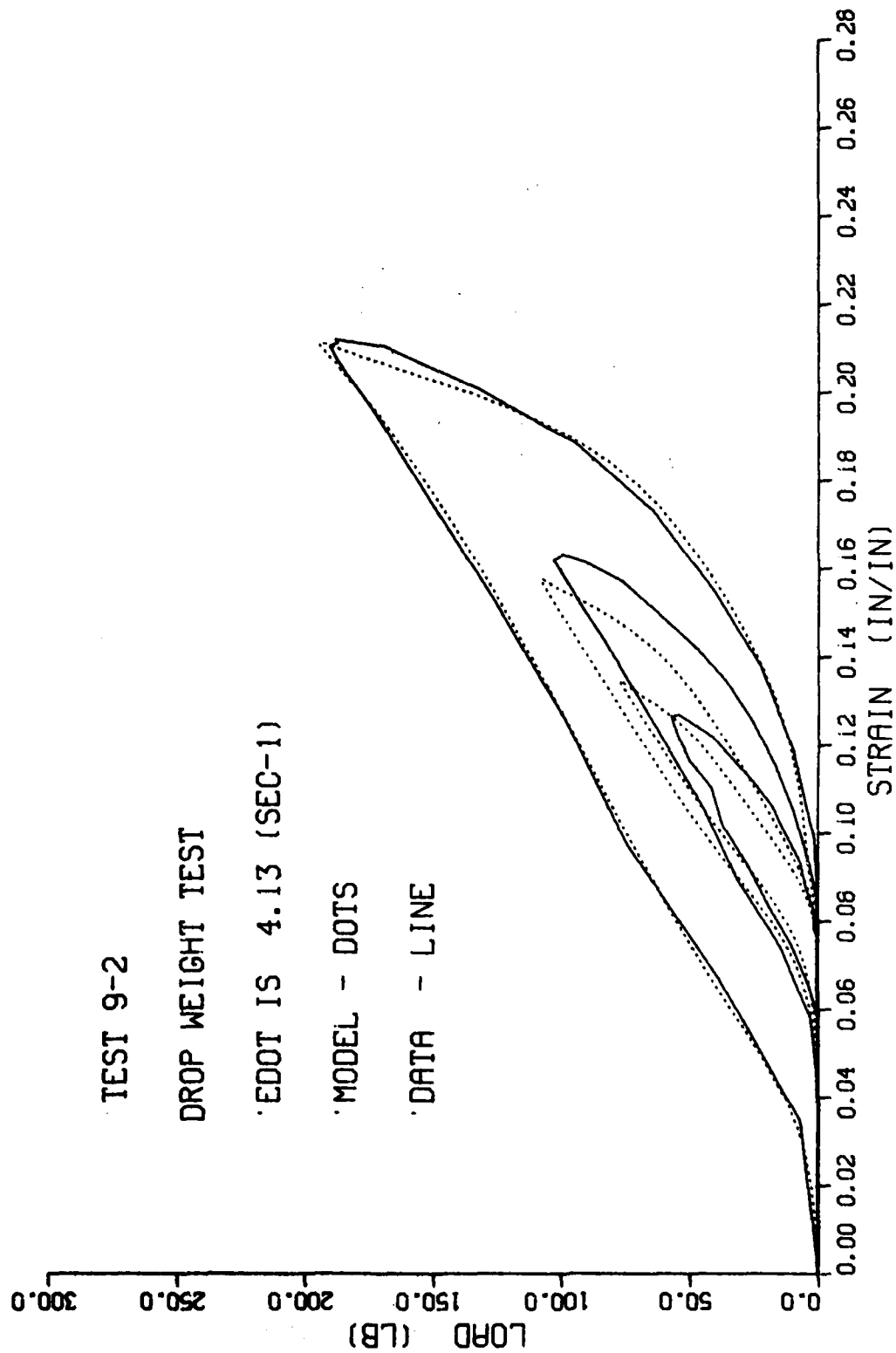
EDOT IS 4.13 (SEC-1)

MODEL - DOTS

DATA - LINE







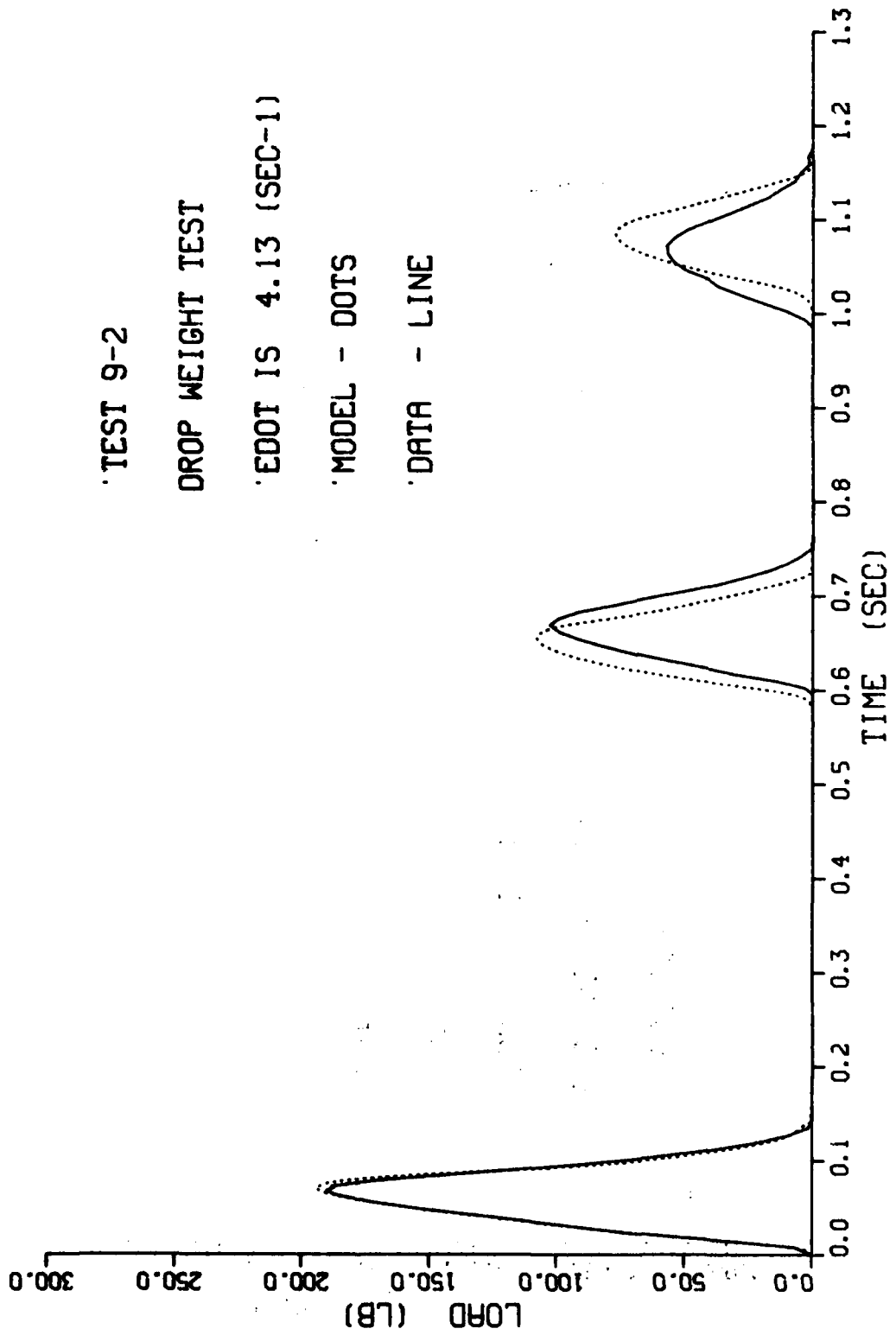
TEST 9-2

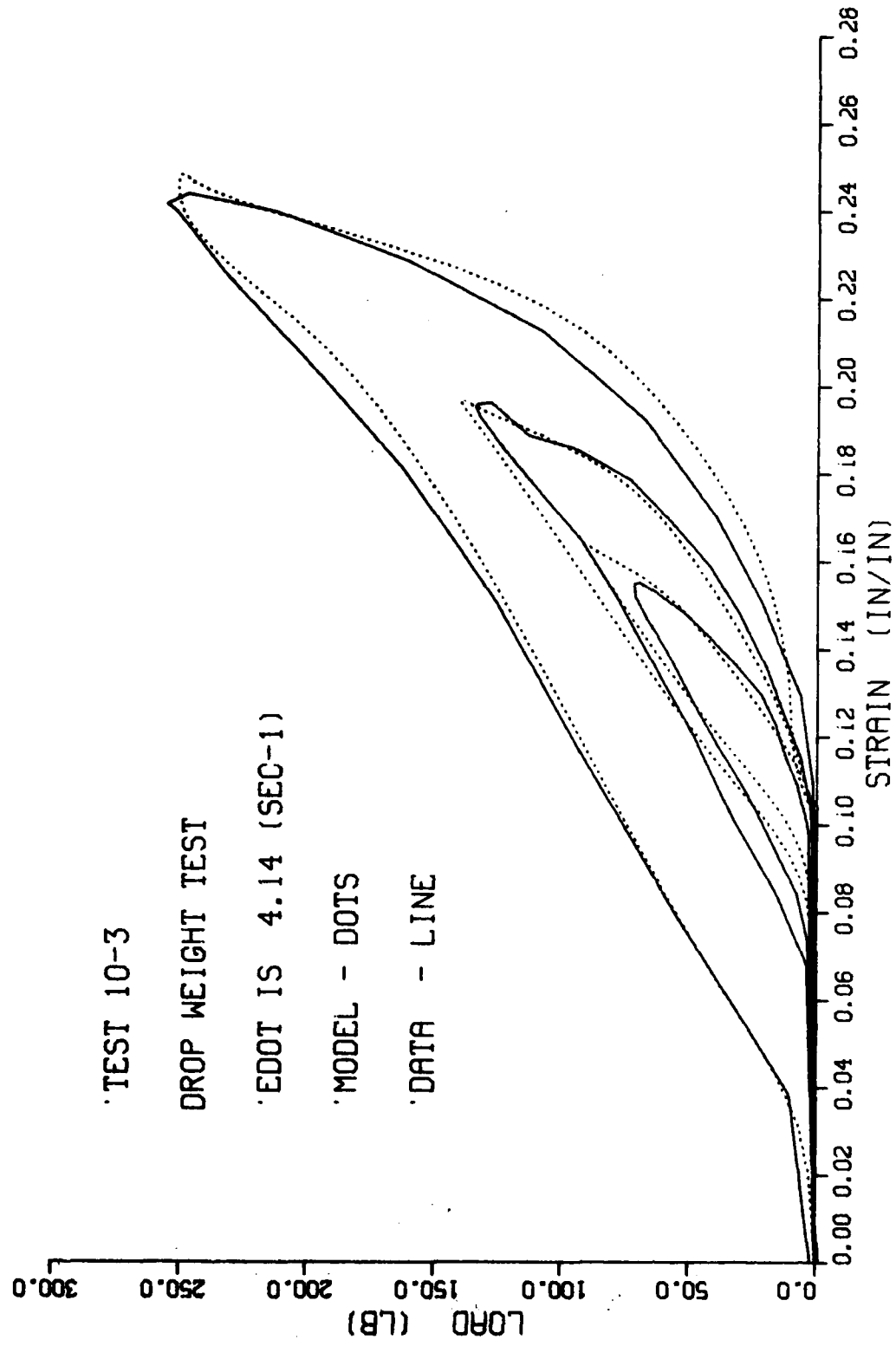
DROP WEIGHT TEST

EDOT IS 4.13 (SEC-1)

MODEL - DOTS

DATA - LINE





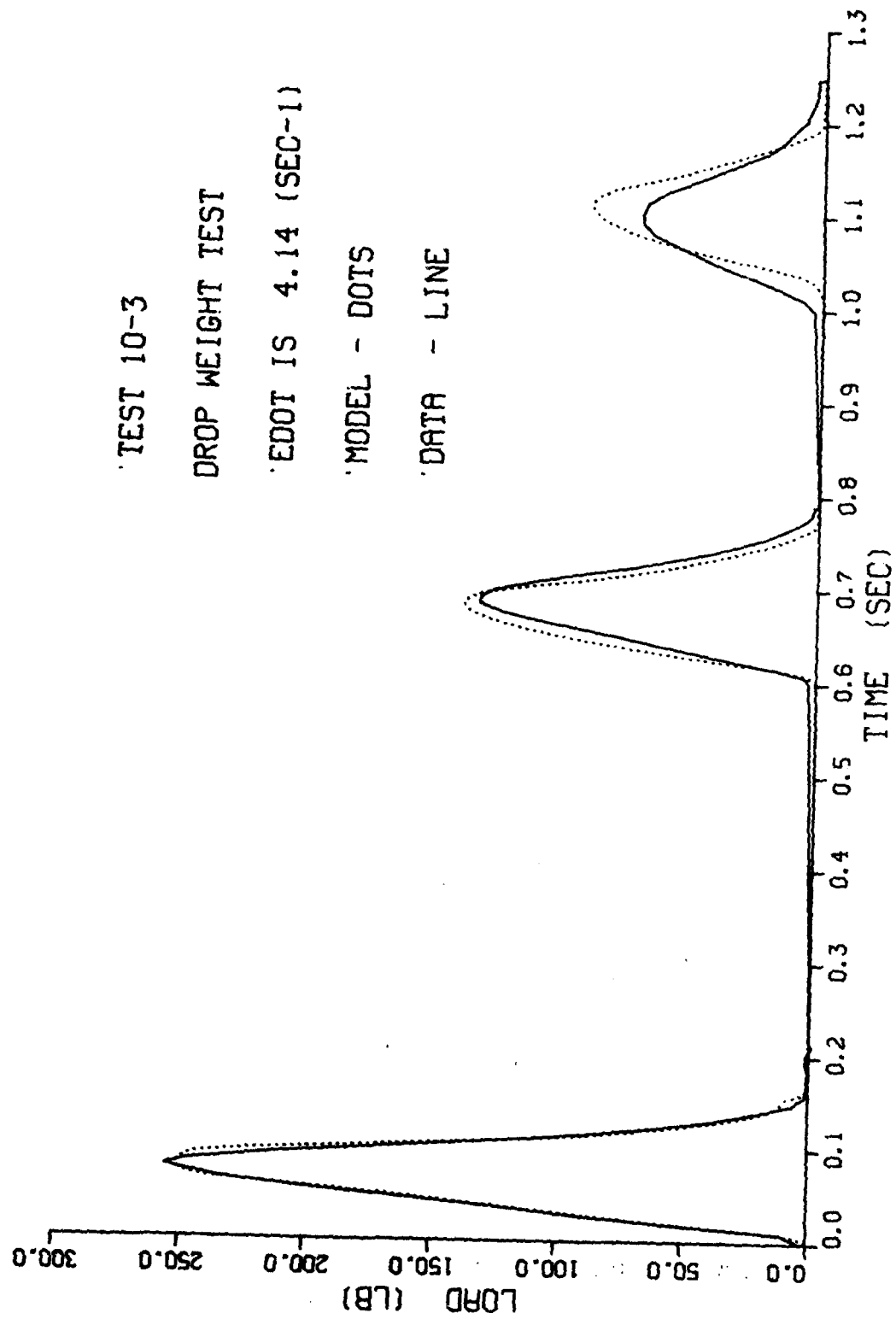
TEST 10-3

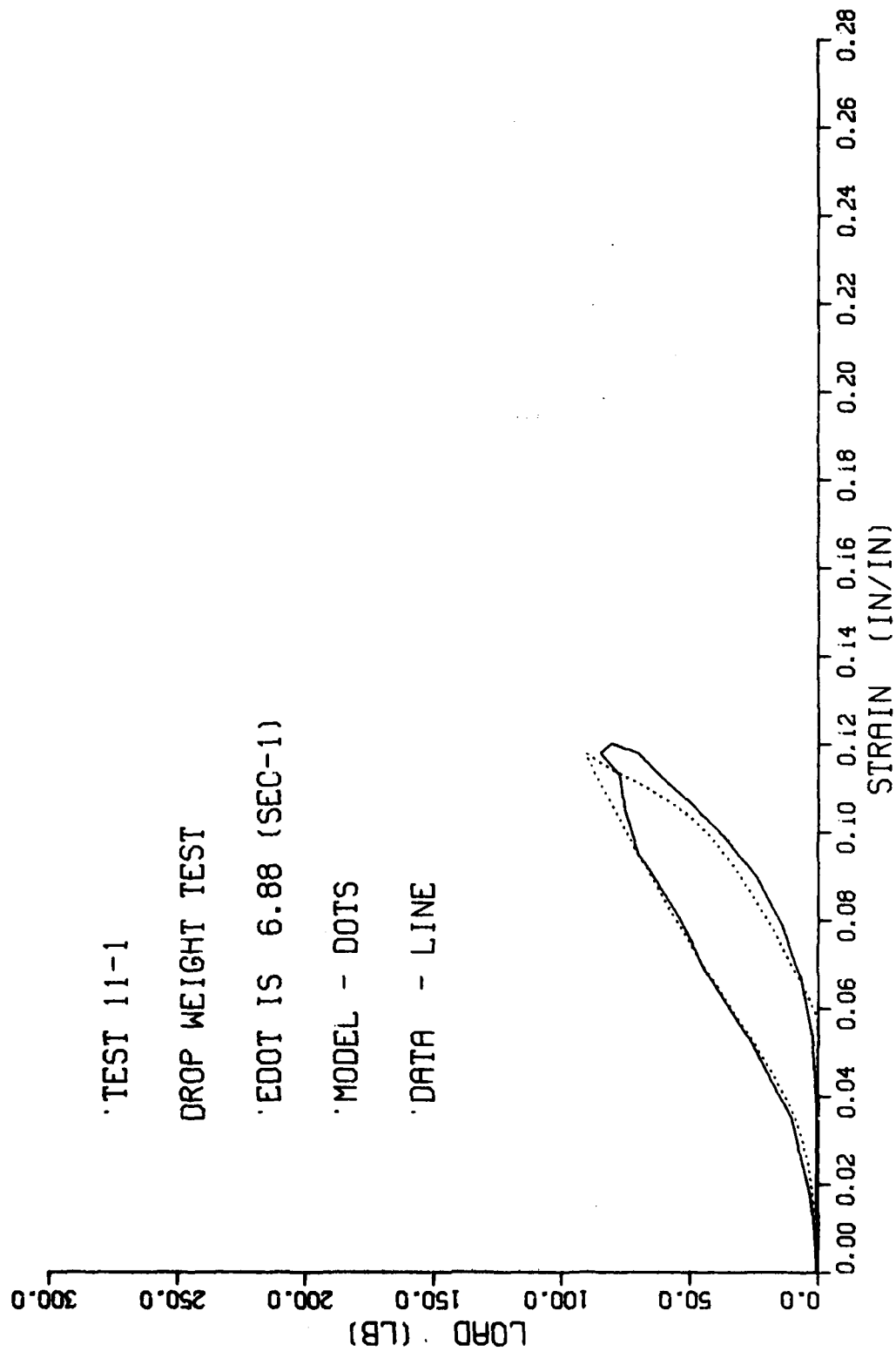
DROP WEIGHT TEST

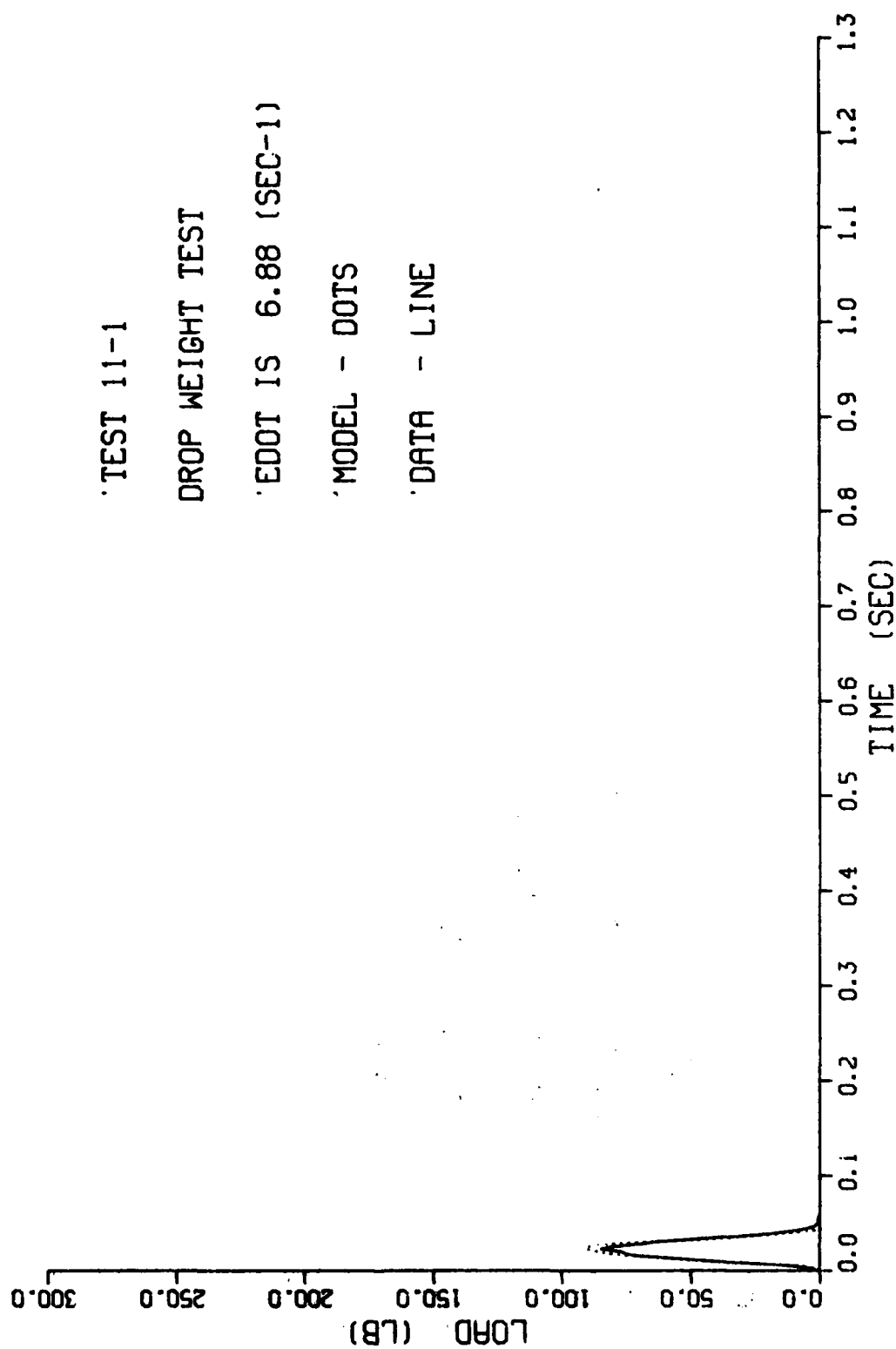
EDOT IS 4.14 (SEC-1)

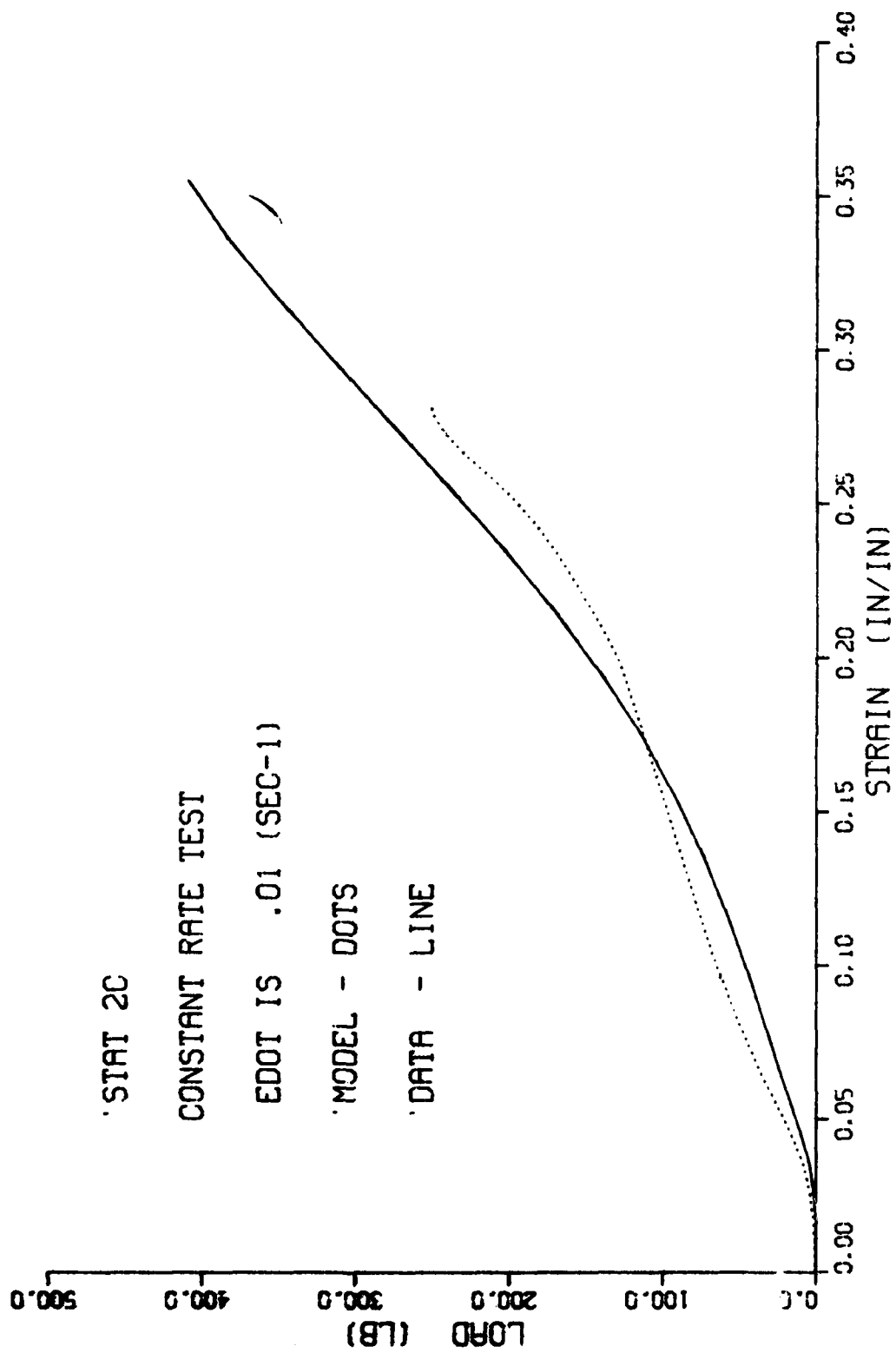
MODEL - DOTS

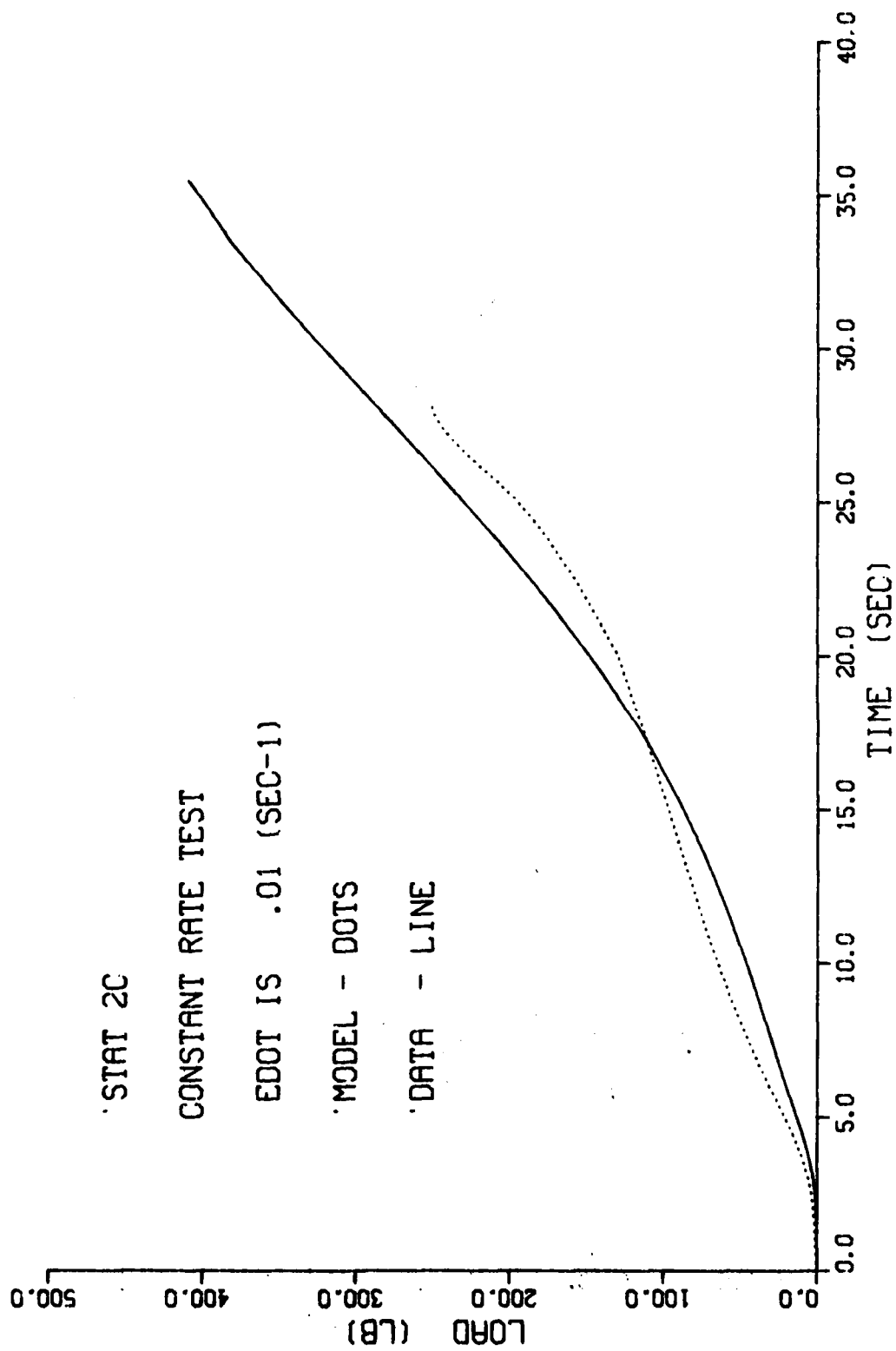
DATA - LINE



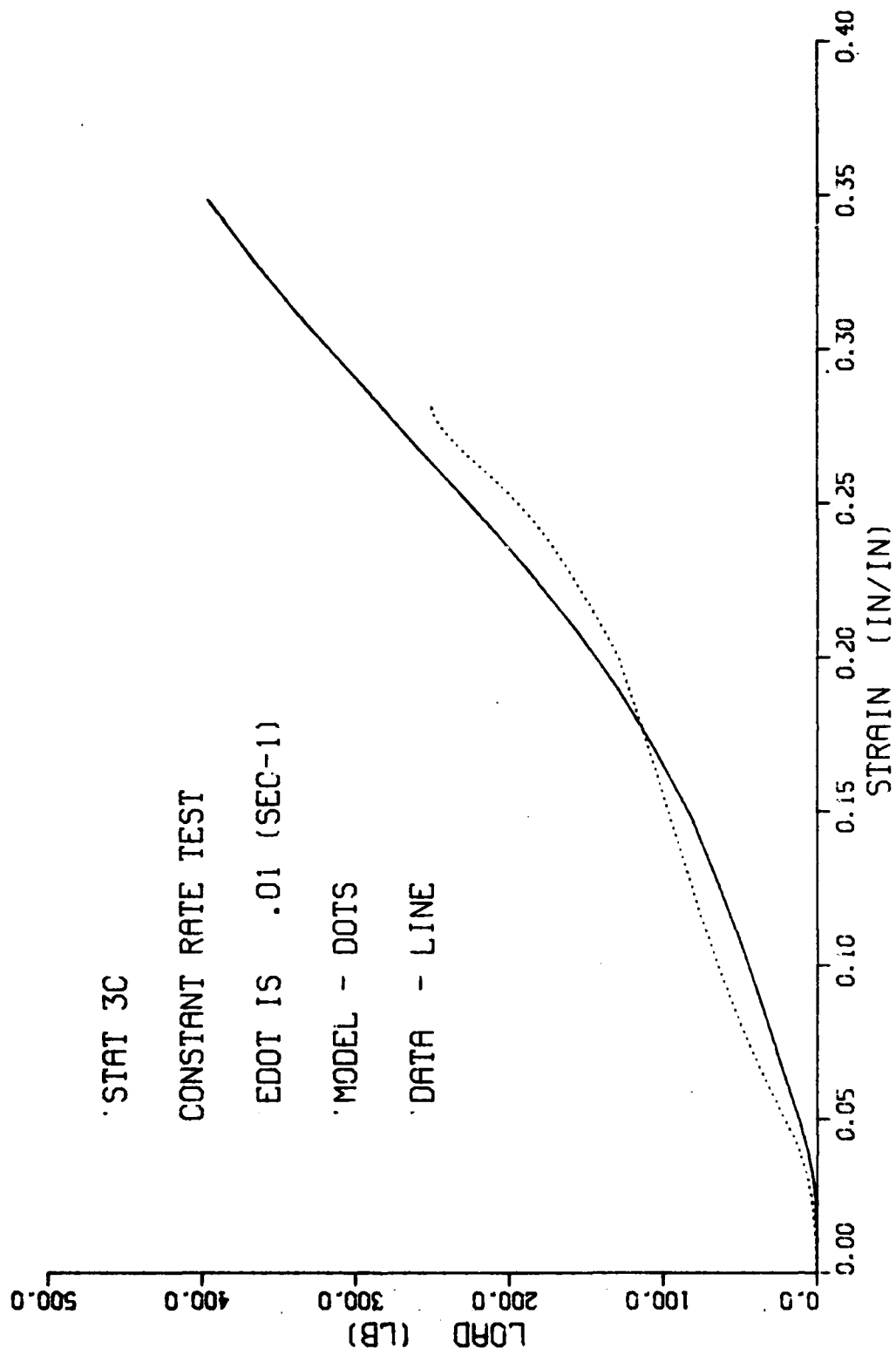


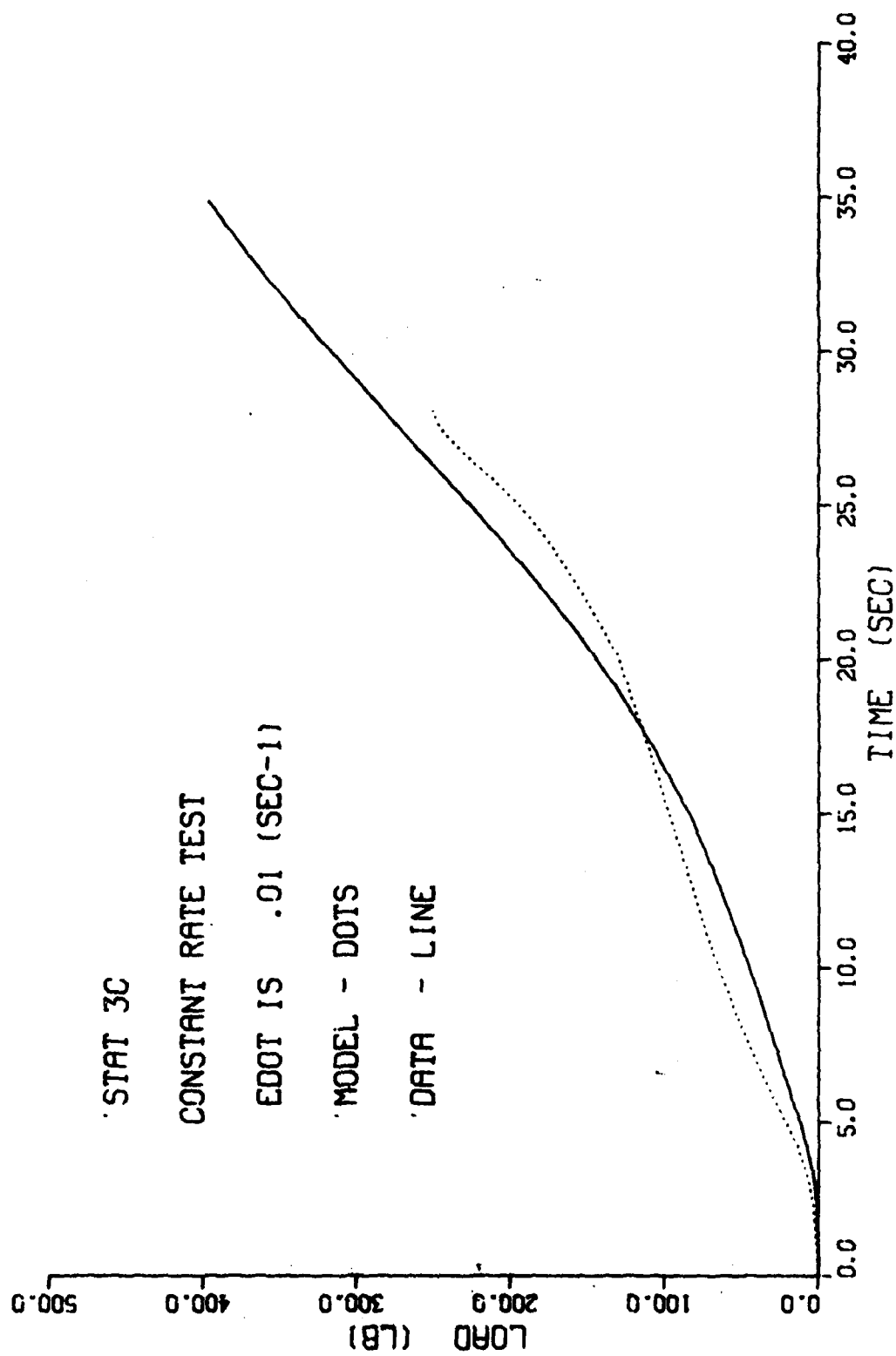


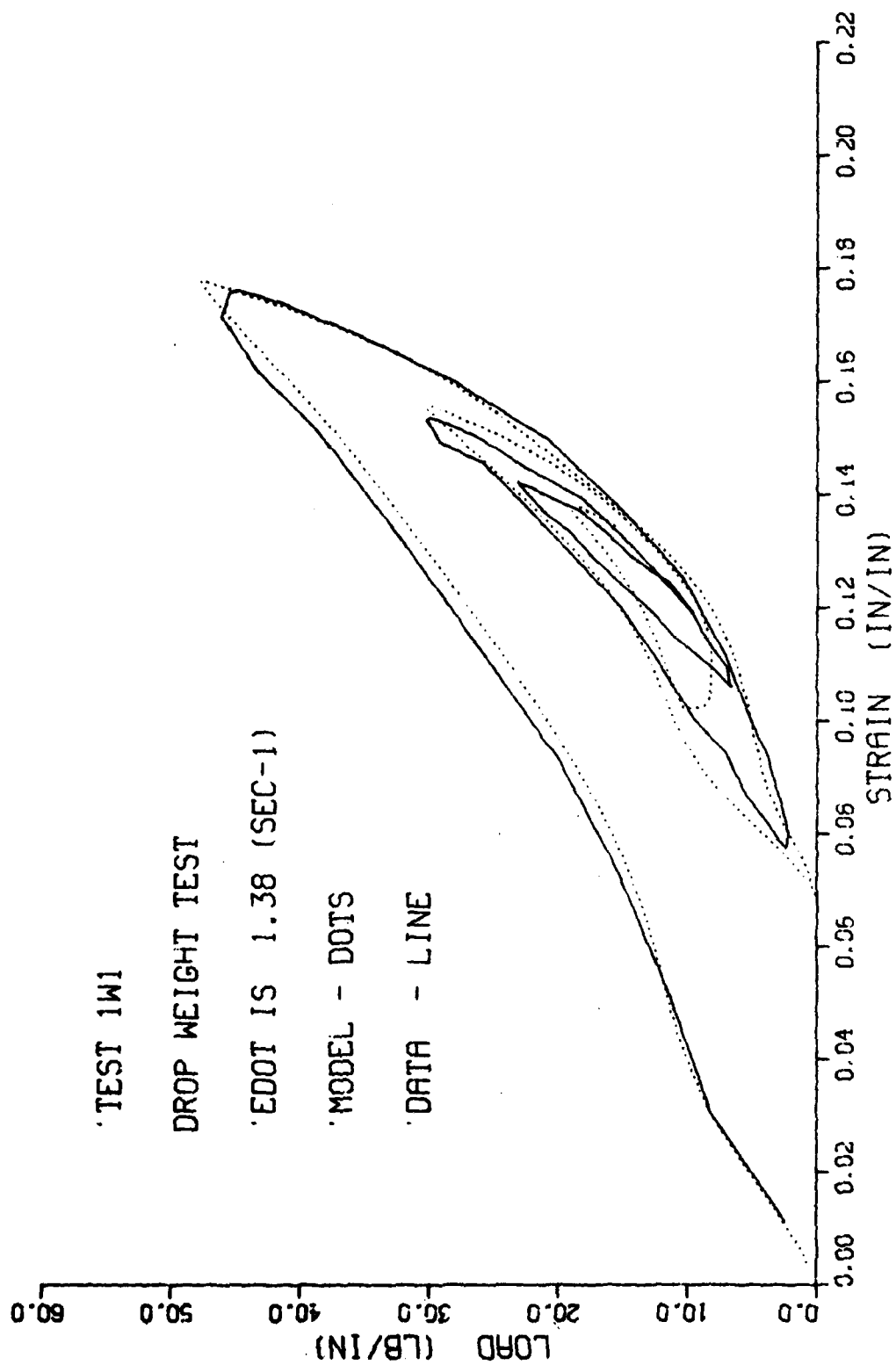


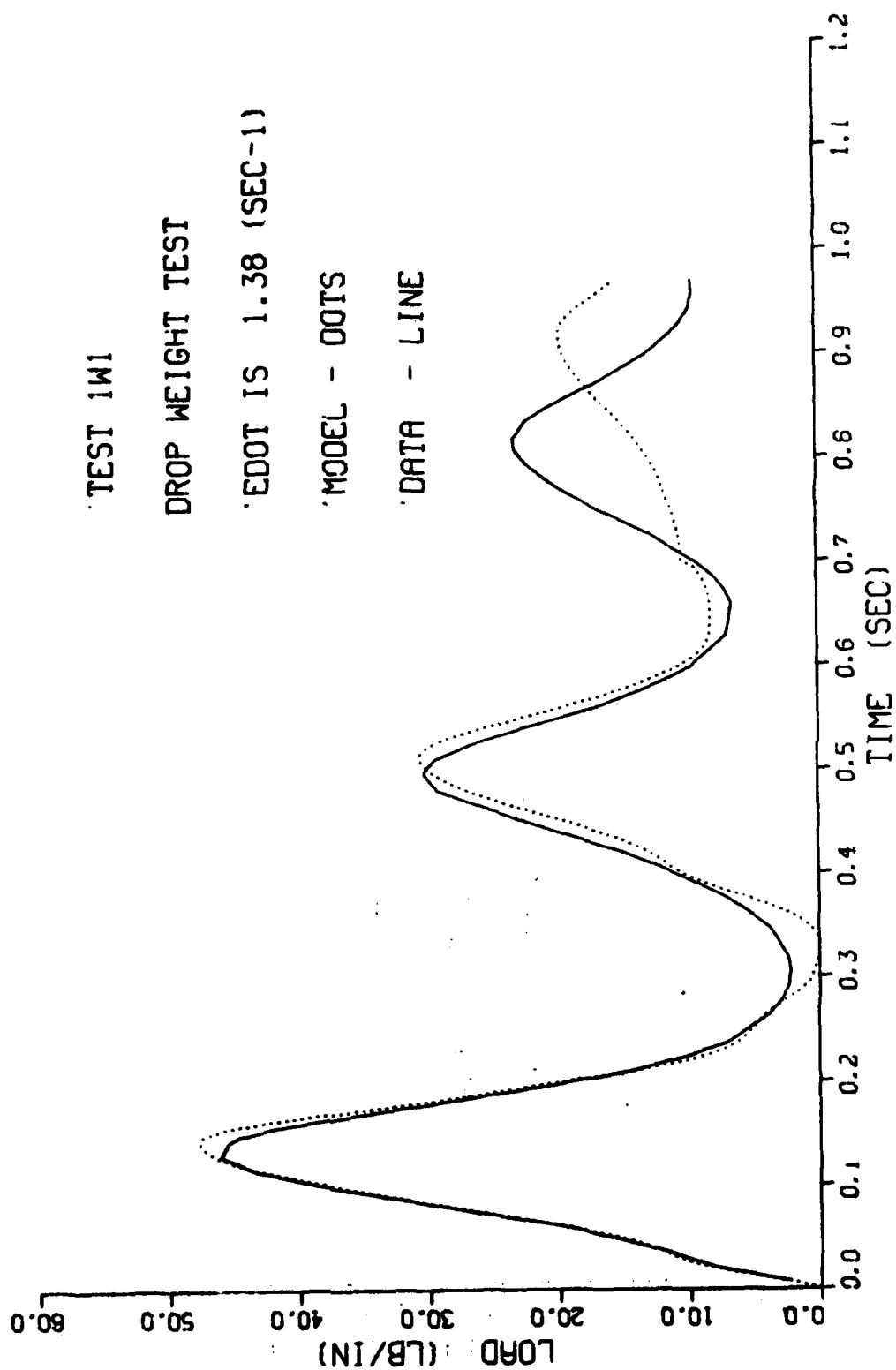


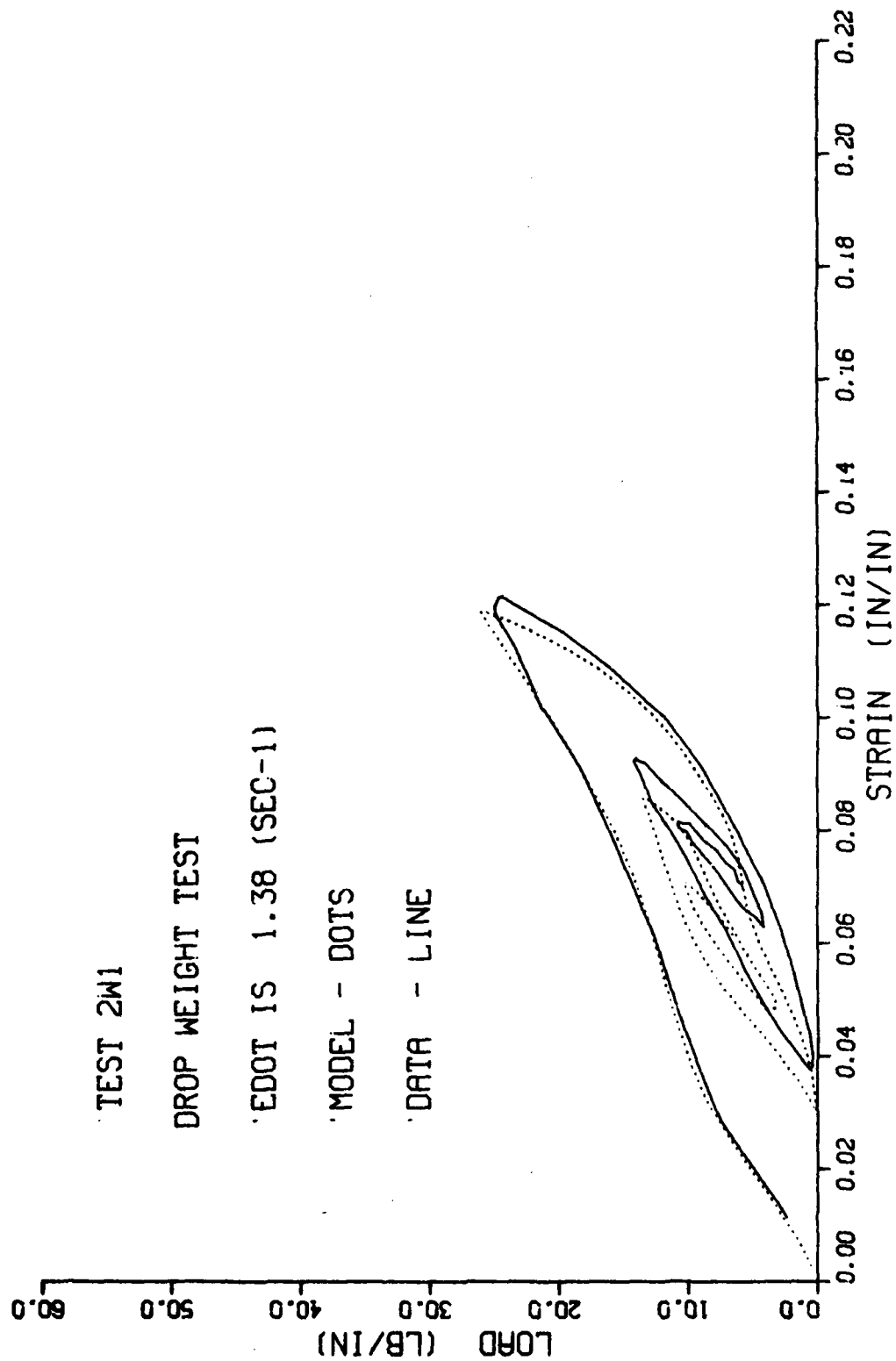












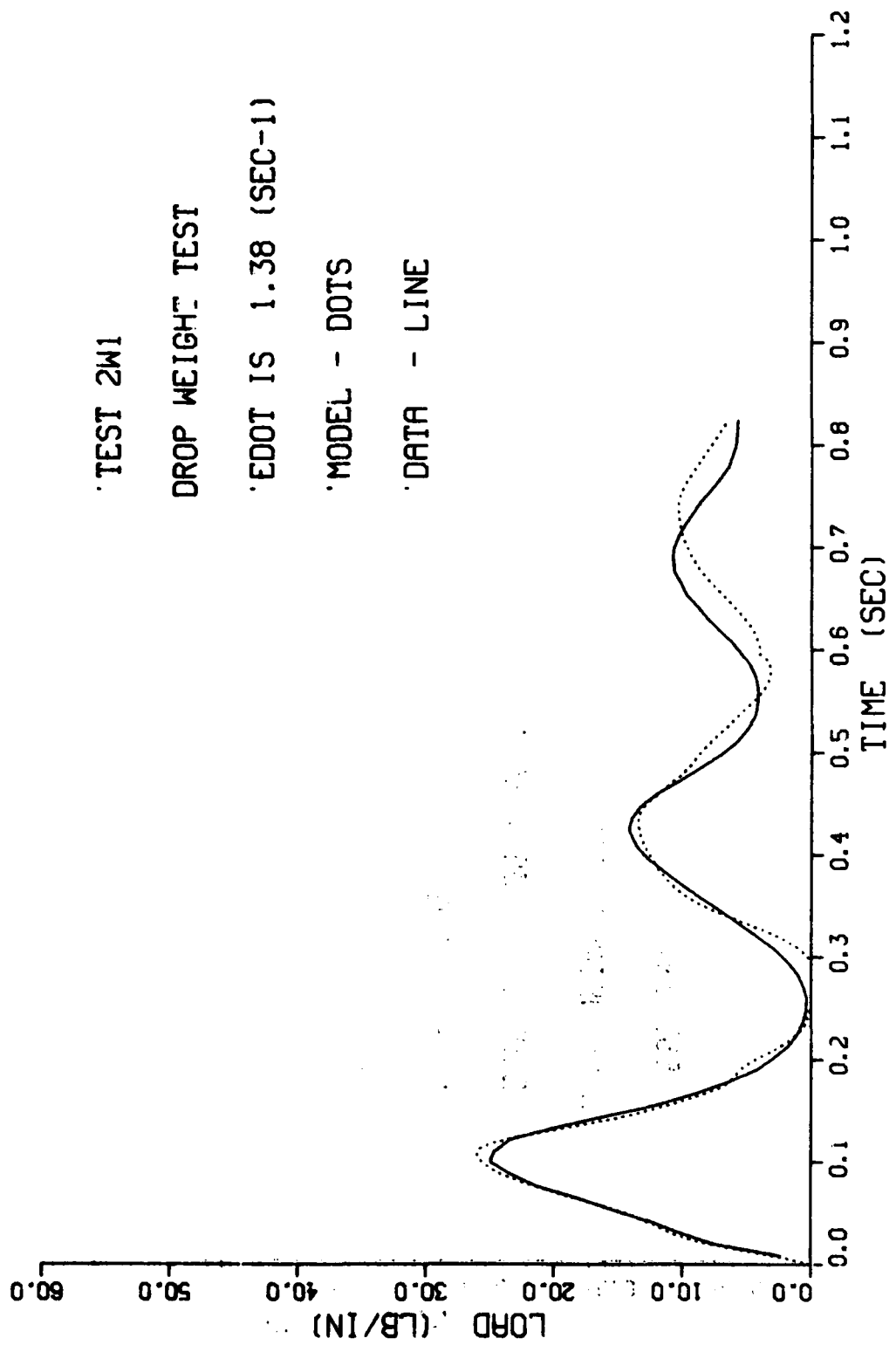
TEST 2W1

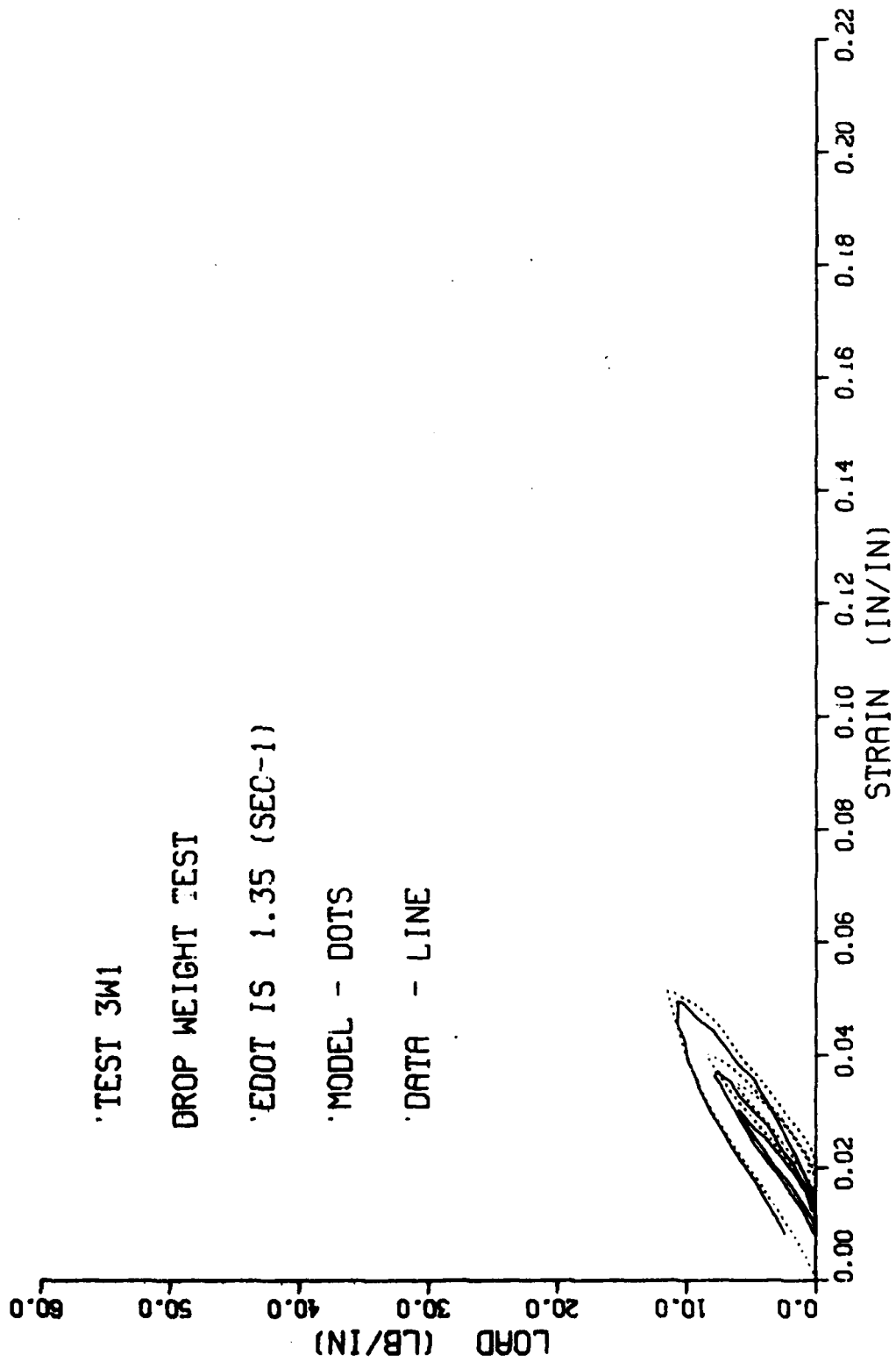
DROP WEIGHT TEST

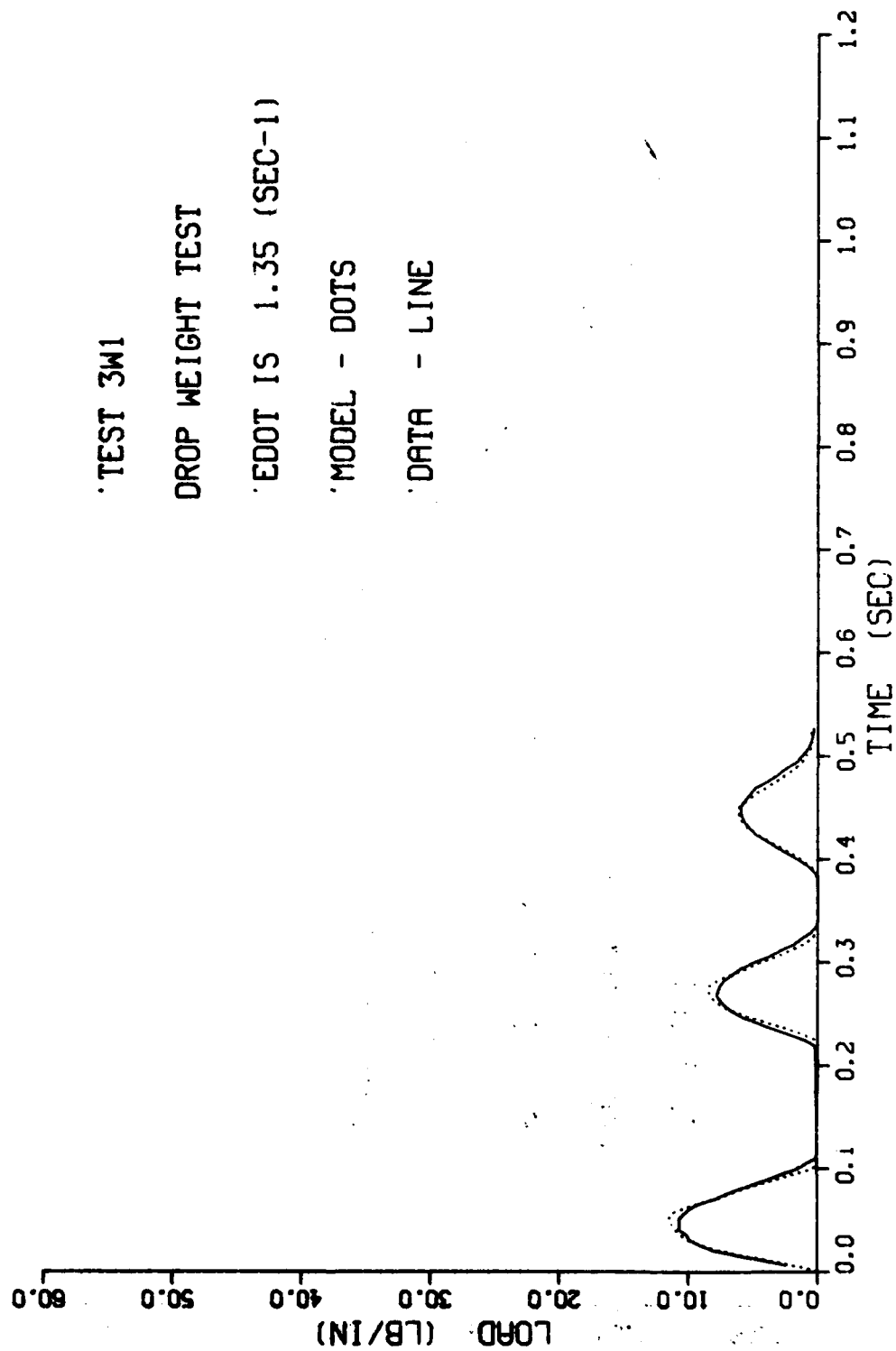
EDOT IS 1.38 (SEC-1)

MODEL - DOTS

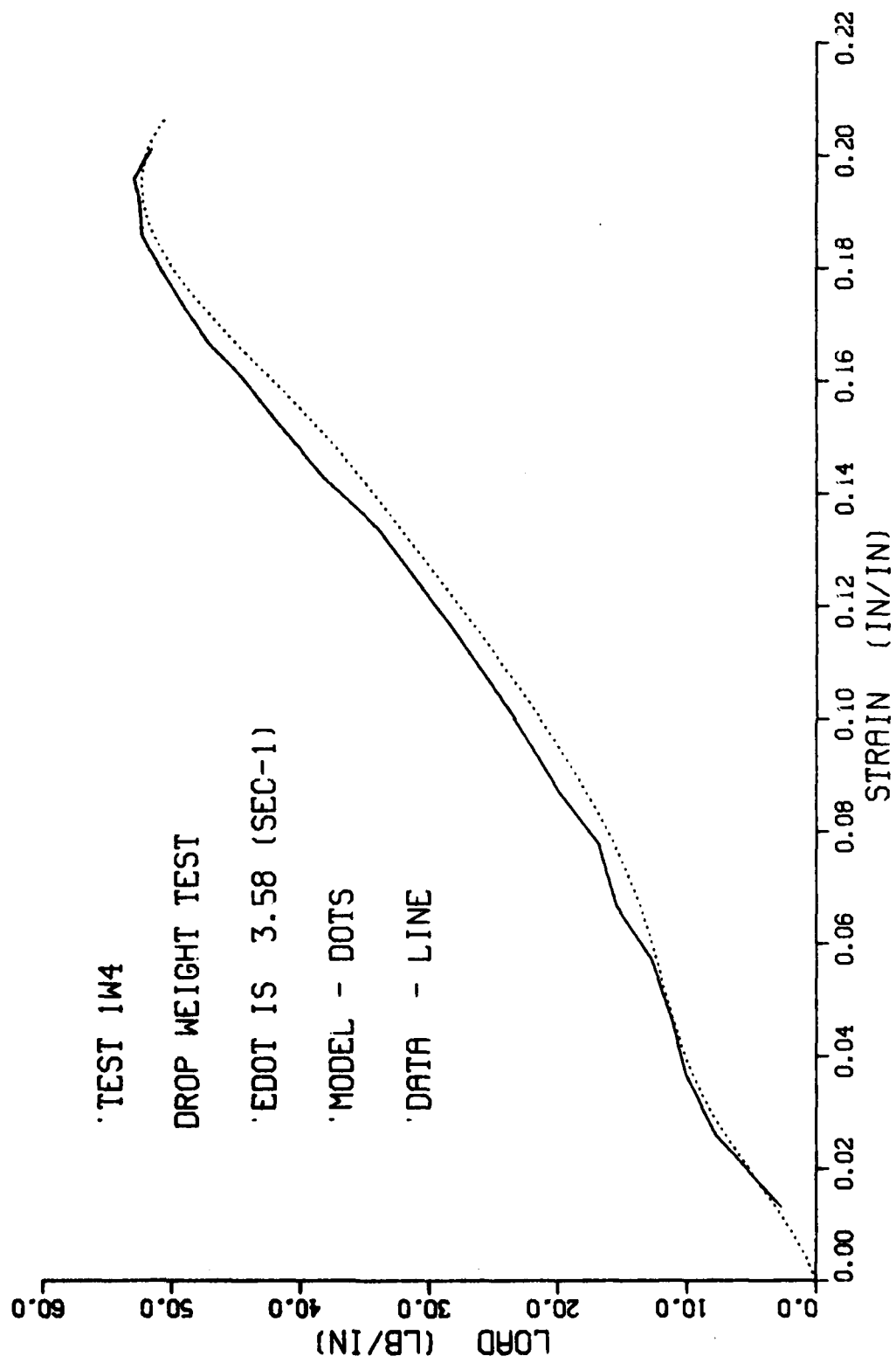
DATA - LINE











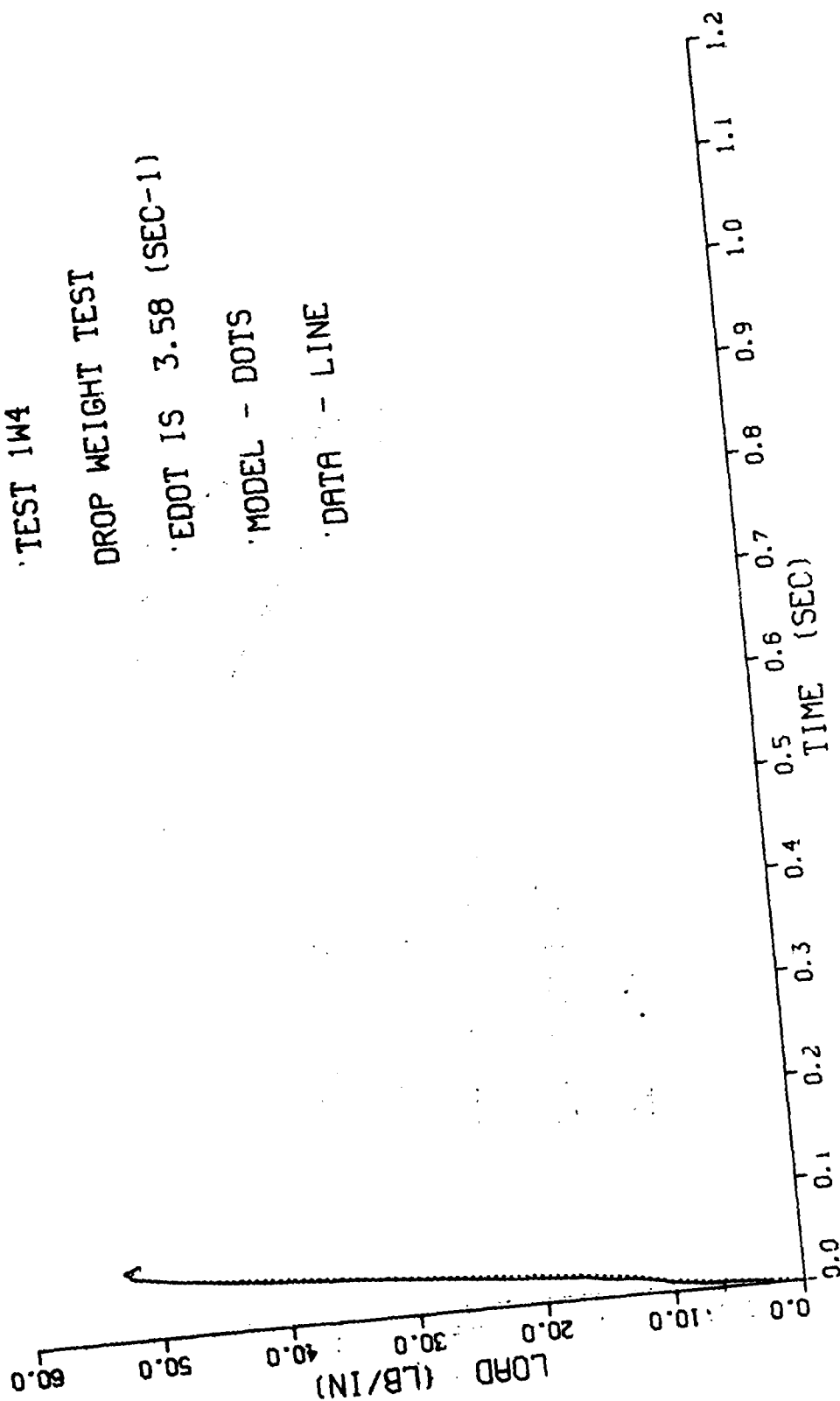
TEST 1W4

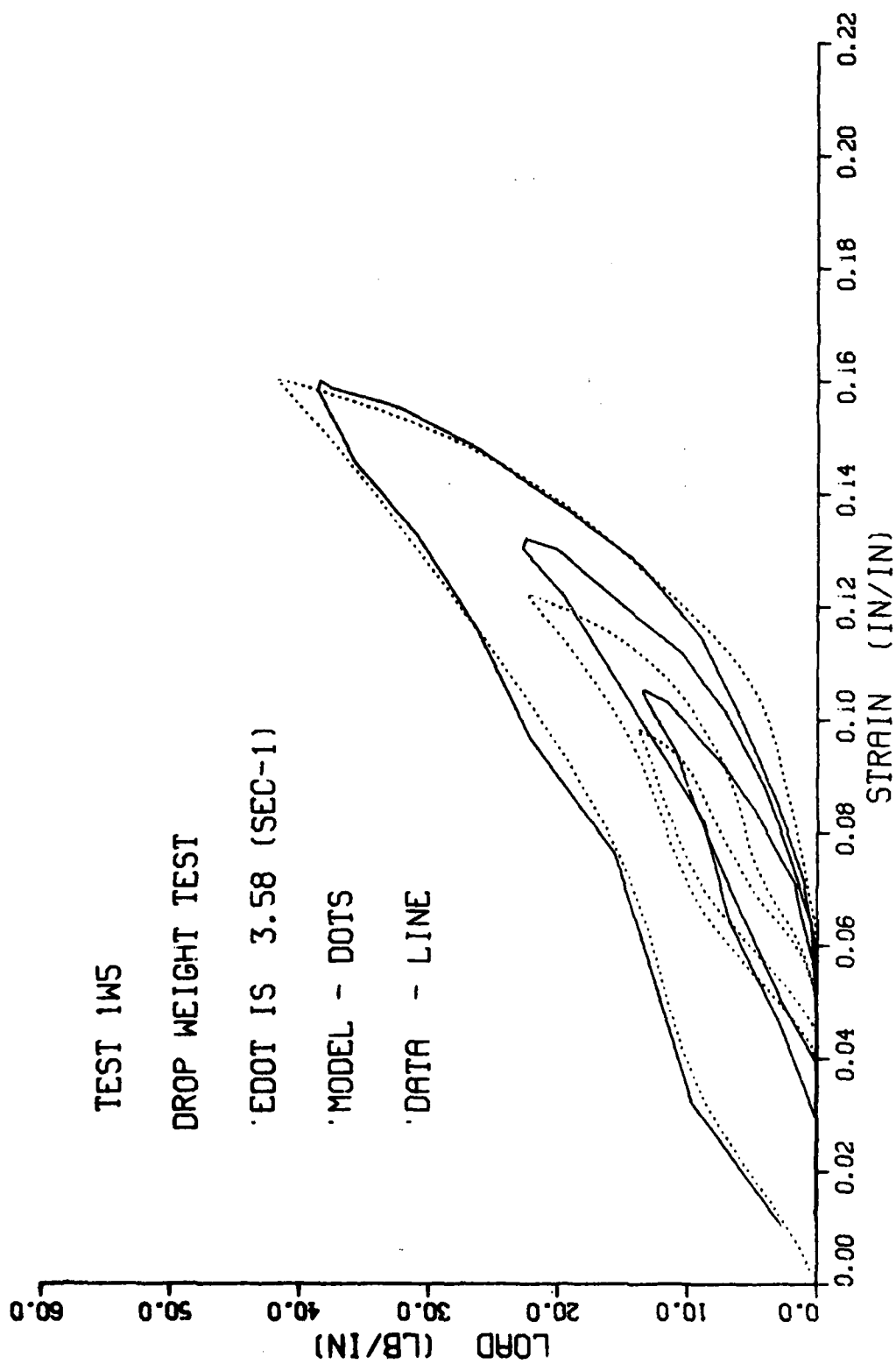
DROP WEIGHT TEST

EDOT IS 3.58 (SEC-1)

MODEL - DOTS

DATA - LINE





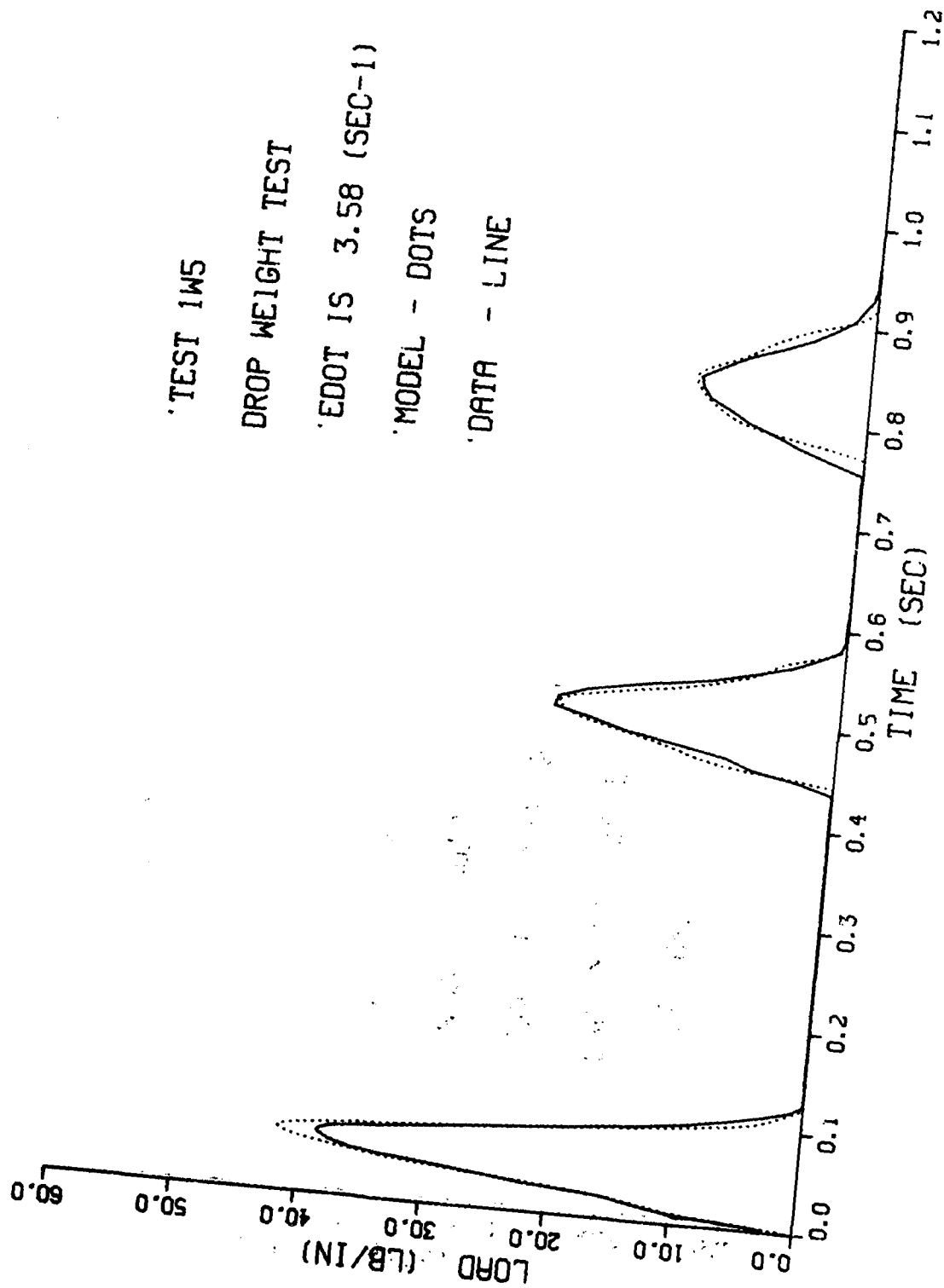
TEST 1W5

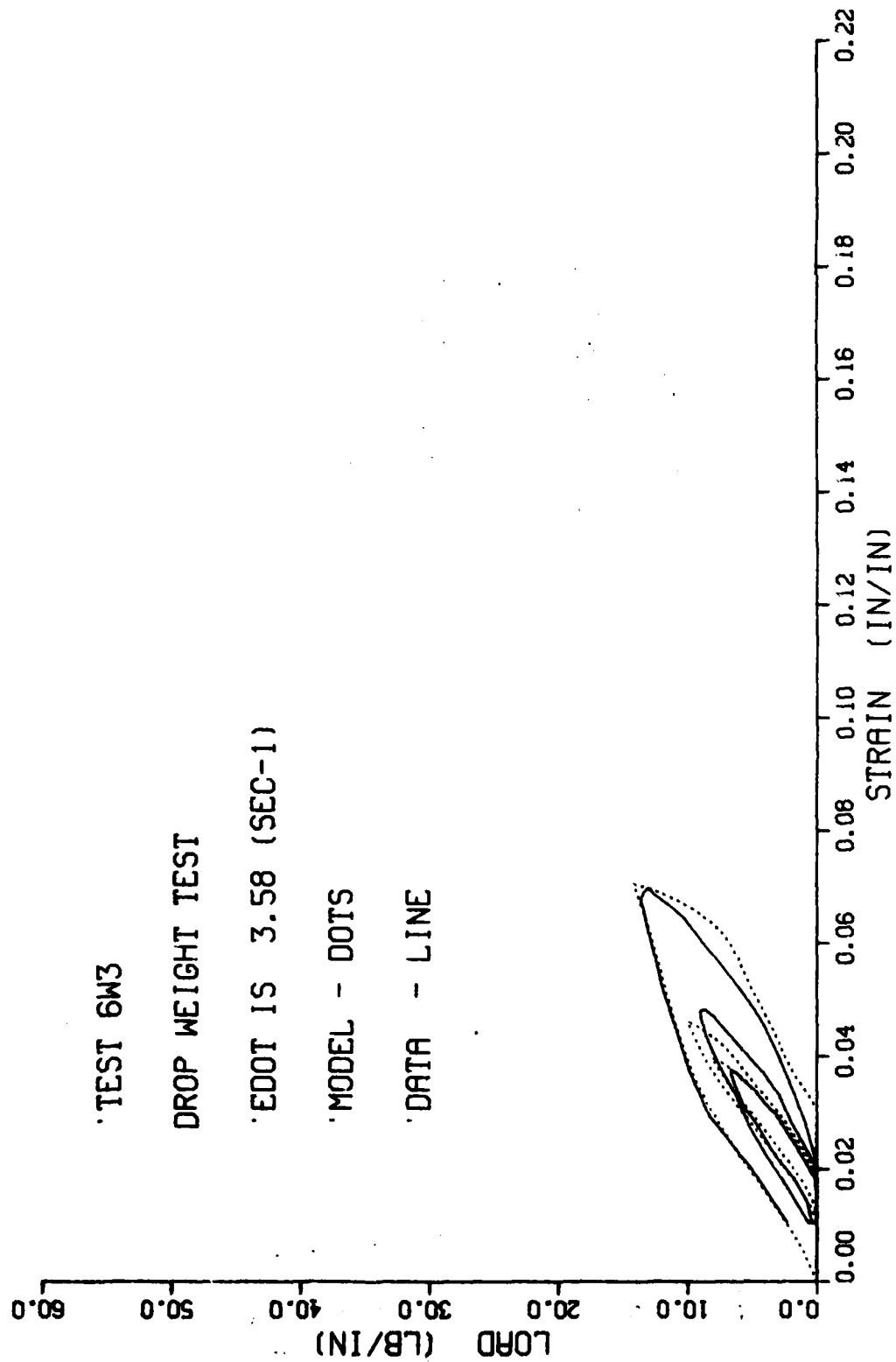
DROP WEIGHT TEST

EDOT IS 3.58 (SEC-1)

MODEL - DOTS

DATA - LINE





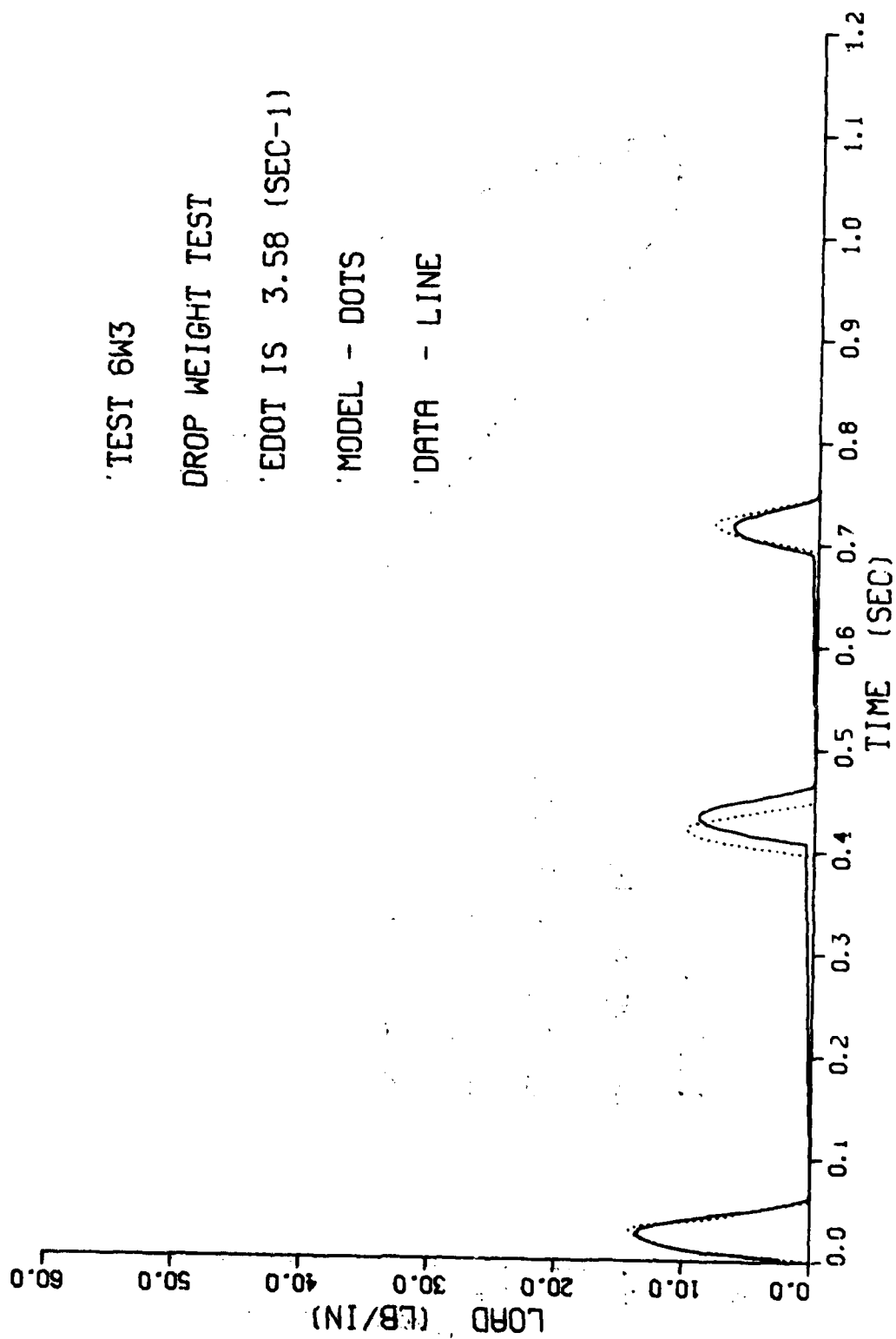
'TEST 6W3

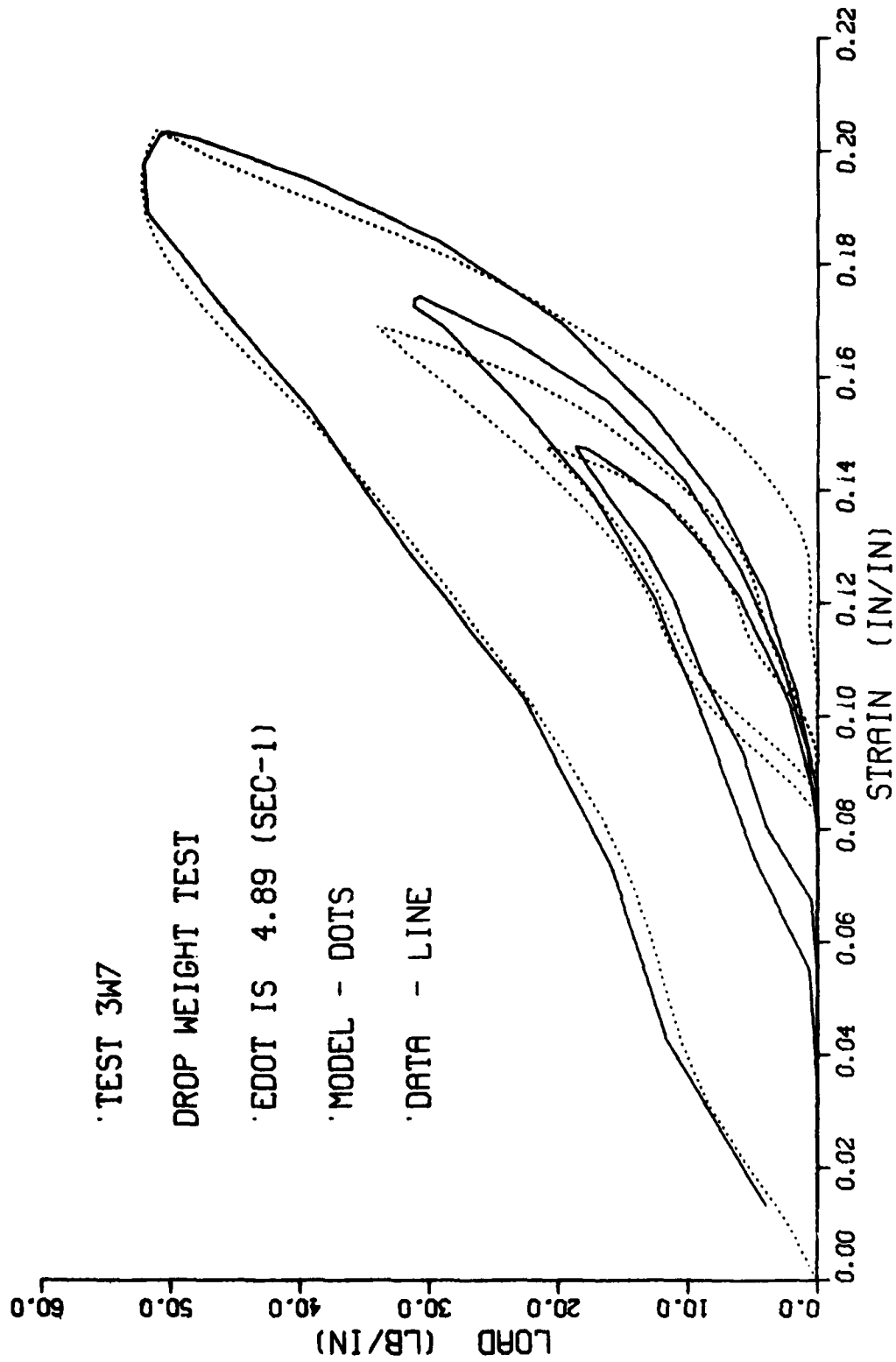
DROP WEIGHT TEST

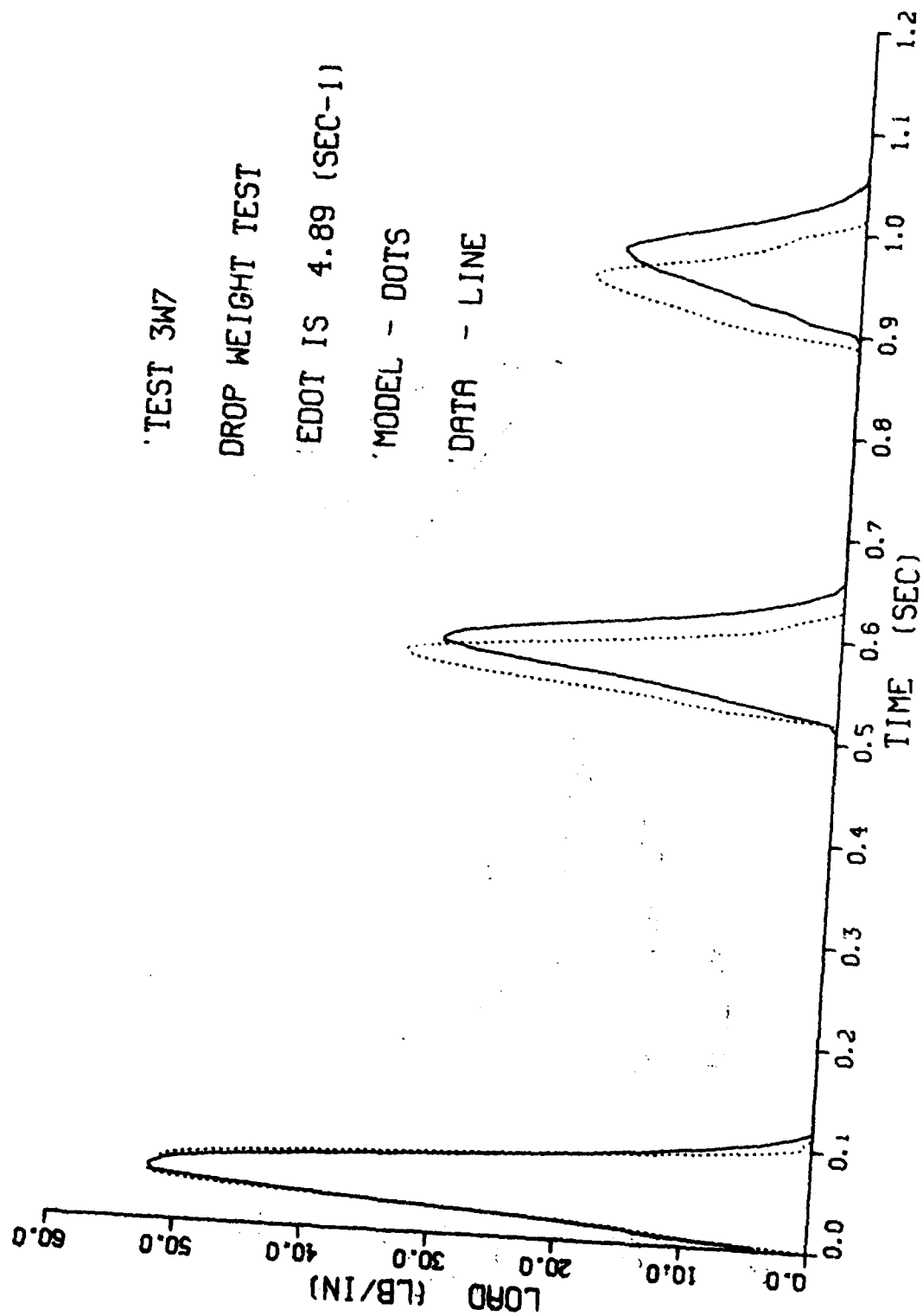
'EDOT IS 3.58 (SEC-1)

'MODEL - DOTS

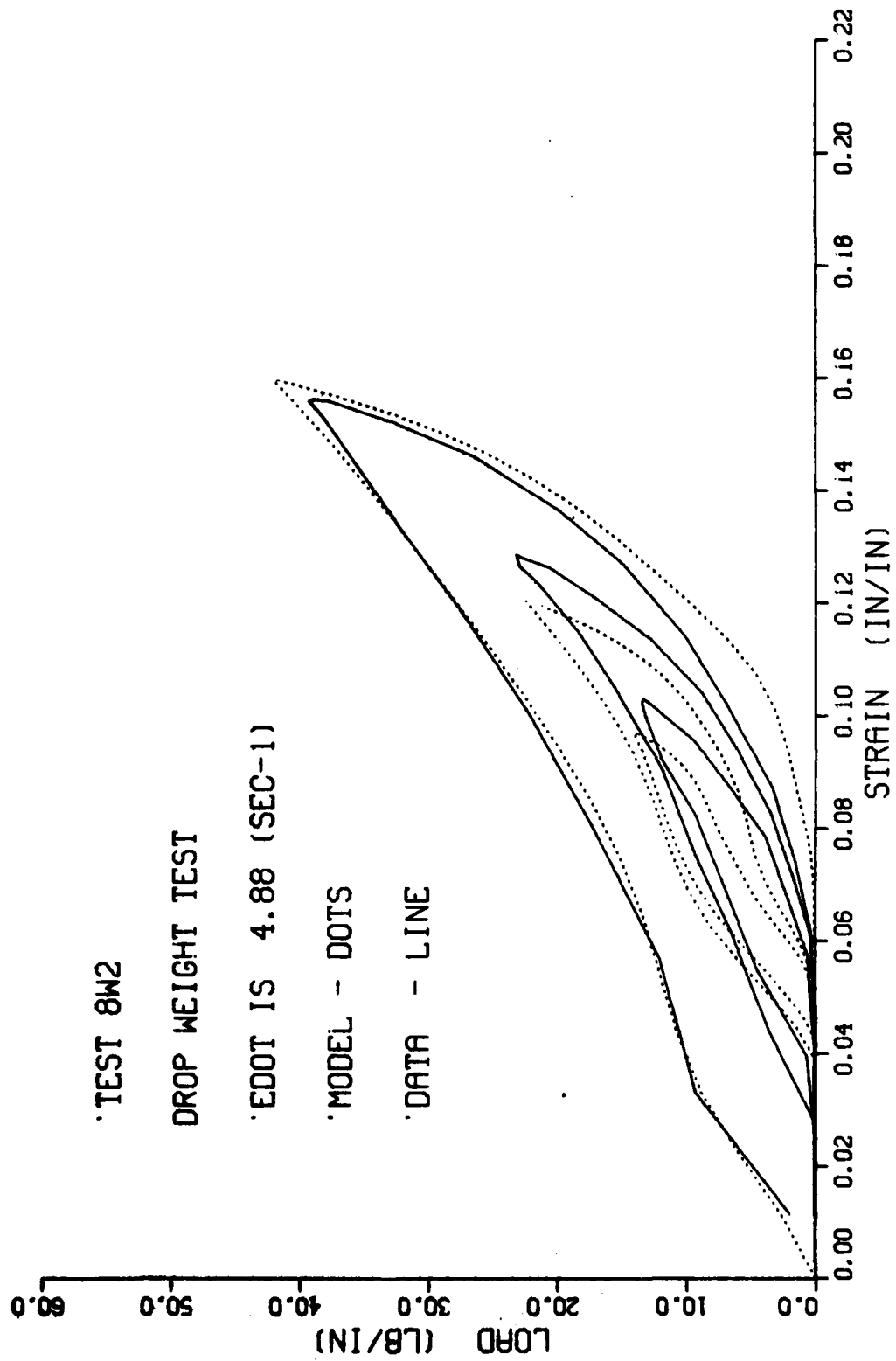
'DATA - LINE











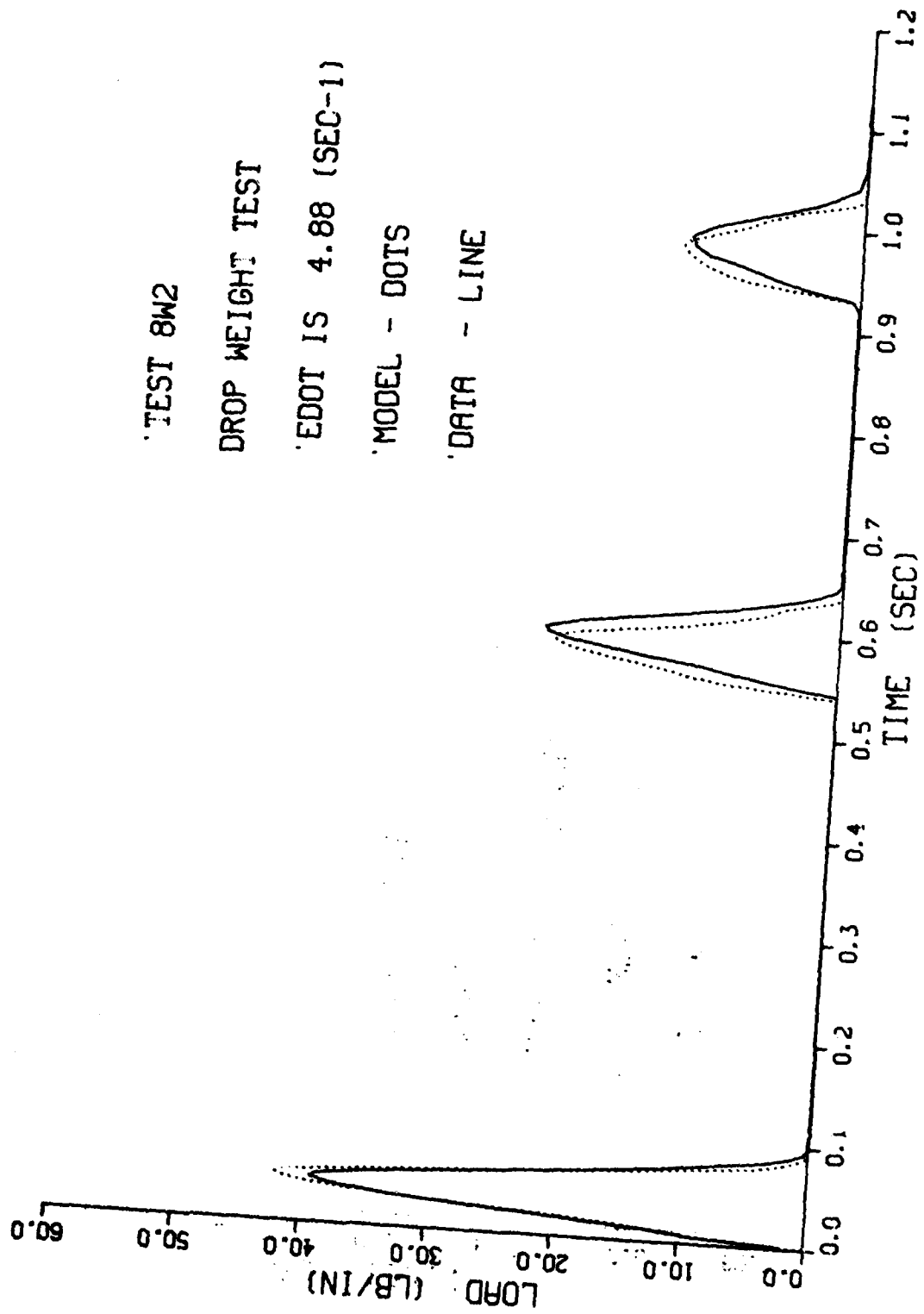
TEST 8W2

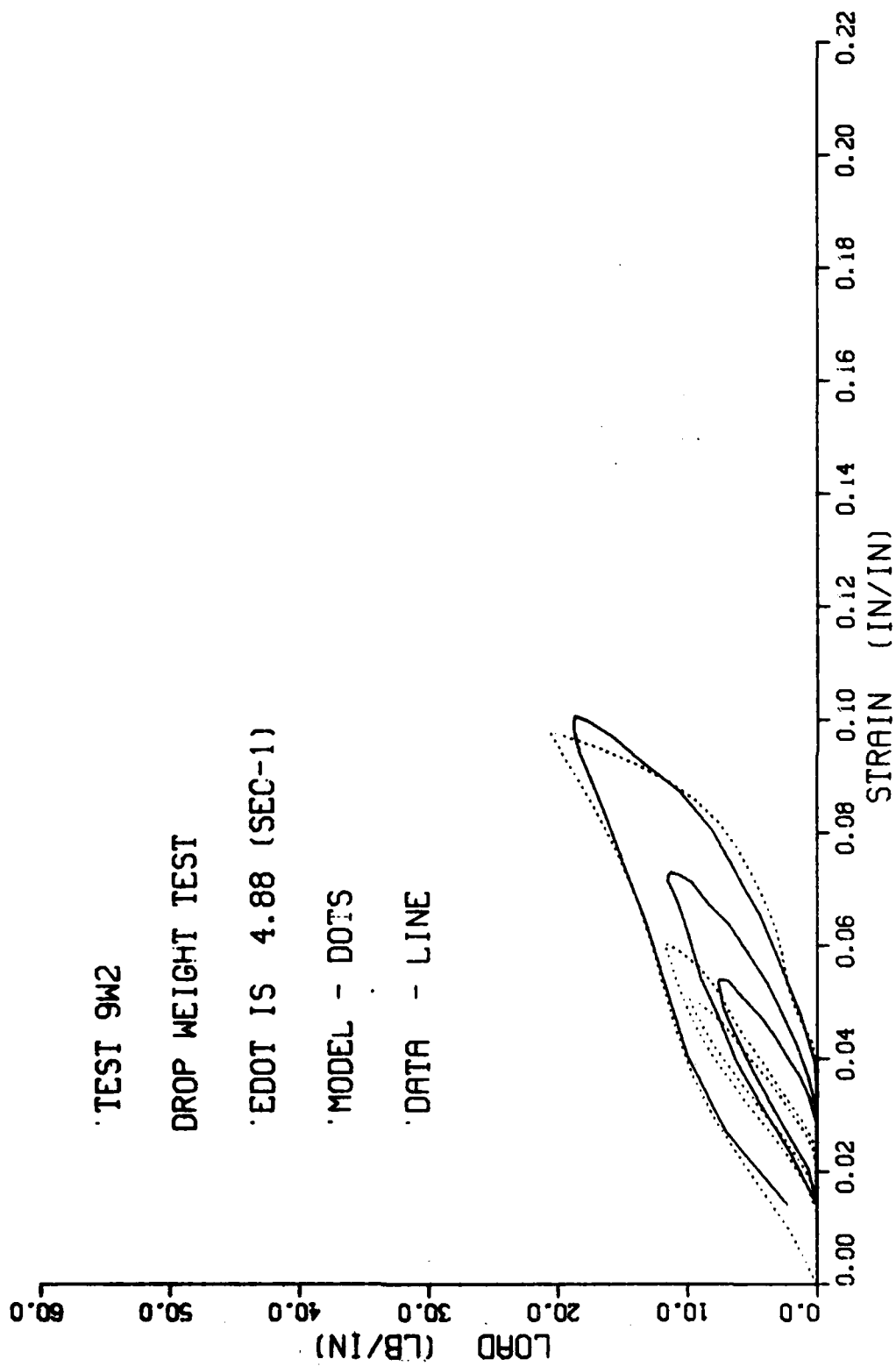
DROP WEIGHT TEST

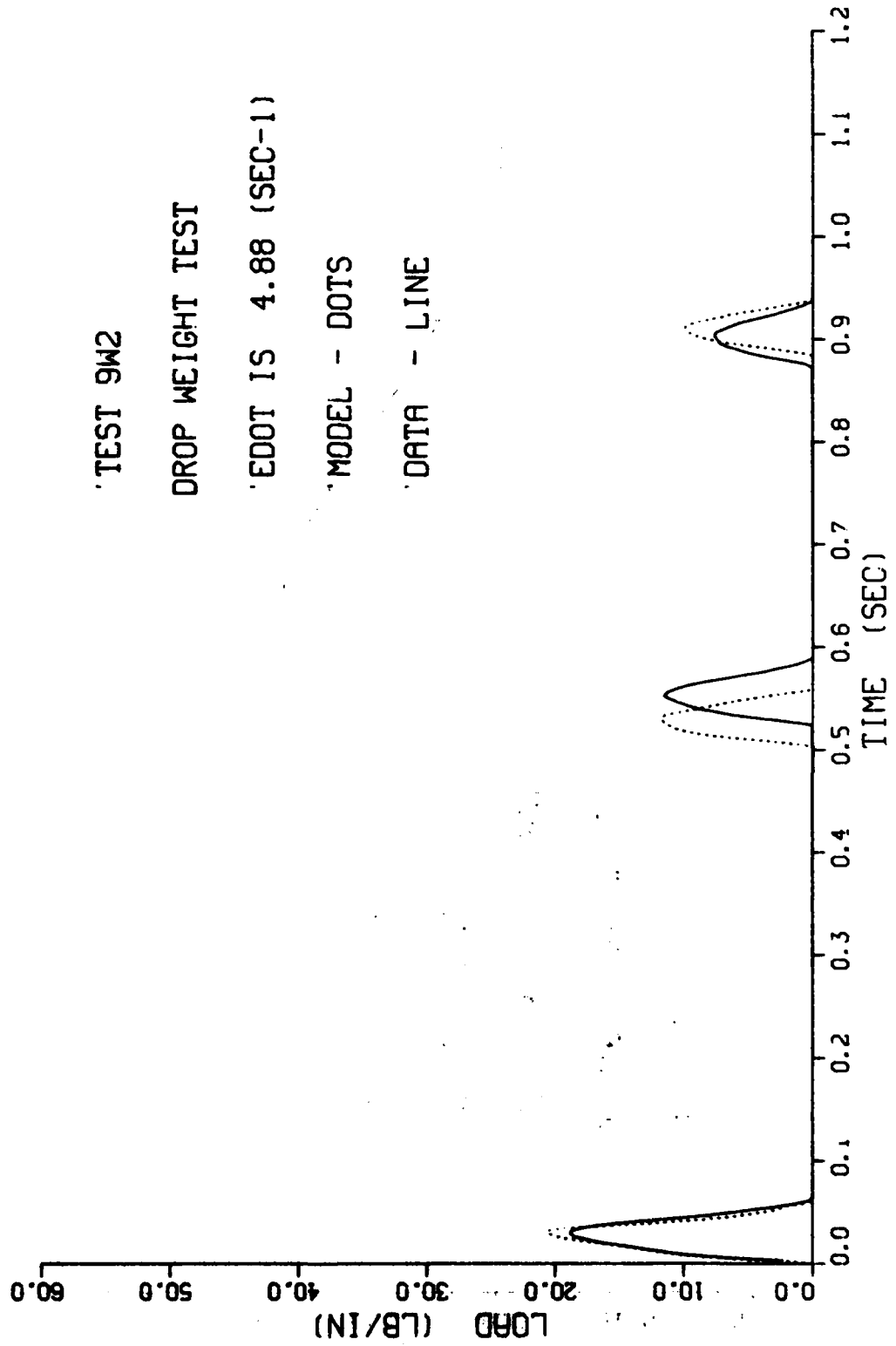
EDOT IS 4.88 (SEC-1)

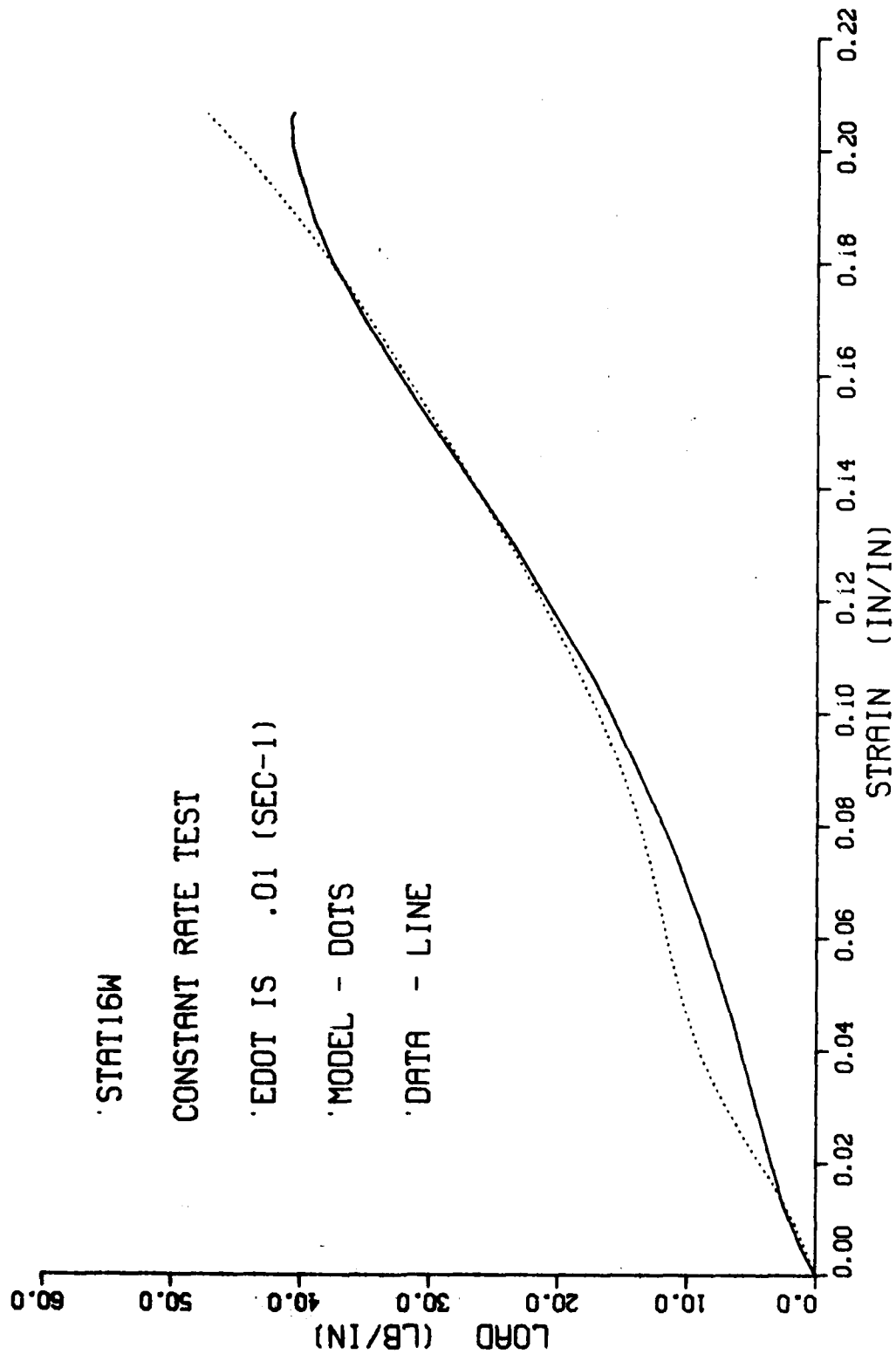
MODEL - DOTS

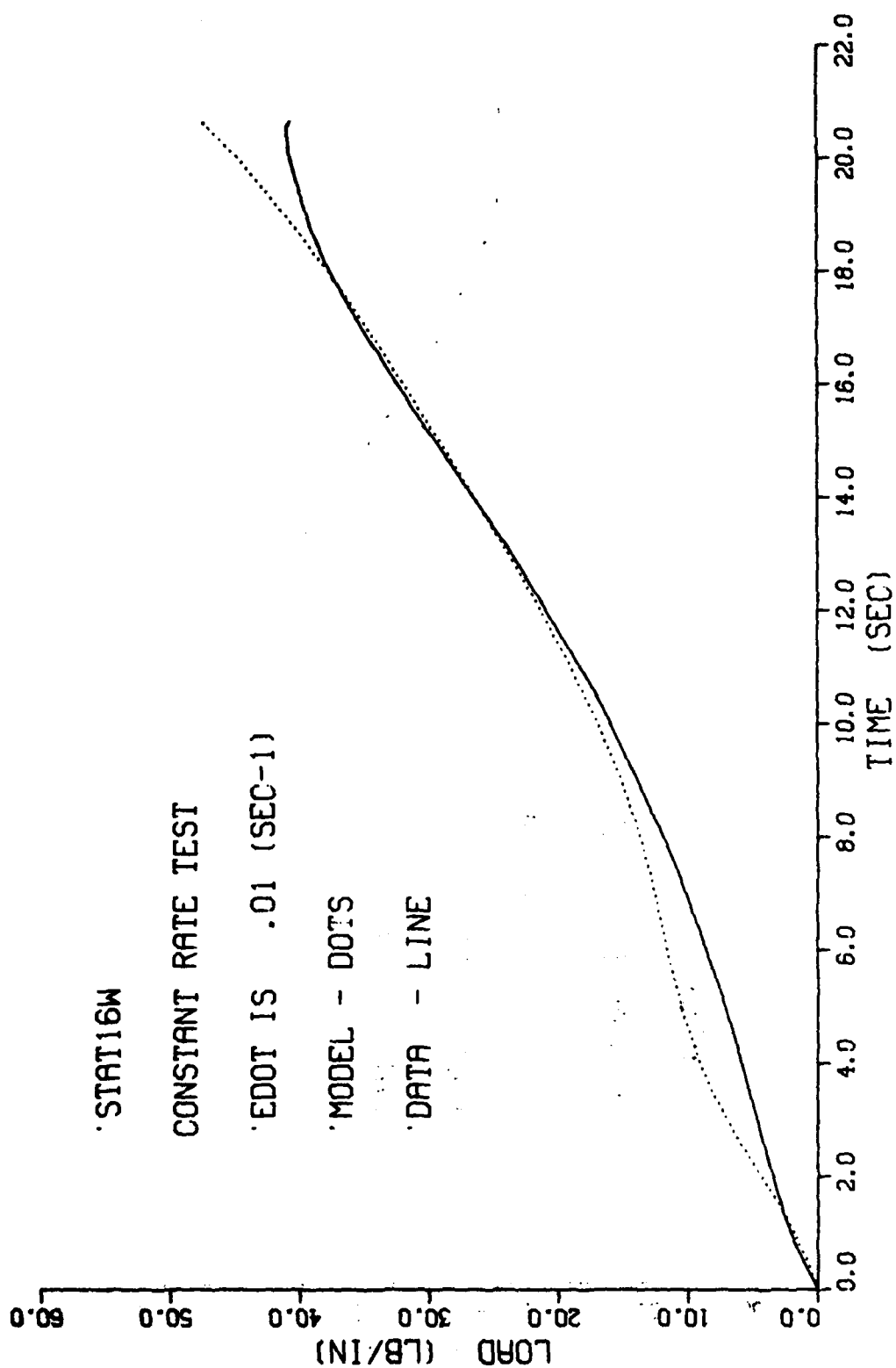
DATA - LINE

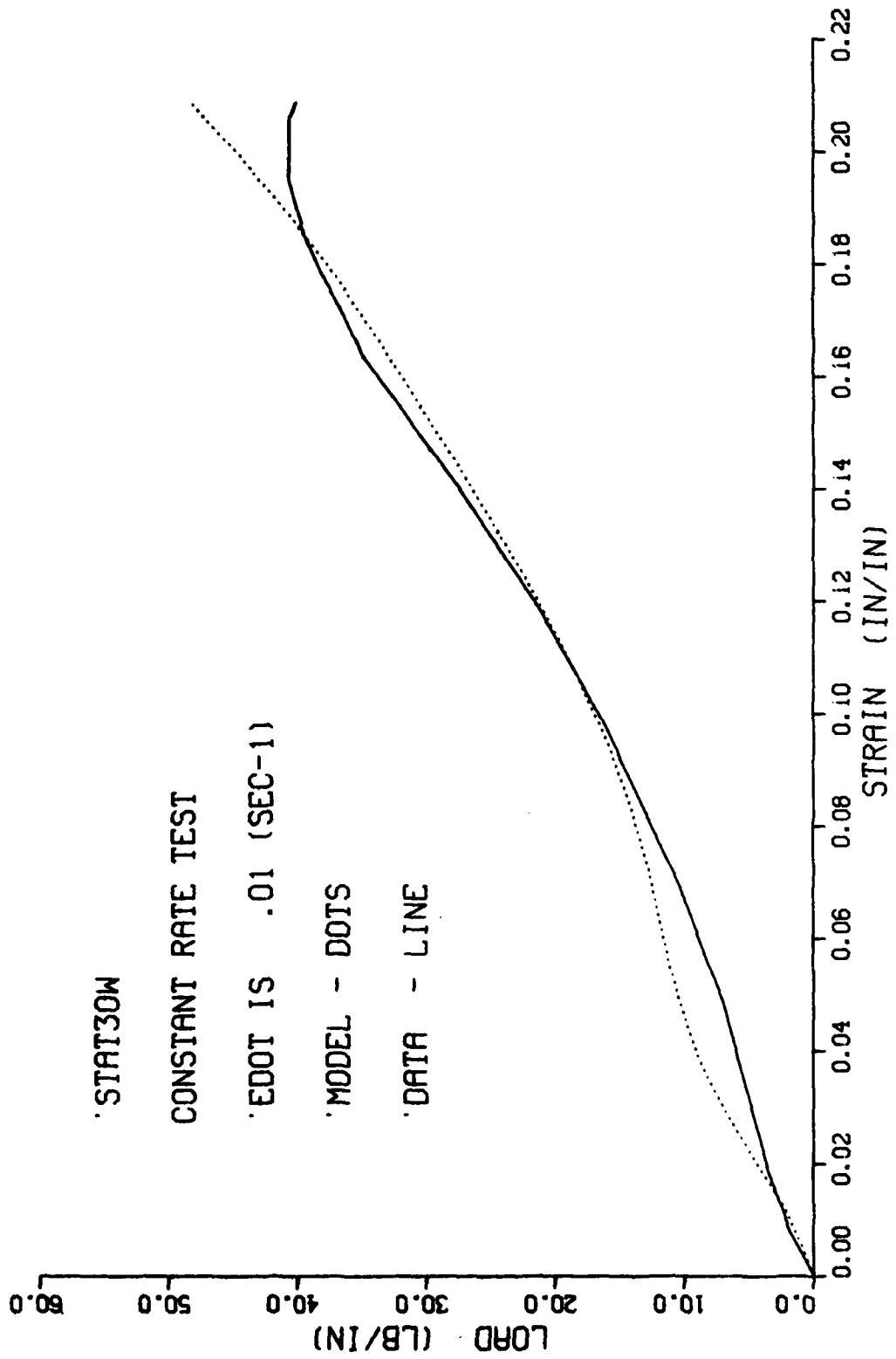


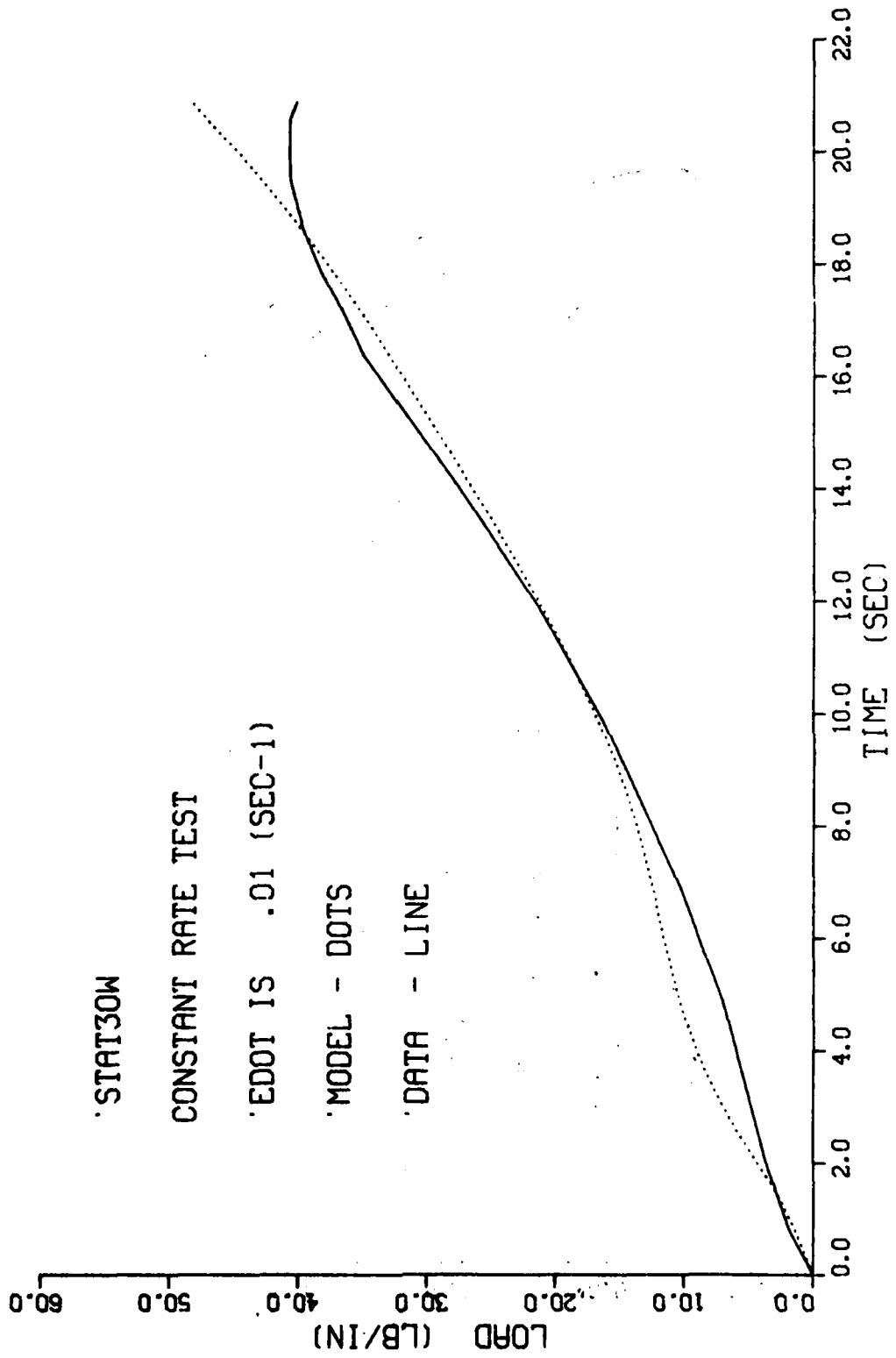




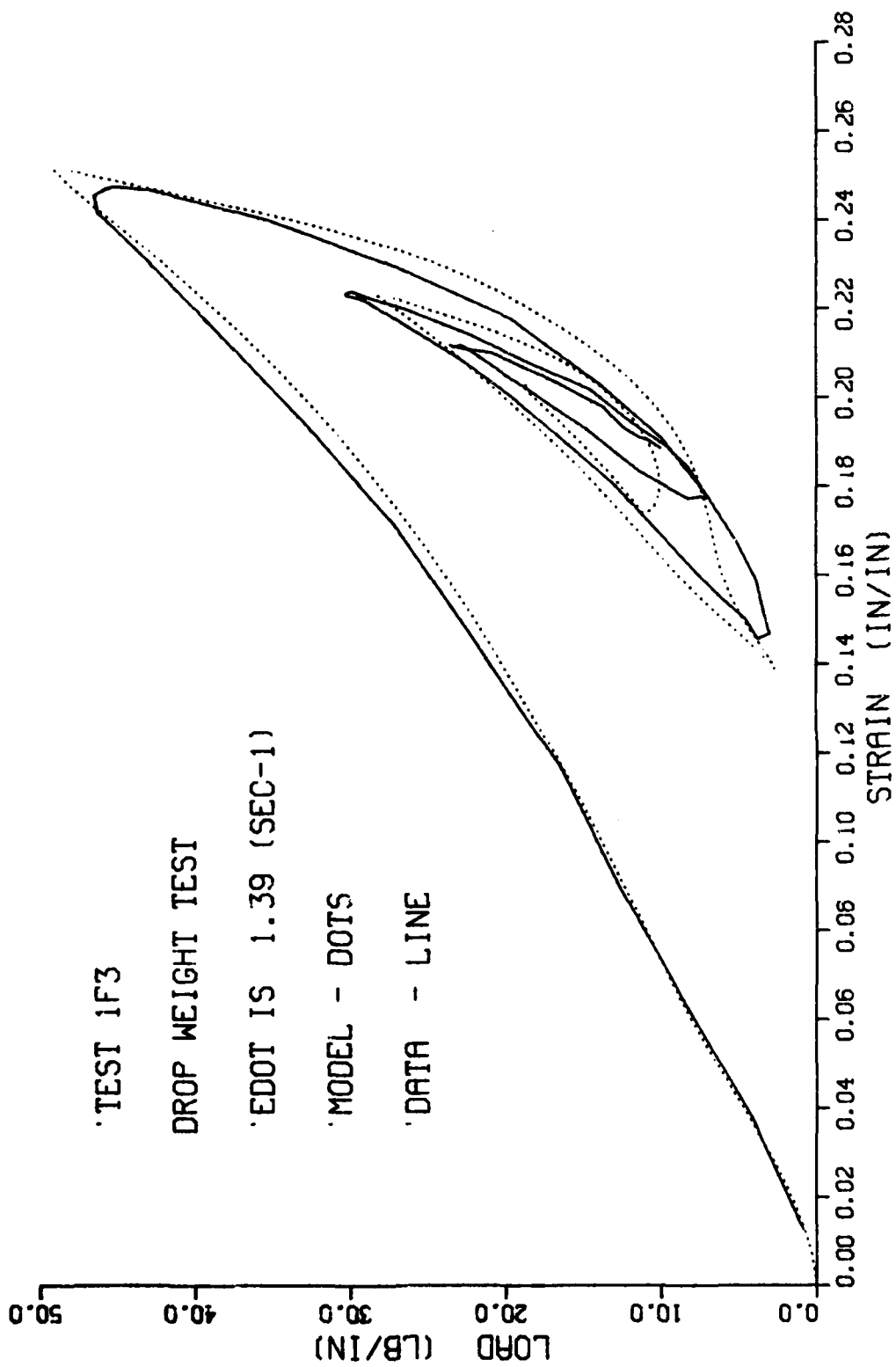


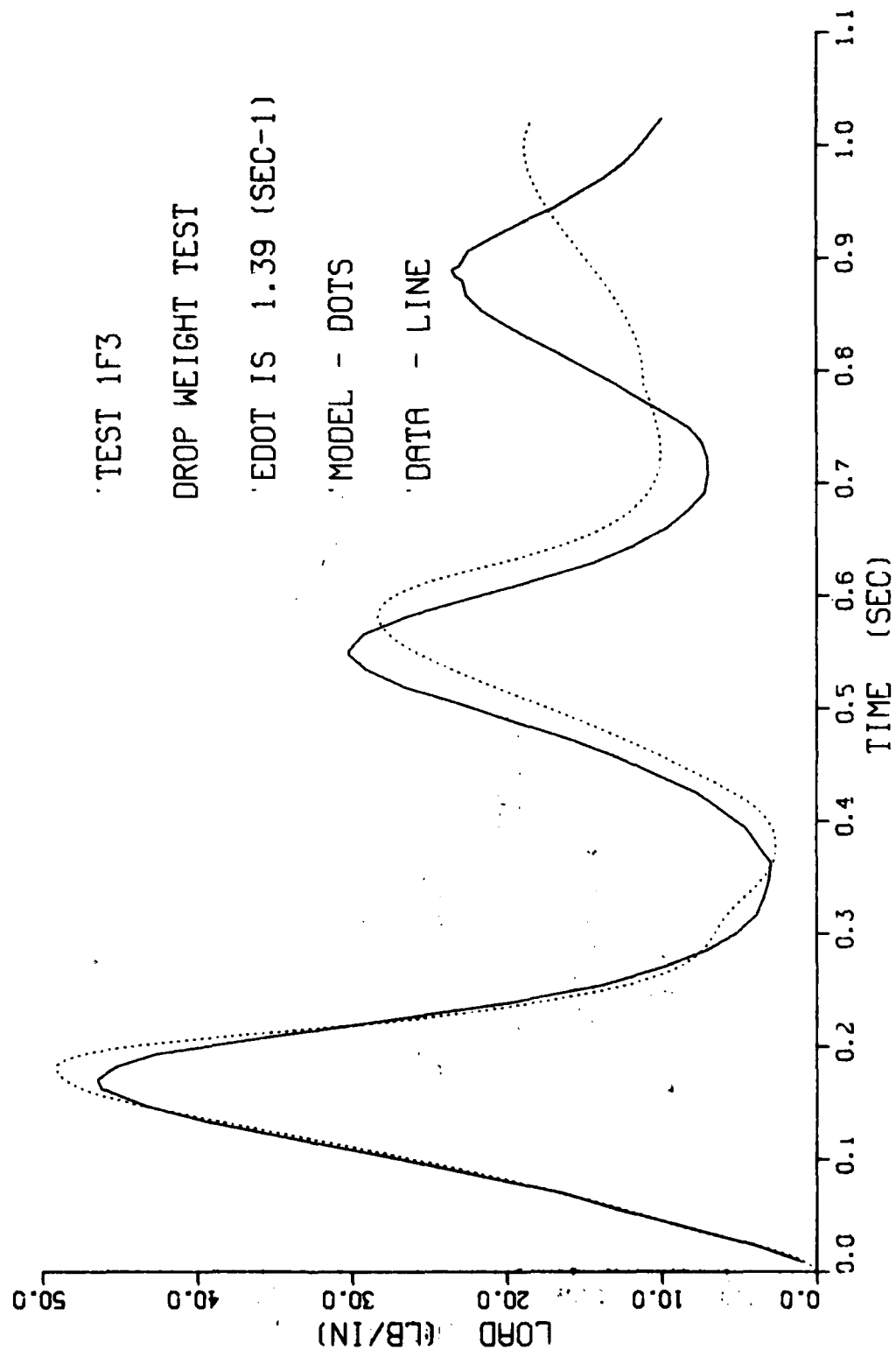


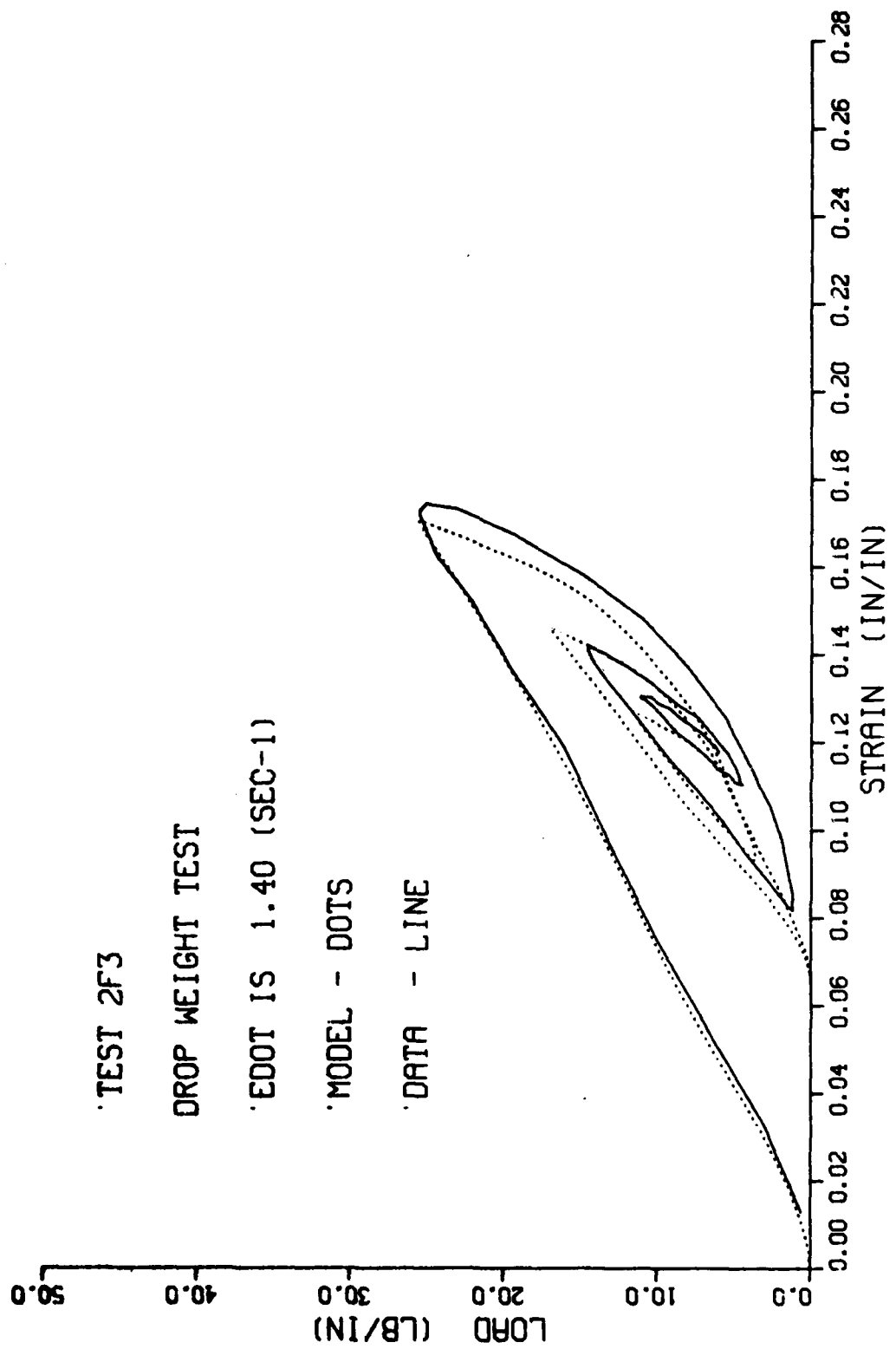


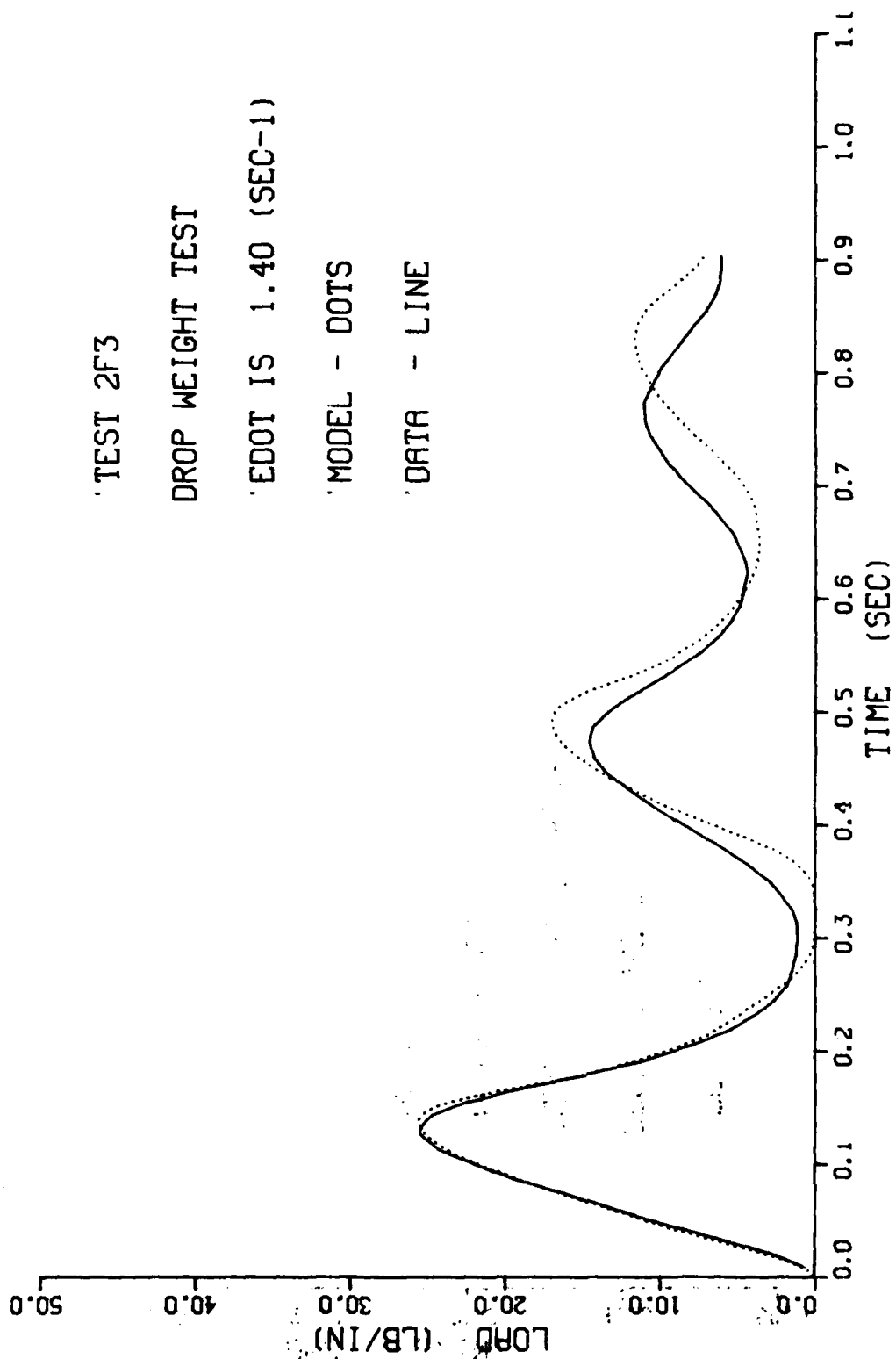


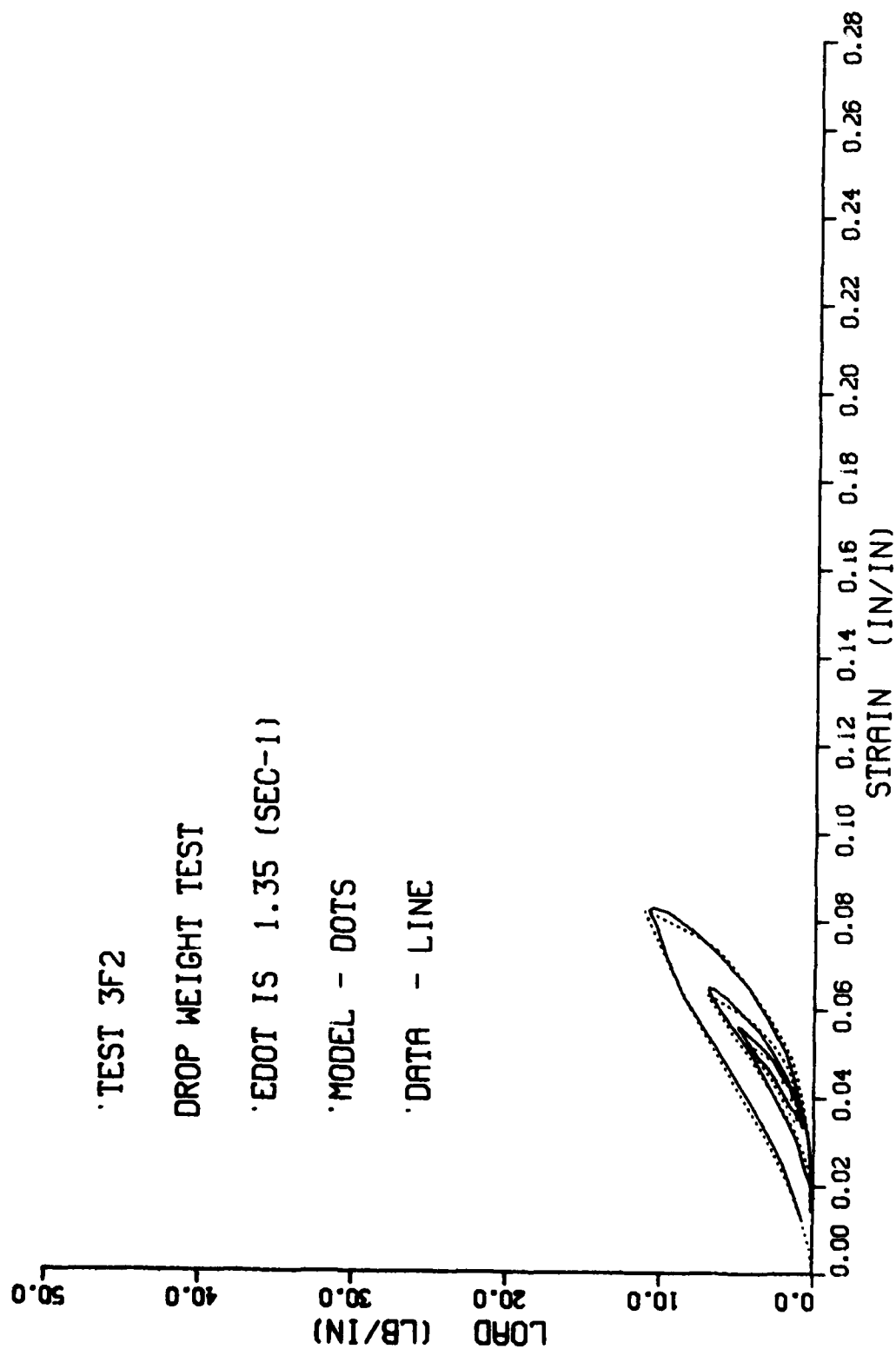












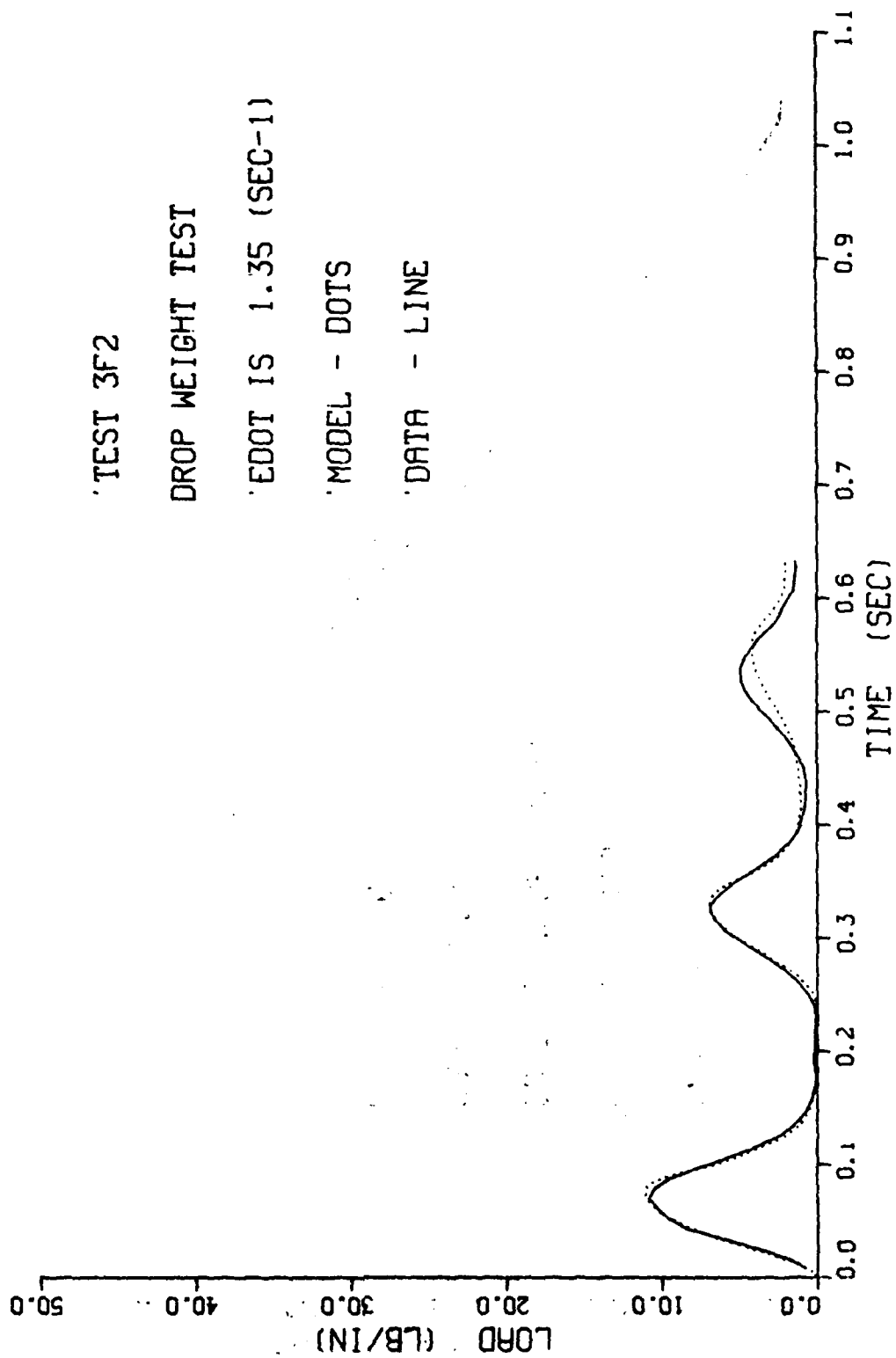
'TEST 3F2

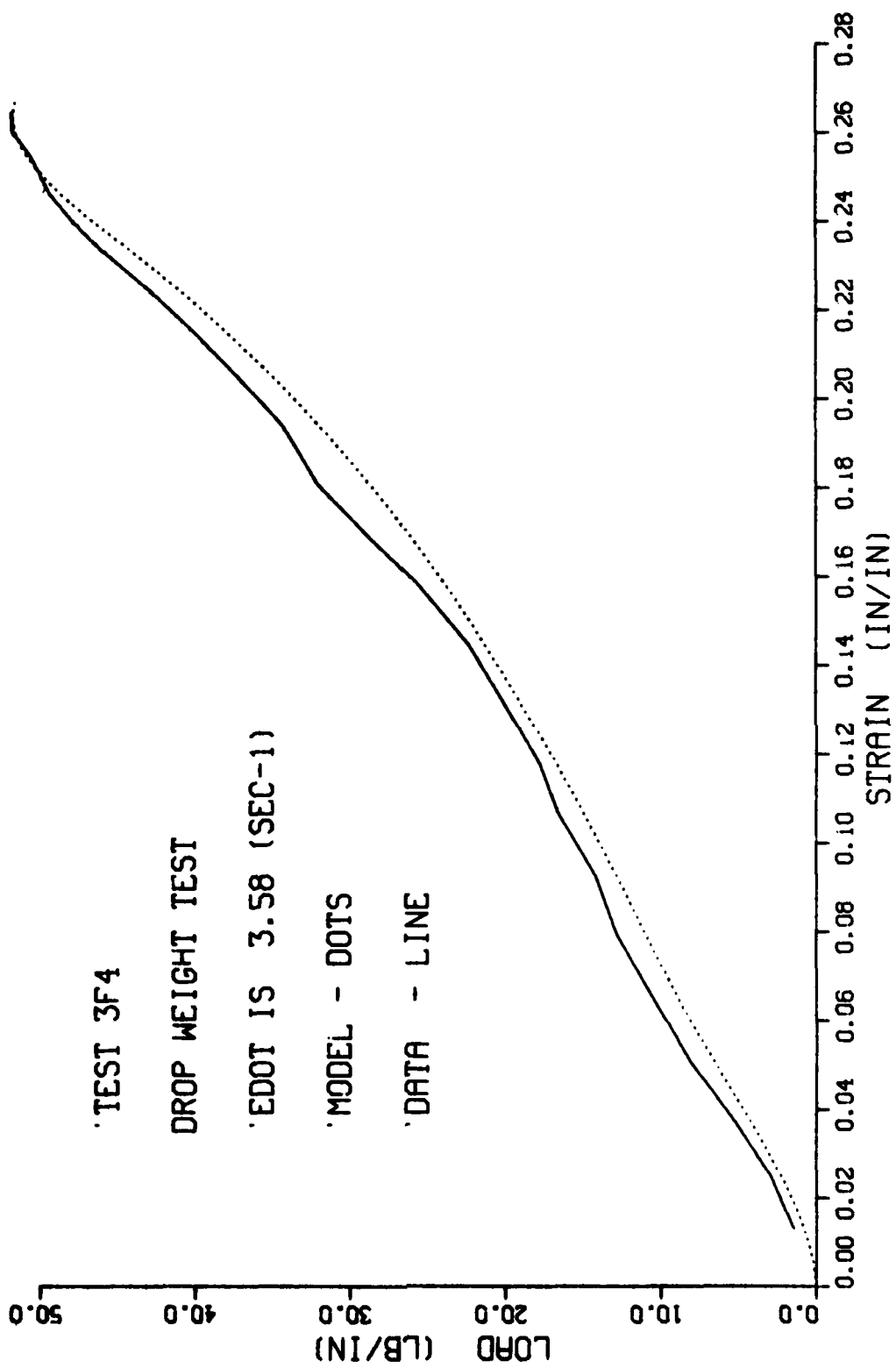
DROP WEIGHT TEST

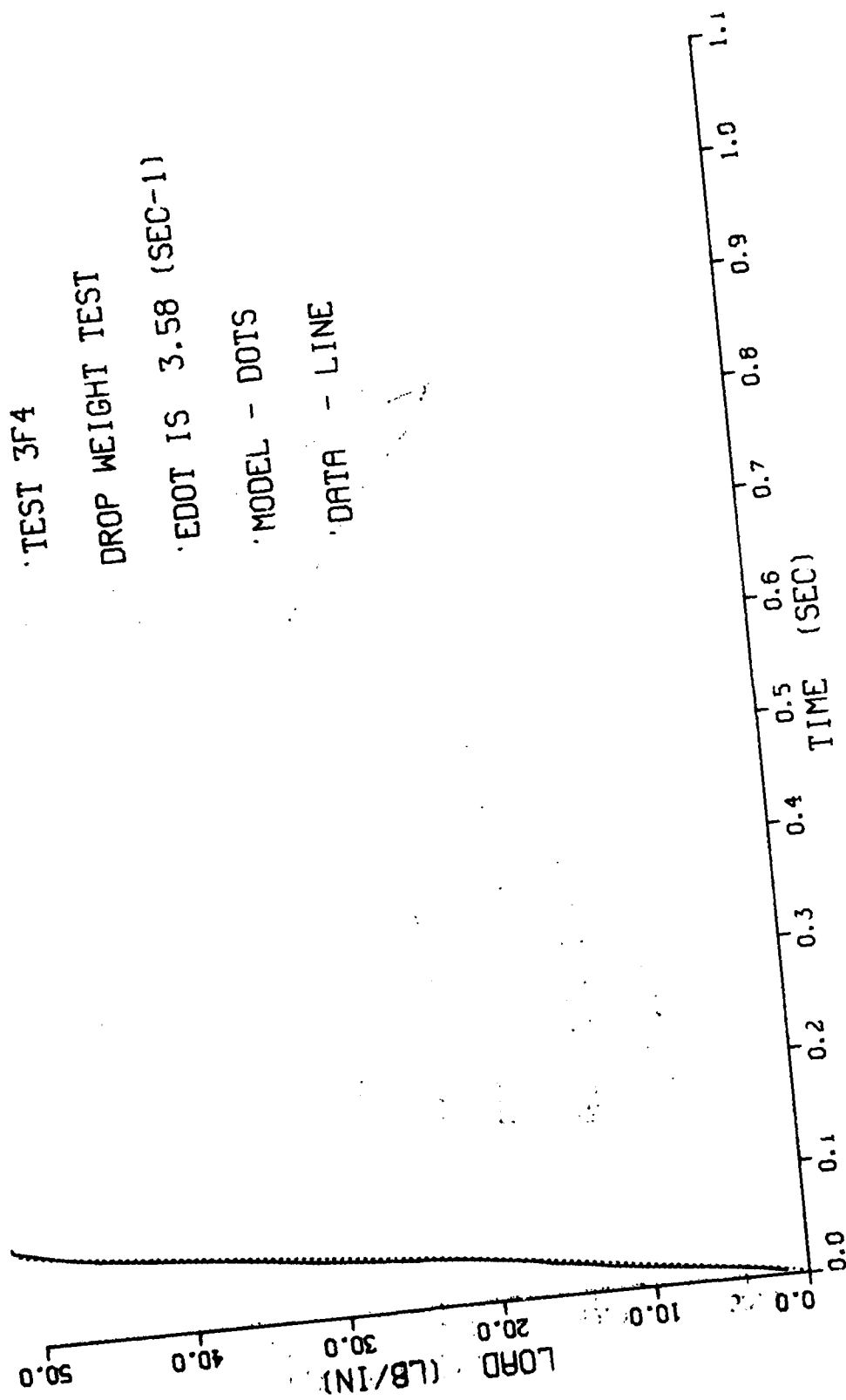
'EDOT IS 1.35 (SEC-1)

'MODEL - DOTS

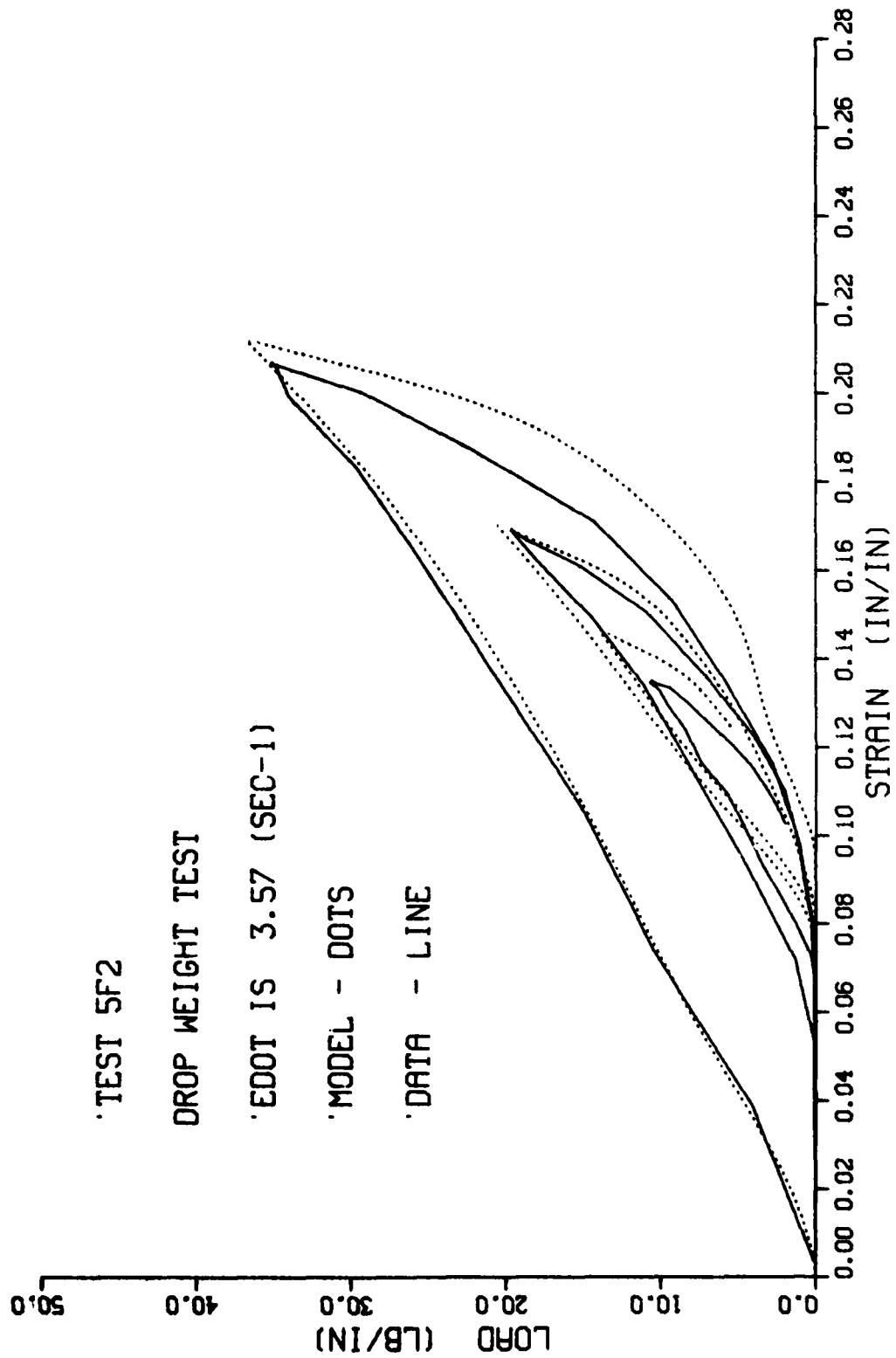
'DATA - LINE











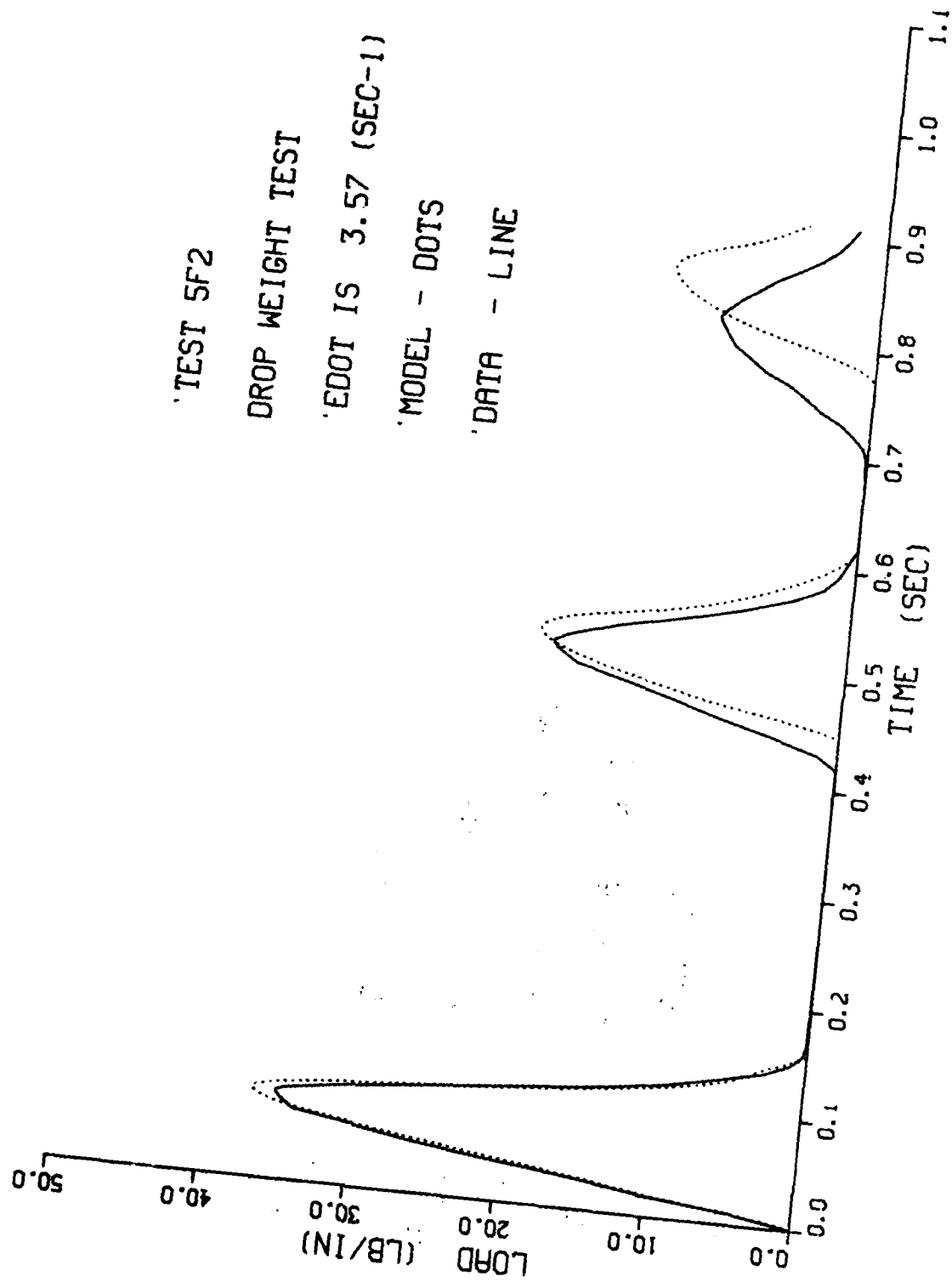
'TEST 5F2

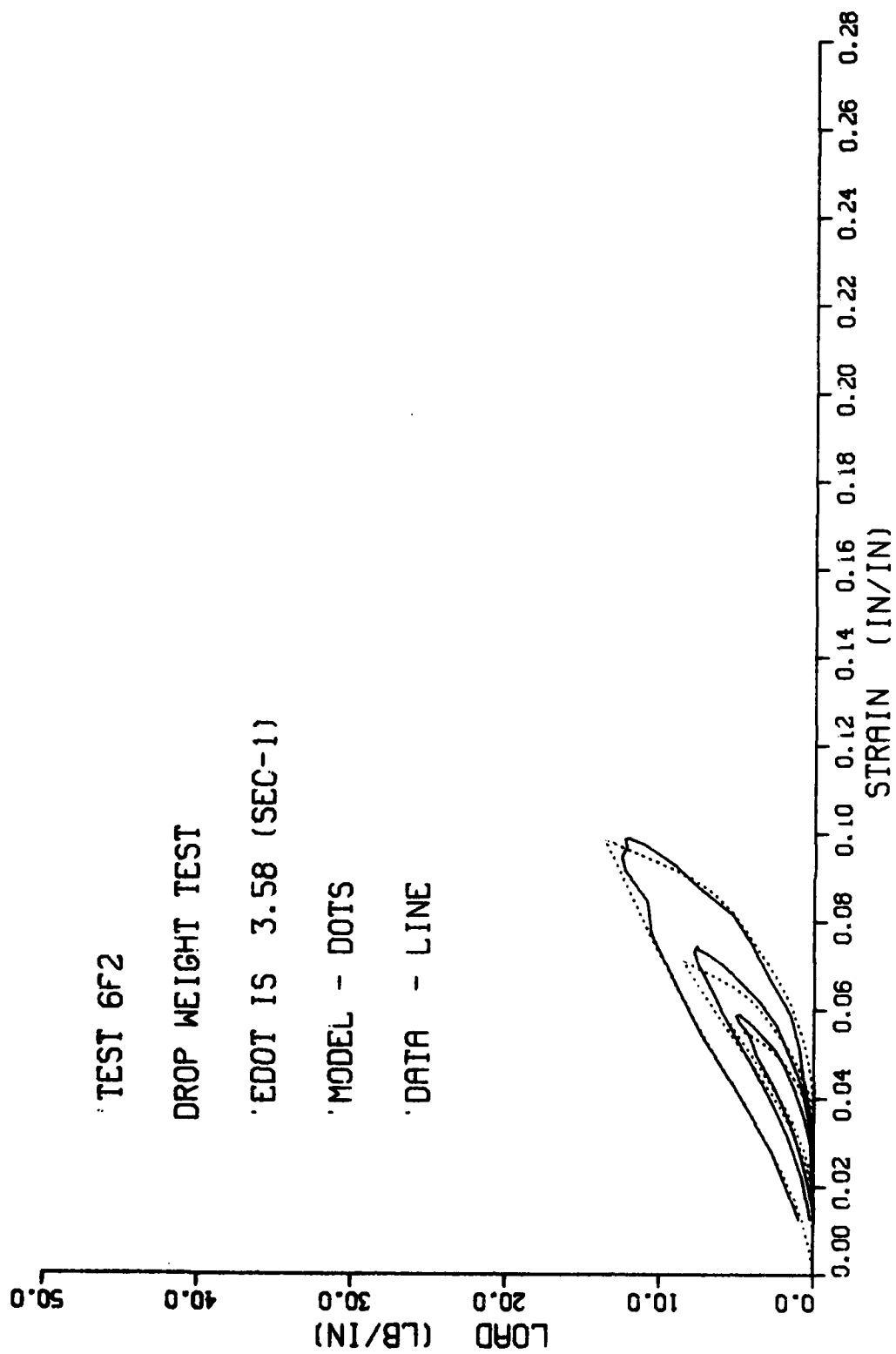
DROP WEIGHT TEST

'EDOT IS 3.57 (SEC-1)

'MODEL - DOTS

'DATA - LINE





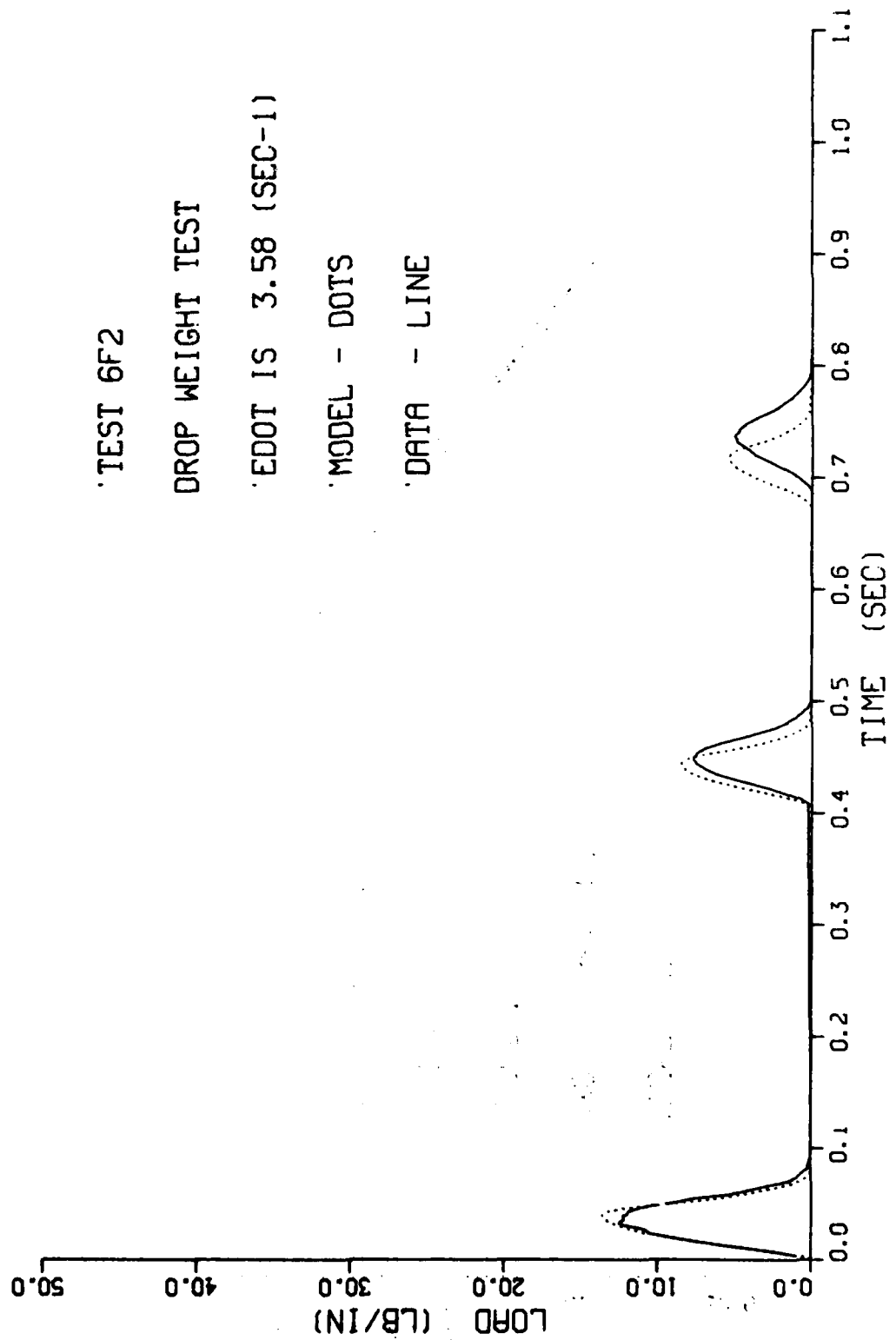
TEST 6F2

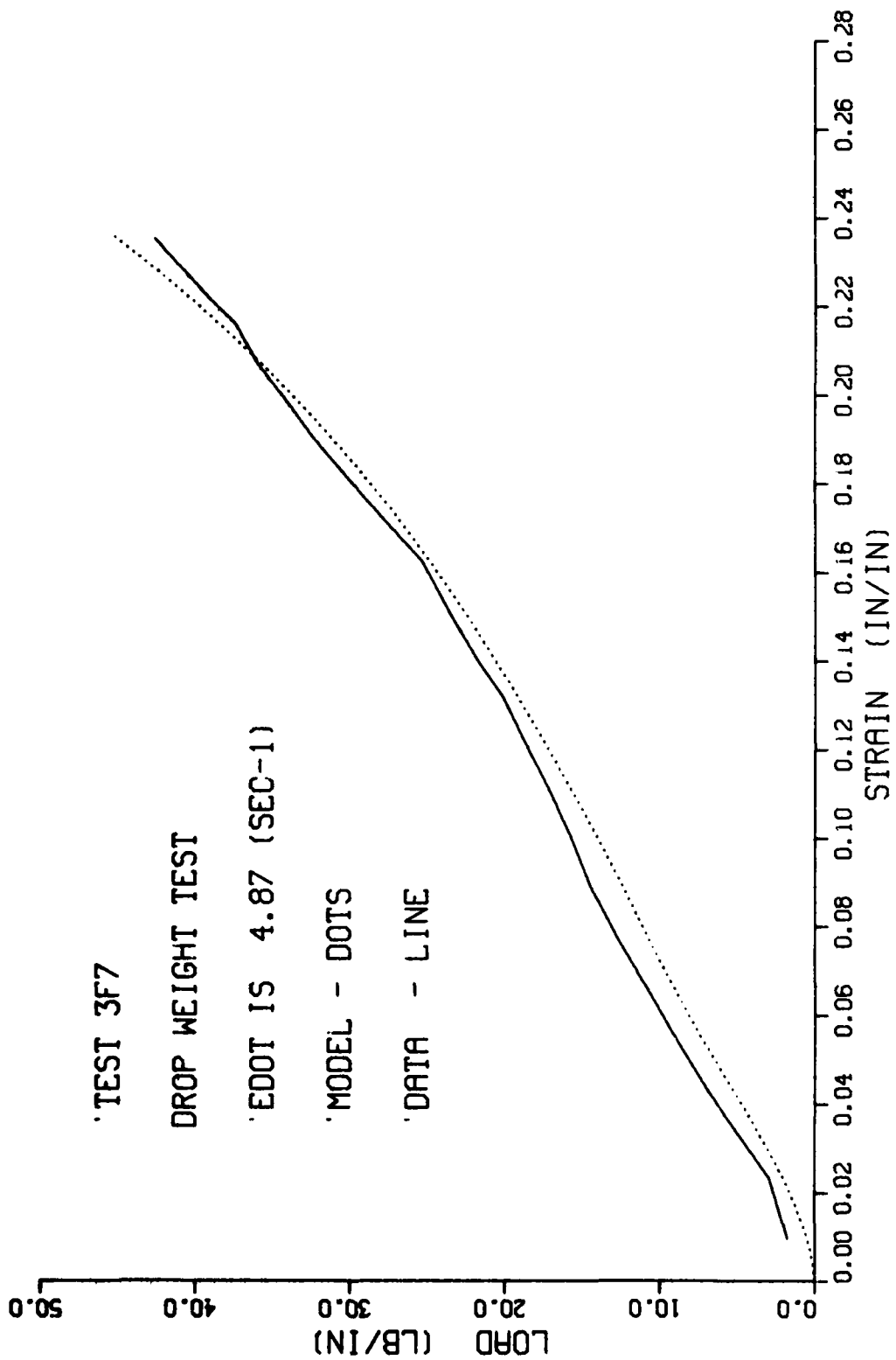
DROP WEIGHT TEST

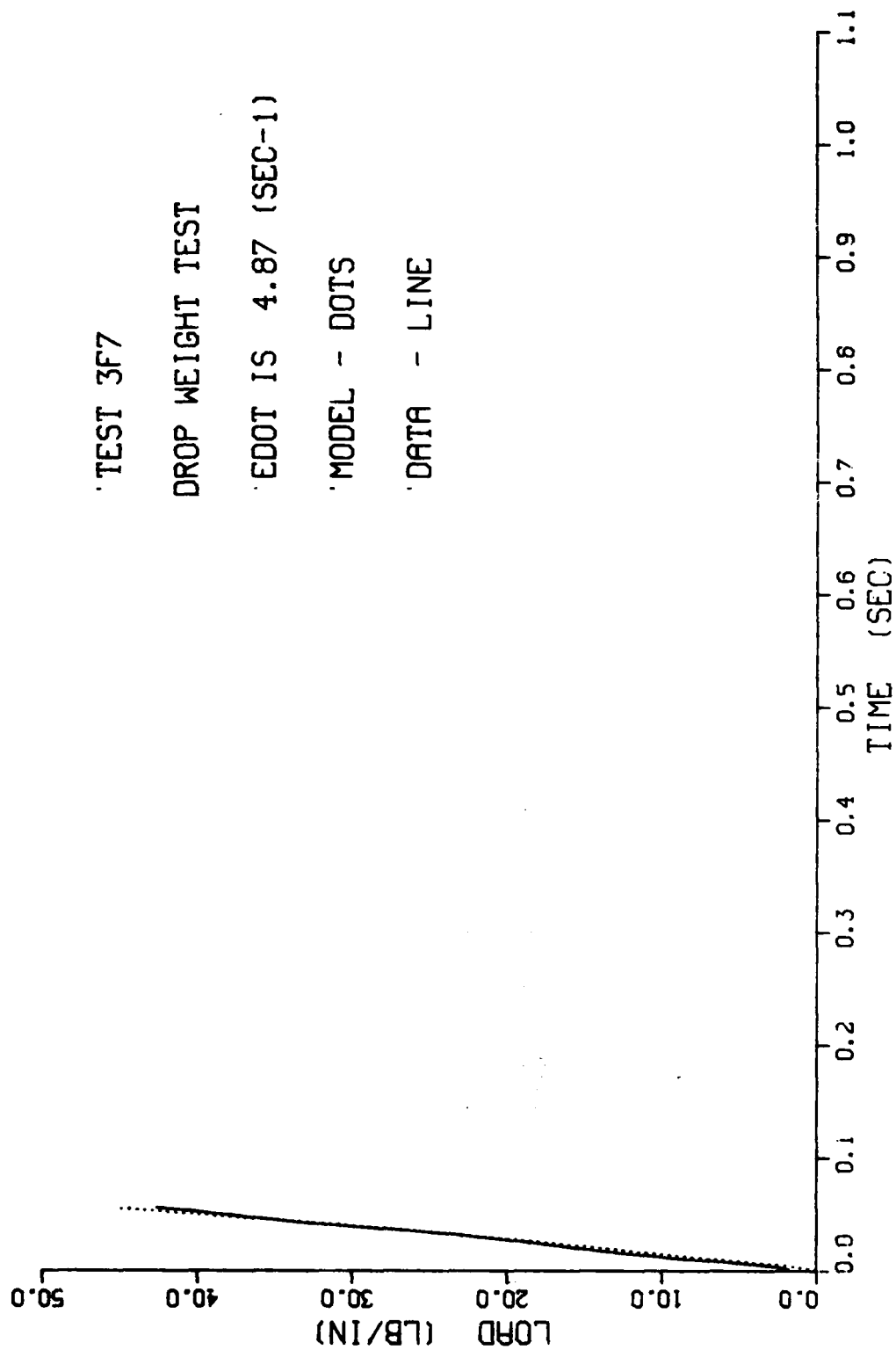
EDOT IS 3.58 (SEC-1)

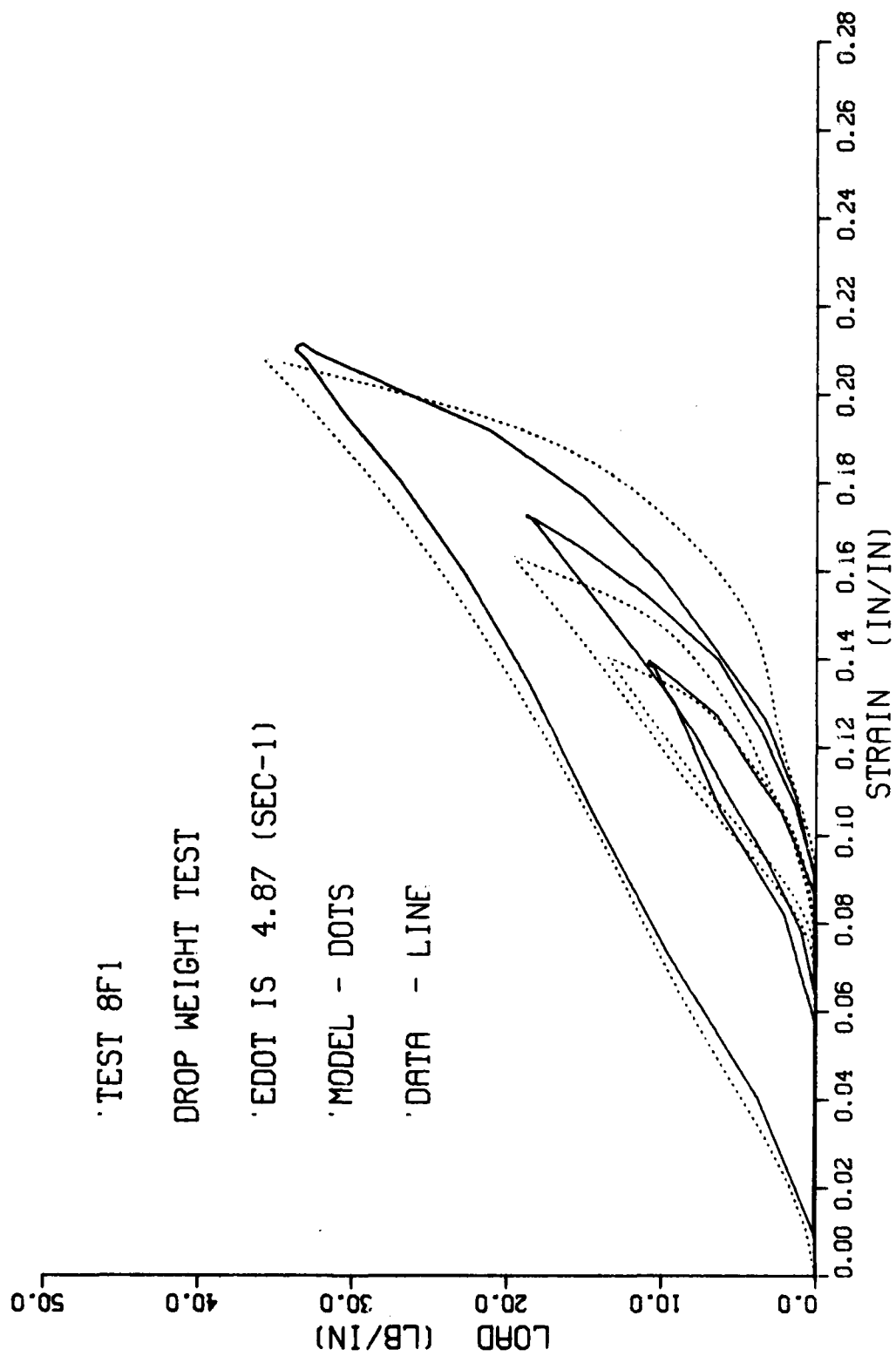
MODEL - DOTS

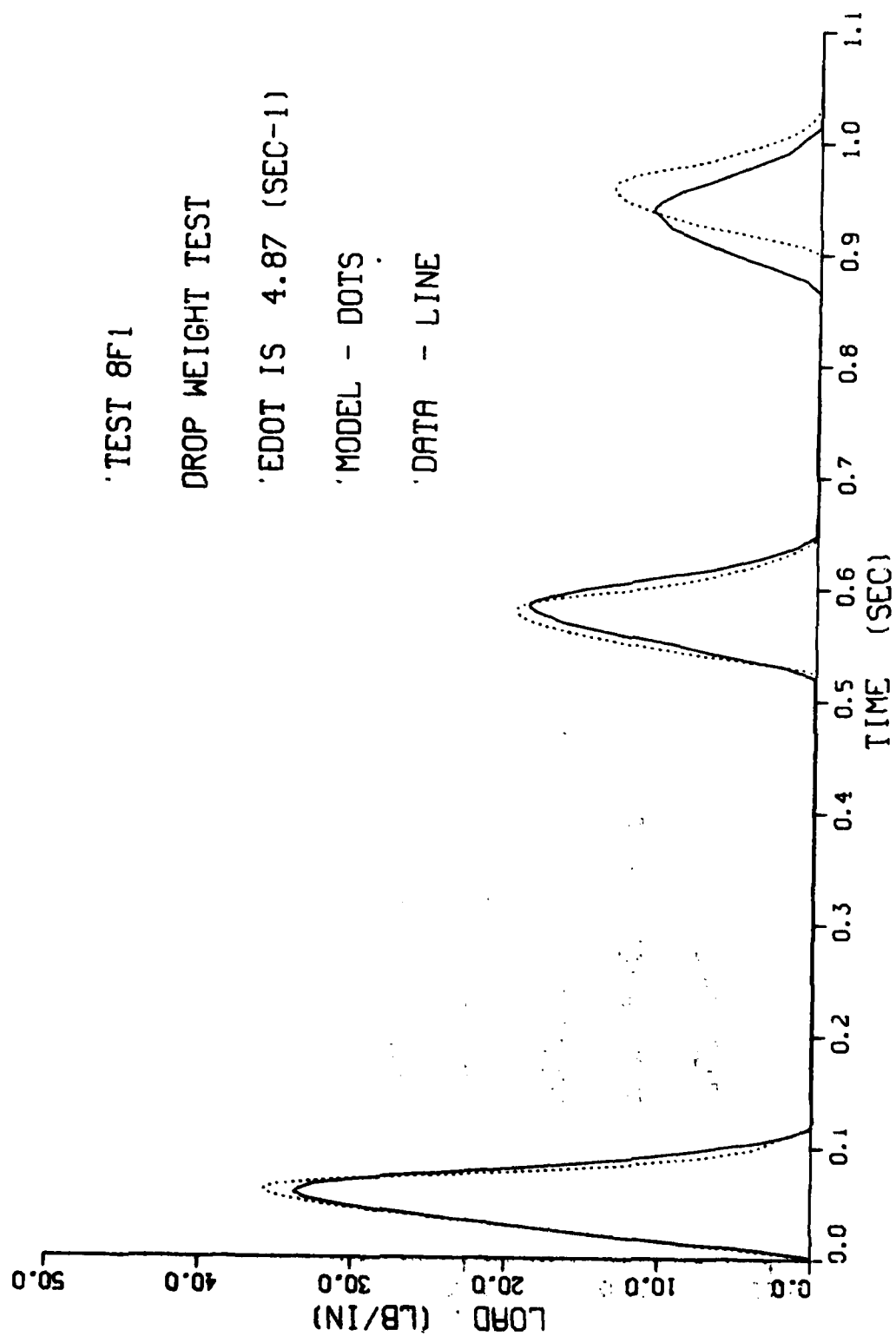
DATA - LINE



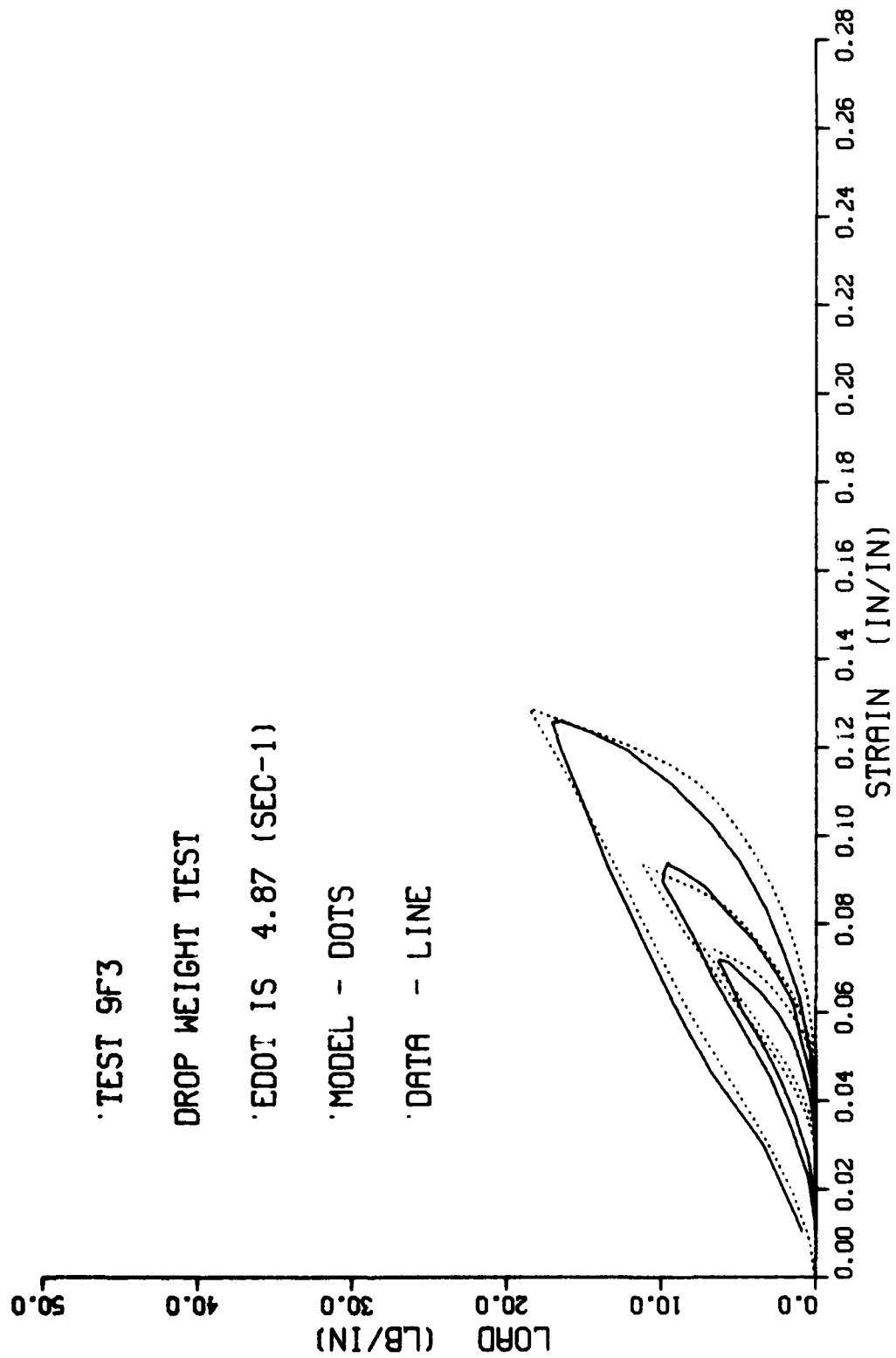












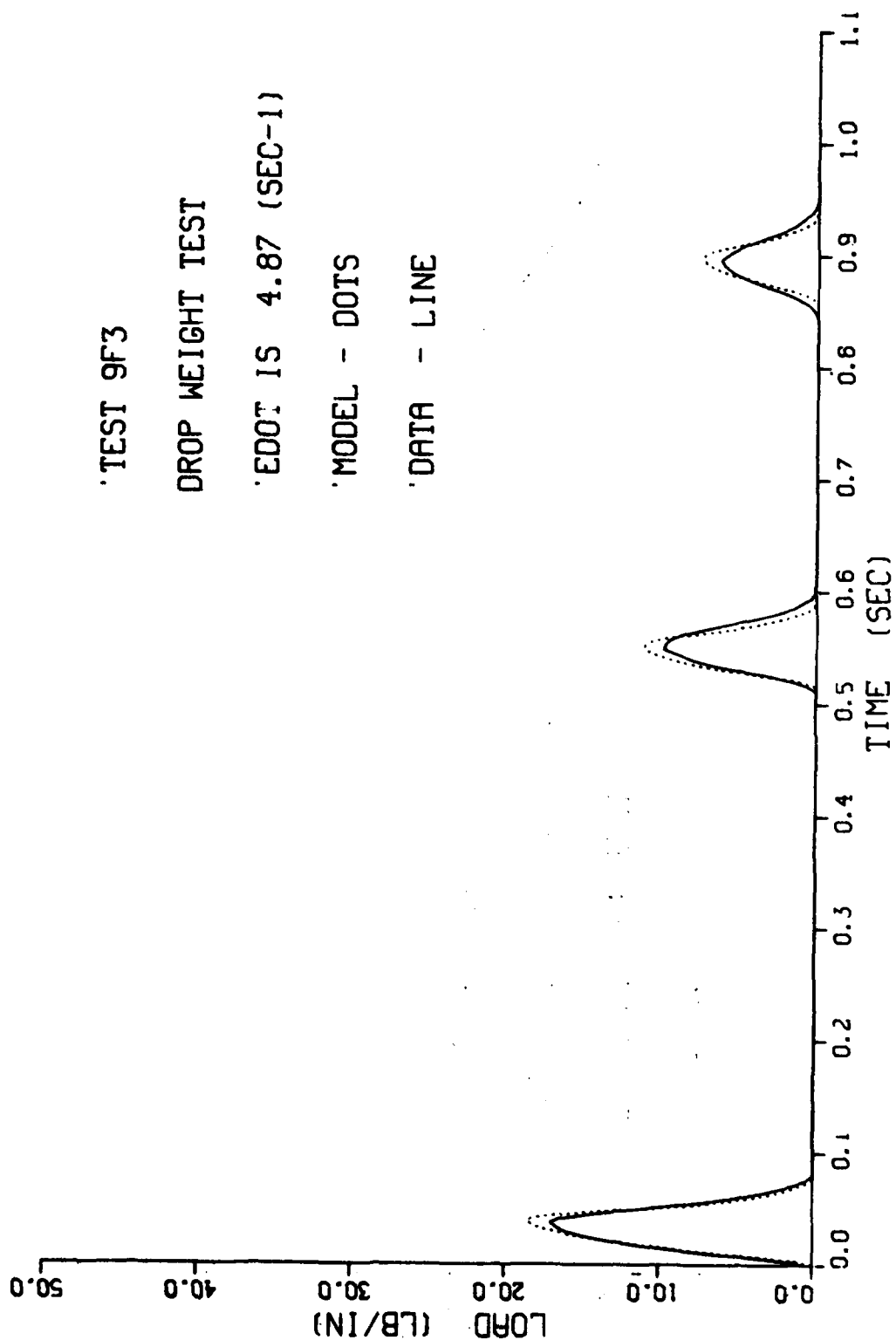
'TEST 9F3

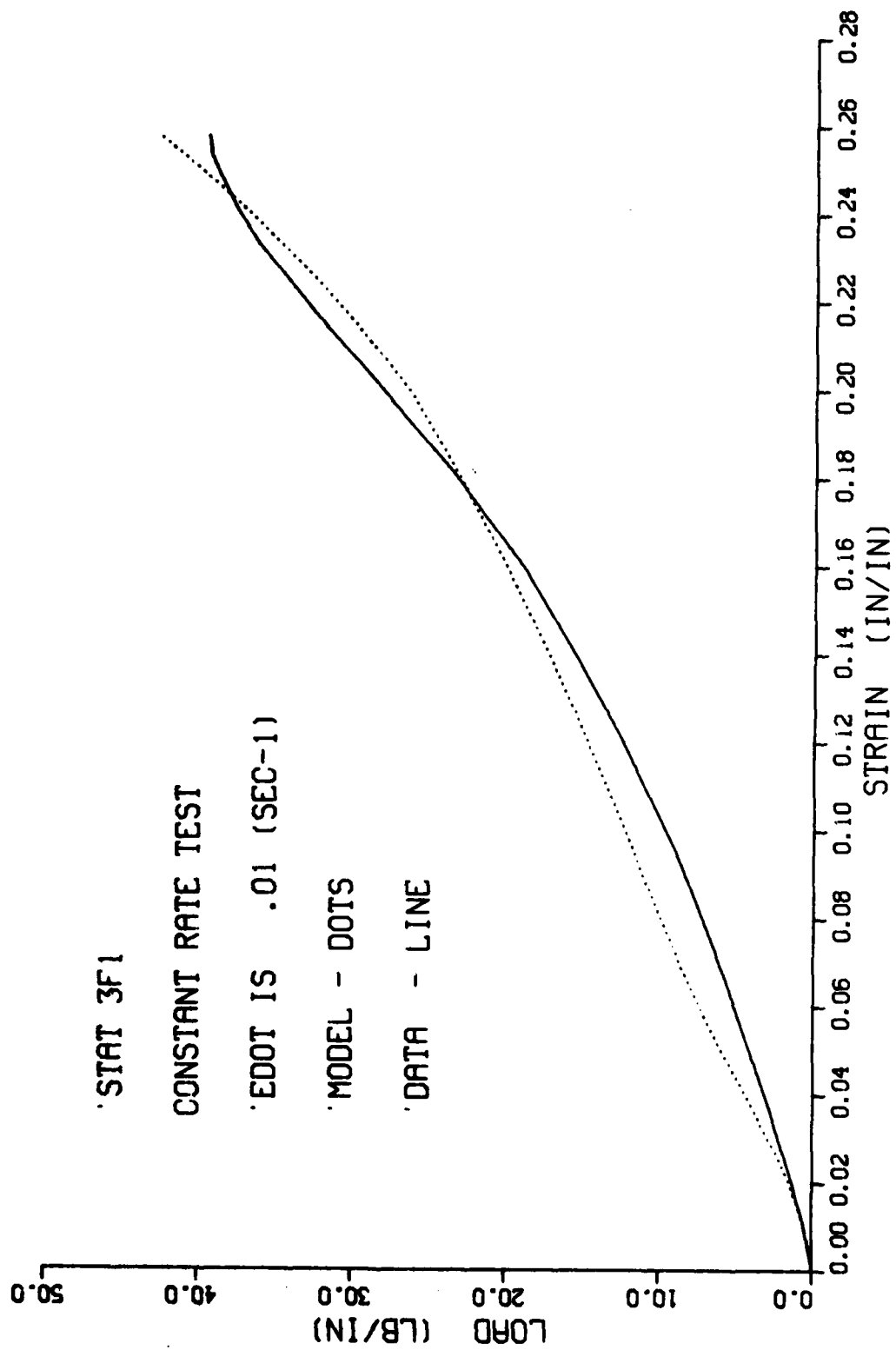
DROP WEIGHT TEST

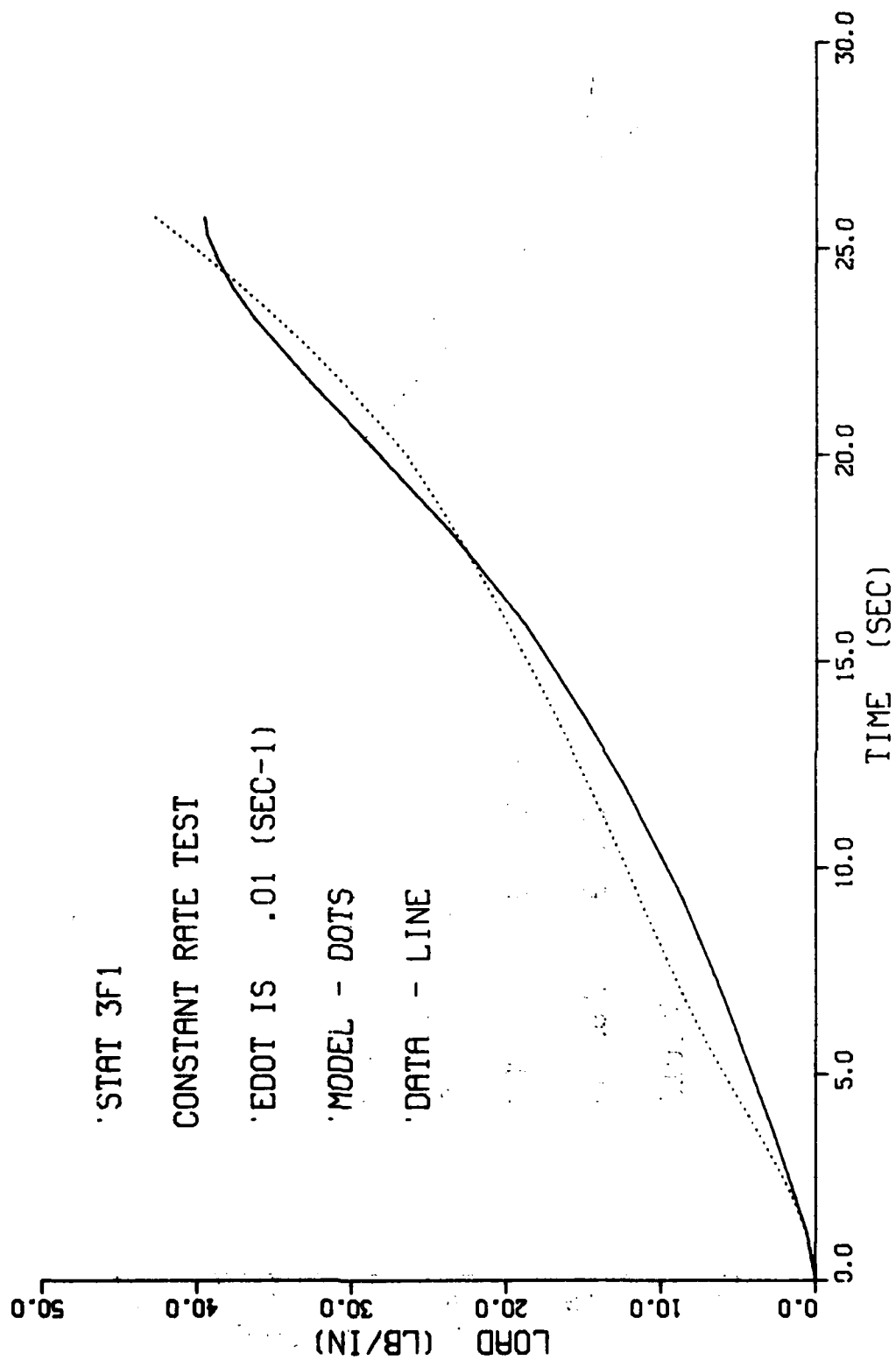
'EDOT IS 4.87 (SEC-1)

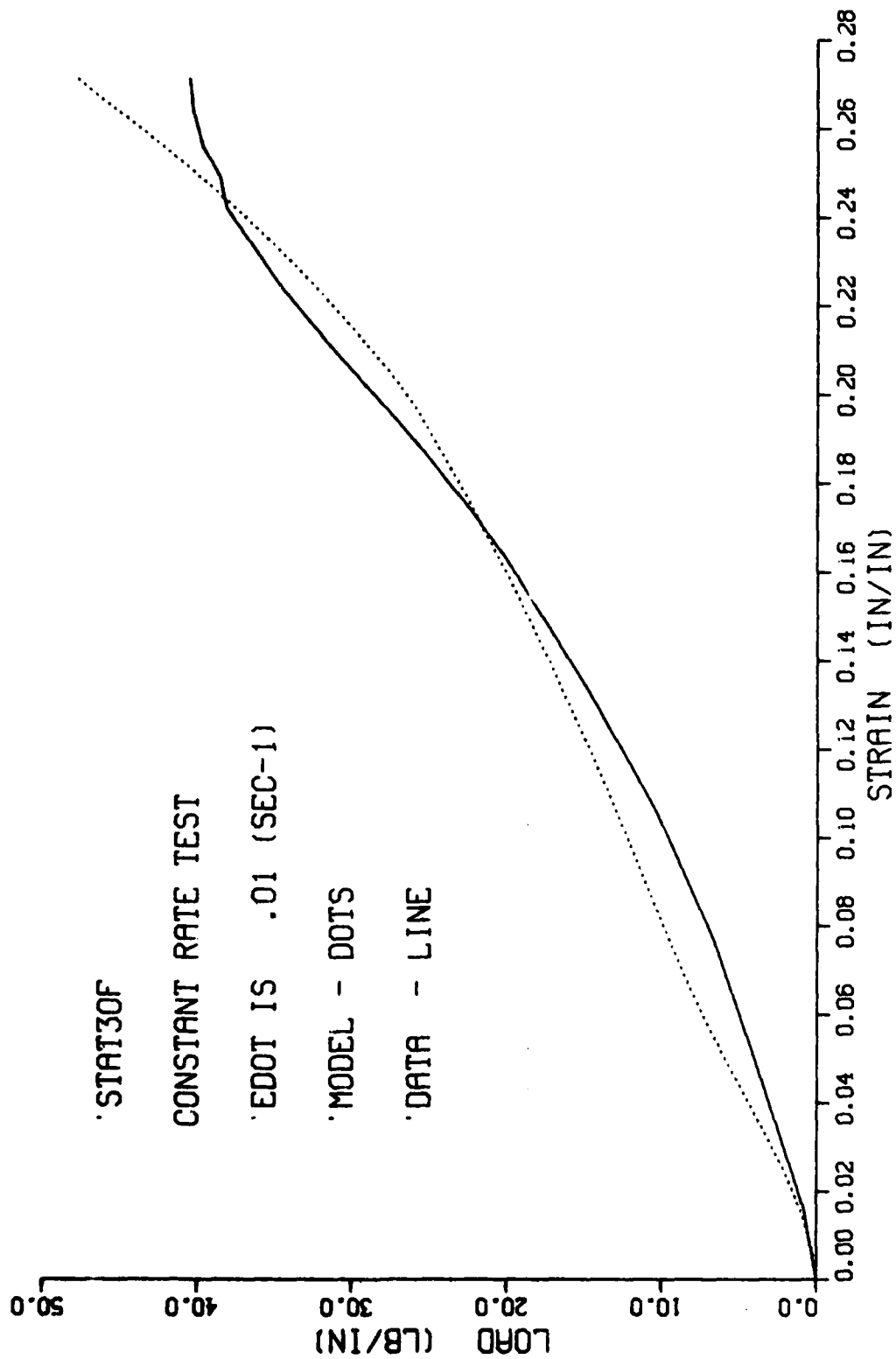
'MODEL - DOTS

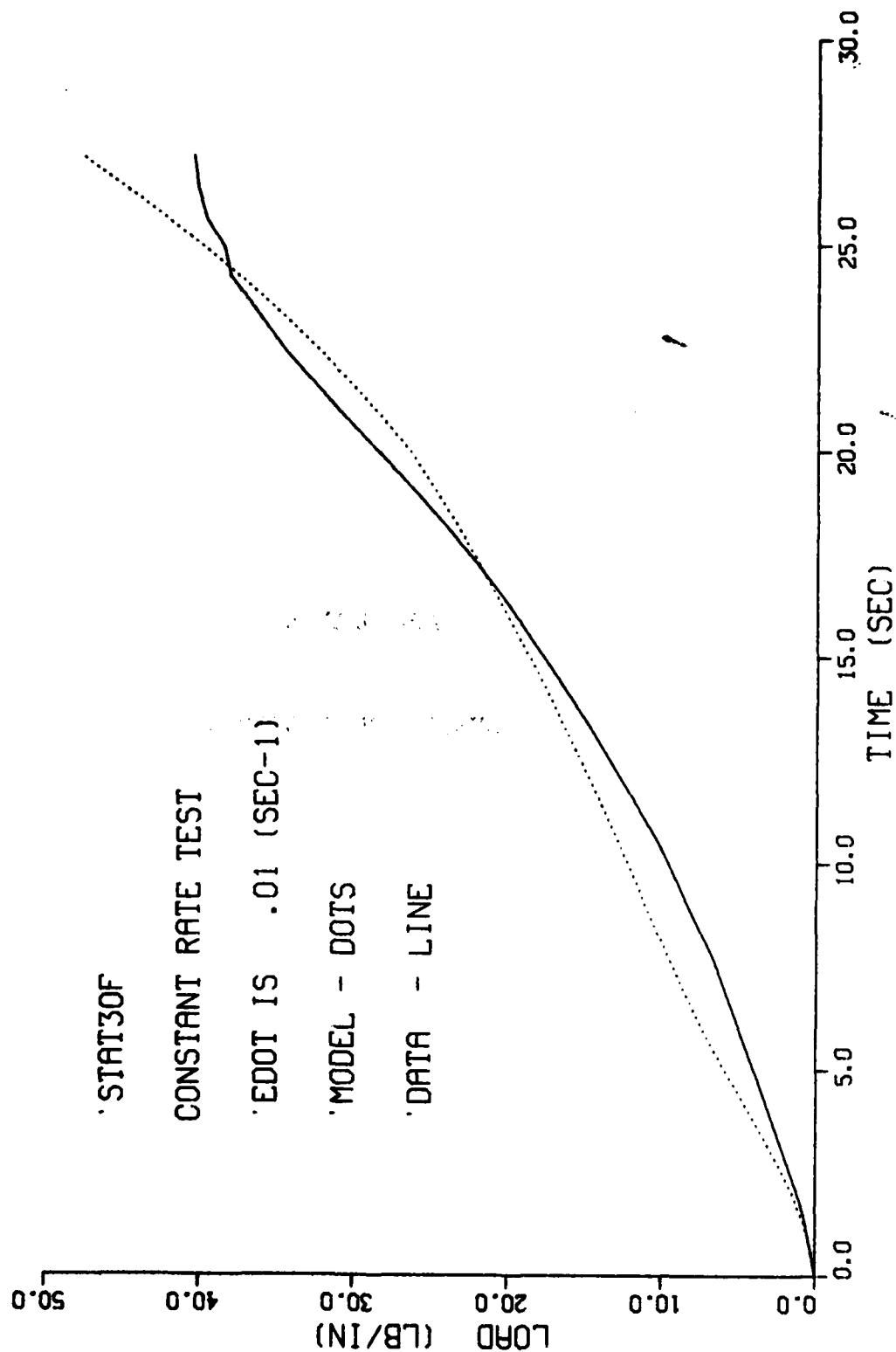
'DATA - LINE











## **APPENDIX B**

### **SUBROUTINE LISTINGS**

SUBROUTINE MODEL FOR  
NYLON CORD, MIL-C-5040E

TYPE II



```

*DECK FCORD
SUBROUTINE F(T,Y,P)
C
C   JANUARY 1978 EDITION OF TENSILE LOAD-ELONGATION ANALOG FOR
C   MIL-C-5040E NYLON CORE-SLEEVE CORD . . .
C
C   DIMENSION Y(3),P(3),EXA(6),EXO(6),EXC(5,3),TC(6),FC(3),CSR(6,3)
C   C,DPA(6),DPO(6),DPC(5,3),ELRLC(3),ELRRC(3),RATC(3)
C   COMMON/INFO/EL,FTR,LC,M,WIDTH,ELM,KRL,KCR,KOP,ELM1,RMAXD2,EC,TF,
C   C TS,IMODE,DELOMAX
C   REAL KRL,KCR,KOP,KPU,LO,M,L
C   CREEP STRAIN RATE DATA FROM PROGRAMS CREEP & BOUNCE
C   DATA TC/0.,.2,.5,.9,1.8,20./
C   DATA FC/0.,80.,1000./
C   DATA CSF/0.,0.,0.,0.,0.,0.,.06779,.03510,.01870,.01010,.
C   C001919,.001919,.06779,.03510,.01870,.01010,.001919,.001919/
C   COAMPING CHARACTERISTIC FROM PROGRAMS HYSTER & BOUNCE
C   DATA DPA/ 0.0, 0.072, 0.272, 0.65359, 0.73397, 1.0/
C   DATA DPO/ 0.67719, 15.140, 30.968, 17.945, 11.383, 0.0/
C   DATA DPC/ 91.851, 218.90, 2.3375, -80.664, -71.035,
C   C 2778.2, -1013.6, -69.191, -148.32, 260.65,
C   C -17555.0, 1574.1, -69.126, 1696.0, -603.77/
C   CEXTENSION CHARACTERISTIC FROM PROGRAMS EXTEND & OKDATA
C   DATA EXA/ 0.0, .037226, .058052, .179808, .210448, .237515/
C   DATA EXO/ 0.0, 10.7213, 33.0281, 156.476, 205.580, 251.117/
C   DATA EXC/ 122.991, 756.471, 1133.19, 1216.87, 2107.30, -3718.97,
C   C20735.9, -3315.61, 4012.75, 24201.0, 218974., -370731.,
C   C20350.3, 213226., -148*210./
C   CPLASTIC STRAIN CHARACTERISTICS FROM PROGRAMS POLYFIT & BOUNCE
C   DATA ELRLC/-.0508,.2178,3.5989/
C   DATA ELRRC/-.0508,.2178,3.5989/
C   COAMPING STRAIN DEPENDENCE DATA FROM PROGRAMS HYSTER & BOUNCE
C   DATA RATC/ -2.7208, 122.01, -272.36/
C   VX=Y(1)
C   X=Y(2)
C   CELONGATION

```

```

EC=Y(3)
EL=FSW(X/LO-1,0.,0.,X/LO-1)
ELO=FSW(EL-EC,0.,0.,EL-EC)
ELM=AMAX1(ELO,ELM)
ELM1=FSW(VX,AMAX1(ELC,ELM1),ELO,ELO)
ELRL=((ELRLC(3)*ELM+ELRLC(2))*ELM+ELRLC(1))*ELM+.0018
ELRR=((ELRRC(3)*ELM+ELRRC(2))*ELM+ELRRC(1))*ELM+.0018
TN=T
TS=T-TF
TSS=FSW((TS/.3)-1.,TS/.3,1.,1.)
ELR=ELRL-TSS*ABS(ELRL-ELRR)
ELR=RLIM(KRL*ELR,0.,KRL*ELR)
ELOT=(ELO-ELR)*ELM/(ELM-ELR+.00001)
ELS=(ELM1-ELO)/(ELM1-ELR+.00001)
ELS=FSW(ELS-1,ELS,ELS,1.0)
ELS=FSW(ELS,0.,0.,ELS)
L=LO*(1.+ELR)
ELOT=RLIM(ELOT,0.,ELO)
DELO=VX/LO
IF(DELO.GT.7.0) STOP "MODEL STRAIN RATE RANGE EXCEEDED"
DELOMAX=AMAX1(DELO,DELOMAX)
RMAXD1=FSW(DELO,DELO,0.00001,0.00001)
RMAXD2=FSW(DELO,AMIN1(RMAXD1,RMAXD2),0.00001,0.00001)
C SPRING FORCE
I=1
DO1 I=1,5
IF(EXA(I).LE.ELO.AND.ELO.LT.EXA(I+1)) GO TO 10
1 CONTINUE
J2=J2+1
IF(J2.GT.1) GO TO 11
PRINT 100
100 FORMAT(10X,"ELO EXCEEDS MODEL RANGE")
11 I=5
10 CONTINUE
O=ELO-EXA(I)
FSO=((EXC(I,3)*O+EXC(I,2))*O+EXC(I,1))*O+EXO(I)-EXO(1)

```

```

I=1
002 I=1,5
IF(EXA(I)).LE.ELOT.AND.ELOT.LT.EXA(I+1)) GO TO 20
2 CONTINUE
J1=J1+1
IF(J1.GT.1) GO TO 21
PRINT 200
200 FORMAT(10X,*ELOT EXCEEDS MODEL RANGE*)
21 I=5
20 CONTINUE
D=ELOT-EXA(I)
FSR=((EXC(I,3)*D+EXC(I,2))*D+EXC(I,1))*D+EXO(I)-EXO(1)
FSOL=RLIM(FSO,0.,FSO)
FSRL=RLIM(FSR,0.,FSR)
FS2=FSW(ELO-ELM,FSRL,FSOL,FSOL)
FS1=FSW(ELO-ELR,0.0,0.0,FS2)
FS=FS1
RATIO=((RATC(3)*ELM1+RATC(2))*ELM1+RATC(1))*ELM1
I=1
004 I=1,5
IF(DPA(I)).LE.ELS.AND.ELS.LT.DPA(I+1)) GO TO 30
4 CONTINUE
I=5
30 CONTINUE
D=ELS-DPA(I)
FD4=((DPC(I,3)*D+DPC(I,2))*D+DPC(I,1))*D+DPO(I)
VSFDM=0.1775.0
VSFD=0.90+VSFDM*DELOMAX
F03=FD4*RATIO*KDP*VSFD*(ELM1-ELR)/(ELM-ELR+1.E-6)
FD3=FSW(FD3,0.,0.,FD3)
F03=FSW(FD3-FS,FD3,FC3,FS)
FD1=FSW(VX,FD3,0.,0.)
FD2=FSW(L-X,FD1,0.0,0.0)
FU=FSW(M*32.155-FTR,F02,F02,((DELO/RMAXD2)**0.5)*FD2)
CTOTAL FORCE
FI=FS-FD

```

```

      FTR=FT*WIDTH
      FIND CURRENT CREEP STRAIN RATE
      NY=6
      NX=3
      NDY=NY
      TF=FSM(FTR,TF,TF,TF+TN-TT)
      TT=T
      IF(TF.GT.TC(6)) GO TO 3
      CALL TBL2(TC,FC,CSR,NY,NX,NOX,TF,FT,DEC,IER)
      C EQUATION OF MOTION
      3 P(1)=AX=32.155-FTR/M
      P(2)=Y(1)
      IF(FT.LE.0.0) DEC=0.0
      IF(TF.GT.TC(6)) DEC=0.0
      P(3)=DEC*KCR*1.8
      RETURN
      END

```

SUBROUTINE MODEL FOR NYLON

FABRIC WARP, MIL-C-7020F

TYPE I

```

*DECK FWARP
SUBROUTINE F(T,Y,P)
C
C   FEBRUARY 1978 EDITION OF TENSILE LOAD-ELONGATION ANALOG FOR
C   MIL-C-7020F NYLON FABRIC WARP . . .
C
C   DIMENSION Y(3),P(3),EXA(6),EXO(6),EXC(5,3),TC(6),FC(3),CSR(6,3)
C,DPA(6),DPO(6),DPC(5,3),ELRLC(3),ELRRC(3),RATC(3)
COMMON /INFO/EL,FTR,LO,M,WIDTH,ELM,KRL,KCR,KDP,ELM1,RMAXD2,EC,TF,
C TS,IMODE,DELOMAX
REAL KRL,KCR,KDP,KPU,LO,M,L
CCREEP STRAIN RATE DATA FROM PROGRAMS CREEP & BOUNCE
DATA TC/0.,.2,.5,.9,1.8,20./
DATA FC/0.,8.,100./
DATA CSR/0.,0.,0.,0.,0.,0.,.06779,.03510,.01870,.01010,.001919/
C001919,.001919,.06779,.03510,.01870,.01010,.001919,.001919/
CDAMPING CHARACTERISTIC FROM PROGRAMS HYSTER & BOUNCE
DATA DPA/ 0.0,.31482,.48706,.61765,.78290,1.0 /
DATA DPO/ 0.0,10.434,10.845,9.7124,8.0092,0.7 /
DATA DPC/ 98.799,3.8845,-4.4891,-7.7518,-23.057,
C-324.06,22.611,-71.229,46.245,-138.86,
C367.06,-181.61,299.86,-373.35,433.78 /
CEXTENSION CHARACTERISTIC FROM PROGRAMS EXTEND & OKDATA
DATA EXA/ 0.0,0.03078,0.06535,0.12983,0.14959,0.19442 /
DATA EXO/ 0.0,8.3751,13.594,31.65,38.846,52.14 /
DATA EXC/ 159.89,243.76,155.14,341.18,410.92,
C 8214.6,-5489.3,2926.0,-40.606,3570.1,
C -148419.,81135.,-15337.,60906.,-136541. /
CPLASTIC STRAIN CHARACTERISTICS FROM PROGRAMS POLYFIT & BOUNCE
DATA ELRLC/ 0.3483,-4.057,23.30 /
DATA ELRRC/ 0.2415,-3.211,19.62 /
CDAMPING STRAIN DEPENDENCE DATA FROM PROGRAMS HYSTER & BOUNCE
DATA RATC/ 10.6,-26.3,26.3 /
/X=Y(1)
X=Y(2)
CELONGATION

```

```

EC=Y(3)
EL=FSW(X/LO-1,0.,0.,X/LO-1)
ELO=FSW(EL-EC,0.,0.,EL-EC)
ELM=AMAX1(EL0,ELM)
ELM1=FSW(VX,AMAX1(EL0,ELM1),ELO,ELO)
ELRL=((ELRLC(3)*ELM+ELRLC(2))*ELM+ELRLC(1))*ELM
ELRR=((ELRRC(3)*ELM+ELRRC(2))*ELM+ELRRC(1))*ELM
TN=T
TS=T-TF
TSS=FSW((TS/.3)-1.,TS/.3,1.,1.)
ELR=ELRL-TSS*ABS(ELRL-ELRR)
ELR=RLIM(KRL*ELR,0.,KRL*ELR)
EL0T=(ELO-ELR)*ELM/(ELM-ELR+.00001)
ELS=(ELM1-ELO)/(ELM1-ELR+.00001)
ELS=FSW(ELS-1,ELS,ELS,1.0)
ELS=FSW(ELS,0.,0.,ELS)
L=LO*(1.+ELR)
EL0T=RLIM(EL0T,0.,ELC)
DELO=VX/LO
IF(DELO.GT.5.0) STOP "MODEL STRAIN RATE RANGE EXCEEDED"
DELOMAX=AMAX1(DELO,DELOMAX)
RMAX01=FSW(DELO,DELO,0.00001,0.00001)
RMAX02=FSW(DELO,AMIN1(RMAX01,RMAX02),0.00001,0.00001)

C SPRING FORCE
I=1
001 I=1,5
IF(EXA(I).LE.ELO.AND.ELO.LT.EXA(I+1)) GO TO 10
1 C CONTINUE
J2=J2+1
IF(J2.GT.1) GO TO 11
PRINT 100
100 FORMAT(10X,'ELO EXCEEDS MODEL RANGE')
11 I=5
10 CONTINUE
D=ELO-EXA(I)
FS0=((EXC(I,3)*D+EXC(I,2))*D+EXC(I,1))*D+EX0(I)-EX0(1)

```

```

I=1
002 I=1,5
IF(EXA(I).LE.ELOT.AND.ELOT.LT.EXA(I+1)) GO TO 20
2 CONTINUE
J1=J1+1
IF(J1.GT.1) GO TO 21
PRINT 200
200 FORMAT(10X,'ELOT EXCEEDS MODEL RANGE')
21 I=5
20 CONTINUE
D=ELOT-EXA(I)
FSR=((EXC(I,3)*D+EXC(I,2))*D+EXC(I,1))*D+EX0(I)-EX0(1)
FSOL=RLIM(FSO,0.,FSO)
FSRL=RLIM(FSR,0.,FSR)
FS2=FSW(EL0-ELM,FSRL,FSOL,FSOL)
FS1=FSW(EL0-ELR,0.0,0.0,FS2)
FS=FS1
RATIO=((RATC(3)*ELM1+RATC(2))*ELM1+RATC(1))*ELM1
I=1
004 I=1,5
IF(DPA(I).LE.ELS.AND.ELS.LT.DPA(I+1)) GO TO 30
4 CONTINUE
I=5
30 CONTINUE
D=ELS-DPA(I)
FD4=((DPC(I,3)*D+DPC(I,2))*J+DPC(I,1))*D+DP0(I)
VSFD=((0.013*DELOMAX-0.148)*DELOMAX+0.619)*DELOMAX
FD3=FD4*RATIO*KDP*VSFD*(ELM1-ELR)/(ELM-ELR+1.E-6)
FD3=FSW(FD3,0.,0.,FD3)
FD3=FSW(FD3-FS,FD3,FD3,FS)
FD1=FSW(VX,FD3,0.,0.)
FD2=FSW(L-X,FD1,0.0,0.0)
FD=FSW(M*32.155-FTR,FD2,FD2,((DELO/RMAXD2)**0.5)*FD2)
CTOTAL FORCE
FT=FS-FD
FTR=FT*WIDTH

```



```

C      FIND CURRENT CREEP STRAIN RATE
      NY=6
      NX=3
      NDX=NY
      TF=FSW(FTR,TF,TF,TF,TF+TN-TT)
      TT=T
      IF(TF.GT.TC(6)) GO TO 3
      CALL TBL2(TC,FC,CSR,NY,NX,NDX,TF,FT,DEC,IER)
C EQUATION OF MOTION
      3 P(1)=AX=32.155-FTR/M
      P(2)=Y(1)
      IF(FT.LE.0.0) DEC=0.0
      IF(TF.GT.TC(6)) DEC=0.0
      P(3)=DEC*KCR
      RETURN
      END

```

SUBROUTINE MODEL FOR NYLON

FABRIC FILL, MIL-C-7020F

TYPE I

```

C
C
C
C
SUBROUTINE F(T,Y,P)

15 NOVEMBER 1977 EDITION OF TENSILE LOAD-ELONGATION ANALOG FOR
MIL-C-7020F RIPSTOP NYLON FABRIC FILL . . .

DIMENSION Y(3),P(3),EXA(6),EXO(6),EXC(5,3),TC(6),FC(3),CSR(6,3)
C,DPA(6),DPO(6),DPC(5,3),ELRLC(3),ELRRC(3),RATC(3)
COMMON /INFO/EL,FTR,LO,M,WIDTH,ELM,KRL,KCR,KDP,ELM1,RMAXD2,EC,TF,T
CS,IMODE,DELOMAX
REAL KRL,KCR,KDP,KPU,LO,M,L
CCREEP STRAIN RATE DATA FROM PROGRAMS CREEP & BOUNCE
DATA TC/0.,.2,.5,.9,1.8,20./
DATA FC/0.,8.,100./
DATA CSR/0.,0.,0.,0.,0.,0.,.06779,.03510,.01870,.01010,.001919/
C001919,.001919,.06779,.03510,.01870,.01010,.001919,
CDAMPING CHARACTERISTIC FROM PROGRAMS HYSTER & BOUNCE
DATA DPA/ 0.0,.10988,.272,.472,.72286,1.0 /
DATA DPO/ .11274,7.2925,10.6327,9.8254,4.9885,0.0 /
DATA DPC/ 50.735,55.465,1.5762,-11.324,-23.955,355.76,-312.7
C1,-19.591,-44.812,-5.5366,-2027.9,602.47,-41.869,52.188,10
C7.82 /
CEXTENSION CHARACTERISTIC FROM PROGRAMS EXTEND & OKDATA
DATA EXA/0.0,.056772,.091612,.13495,.22838,.25952 /
DATA EXO/ .12309,7.8117,13.009,20.059,43.79,51.75 /
DATA EXC/ 23.12,166.,146.95,178.78,368.94,3418.1,-901.43,
C354.67,379.94,1655.4,-25362.,12017.,194.35,4550.8,-170032.
C/
GPLASTIC STRAIN CHARACTERISTICS FROM PROGRAMS POLYFIT & BOUNCE
DATA ELRLC/-.0337,2.8651,-3.5577/
DATA ELRRC/-.0511,2.195,-1.928/
CDAMPING STRAIN DEPENDENCE DATA FROM PROGRAMS HYSTER & BOUNCE
DATA RATC/ 8.5708,-53.620,139.04 /
VX=Y(1)
X=Y(2)
CELONGATION
EC=Y(3)

```

```

EL=FSW(X/L0-1,0.,0.,X/L0-1)
ELO=FSW(EL-EC,0.,0.,EL-EC)
ELM=AMAX1(ELO,ELM)
ELM1=FSW(VX,AMAX1(ELO,ELM1),ELO,ELO)
ELRL=((ELRLC(3)*ELM+ELRLC(2))*ELM+ELRLC(1))*ELM
ELRR=((ELRRC(3)*ELM+ELRRC(2))*ELM+ELRRC(1))*ELM
TN=T
TS=T-TF
TSS=FSW((TS/.3)-1.,TS/.3,1.,1.)
ELR=ELRL-TSS*ABS(ELRL-ELRR)
ELR=RLIM(KRL*ELR,0.,KRL*ELR)
ELOT=(ELO-ELR)*ELM/(ELM-ELR+1.E-6)
ELS=(ELM1-ELO)/(ELM1-ELR+1.E-6)
ELS=FSW(ELS-1,ELS,ELS,1.0)
ELS=FSW(ELS,0.,0.,ELS)
L=LO*(1.+ELR)
ELOT=RLIM(ELOT,0.,ELO)
DELO=VX/LO
IF(DELO.GT.5.0) STOP "MODEL STRAIN RATE RANGE EXCEEDED"
DELOMAX=AMAX1(DELO,DELOMAX)
RMAX01=FSW(DELO,DELO,1.E-6,1.E-6)
RMAX02=FSW(DELO,AMIN1(RMAX01,RMAX02),0.00001,0.00001)
C SPRING FORCE
I=1
001 I=1,5
IF(EXA(I).LE.ELO.AND.ELO.LT.EXA(I+1)) GO TO 10
1 CONTINUE
J2=J2+1
IF(J2.GT.1) GO TO 11
PRINT 100
100 FORMAT(10X,"ELO EXCEEDS MODEL RANGE")
11 I=5
10 CONTINUE
D=ELO-EXA(I)
FSO=((EXC(I,3)*D+EXC(I,2))*D+EXC(I,1))*D+EXO(I)-EXO(I)
I=1

```

```

002 I=1,5
IF(EXA(I).LE.ELOT.AND.ELOT.LT.EXA(I+1)) GO TO 20
2 CONTINUE
J1=J1+1
IF(J1.GT.1) GO TO 21
PRINT 200
200 FORMAT(10X,'*ELOT EXCEEDS MODEL RANGE*')
21 I=5
20 CONTINUE
D=ELOT-EXA(I)
FSR=((EXC(I,3)*D+EXC(I,2))*D+EXC(I,1))*D+EXO(I)-EXO(1)
FSOL=RLIM(FSO,0.,FSO)
FSRL=RLIM(FSR,0.,FSR)
FS2=FSW(EL0-ELM,FSRL,FSOL,FSOL)
FS1=FSW(EL0-ELR,0.0,0.0,FS2)
FS=FS1
RATIO=((RATC(3)*ELM1+RATC(2))*ELM1+RATC(1))*ELM1
I=1
004 I=1,5
IF(DPA(I).LE.ELS.AND.ELS.LT.DPA(I+1)) GO TO 30
4 CONTINUE
I=5
30 CONTINUE
D=ELS-DPA(I)
FD4=((DPC(I,3)*D+DPC(I,2))*D+DPC(I,1))*D+DPO(I)
VSFDM=FSW(ELM-0.10,0.,0.,ELM-0.10)
VSFD=0.53+0.24*(VSFDM/.10)+0.154*DELOMAX
FD3=FD4*RATIO*KDP*/SFD*(ELM1-ELR)/(ELM-ELR+1.E-6)
FD3=FSW(FD3,0.,0.,FD3)
FU3=FSW(FD3-FS,FD3,FD3,FS)
FD1=FSW(VX,FD3,0.,0.)
FD2=FSW(L-X,FD1,0.0,0.0)
FD=FSW(M*32.155-FTR,FD2,FD2,(DELO/RMAXD2)*FD2)
CTOTAL FORCE
FT=FS-FD
FTR=FT*WIDTH

```

```

C      FIND CURRENT CREEP STRAIN RATE
      NY=6
      NX=3
      NDX=NY
      TF=FSW(FTR,TF,TF,TF+IN-IT)
      TT=T
      IF(TF.GT.TC(6)) GO TO 3
      CALL TBL2(TC,FC,CSR,NY,NX,NDX,TF,FT,DEC,IER)
C EQUATION OF MOTION
      3 P(1)=AX=32.155-FTR/M
      P(2)=Y(1)
      IF(FT.LE.0.0) DEC=0.0
      IF(TF.GT.TC(6)) DEC=0.0
      P(3)=DEC*KCR
      RETURN
      END

```

**FUNCTION FSW**  
**REQUIRED BY**  
**SUBROUTINE MODELS**

```
FUNCTION FSW(A,B,C,D)
  IF(A) 1,2,3
1 FSW=B
  RETURN
2 FSW=C
  RETURN
3 FSW=D
  END
```



FUNCTION RLIM  
REQUIRED BY  
SUBROUTINE MODELS

```
FUNCTION RLIM(AA,BB,CC)
IF(AA.LT.BB)GO TO 10
IF(AA.GT.CC)GO TO 20
RLIM=AA
RETURN
10 RLIM=9B
RETURN
20 RLIM=CC
RETURN
END
```

SUBROUTINE TBL2

REQUIRED BY

SUBROUTINE MODELS

```

SUBROUTINE TBL2(X,Y,Z,NX,NY,NDX,XO,YO,ZO,IER)
DIMENSION X(1),Y(1),Z(1)
IF(NX.GT.NDX) GO TO 12
I1=1
IF(XO.LT.X(1)) GO TO 4
IF(XO.GT.X(NX)) GO TO 3
IER=0
I2=NX
1 IF((I2-I1).LT.2) GO TO 5
I=(I1+I2)/2
IF(XO.LT.X(I)) GO TO 2
I1=I
GO TO 1
2 I2=I
GO TO 1
3 I1=NX-1
4 IER=1
5 J1=1
IF(YO.LT.Y(1)) GO TO 9
IF(YO.GT.Y(NY)) GO TO 8
J2=NY
6 IF((J2-J1).LT.2) GO TO 10
J=(J1+J2)/2
IF(YO.LT.Y(J)) GO TO 7
J1=J
GO TO 6
7 J2=J
GO TO 6
8 J1=NY-1
9 IER=1
10 OI/=X(I1+1)-X(I1))*Y(J1+1)-Y(J1)
IF (OI) 12,12,11
11 I11=(J1-1)*NDX+I1
I12=I11+NDX
X20=X(I1+1)-XO
XC1=XO-X(I1)

```

```

Z0=((Y(J1+1)-Y0)*(X20*Z(I11)+X01*Z(I11+1))+
C(Y0-Y(J1))*(X20*Z(I12)+X01*Z(I12+1)))/DIV
RETURN
12 IER=2
RETURN
END

```

## REFERENCES

1. Priesser, J.S. and Green, G.C., "Effect of Suspension Line Elasticity on Parachute Loads," Journal of Spacecraft and Rockets, Vol. 7, No. 10, Oct. 1970, pp. 1278-1280.
2. Poole, L.R., "Effect of Suspension-Line Viscous Damping on Parachute Opening Load Amplification," Journal of Spacecraft and Rockets, Vol. 10, No. 1, Jan. 1973, pp. 92-93.
3. Mullins, W.M., et al., Investigation of Prediction Methods for the Loads and Stresses of Apollo Type Spacecraft Parachutes. Volume 2: Stresses, NASA-CR-134231, 1970.
4. Houmard, J.E., Stress Analysis of the Viking Parachute, AIAA Paper 73-444, 1973.
5. Reynolds, D.T., and Mullins, W.M., An Internal Loads Analysis for Ribbon Parachutes, NVR 75-12, Northrop Corp., Ventura Division, 1975.
6. McVey, D.F., and Wolf, D.F., "Analysis of Deployment and Inflation of Large Ribbon Parachutes," Journal of Aircraft, Vol. 11, No. 2, Feb. 1974, pp. 96-103.
7. Ibrahim, S.K., and Engdahl, R.A., Parachute Dynamics and Stability Analysis, NASA-CR-120326, Feb 1974.
8. Sundberg, W.D., Finite-Element Modelling of Parachute Deployment and Inflation, AIAA Paper 75-1830, 1975.
9. Talay, T.A., Parachute-Deployment-Parameter Identification Based on an Analytical Simulation of Viking BLDT AV-4, NASA-TN-D7678, Aug. 1974.
10. Bobbitt, P.J., "Recent Advances and Remaining Voids in Parachute Technology," AIAA Aerodynamic Deceleration Systems Tech Committee Position Paper, Astronautics and Aeronautics, Oct. 1975, pp. 56-63.
11. McCarty, R.E., A Computer Subroutine for the Load-Elongation of Parachute Suspension Lines, AIAA Paper 75-1362, 1975.
12. Keck, E.L., A Computer Simulation of Parachute Opening Dynamics, AIAA Paper 75-1379, 1975.
13. DeBoor, C., and Rice, J.R., Cubic Spline Approximation II-Variable Knots, Computer Science Department TR-21, Purdue University, April 1968.

14. Crandall, S.H., and Dahl, N.C., An Introduction to the Mechanics of Solids, McGraw-Hill, 1959, pp. 222-223.
15. Bruhn, E.F., Analysis and Design of Flight Vehicle Structures, Tri-State Offset, 1965, pp. B1.12-13.
16. Polakowski, N.H., and Ripling, E.J., Strength and Structure of Engineering Materials, Prentice-Hall, 1966, p. 429.
17. Groom, J.J., Investigation of a Simple Dynamic System with a Woven-Nylon Tape Member Displaying Nonlinear Damping, Thesis for Master of Science, Ohio State University, 1974, pp. 51-54.
18. 777 Interactive Graphics System, Version 2.1, Reference Manual, Control Data Corporation publication number I7321800, Revision B, 30 October 1975.
19. FORTTRAN Extended, Version 4, Reference Manual, Control Data Corporation publication number 60305600, Revision J, 5 March 1976.
20. Swallow, J.E., and Webb, Mrs. M.W., "Single and Repeated Snatch Loading of Textile Yarns, and the Influence of Temperature on the Dynamic Mechanical Properties," Journal of Applied Polymer Science, Vol.8, pp. 257-282 1964.